

TECHNICAL
DESIGN STUDY
BESSY VSR

Technical Design Study

BESSY VSR

Variable pulse length **S**torage **R**ing

Upgrade of BESSY II

– June 2015 –

Publisher

Helmholtz-Zentrum Berlin für Materialien und Energie GmbH

Albert-Einstein-Straße 15

D-12489 Berlin

Germany

Fon: +49 (0)30 8062 0

Fax: +49 (0)30 8062 12990

Mail: info@helmholtz-berlin.de

Homepage: www.helmholtz-berlin.de

Cover

Helmholtz-Zentrum Berlin, Heike Oberdiek

Project Team contributing to the Technical Design Study

Beam Dynamics and Beam Tests

P. Goslawski, P. Kuske, R. Müller, M. Ries,
M. Ruprecht, A. Schälicke, G. Wüstefeld

SRF Systems

W. Anders, A. Burrill, J. Knobloch, A. Neumann, A. Velez

Engineering Support

V. Dürr, D. Pflückhahn, O. Schüler

Photon Science

A. Föhlisch, K. Holldack

Radiation Protection

K. Ott

Editors

A. Jankowiak, J. Knobloch, P. Goslawski, N. Neumann

DOI [doi:10.5442/R0001](https://doi.org/10.5442/R0001)
<http://dx.doi.org/10.5442/R0001>

Copyright by
Helmholtz-Zentrum Berlin für Materialien und Energie GmbH, Berlin 2015

Foreword

Helmholtz-Zentrum Berlin (HZB) operates two large-scale facilities, the neutron source BER II (until 2019) and the photon source BESSY II for an international user community. HZB scientists focus on research with photons and neutrons, accelerator research as well as on materials and energy research. Guidelines for the operation of the large-scale facilities and for HZB's research were formulated and reviewed in the Helmholtz Association's program oriented funding (POF) process in 2014.

HZB in future will focus on BESSY II and strengthen its materials and energy research. HZB's primary goal with regard to BESSY II is to maintain its position among the international synchrotron sources. The midterm goal is to implement a new concept for the operation of BESSY II: the **BESSY Variable pulse-length Storage Ring** concept BESSY VSR. BESSY VSR is central to achieve HZB's strategic goal to be a scientific hub for developing methods, designing soft-X-ray instruments and pushing accelerator technologies for next generation sources. This will also in the long-term prepare for a future successor to BESSY II.

The concept of BESSY VSR finds the unanimous support of HZB's Scientific Advisory Council and the HZB Supervisory Board. The scientific case for BESSY VSR¹ has been conceived by HZB staff and further discussed and developed in a dedicated workshop with the international soft-X-ray user community in late 2013. The BESSY VSR concept and the scientific case in an updated version were presented to and discussed by the user community during a second workshop in early 2015. In the Helmholtz Association's POF evaluation in spring 2014, BESSY VSR was presented to the reviewers as it represents the mid-term upgrade to BESSY II. In addition the accelerator part of the BESSY VSR project was presented to the reviewers, due to its strong significance for future upgrades also of storage ring based light sources other than BESSY II. The reviewers judged BESSY VSR as of highest scientific interest to the accelerator physics community and being the ideal facility to address the future increasing demands to study sub-picosecond, picosecond and longer dynamics in complex systems, complementary to e.g. the E-XFEL facility. The reviewers thus put strong emphasis on encouraging HZB to go further with the

¹The BESSY VSR Scientific Case, as well as other relevant information on the project, is available at http://www.helmholtz-berlin.de/zentrum/zukunft/vsr/index_en.html

BESSY VSR project, developing a Technical Design Study. Within the accelerator community the BESSY VSR concept is seen as complementary to the development of diffraction limited synchrotron radiation sources and many laboratories, including SLAC (SPEAR III, PEP X proposal) and MAXLAB (compact MAX IV ring), are eagerly following the progress of the BESSY VSR project.

HZB has taken up this recommendation immediately after the POF review was finalized. In September 2014 an editorial team of HZB staff has been set-up with the goal of finalizing the Technical Design Study latest in March 2015. This timeline allows for an external review and expert feedback before HZB applies for funding BESSY VSR from the strategic investment funds of the Helmholtz-Association by end of June 2015.

With the present Technical Design Study, HZB will pave the way for BESSY VSR. This upgrade of BESSY II will provide unique possibilities for BESSY II users to choose the appropriate pulse structure for experiments requiring time resolution, in particular in the picosecond time range. BESSY VSR will provide new insights, for instance, into the function and the control of materials properties, into technologically relevant switching processes, chemical dynamics and kinetics. We are very much looking forward to the successful implementation of BESSY VSR for our user community!



A. Kaysser-Pyzalla *Th. Frederking*

Prof. Dr. Anke Kaysser-Pyzalla
Scientific Director

Thomas Frederking
Administrative Director

Contents

Foreword	v
1 Project Overview	1
1.1 Introduction	1
1.2 Scientific Goals	4
1.3 Major System Parameters and Basic Layout	6
1.4 International Context	16
1.5 Project Phases	20
1.6 Costs and Schedule	24
2 Beam Dynamics	29
2.1 Limits of Bunch Length and Intensity	30
2.2 Alternating Bunch Length Scheme	36
2.3 Bucket Fill Pattern	39
2.4 Touschek Lifetime	40
2.5 RF Jitter	43
2.6 Multi Bunch Effects	45
2.6.1 Coupled Bunch Instabilities	45
2.6.2 Transient Beam Loading	49
2.6.3 Robinson's Instability	51
2.7 Low α Optics	53
2.7.1 Low α Lattice	55
2.7.2 Bunch Length Limits	55
2.8 Transparent Operation of the SC Cavities	59
2.8.1 Fundamental Cavity Mode	59
2.8.2 Higher Order Cavity Modes	62
2.9 Beam Injection	64
2.9.1 Ramping of the SC Cavities	67
2.9.2 Short Bunches in the Booster Synchrotron	68
3 Superconducting RF Systems	73
3.1 SRF Parameters	75
3.2 Cavity Design	79
3.2.1 Mid-Cell Design	79

3.2.2	Five-Cell 1.5 GHz Cavity	81
3.2.3	Modal Spectrum, End-groups and HOM absorbers	83
3.2.4	Transparent operation	95
3.3	Cryomodule Design	97
3.3.1	Cryomodule Components for Preparatory Phase	98
3.3.2	Cryomodule Components for Final BESSY VSR Setup	100
3.4	Ancillary Components	100
3.5	RF Systems	105
3.5.1	RF Transmitters	105
3.5.2	RF Transmission Lines	106
3.5.3	RF System for the Booster Synchrotron	107
3.6	RF Control and LLRF, Microphonics	108
3.6.1	Combined LLRF-Cavity Beam Dynamics Simulations	115
3.6.2	A Generic LLRF System	121
4	Cryogenics	131
4.1	Cryogenic Loads	132
4.2	Cryogenic Plant	133
4.3	Cryogenic Transferlines	135
4.4	Cryogenics for Preparatory Phase	136
4.5	Warm Operation of SC Cavities	137
5	Machine Integration	139
5.1	Module Integration in Storage Ring	140
5.2	Vacuum System	140
5.3	Impedance Upgrade	143
5.4	Installations, Run-In, Dark Times, Precautions	151
5.4.1	Operation Constraints for Hardware Implementation	152
5.4.2	Installation, Commissioning in the Preparatory Phase	153
5.4.3	Installation, Commissioning of the Booster Synchrotron Cavity	154
5.4.4	Installation, Commissioning of Final BESSY VSR	154
5.4.5	Precautional Measures	155
6	Beam Diagnostics	157
6.1	Required Information	157
6.2	Diagnostic Beamline	157
6.2.1	General Setup	158
6.2.2	Bunch Length Diagnostics	160
6.2.3	Source Size Diagnostics	161
6.3	Digital Feedback System	162
7	Bunch Separation Schemes	167

7.1	Chopper Systems	167
7.2	Incoherent Excitation	170
7.3	Transverse Deflecting Structure	172
7.4	Resonance Island Buckets	177
8	Beamlines, Endstations and Experiments	183
8.1	Photon Beams	183
8.2	Timing and Synchronization	184
8.3	Endstations and Experiments	186
9	Radiation Protection Issues of BESSY VSR	189
9.1	Electron Loss Limitation	189
9.2	Life Time	190
9.3	Doses Prediction of Cavity Tests by FLUKA Calculations	191
9.4	Dose Measurements	192
9.5	Conclusion	193
10	Testing Equipment	195
11	Cost and Schedule	199
11.1	Costs	199
11.2	Schedule	199
12	Future Upgrade Options	203

1 Project Overview

1.1 Introduction

Synchrotron radiation sources have developed into highly sophisticated and reliable facilities that enable cutting-edge materials research which otherwise would not be possible. From a user perspective, the photon beam-parameters of interest are wavelength, flux, peak and average brilliance, coherence (longitudinal and transverse), and pulse length. Depending on the experiment being performed, the focus will lie on different parameters. For example, BESSY II users performing protein crystallography requires high-flux X-rays while the pulse length is of no concern. On the other hand, a large and growing fraction of BESSY's user community focuses on "functional materials" where dynamics in the picosecond and sub-picosecond range are essential, for example in magnetization dynamics for future information technologies.

At BESSY II, short pulses are provided during dedicated low α operation or with the femto-slicing facility, albeit at only a small fraction of the photon flux provided during standard operation. Other, flux-hungry users are then literally left in the dark so that low α operation must be limited to few weeks per year. Nevertheless, an extensive user community focusing on dynamics research in the VUV to soft-X-ray range has established itself at HZB and the demand for increased short pulse operation continuous to grow rapidly.

An important feature of future synchrotron sources will thus be the flexibility to tune the beam parameters to the various user needs, while ideally maintaining a high average flux. Since HZB's users are multifaceted this aspect will certainly be a key element of a next-generation facility to succeed BESSY II in the late 2020's. Several options exist and HZB is in the process of evaluating the merits of each. For example, HZB is constructing bERLinPro, a high-current ERL demonstration facility that is designed to evaluate the physics and technology as a suitable driver for flexible future light sources.

Even at present, HZB faces the challenge to significantly improve the flexibility of BESSY II to address the needs of its increasingly diverse user community. HZB

plans to perform a major upgrade by 2020 with superconducting RF cavities to provide high-flux and picosecond-pulse beams simultaneously. The world-wide unique feature of the BESSY Variable pulse length Storage Ring (BESSY VSR) will be the simultaneous operation of long (ca. 15 ps rms) and short (ca. 1.7 ps rms) pulses, both at high bunch current, while still providing the average beam brilliance and flux users have come to expect from 3rd generation facilities. The photon beam appropriate for the individual experiments can be selected by each user at will. Dedicated low α operation with 300 fs bunches or femtoslicing of high-charge picosecond bunches will even enable the study of femtosecond dynamics.

The concept of BESSY VSR was originally proposed in 2006 [1]. It relies crucially on 1.5 GHz CW superconducting RF (SRF) cavities to provide 80 times more longitudinal focusing than from the normal-conducting system in BESSY II. The bunches are compressed by roughly a factor of $\sqrt{80}$ into the low picosecond range. For some time the concept was considered technically doubtful: In particular, stable 300 mA operation is unfeasible with a beam whose spectral components extend into the 100 GHz range and many special short-bunch shifts with reduced current leave other users in the dark. In 2011 [2] a vital modification of the scheme was proposed. The installation of additional 1.75 GHz SRF cavities generates a beating of the voltages of the two SRF systems, thereby creating alternating buckets for long and short bunches. One may then store many long bunches to provide the standard high photon flux while only a few short-bunch buckets are populated with high charge for short-pulse experiments. Thus one bypasses the impedance and Touschek lifetime problems. Importantly, both short and long pulses are available at every beam line. Of course, users must then be able to select the appropriate photon pulses for their experiment—several schemes to do so have been identified.

Installation of the full BESSY VSR scheme and the start of user operation is planned for 2020. Here, it will be essential to guarantee rapid transition to the user operation which requires high risk issues to be retired well before 2020. These include the operation of L-Band multicell SRF cavities in a high-current storage ring that was not originally designed for such devices, the question of being able to “park” the SRF cavities making them transparent for the beam in case of a system failure and in general the question of beam dynamics/stability. Hence a preparatory phase has been defined which will culminate in the installation of a reduced number of cavities in the ring by 2018, operating at moderate voltage. This prototype phase should allow most of the technical risks to be addressed at that time and to provide feedback for the final system design.

Other options for short-pulse operation were also investigated. Argonne National Laboratory pioneered a powerful scheme based on bunch rotation by superconducting deflecting cavities (SPX). Such a setup is well suited for high-beam-energy facilities such as APS (7 GeV) whereas the BESSY VSR scheme would require the

installation of significantly more SRF voltage than in BESSY VSR. But the concept also requires the development of a whole new class of SRF cavities, adding significantly to the technical risk. Importantly, SPX only provides short pulses at limited number of beam lines and at reduced flux because only a fraction of each bunch contributes to the photon pulse. HZB thus came to the conclusion that BESSY VSR is better suited to BESSY II and its community than an SPX-type system.

The CW SRF system for BESSY VSR is technically very challenging. Fortunately, HZB is in a position to take advantage of the development currently underway for bERLinPro. Many concepts and much of the technology can be directly transferred to BESSY VSR, thereby shortening the development time. This parallel development is also an ideal fit for HZB's strategy in designing a successor to BESSY II. While BESSY VSR addresses the immediate needs of the user community, together with bERLinPro it also will provide invaluable insight in evaluating various options for HZB's next-generation light source, e.g., the integration of a BESSY VSR scheme in a diffraction-limited storage ring. As part of this strategy, BESSY VSR and bERLinPro will ensure that the necessary know how, personnel and SRF infrastructure will be in place at HZB to quickly transition to the BESSY III design & construction phase in the 2020's.

In pursuing BESSY VSR, HZB intentionally has chosen an upgrade path that differs from that of other facilities such as ESRF or ALS. Here plans call for the installation of a diffraction-limited storage ring (DLSR) using multi-bend achromats. DLSRs promise to reduce the beam emittance by nearly a factor of 100 and they provide full transverse X-ray coherence into the keV range—features that are essential to the ESRF user community. However, to maintain an acceptable beam life time, the bunches must intentionally be lengthened to several 10 ps to 100 ps. Such an operating mode runs contrary to the needs of many core BESSY II users. Beyond this, a DLSR upgrade requires a nearly complete revamp of the ring and is difficult to realize within a relatively small facility such as the BESSY II ring. The associated cost and installation time (dark time for users — minimum one years for ESRF) far exceeds that of the BESSY VSR proposal. While a BESSY VSR upgrade of high-energy rings such as APS, ESRF, Spring8 is not feasible because a much higher voltage must be installed (i.e., many straights used), BESSY II's low energy (1.7 GeV) allows the whole BESSY VSR system to fit in a single straight. HZB considers the BESSY VSR upgrade to be a complementary development to DLSRs that is the better choice for the BESSY II portfolio. It offers a cost effective and minimally invasive option for a major improvement of BESSY II with a far-reaching scientific impact.

1.2 Scientific Goals

With the novel BESSY VSR approach to create long and short photon pulses simultaneously for all beam lines, pulse-picking schemes will allow each individual user to freely switch between high average flux for X-ray spectroscopy, microscopy and scattering and picosecond pulses up to 250 MHz repetition rate for dynamic studies. Thus BESSY VSR preserves the present average brilliance of BESSY II and adds the new capability of user accessible picosecond pulses at high repetition rate. In addition, high intensities for THz radiation with intrinsic synchronization of THz and X-ray pulses can be extracted.

For the scientific challenges of quantum materials for energy, future information technologies and basic energy science BESSY VSR is the multi-user synchrotron radiation facility that allows with the flexible switching between high repetition rate for picosecond dynamics and high average brightness. This moves classical 3rd generation synchrotron radiation science from the observation of static properties and their quantum mechanical description towards the function and the control of materials properties, technologically relevant switching processes and chemical dynamics and kinetics on the picosecond time scale.

Scientific Drivers

BESSY VSR creates for the highly productive Synchrotron Radiation community a uniquely attractive multi user facility. In particular investigations on reversible dynamics and switching in molecular systems and materials are accessible in a non-destructive way. The investigations with X-ray beams from BESSY VSR are highly complementary and compatible to dynamic studies conducted by users with optical lasers at their home universities and laboratories. BESSY VSR also represents a missing link between the extreme average brilliance of ultimate storage rings like PETRA III and free electron lasers.

Science with BESSY VSR will excel to correlate chemical function with molecular dynamics on multidimensional potential energy surfaces and to determine principles underlying functional materials for reversible processes such as switching. The ability to determine through high quality synchrotron radiation spectroscopy, scattering and microscopy the geometric and electronic structure as well as the nanoscale composition is the first step to then create and investigate transient states and their picosecond dynamics that govern materials' function. For future information technologies, BESSY VSR is a key facility for the science and technology of efficient and reversible magnetic and all optical switching. X-ray probes in combination with picosecond dynamics will elucidate phonon and magnon driven

processes, precessional magnetization dynamics, resistive switching dynamics, and the switching of nanostructures relevant for information storage. In a more general way, phase transitions determine materials functionality and BESSY VSR will allow for the observation and the control of phases far from equilibrium in order to answer the key questions of “What is the most efficient way to control properties?” And “How fast can properties be changed, and how stable are the states?” Reversible switching extends far beyond the solid state toward molecular switches through e.g. isomerisation, tautomerisation or spin-cross over excitations that are the basis of molecular electronics. Here both X-ray probes and IR/ THz pulses from BESSY VSR uniquely enable THz-EPR experiments with picosecond time resolution to reveal the structure-dynamic-function relationship of functional molecular systems.

In basic energy science BESSY VSR will address challenges in photochemistry, photosynthesis, photovoltaics, catalysis and the basic reaction steps underlying solar fuels. Understanding and controlling photochemistry, i.e., the correlated motion of electrons and nuclei holds the key in controlling the reaction kinetics and motivates the need for information on photoexcited electronic and structural changes in molecular systems. Following the structural dynamics and the valence charge density in ground and excited transient states with time-resolved X-ray spectroscopy at BESSY VSR uniquely addresses fundamentals of charge-transfer reactions in metalloenzymes, photo-triggered proton-transfer reactions and nonequilibrium processes in hydrogen-bonded systems. For photosynthesis, the key process for oxygen regeneration on earth by photosynthetic water oxidation, BESSY VSR will enable explaining the reaction kinetics resulting from the dynamic pathways of the photosystem II membrane protein complex *in vivo* in solution by X-ray spectroscopic characterization of the catalytic reaction center on nano- and millisecond time scales. In photovoltaics, time-resolved X-ray spectroscopy will reveal the coupling of charge carrier dynamics and interface properties, a key in understanding and controlling the efficiency of photovoltaic devices. For catalysis in general, time-resolved soft X-ray spectroscopy at BESSY VSR will be used to address the pathways that govern chemical rate and selectivity in heterogeneous catalysis and surface chemistry. The catalyst or the adsorbate will be driven through external stimuli and the interplay between femtosecond charge transfer, local coordination and the electronic or vibrational excitations present in the system will be probed to pave the way towards insight-driven design of future catalysts with applications to solar fuels, clean combustion and green chemistry. For solar fuels, finally, photoelectrochemistry will be used to combine photovoltaic and electrocatalytic functionalities within a single material or composite. BESSY VSR will be used to probe the generation, recombination and charge-transfer dynamics and charge-carrier lifetimes in solar fuel materials. In addition, BESSY VSR will allow addressing the time scales and energy losses associated with charge transfer across semiconductor-

catalyst interfaces to elucidate the complex four-electron proton-coupled electron transfer process in water oxidation in solar fuel devices.

1.3 Major System Parameters and Basic Layout

To address the increasing request for time resolved measurements, BESSY VSR presents an innovative new scheme of longitudinal bunch length manipulation. This scheme allows to generate simultaneously 15 ps and 1.7 ps (rms-values)¹ long photon pulses in the BESSY II user optics, emitted by long and short electron bunches of corresponding lengths. These pulses are supplied to all dipole, undulator and wiggler beamlines. The overall current of 300 mA, mostly stored in the long pulses, ensures a continuation of the present user mode with high average brilliance including the full operation of all undulators, wigglers, superconducting wavelength shifter and the TopUp operation. In addition, the short pulses offer new possibilities for time resolved X-ray and THz measurements.

The alternating bunch length schema is proposed, to avoid impedance heating effects of the machine and to limit the Touschek loss rate. Both effects are strongly dependent on the total currents in the short bunches and these are only a smaller fraction compared to the current in the long bunches.

This new operating mode is achieved by installing longitudinally focusing superconducting (SC) radio frequency (RF) cavity systems of 1.5 GHz and 1.75 GHz in addition to the normal conducting (NC) 0.5 GHz RF system into one of the low β straights of the BESSY II ring, as sketched in Figure 1.1.

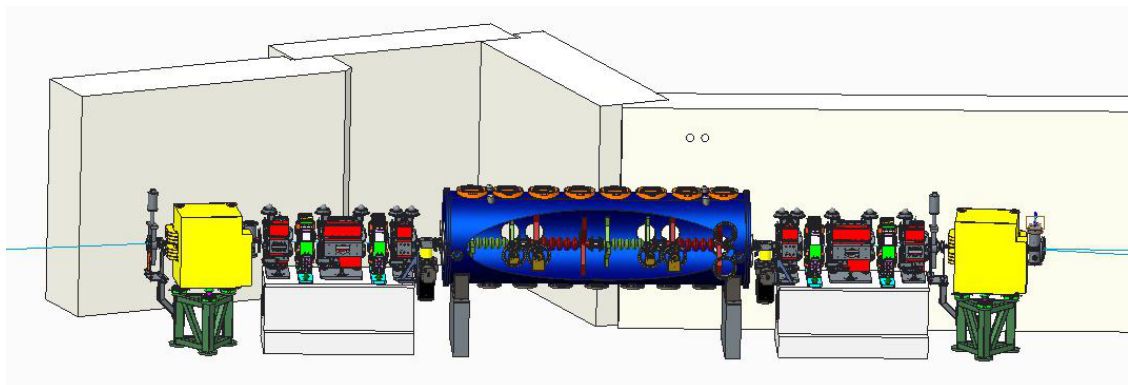


Figure 1.1: Schematic view of the BESSY VSR cavities straight.

¹If not stated differently, always rms-values are used.

The two different frequencies cause a beating of the voltage creating fixed points where the voltages add and others where they cancel. Short bunches are located at the high-voltage gradient points and long bunches at the cancellation points. An enhancement of the longitudinal, temporal focusing gradient, proportional to the voltage gradient $V' = dV/dt$, by a factor of 80 compared to the present 0.5 GHz cavities is achieved. The transverse beam optics and emittance remains unchanged, the longitudinal focusing acts only on the length of the bunches. Methods to separate long and short photon pulses are available, so that users can select the different pulses at will.

BESSY VSR addresses several innovative topics of storage ring operation, specifically:

- the alternating bunch length scheme generated by voltage beating,
- the continuous wave (CW) operation of SC multi-cell cavities at high currents of 300 mA in a storage ring,
- very short bunches of high currents in synchrotron radiation equilibrium in the BESSY VSR user and low α optics:
 - bunches of 1.7 ps length of up to 0.8 mA (0.64 nC)
 - bunches of 0.3 ps length and currents of 0.04 mA (0.03 nC).

For an overview of relevant BESSY II parameters see Table 1.1.

Beam Current Limit of Short Bunches

The promise of BESSY VSR lies in a significantly higher short-bunch current than is presently feasible in the low α mode. Above a critical, bunch length dependent “threshold current”, described by the “microwave” or “bursting” instability, bunches become unstable but are not lost, see Section 2.1. These unstable bunches emit bursts of coherent synchrotron radiation (CSR) in the THz range. These threshold currents are used as a figure of merit for the upper limit for the various bunch lengths. This is a single bunch effect, most likely not affected by other bunches. The threshold currents for the different optics modes and bunch lengths are summarized in Table 1.2.

There are two possible ways to produce short bunches: first, reducing the value of the “momentum compaction factor” α or, second, increasing the focusing gradient V' , by applying the relation of the bunch length $\sigma_z \propto \sqrt{\alpha/V'}$. The relation between the threshold current and the related bunch length can be described by a scaling law. Within the validity of this law the threshold current for a fixed bunch length

Table 1.1: Overview of relevant BESSY II parameters.

Parameter	Value
Energy E	1.7 GeV
Emittance ϵ	5 nm rad
Coupling	2 %
Beam optics, DBA cells	2×8
Circumference	240 m
Max. beam current I	300 mA
Harmonic number h	400
RF frequency f_{rf}	500 MHz
RF sum voltage V_{rf} at 500 MHz	1.5 MV
Landau cavities frequency	1.5 GHz
Landau cavities sum voltage	0.225 MV
Revolution frequency f_{rev}	1.25 MHz
Momentum compaction factor α	7.3×10^{-4}
Relative natural energy spread, rms δ_0	7×10^{-4}
Transversal tunes Q_x, Q_y	17.85, 6.74
Synchrotron frequency f_s	7.6 kHz *
Longitudinal radiation damping time τ_z	8 ms
Transverse radiation damping time $\tau_{x,y}$	16 ms

* without Landau cavities

is proportional to α . If V' is increased, α must increase by the same factor to maintain a fixed bunch length. The benefit in doing so lies in the fact that the threshold current increases by the same factor. For BESSY VSR with an 80 times stronger focusing compared to BESSY II we expect to store 80 times more current in short bunches, Figure 1.2. Note however that in the ps-bunch length range the simple scaling could deviate from this law; this is discussed in Section 2.1.

Ultra Short Bunches - Low α Optics

The SC cavity fields of the π -TM₀₁₀ mode have only minor effects on the transverse beam optics parameters such as beta functions, natural emittance and energy spread. The transverse optics of the present BESSY II user and low α optics is not affected by the BESSY VSR scheme and it can be also applied to the well

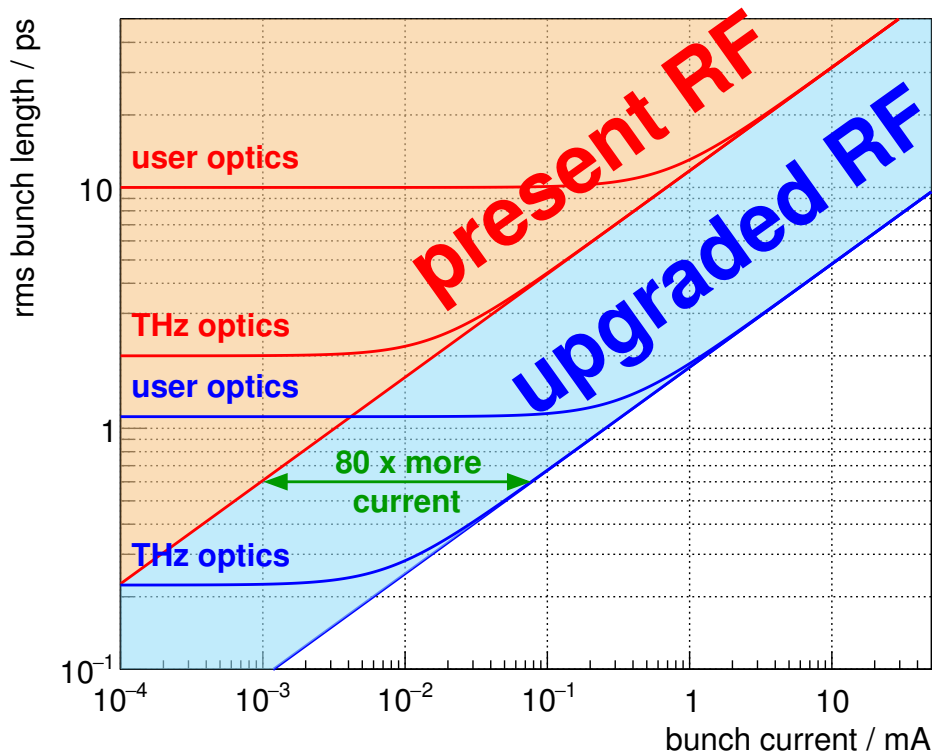


Figure 1.2: Schematic bunch length current relation of BESSY II shown by the red line and for the short bunches of BESSY VSR with the upgraded RF focusing by the blue line.

established BESSY II low α optics, Section 2.7. There are again alternating long and short bunches, up to 150 bunches of 3ps length with a current per bunch of 0.045 mA and 150 bunches of 300 fs length with 0.04 mA. This low α optics will be operated with about 15 mA beam current, 20 times less compared to the user optics. Therefore, this BESSY VSR operation mode has a small Touschek loss rate and is very stable with respect to the later discussed high current instabilities.

Bunch Lengths and Currents

A summary of the expected bunch lengths and bunch currents is given in Table 1.2. For the bunches the values are the expected single bunch stability limits with respect to the bursting instability, see Section 2.1. The zero current bunch lengths σ_0 are modified by the potential well effect by up to a factor 1.5 to achieve the presented bunch length values σ_z , see discussion in Section 2.1.

Table 1.2: Bunch lengths and bunch threshold currents for the standard user and low α optics of BESSY VSR.

	Bunch length σ_z/ps	Threshold current I_{th}/mA
Standard optics		
long bunch	15	1.8
short bunch	1.7	0.8
Low α optics		
long bunch	3	0.045
short bunch	0.3	0.04

Photon Beam Parameter

It is the goal that BESSY VSR preserves the average brilliance of BESSY II undulators as illustrated by Table 1.3. As an example, the maximum brilliance values of the UE49 are given and compared to predicted values of BESSY VSR according to the extended fill pattern of Figure 2.6, which also includes 150 short bunches of 1.1 ps length.

Table 1.3 shows that the peak brilliance of almost all bunches in the fill is of the order of 10^{22} , meaning that any time resolved application at BESSY VSR can be performed always at the same peak brilliance regardless of the different repetition rates.

When approaching very short bunches by combining BESSY VSR and the low α mode, losses in brilliance due to increased emittance are partly compensated by upcoming in-vacuum undulators, like UE30, which will deliver up to an order of magnitude higher brilliance than the existing conventional undulators in BESSY II.

Bunch Fill Pattern

The beam current is limited by radiation safety requirements to 300 mA. Two bunch trains of 300 ns each are chosen for the bunch fill pattern, separated by two 100 ns long gaps, see Section 2.3. In the example of Figure 1.3 the bunch trains contain 150 long bunches of 1.8 mA each. For explicit time dependent measurements there are additionally three short hybrid bunches inside the bunch trains for laser slicing experiments and a short and a long bunch in the filling gap for time resolved

Table 1.3: Photon beam properties of BESSY VSR compared to different modes of BESSY II. Brilliance values refer to the UE49 undulator in planar mode at the BESSY II design emittance of 5 nm rad and 2% coupling.

Facility	Peak brilliance ph/s/mrad ² /mm ² /0.1 %BW	Average brilliance (multi bunch curr.)	Number of bunches	Pulse duration ps (rms)
BESSY II				
standard	6.1e21	4e19 (300 mA)	350	15
low α	1.9e20	2.5e17 (15 mA)	350	3
BESSY VSR				
total	varying	4e19 (300 mA)	varying	varying
std. long pulses	1.2e22	3.3e19 (248 mA)	150	15
std. short pulses	1.7e22	3.6e18 (27 mA)	150	1.1
long camshaft	3.95e22	1.3e18 (10 mA)	1	27
short camshaft	5.1e22	1e17 (0.8 mA)	1	1.7
low α	2.2e21	1.2e17 (7.5 mA)	150	0.3

measurements. The length of the gap is demanded by the mechanical chopper, as discussed in Section 7.1, which separates photons of the single bunch of 1.25 MHz repetition rate, suppressing all other X-ray pulses. By applying a different method, the resonant bunch excitation, see Section 7.2, any chosen bunch can be excited and the emitted X-ray pulses will be separated from the core beam spatially. Further concepts for bunch separation are discussed in Sections 7.3 and 7.4. There is a variant of this fill pattern, see Section 2.3, where additionally 150 short pulses of 1.1 ps length are populated for production of intense THz radiation and further time resolved measurements.

Technical Realization

The key elements of BESSY VSR are SC cavities, cooled down to 1.8 K and operating at two different frequencies, to shape the longitudinal phase space, see Section 2.2. One set of the cavities operates at a frequency of 1.5 GHz and 20 MV voltage amplitude and one at 1.75 GHz and 17.1 MV. These frequencies produce a beating of the RF voltage and modulate the RF focusing, depending on the bucket

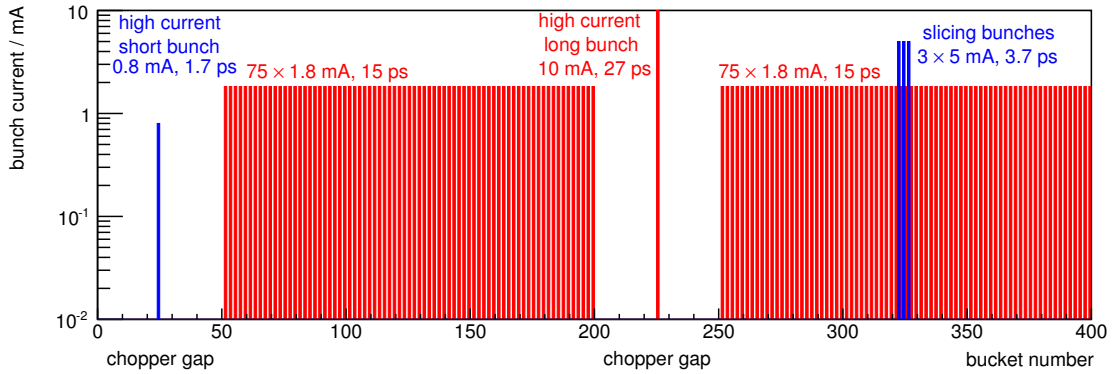


Figure 1.3: Example of bunch fill pattern with long and short pulses. There are 400 buckets with 2 ns spacing and a revolution time of 800 ns.

position. There are still 400 buckets, but divided into two different groups, located 2 ns apart in the fill pattern. At the odd numbered positions, where the voltage gradients cancel exactly, 15 ps long electron bunches are generated. At the even bucket position, the voltage gradients add up and generate a strong, longitudinal bunch focusing, resulting in 1.7 ps short electron bunches, Figure 1.4. The longitudinal RF focusing by the SC cavities at BESSY II is very efficient because of the moderate beam energy of 1.7 GeV.

This alternating bunch length scheme for BESSY VSR was proposed [2], compared to an earlier suggestion of only short bunches [1], to avoid impedance heating effects by the beam and to relax the Touschek life time. In the BESSY VSR scheme, most of the beam is stored in long bunches of 250 MHz repetition rate, nearly similar to the present BESSY II operation of 500 MHz repetition rate.

The SC cavities are only used for bunch focusing; no source power is extracted by the beam. Only a relatively small external RF power supply is required to control the cavities, which simplifies the technical realization. The energy lost by synchrotron radiation is recovered from the present 0.5 GHz cavities. An extended vacuum section of the ring must be specially prepared to provide the cleanliness and vacuum conditions required by the SRF system, Chapter 5. Two 1.5 GHz cavities and two 1.75 GHz cavities, see Table 1.4 will be placed into one cryomodule that fits into one straight of BESSY II. A second cryomodule will be assembled as spare unit. An dedicated diagnostic beamline is installed to monitor and analyze beam parameters, see Chapter 6, including streak camera, electronics diagnostics and THz monitors.

BESSY VSR will not lead to a drastic change in beam size as expected, e.g., for diffraction limited light sources. Most of the beam current is stored in the long

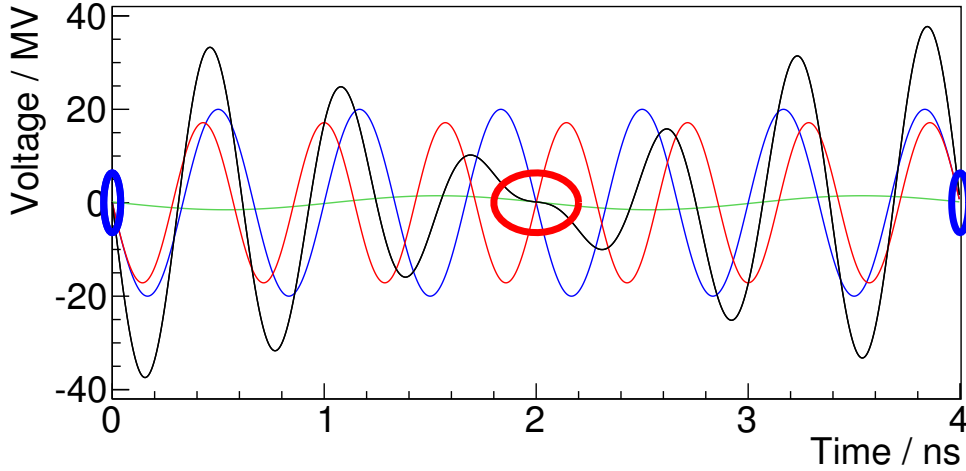


Figure 1.4: Example of bunch fill pattern with long and short pulses, indicated by the ellipses. The colored sinusoidal oscillations represent the individual voltages, green 500 MHz, blue 1.5 GHz, red 1.75 GHz. The black line shows the resulting sum voltage, which defines bucket sizes and locations.

Table 1.4: Cavity systems for BESSY VSR.

Cavity	Frequency f/GHz	Integrated voltage V/MV	Number of cavities
NC	0.5	1.5	4
SC ₁	1.5	20	2 × 5 cells
SC ₂	1.75	17.14	2 × 5 cells

bunches, which are comparable in size to the present BESSY II bunches, but with twice as much current. Since the upgrade to BESSY VSR will not lead to a strongly increased loss rate of electrons, no special change in the radiation protection concept is required, see Chapter 9. The loss rate, if required, can be further controlled by a vertical transverse noise excitation of the beam, as presently applied for the BESSY II TopUp operation.

Beam Cavity Interactions

A major challenge concerning the operation of SC multi-cell cavities in a high current storage ring is the beam stability. Higher order modes (HOMs) are excited

in the cavity and could destabilize the beam. However, the calculations presented in Section 2.6 conclude that the presented cavity design in combination with active feedback systems, which may need to be upgraded, suppresses the multi bunch instability in all desired operation modes. The recent HZB design of the 1.5 GHz cavity, shows a strongly damped HOM spectrum which relaxes the constraints for the feedback systems, see Figures 2.10 and 2.11 and Section 3.2. The beam interaction with the fundamental cavity π -TM₀₁₀ mode, the “Robinson effect”, is controlled by the low-level RF electronics, see Sections 2.6.3 and 3.6.

Parking of the cavities, i.e., making them transparent to the beam, is required in case of problems arising during operation of the system. Even when the SC cavity is maximum detuned in the cold state, the beam still induces a voltage in the order of 0.3 MV, and 3 times less if it is warmed up. But because there are two equal cavities of each type, they can be detuned in such a way, that the fundamental accelerating modes compensate each other, thus not affecting the beam, see Section 2.8.

Transient Beam Loading

The bunch pattern excites a periodic beam loading in the cavities. The gap in the bunch fill pattern causes a particular strong transient, Section 2.6.2. This leads to a modulation of the focusing strength and the bunch phase position along the filling. Bunches pass the cavities at different phases of the voltage. For the short bunches, where the SC cavity voltages add up, this has only a minor effect. But for the long bunches, the exact canceling of the two strong RF voltage amplitudes becomes disturbed. The phase position of the long bunch centers varies continuously from -40 ps to 40 ps along the bunch train. Additionally, the focusing of the long bunches is modulated in a similar way; the synchrotron frequencies could vary by about 30 %. The overall result is that the long bunches on average are stronger focused than expected, which leads to shorter bunches and enhanced Touscheck loss rate. For averaging times longer than the revolution period, the phase and amplitude of the SC cavity voltages stay constant.

Cavity RF Design

The higher harmonics frequencies chosen are a compromise between required high gradient for longitudinal focusing, the limited available real estate space and limits imposed by the BCS theory for RF superconductivity favoring lower frequencies as this results in lower surface resistance. Also, a larger diameter structure is less prone to any wake field driven instability of the beam. The chosen harmonics of 1.5 GHz and 1.75 GHz are well within the range of current operating SRF cavities.

A five-cell design, see Figure 1.5 was chosen as a reasonable compromise between conflicting requirements to maximize HOM damping while minimizing the installation length and operating field. Heavy HOM damping is achieved by waveguide couplers originally developed at the Thomas Jefferson Laboratory (JLab) [3]. Detailed cavity end-group studies have been performed that resulted in an enlarged beam tube design for the 1.5 GHz cavity. The HOM spectrum was used as basis for beam stability calculations. The design for the 1.75 GHz system will be based on the 1.5 GHz design.

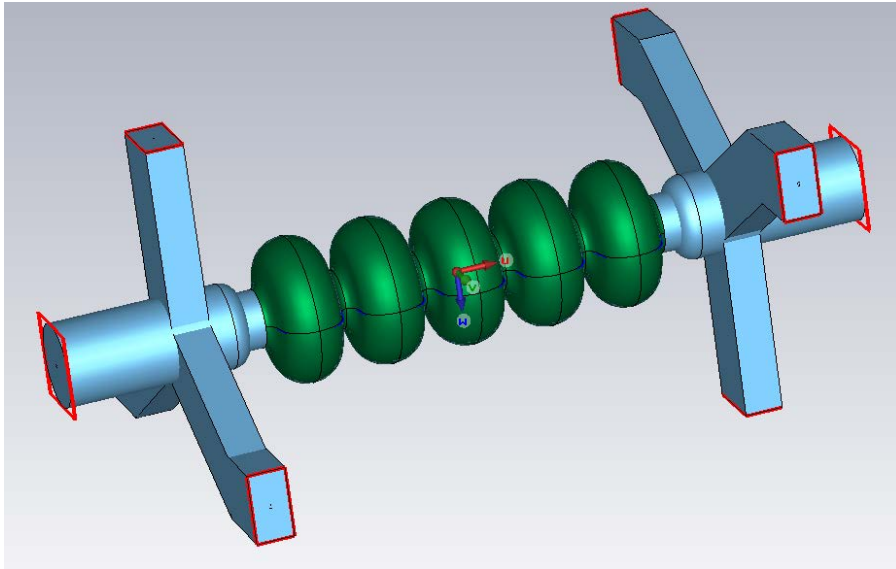


Figure 1.5: Five cells 1.5 GHz cavity design with end-groups attached.

Cavity Control and Operation

Another aspect of BESSY VSR is given by the required high reliability and stability of operating the cavities as they have to support a 24/7 running user facility. One challenge is given by the rather high CW field level of about 20 MV/m at a high loaded quality factor Q_L to allow operation at power levels within the 10 kW range. The latter is of importance, as this is a power range where reliable coupler designs are available and also the cost for RF transmitters can be kept within acceptable limits.

Operating SRF cavities at high Q_L , thus narrow bandwidth necessitates a precise tuning and therefore compensation of microphonics and coupled Lorentz-force detuning driven instabilities. Precise regulation of CW driven RF fields at high loaded Q was already demonstrated and CW field levels of 20 MV/m are within

reach [3, 4]. Nonetheless, routinely CW detuning compensation still needs to be demonstrated.

Beam loading is a second major challenge the SRF system faces. As the cavities are operated in zero-crossing of the RF field with respect to the beam, they experience strong reactive beam loading leading to a phase shift of the field. This will be compensated by proper detuning in the kHz range, so that only the power to maintain the cavity field and some compensation for unwanted detuning is required.

Finally, given the high impedance of the SRF system and the high current stored in the ring, special attention must be paid to DC and AC Robinson instabilities [5], see Sections 2.6.3 and 3.6. In the BESSY VSR concept, the 1.75 GHz frequency system is intrinsically operated in the Robinson unstable regime. However, the combined system of all frequencies is stable again, but it needs to be studied how robust this combined system is to any perturbation. To some extent, this effect can be controlled by high gain amplitude and phase control, reducing any deviation to a minimum, so that any rise towards this instability is suppressed.

Injection into Short Buckets

Presently, bunches extracted from the booster are typically 60 ps long, too long to maintain a $\geq 90\%$ injection efficiency demanded by radiation safety. For efficient TopUp injection into the short buckets a bunch compression in the booster by a factor of 6 is necessary. This can be achieved by improving the low α lattice of the booster and/or by installing additional cavities, i.e., 3 GHz cavities of 4 MV, for shortening the booster bunches. These cavities need to be redesigned, based on existing cavities of the Institute for Nuclear Physics of the University of Mainz (Germany). The other option, to ramp down the BESSY VSR SC cavities to low fields just for TopUp injection into the short buckets seems not to be feasible. High fields are induced in the SC cavities by the beam and there is no sufficiently fast detuning possible to drive the fields to zero.

With the low current in the low α optics the situation is different. The beam has a very low Touschek loss rate and operation in decay mode is possible. The injection can be done by slowly ramping the SC cavities to zero fields or even a fast ramping could be possible, because of the low current.

1.4 International Context

Over the last decades third generation light sources have evolved considerably. Petra III has reached a record emittance of 1 nm rad with an energy of 6 GeV thanks

to the large circumference of 2.3 km [6]. Most recently NSLS-II went into operation and should achieve an emittance of 0.5 nm rad once all damping wigglers are in place [7]. Modern synchrotron light source projects, like MAX IV in Sweden or SIRIUS in Brazil, take advantage of innovative accelerator technologies in order to lower the beam emittances by an additional factor of 2 to 3 down to the 0.2 nm rad-level. New computing techniques are available to model the complex beam dynamics and optimize the magnet parameters for maximum dynamic apertures. The resulting high field strength leads to a small bore radius of the magnets and therefore to small vacuum chamber cross sections which require distributed pumping by NEG coatings. Today the accelerator community has the ability to build these very compact magnet lattices and fulfill the tight alignment tolerances, including non-linear elements like sextupole and octupole magnets. The improved emittance will increase the brilliance of the source by orders of magnitude. The emittance can be so small that the radiation from these sources reaches the diffraction limit, $\epsilon \lesssim \frac{\lambda}{4\pi} \dots \frac{\lambda}{2\pi}$, up to a few keV, with a much higher degree of transverse coherence of the emitted radiation [8].

Nowadays, many of the existing light sources plan to develop into this direction and reduce the emittance by changing their current magnet lattice configuration into the more compact multi-bend achromat lattice (MBA) [9]. The increased number of bending magnets is the key to achieve smaller emittance. The higher degree of coherence and the increased brilliance of the radiation are the driving forces from the user's point of view. Examples are the major upgrades planned at the high energy rings ESRF, APS and Spring8 as well as projects, for example at the ALS, to reach an extremely small natural emittance on the order of only ~ 50 pm rad with a nine-bend achromat [10]. Elettra proposes an upgrade with an emittance of 300 pm rad [11]. The drawback of bunches approaching the diffraction limit is the large bunch length needed to reduce the electron density in order to reach decent Touschek life time and avoid beam blow-up due to the strong intra-beam scattering. This can be achieved by using either much lower RF frequencies (MAX-IV uses a 100 MHz RF system instead of the more common 350 MHz to 500 MHz systems) and bunch lengthening utilizing higher harmonic cavities (NSLS-II and other light sources, among them BESSY II). In many projects the emittance is further reduced by including damping wigglers in the lattice. Their radiation will increase the natural energy spread of the electron beam which also leads to bunch lengthening and a corresponding lowering of the particle density within the bunch.

The HZB has opted to not follow this upgrade path for several reasons. From the very beginning the BESSY II lattice was very densely packed with magnets and at the time of its construction it offered the largest ratio of straight section length to circumference of all existing light sources. In order to maintain the circumference and the footprint of the beamlines as well as the energy of the ring at least a five-bend achromat would be required for the reduction of the emittance by only

one order of magnitude [12]. The modification would not only be expensive but would also lead to a dark time of at least one year. Additionally it would reduce the available length of the straight sections similar to the upgrade plan at the ESRF [13].

On the other hand, the light sources BESSY I and BESSY II have always supported time resolved experiments by offering operation in the single bunch mode. With the request for even shorter light pulses laser-slicing was introduced [14] and for the first time 100 fs-long light pulses (FWHM) from an APPLE-II undulator were offered to the user community during normal routine operation [15]. Over the years the slicing facility was constantly improved and today, with the increased photon flux per pulse, serves a growing user community [16]. At the same time, the short bunch length mode based on a low α lattice configuration was developed and put into operation at BESSY II [17] for the first time. This mode delivers bunches which are 3 ps long and which are used for time resolved experiments and for experiments requiring coherent radiation in the THz-region. BESSY II is operated for two weeks in short bunch low α mode and during additional four weeks in single bunch mode each year. With the introduction of the angular resolved TOF (time of flight) set-up, ARTOF, the interest in the single bunch, short pulse mode operation has increased even further.

HZB therefore is convinced that an MBA - low emittance upgrade is unsuited for the wide portfolio of dynamic and THz experiments performed at BESSY II. Rather HZB believes that the users are better served by upgrading the facility towards the production of shorter light pulses with repetition rates up to the MHz-range while keeping the emittance, brilliance, and flux at the level of today. Such a facility would be complementary to the diffraction limited storage rings (DLSR).

BESSY VSR is only one of the possible paths to shorter and intense light pulses. Other proposals are limited to either low intensity, low repetition rate, availability at only few beamlines or all of those together. BESSY VSR promises to provide short bunches with full intensity and at a high rate to all beamlines on demand, and in parallel to the 'usual' user operation.

Short bunches in the low α mode suffer from a very low threshold for the single bunch longitudinal instability driven by the interaction with the coherent radiation emitted by the bunch in the metallic surrounding of the dipole vacuum chamber. More on this subject can be found in Chapter 2. Therefore, the low α mode is best suited for producing many short, but low intensity bunches creating coherent THz-synchrotron radiation and less suited if short and high intensity pulses are requested for time resolved experiments with MHz-repetition. Nevertheless, short bunches by operating in low α mode has become an attractive feature of many other light sources and is offered to users on a more or less regular basis at ANKA, BESSY II, CLS, Diamond, MLS, Soleil, SPEAR3, and others.

Laser slicing produces light pulses as short as 100 fs (FWHM), however, since only a small fraction of the electrons inside the bunch are contributing to the radiation, the intensity is very low and the repetition rate is limited by the available average laser power. Short pulses of radiation produced by laser slicing will be available at the Swiss light source until the Swiss FEL becomes operational and in the future at Soleil where the slicing set-up is in the commissioning phase [18]. Like the short bunches produced in the low α mode laser sliced bunches can radiate all around the circumference of the storage ring. In principle many beamlines can take advantage of the short pulses which for the laser slicing tend to become longer the larger the distance between the beamline and the location of the laser interaction.

Another technique to create short pulses on many beamlines and experiments along the circumference of the storage ring would be the injection of short bunches as can be delivered by a full energy injection LINAC [19]. Only a few light source facilities have or potentially could use such an injector. Spring8 could employ the SACLA LINAC or MAX-IV could utilize their injector LINAC. At SLAC part of the existing infrastructure could be used for this purpose and detailed studies for injecting short bunches into the SPEAR3 ring have been performed [20]. LINACs tuned to be useful for FELs deliver the desired bunch characteristics: short length with sufficient charge of ~ 300 pC and small transverse emittance leading to very brilliant light pulses in the ring. Bunches have to be injected on-axis and are useful for up to 10 turns. With increasing number of turns the beam quality deteriorates quickly through the microwave instability due to the coherent synchrotron radiation, the same instability mechanism that limits the single bunch current in the low α mode. With LINAC repetition rates of up to 100 Hz the overall pulse rate is far from the desired MHz-region and rather similar to what is available by laser slicing. CW LINACs to allow for higher injection rates would be very expensive to build and operate and dumping the spoiled bunches puts high demands on radiation protection.

Producing shorter light pulses down to the ps-range (FWHM) with deflecting cavities [21] seems to be a more promising approach. The deflecting cavity produces a vertical kick which varies along the length of the bunch. After the interaction the bunch develops a vertical offset - time correlation in the insertion device, which can be used to produce light pulses down to the ps-region either behind a horizontal slit or with the help of suitably cut crystals. This reduces the intensity in the light pulse to the percent level of the total intensity the bunch could deliver. The repetition rates can be high. A second deflecting cavity has to take out the correlation further downstream. This allows only some beamlines between the two cavities to take advantage of the short pulses. The approach has been studied extensively for an earlier upgrade plan at the APS [22] and an attractive science case was developed. Over the years a very promising SC transverse deflecting cavity was designed and built [23] achieving a kick voltage of more than 2 MV. However, the project

had been terminated and was replaced by an emittance upgrade project similar to the ESRF [24].

BESSY VSR overcomes the deficiencies of the approaches mentioned above. It thus supports a multi-user facility for high-flux time resolved experiments and complements DLSRs, in their quest for lowest emittance, very nicely. This upgrade project is better suited for the BESSY II user community than an emittance upgrade of the existing ring. BESSY VSR represents an ideal testbed for the concept and, given its success, may be a strong candidate for implementation in future DLSRs for a combination of low emittance and short bunch operation.

1.5 Project Phases

The realization of the BESSY VSR concept will be subdivided into two project phases:

1. A preparatory phase and
2. The final BESSY VSR phase,

to guarantee a straightforward and smooth implementation of the SC cavities into the BESSY II ring with the objectives of minimal dark time and first user operation in 2020. The separation in two phases aims at decoupling the costly and time consuming infrastructure installations, from studies needed to finalize the beam dynamics issues, and to validate the design of the new superconducting RF system, i.e., cavities with couplers and cryomodule.

In order to establish full BESSY VSR operation, a new cryo plant (L700) is needed for cooling down the cavities to a temperature level of 1.8 K. To avoid time consuming purchase and setup of the cryogenic system, the preparatory phase will be realized using the existing cryogenic infrastructure of BESSY II. By applying only moderate modification to the available cryo system, the existing Linde TCF50 helium liquefier can be used for a proof of principle installation consisting of two 1.5 GHz cavities operating at 4.4 K. The cryogenics needed for BESSY VSR and the modifications for the preparatory phase are discussed in detail in Chapter 4 and Section 4.4.

Table 1.5 lists new hardware required for both phases and indicates components which will be reused from the preparatory phase in full BESSY VSR.

The nonrecoverable investment costs for the preliminary phase amount only some percent of the full BESSY VSR investment, mainly for adapting the existing cryogenic system, while the remainder flows into the final phase. Costs and schedule

Table 1.5: Hardware for the two project phases. Most of the hardware of the preparatory phase will be reused for the final BESSY VSR setup (indicated by arrow \rightarrow).

Preparatory phase		Final BESSY VSR phase
1 cryomodule	\rightarrow	1 cryomodule + 1 spare
3 cavities + 1 spare	\rightarrow	5 cavities + 5 spare
2 transmitters	\rightarrow	4 transmitters + 2 spare
Diagnostics beamline	\rightarrow	Diagnostics beamline
BESSY II cryogenics (4.4 K)		1.8 K cryo system
		Upgrade feedback-system
		Upgrade vacuum components
Partial booster upgrade	\rightarrow	Final booster upgrade

for the BESSY VSR project are summarized in Section 1.6 and discussed in detail in Chapter 11.

Preparatory Phase

The main objective of the preparatory phase is an early evaluation of the new SRF components with stored beam. It has already been launched in 2014 and aims for an installation of one prototype cryomodule hosting two 1.5 GHz cavities in BESSY II in 2018. This will allow to investigate the interaction of the stored beam with SC multi-cell cavities in CW operation. But already now studies and measurements have been conducted and will be continued at the MLS and BESSY II preparing for BESSY VSR, for example, studies of bursting thresholds, beam based damping of CBIs, beam loading, fill pattern, and injection studies. The preparatory phase also includes a partial upgrade of the booster synchrotron improving the injection into short buckets, see Chapter 2.9. The following list summarizes the project goals to be achieved in the preparatory phase with the installed prototype cryomodule.

From the perspective of the **SC RF system**:

- Design and production of two 1.5 GHz cavities with power and HOM couplers.
- Design and assembly of one prototype cryomodule equipped with two 1.5 GHz cavities.
- Development of a 1.75 GHz cavity design.
- Purchase and testing of solid state transmitters, LLRF and waveguide system.

- Modification of the existing BESSY II cryogenic system based on the TCF50 liquefier.
- Machine integration of the prototype cryomodule equipped with two cavities in BESSY II and operation at 4.4 K.

From the perspective of **beam dynamics**:

- Verification of transparent operation of the cavities when necessary.
- Phase and amplitude stability studies under full operation and the synchronization of the NC and the SC cavities.
- Storage of 300 mA in BESSY II with respect to CBIs conserving the emittance and the TopUp capabilities.
- Studying beam loading in the cavity system and consequences on bunch length and Robinson instability.
- Injection into short buckets, which needs a partial upgrade of the booster synchrotron.
- Setup up and commissioning of diagnostic beamline for short bunches.
- Tracking down and eliminate remaining noise sources.

In contrast to the full BESSY VSR installation with one cryomodule hosting four cavities, the preparatory phase is reduced to two 1.5 GHz cavities. Contrary to the scheme with two different frequencies there will be no alternation in the bunch length anymore. Although the two 1.5 GHz cavities will act as classical, active, 3rd harmonic Landau cavities allowing for bunch lengthening or shortening of all bunches, the CW operation of the multi-cell SRF cavities with high stored current of 300 mA is an important step for the project.

The SC cavities, designed to operate at 1.8 K will be cooled to 4.4 K using the existing TCF50 helium liquefier, providing a cooling capacity of 120 W. However, losses on cryolines and other components will reduce the power to ≈ 80 W, i.e., 40 W for each cavity, see Section 4.4. Due to the increased temperature, the quality factor is only $Q_0 = 1.5 \times 10^8$, decreasing the accelerating field to 3.6 MV/m to remain in the cryogenic budget. The cavity voltage seen by the beam is then 3.6 MV for a setup with two 1.5 GHz cavities. The total RF gradient will be increased by a factor of 8.1 compared to BESSY II, reducing the effective bunch length by a factor of ≈ 2.8 down to 5.4 ps. In the low α mode the effective bunch length will be even reduced down to 1.2 ps. By further reducing the momentum compaction factor in dedicated machine shifts, the zero current bunch length could be decreased down to ≈ 0.3 ps.

The threshold current for the 5.4 ps long bunches is 1.4 mA. In the low α mode the bunch length reaches into the region of a weak instability, so that the prediction of the threshold current suffers from greater uncertainty. The bunch current at the bursting threshold is summarized in Table 1.6.

Table 1.6: Bursting threshold current I_{th} and bunch length σ_z for BESSY II, the preparatory phase and the final BESSY VSR setup.

	Standard mode	Low α mode
	I_{th} at σ_z	
BESSY II	1.8 mA at 15 ps	0.045 mA at 3 ps
Preparatory BESSY VSR phase	1.4 mA at 5.4 ps	0.04 mA at 1.2 ps
Final BESSY VSR phase	0.8 mA at 1.7 ps	0.04 mA at 0.3 ps

Final BESSY VSR Phase

While the preparatory phase aims to verify the technical setup with beam and to study open questions concerning beam dynamics, the final phase focuses on upgrading the required infrastructure for full BESSY VSR user operation.

The outcomes and experiences gained at the prototype commissioning in the preparatory phase enables further optimization of the final implementation. If necessary, adaptations can be made at different points, i.e., the design of the SRF components, such as cavities, couplers, tuners and others components can be optimized as well as the process of assembly of the cryomodule and its integration into BESSY II. The injection studies into short bunches will define the way of upgrading the booster synchrotron.

The primary task of the final phase will be to setup the mandatory infrastructure for realizing full BESSY VSR, which covers a 1.8 K cryogenic system and the required RF infrastructure. The main field of activity will be the purchase and setup of the new cryogenic infrastructure providing a temperature level of 1.8 K in the ring, see Chapter 4. Compared to the preparatory phase, the reduced temperature will enables focusing gradients that are larger by one order of magnitude.

In order to prevent performance degradation of the SC cavities due to dust, particle free operation at high gradients must be guaranteed. Therefore, a vacuum upgrade of the ring is foreseen, including cleaning of the vacuum chambers near the cryomodule, installation of new valves for particle free venting and ion pumps with internal NEG cartridges, see Section 5.2.

1.6 Costs and Schedule

Project Costs

BESSY VSR will be carried out in the two aforementioned phases: the preparatory and the final BESSY VSR phase. Many of the components purchased for the preparatory phase will be re-used during the BESSY VSR phase in order to mitigate technical risks as well as best utilize the funds available for the project. In the preparatory phase only two SRF cavities will be installed in a full size cryomodule. The system will be operated at 4.4 K in lieu of 1.8 K as this will be possible utilizing the existing cryogenic infrastructure with minor modification. The 1.8 K system for the BESSY VSR phase will be entirely new and thus will take several years to be designed and delivered.

The summary budget based on the hardware requirements in Table 1.5 is provided in Table 1.7 with more details in Chapter 11.

Table 1.7: The cost breakdown for the two BESSY VSR phases.

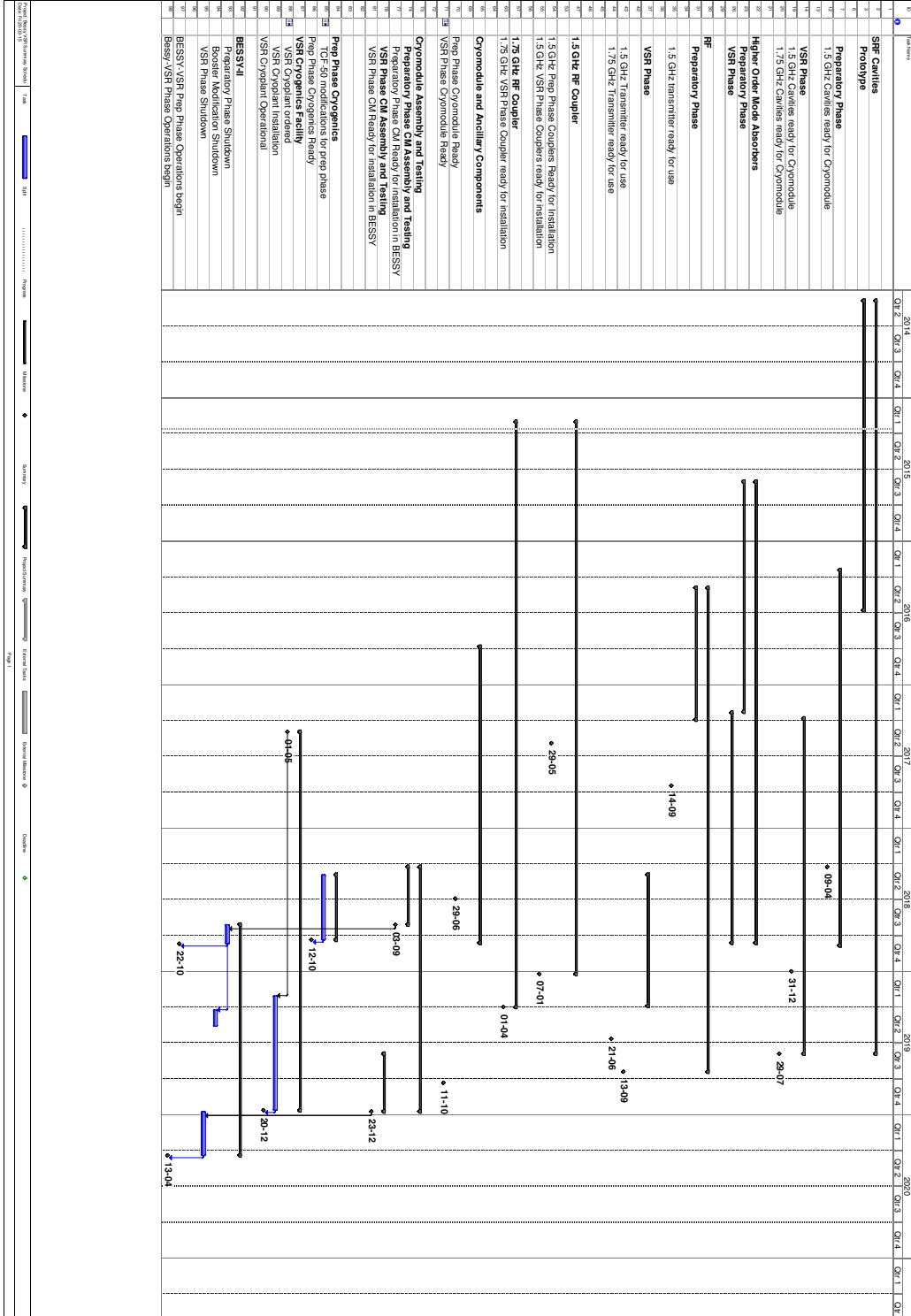
Sub-system	Preparatory phase Cost/k€	Final project phase Cost/k€
SRF components (cavities, couplers, absorbers, cryomodule)	2464 k€	2728 k€
Cryogenics (TCF-50 upgrade, 1.8 K facility)	1460 k€	8270 k€
RF components (transmitters, LLRF)	1468 k€	2468 k€
BESSY II modification (booster, vacuum, BPM, Feedback system, pseudo single bunch kicker, chopper)	2143 k€	5823 k€
Diagnostics (diagnostic beamline, X-ray diagnostic)	930 k€	1175 k€
Subtotals	8465 k€	20 464 k€
Project total	28 929 k€	

In addition to the project specific hardware necessary to realize BESSY VSR there is also other testing infrastructure that must be installed. The two main items needed for BESSY VSR are a new vertical testing dewar for the SRF cavities and a Cryomodule Test Facility (CTF) where the BESSY VSR cryomodules can be commissioned prior to installation into the storage ring.

Project Schedule

The schedule showing the key dates for the project is shown in Table 1.8, with a more detailed schedule found in Section 11.2. Due to the compressed nature of the project, there will be a great deal of overlapping orders being placed in order to keep the project on track. This will be most critical for the SRF cavities, as three different orders need to be placed for a copper prototype, the preparatory phase cavities and the final BESSY VSR cavities. As noted on the schedule, there are HZB infrastructure upgrades which are necessary. The construction of Testing Hall 1 for the vertical testing dewar is underway, so its delivery date is established, and therefore the date of the vertical testing dewar availability.

Table 1.8: The summary BESSY VSR schedule.



References

- [1] J. Feikes, P. Kuske, and G. Wuestefeld. “Towards Sub-picoseconds Electron Bunches: Upgrading Ideas for BESSY II”. In: *Proceedings of EPAC2006* (2006), pp. 157–159 (cit. on pp. 2, 12).
- [2] G. Wüstefeld et al. “Simultaneous long and short electron bunches in the BESSY II storage ring”. In: *Proceedings of IPAC2011 THPC014* (2011), pp. 2936–2938 (cit. on pp. 2, 12).
- [3] F. Marhauser et al. “Status and Test Results of high Current 5-Cell SRF Cavities developed at JLAB”. In: *Proceedings of EPAC2008 MOPP140* (2008), pp. 886–888 (cit. on pp. 15, 16).
- [4] A. Neumann et al. “CW Measurements of Cornell LLRF System at HoBi-CaT”. In: *Proceedings of SRF2011 MOPO067* (2011), pp. 262–266 (cit. on p. 16).
- [5] K. W. Robinson. *STABILITY OF BEAM IN RADIOFREQUENCY SYSTEM*. Feb. 1964. URL: <http://www.osti.gov/scitech/servlets/purl/4075988> (cit. on p. 16).
- [6] URL: http://photon-science.desy.de/facilities/petra_iii/machine/parameters/index_eng.html (cit. on p. 17).
- [7] URL: <http://www.bnl.gov/ps/accelerator/> (cit. on p. 17).
- [8] R. Hettel. “DLSR design and plans: an international overview”. In: *Journal of Synchrotron Radiation* 21.5 (Sept. 2014), pp. 843–855. URL: <http://dx.doi.org/10.1107/S1600577514011515> (cit. on p. 17).
- [9] D. Einfeld et al. “First multi-bend achromat lattice consideration”. In: *Journal of Synchrotron Radiation* 21.5 (Sept. 2014), pp. 856–861. URL: <http://dx.doi.org/10.1107/S160057751401193X> (cit. on p. 17).
- [10] H. Tarawneh et al. “ALS-II, a Potential Soft X-ray, Diffraction Limited Upgrade of the Advanced Light Source”. In: *Journal of Physics: Conference Series* 493.012020 (2014). 17th Pan-American Synchrotron Radiation Instrumentation Conference (SRI2013) (cit. on p. 17).
- [11] E. Karantzoulis. *Status of Elettra and Future plans*. Conference Website. ESLS XXII Workshop. Nov. 2014. URL: http://www.esrf.eu/files/live/sites/www/files/events/conferences/XXII%20ESLS/Karantzoulis_Elettra_ESLSXXII_Nov2014-4_final.pdf (cit. on p. 17).
- [12] R. Bartolini. *Design, status and roadmap of next generation low emittance ring*. Conference Website. ESLS XXII Workshop. Nov. 2014. URL: <http://www.esrf.eu/home/events/conferences/esls-xxii-workshop/presentations.html> (cit. on p. 18).

- [13] P. Raimondi. *ESRF Operation Status Report & Accelerator Upgrade Programme*. Conference Website. ESLS XXII Workshop. Nov. 2014. URL: <http://www.esrf.eu/home/events/conferences/esls-xxii-workshop/presentations.html> (cit. on p. 18).
- [14] A. A. Zholents and M. S. Zolotarev. “Femtosecond X-Ray Pulses of Synchrotron Radiation”. In: *Physical Review Letters* 76.6 (Feb. 1996), pp. 912–915. URL: <http://link.aps.org/doi/10.1103/PhysRevLett.76.912> (cit. on p. 18).
- [15] S. Khan et al. “Femtosecond Undulator Radiation from Sliced Electron Bunches”. In: *Phys. Rev. Lett.* 97 (7 Aug. 2006), p. 074801. URL: <http://link.aps.org/doi/10.1103/PhysRevLett.97.074801> (cit. on p. 18).
- [16] K. Holldack et al. “FemtoSpeX: a versatile optical pump-soft X-ray probe facility with 100 fs X-ray pulses of variable polarization”. In: *Journal of Synchrotron Radiation* 21.5 (2014), pp. 1090–1104 (cit. on p. 18).
- [17] M. Abo-Bakr et al. “Steady-State Far-Infrared Coherent Synchrotron Radiation detected at BESSY II”. In: *Phys. Rev. Lett.* 88 (June 2002), p. 254801. URL: <http://link.aps.org/doi/10.1103/PhysRevLett.88.254801> (cit. on p. 18).
- [18] M.-A. Tordeux. *Femto-Slicing project at SOLEIL*. Conference Website. ESLS XXII Workshop. Nov. 2014 (cit. on p. 19).
- [19] Y. Shoji et al. “Circulation of a Short, Intense Electron Bunch in the New SUBARU Storage Ring”. In: *Proceedings of EPAC 2006 MOPCH055* (2006), pp. 163–165 (cit. on p. 19).
- [20] X. Huang, T. Rabedeau, and J. Safranek. “Generation of picosecond electron bunches in storage rings”. In: *Journal of Synchrotron Radiation* 21.5 (Sept. 2014), pp. 961–967. URL: <http://dx.doi.org/10.1107/S1600577514010509> (cit. on p. 19).
- [21] A. Zholents et al. “Generation of subpicosecond X-ray pulses using RF orbit deflection”. In: *Nuclear Instruments and Methods in Physics Research* 425 (1999), pp. 385–389 (cit. on p. 19).
- [22] *Advanced Photon Source Upgrade Project*. Conceptual Design Report. The Advanced Photon Source (APS), May 2011. URL: <http://www.aps.anl.gov/Upgrade/Documents/CDR> (cit. on p. 19).
- [23] Z. Conway et al. “Development and Test Results of a Quasi-waveguide Multi-cell Resonator”. In: *Proceedings of IPAC2014 WEPRI050* (2014), pp. 2595–2597 (cit. on p. 19).
- [24] URL: <http://dlsr-workshop-2014.aps.anl.gov/index.html> (cit. on p. 20).

2 Beam Dynamics

The BESSY VSR proposal is a novel approach to manipulate the longitudinal phase space to obtain simultaneously short and long bunches. The goal is, to have about 80 times more current in the short bunches compared to what has been achieved by the present BESSY II low α optics. Various beam dynamical aspects are discussed in the present chapter. An analysis of the expected bunch current limits derived from actual scaling relations, multiparticle simulations and measured data is presented in Section 2.1. The voltage requirements to achieve the short and intense bunches are discussed in Section 2.2, where the alternating focusing scheme is presented and the specification of the voltage and frequencies of the cavities are derived. The bunch fill pattern based on user demands and the related Touschek life time are discussed in Section 2.3 and Section 2.4. Bunch separation schemes, to allow a choice between short or long bunches at the user beam port are subject of Chapter 7.

Interactions between beam and cavities are topic of Section 2.5 and Section 2.6, where single particle und coherent high current effects are discussed. Section 2.6 on coupled multi bunch instabilities (CBI), beam loading and Robinson's instability concludes that with a realistic longitudinal and transverse feed back system and HZB's recent cavity design, see Chapter 3, beam stability can be achieved. A modified low α optics is discussed in Section 2.7 with vanishing dispersion at the cavity location, to minimize longitudinal-transverse beam coupling. Also the ultimate bunch length limits achievable with BESSY VSR in radiation damping equilibrium are discussed and a limit of about 300 fs is found for the present low α optics. A discussion is presented in Section 2.8 on parking the cavities and transparent beam operation in case a switch back to standard operation is required. The fundamental cavity mode is easily compensated for cold cavities, if pairs of equal cavities are installed.

Beam injection into the SC cavities, subject of Section 2.9, is feasible with the present booster synchrotron for the long bunches, but for the short bunches special care is required. The bunches extracted from the booster are too long. By bunch rotation inside the short BESSY VSR buckets they will blow up in momentum with enhanced particle losses. The presently favored solution is an upgrade of the booster RF by additional bunch compressing cavities.

2.1 Limits of Bunch Length and Intensity

One of the main promising features of the BESSY VSR concept is the increased bunch current for short bunches. The presently applied BESSY II low α optics can deliver short bunches of 3 ps length, but at low currents of 45 μ A per bunch. The goal of BESSY VSR is to deliver bunches of 1.7 ps length at currents of about 0.8 mA. To predict reliable values for bunch length and current requires an extrapolation beyond the presently achievable values by more than one order of magnitude.

In the limit of vanishing bunch currents it is quite reliable to predict the "zero current" bunch length. With increasing current bunches will pass an instability threshold, beyond which they are unstable. These bunches are not lost, but with increasing current they gradually blow up in energy spread and bunch length¹. This threshold current has a well-defined value, it can be predicted by simulation codes and detected by the sudden emission of intense bursts of coherent synchrotron radiation (CSR) in the THz frequency range. This instability is called the "microwave" or "bursting" instability. The relation between the bunch length and current at the stability limit follows a "universal scaling law", already suggested 1990 [1], but needs to be refined for the short bunches discussed here. The most recent review of the scaling law as presented by [2], together with recent simulations and measurements for BESSY II [3–5], will be discussed to derive predictions of lengths and currents of short bunches of BESSY VSR.

In the limit of low currents, the relative rms-energy spread δ_0 of electron bunches circulating in a storage ring is called "natural" or "zero current" energy spread and follows from a Gaussian distribution. This energy spread is, apart from very special optics tuning, independent of the beam optical parameters. Unlike the energy spread, the rms-length σ_0 of electron bunches in a storage ring is dependent on the machine optics and given by the relation

$$\sigma_0 = \frac{\alpha \delta_0}{2\pi f_s} = \delta_0 \sqrt{\frac{E}{e f_{\text{rev}} V'_{\text{rf}}}} \frac{\alpha}{V'_{\text{rf}}} \quad (2.1)$$

where $f_s^2 = (f_{\text{rev}} \alpha e V'_{\text{rf}})/(4\pi^2 E)$ with the synchrotron frequency f_s , the beam revolution frequency f_{rev} , the momentum compaction factor α , the applied RF voltage V_{rf} , the voltage temporal gradient at the bunch position $dV_{\text{rf}}(t)/dt = V'_{\text{rf}} = 2\pi V_{\text{rf}} f_{\text{rf}}$ with the radio frequency f_{rf} , the total electron energy E , and the electron charge e . This length σ_0 is called "natural" or "zero current" bunch length and is valid in the limit of low currents. Energy and position of individual electrons are the

¹The BESSY II low α optics is presently running during half of its scheduled time at 100 mA by user demands, which is 7 times above the bursting threshold of 15 mA (0.04 mA/bunch).

result of quantum emission, radiative damping and longitudinal focusing, yielding an equilibrium distribution of a Gaussian bunch shape.

The zero current values of bunch length and energy spread become distorted at the onset of the instability, detectable as coherent bunch shape oscillations in the kHz-range. The instability is a result of the interaction of the bunch current with its impedance surrounding, including the interaction with its own emitted synchrotron radiation. This radiation field in the sub-THz-range is the dominant impedance contribution. The instability threshold can be shifted to higher currents by shielding the THz radiation by the metallic vacuum chamber, characterized by the dipole bending radius ρ (4.35 m, BESSY II) and the vacuum chamber full height h (0.035 m, BESSY II). A recent version of the scaling law derived from interactions with the radiation field [2] is shown in Figure 2.1. In the presentation two scaling parameters, χ and ξ , are applied. The first parameter is defined as $\chi = c\sigma_0\rho^{1/2}/h^{3/2}$, depending on the length σ_0 , height h and radius ρ describing the strength of the shielding. The second scaling parameter is defined as $\xi = I_n\rho^{1/3}/(c\sigma_0)^{4/3}$. Here I_n is a normalized current given by $I_n = c\sigma_0 I_b/(\alpha\gamma\delta_0^2 I_A)$, with I_b the bunch current and I_A the Alfvén current of 17 045 A. The figure is divided into a lower and an upper part by the line resp. circles, representing results from different theoretical models. A given bunch length fixes a position on the horizontal axis, the value on the vertical axis is then proportional to the bunch current. As long as the selected values of bunch length and current yield a point located in the lower part of the figure the bunch is stable; in the upper part it would be unstable. The predicted transition, the bursting threshold, is indicated by the line or circles.

The red line in Figure 2.1 indicates a threshold calculation, based on the "coasting beam" model. The functional relation is given by $\xi = 3\sqrt{2}\chi^{2/3}/\pi^{3/2}$. More refined calculations are based on "bunched beam" theory or the solution of the "Vlasov-Fokker-Planck" (VFP) equation, marked by the circles. Results of the two last methods can be approximated by the simple relation, $\xi = 0.5 + 0.34\chi$. Additionally, there is a dip at around $\chi = 0.25$, ranging from about $\xi = 0.1$ to $\xi = 0.5$, indicating a further instability mechanism, the "weak instability", which results from a mixing of radial bunch modes. This is different to the microwave instability, described by azimuthal bunch mode mixing.

A comparison of thresholds derived from measurements and simulations is shown in Figure 2.2, with axis parameters σ_0 and I_b/V , the bunch current divided by the effective RF voltage applied for longitudinal bunch focusing. Results of the coasting beam model of Figure 2.1 are transformed into the red line of Figure 2.2, the bunched beam and VFP simulation of Figure 2.1 to the blue line. The dip of Figure 2.1 is transformed into the blue hump in Figure 2.2. The hump is placed at $\sigma_0 = 2.5$ ps (zero current value) for BESSY II parameters, the shape of the

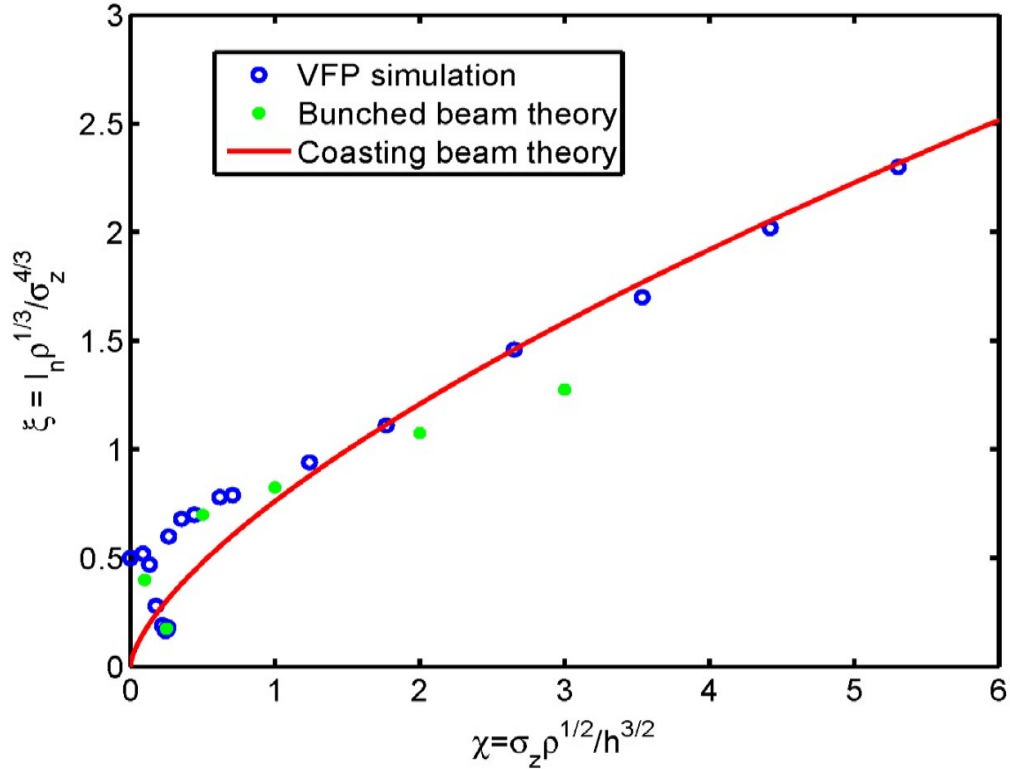


Figure 2.1: Instability threshold relation in scaled variables, reproduction of Figure 5 of [2]. In this figure σ_z is given in units of a length, not time.

hump is only a qualitative indication. For BESSY VSR cavities of different RF frequencies and voltages are foreseen. An equivalent effective voltage is required for the scaling parameter to take into account the combination of different voltages and frequencies. BESSY VSR will achieve an 80 times stronger RF focusing, equivalent to an 80 times enhanced voltage of the present RF voltage of 1.5 MV at 0.5 GHz frequency. This equivalent, 80 times stronger voltage is applied for the scaling.

Additionally, in Figure 2.2 data points from measurements at BESSY II [3–5] are shown and results of simulations [3, 4] derived from multi particle tracking and solution of the VFP equation. The green line shows a simulation for the present BESSY II parameters, the black line a simulation for BESSY VSR with the enhanced RF focusing. The data points agree well with the simulation for bunch lengths longer than 3 ps, but differ in the range below 3 ps. Here, data points deviate from the green line, the reason is not understood. The coherent signals of the THz bursts could indicate signals from different sources, like Schottky noise [3]. The bunch length and focusing voltage could also be modified by other impedance contributions of the ring and their "potential well effect" [6], where the applied

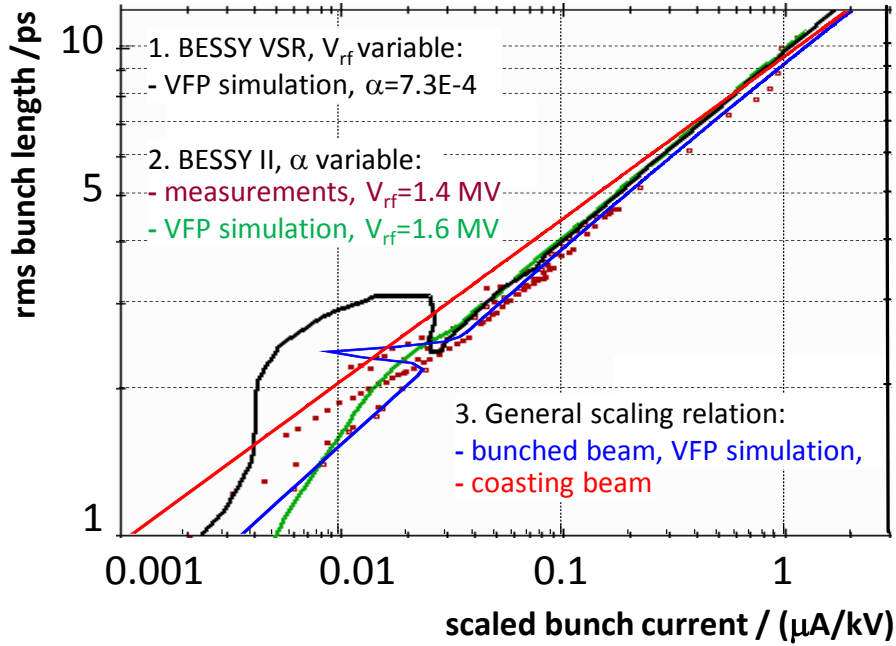


Figure 2.2: Instability threshold scaling relation with bunch current/voltage on horizontal axis and zero current bunch length σ_0 on vertical axis. The comparison shows results of 1. BESSY VSR with the enhanced, longitudinal focusing, 2. the present BESSY II optics and 3. the universal scaling relation [2].

external RF voltage is superimposed by an additional voltage induced by the interaction of the bunch current with chamber impedances to an effective voltage V_{eff} . This would lead to revised scaling values σ_0 and I_b/V_{eff} .

The simulation takes into account only the potential well distortion from the shielded CSR impedance, which does not generate a bunch lengthening. However, this is different to the bunch lengthening found by streak camera measurements at BESSY II, where bunches at the bursting threshold are nearly 50% longer than predicted by the zero current bunch length [7]. This was also observed at other storage rings. A 2 ps long bunch, for example, would be lengthened to 3 ps at the instability threshold. The potential well lengthening just below the bursting instability is a static deformation and does not increase the energy spread, the zero current value is preserved. These bunches are considered as stable. This effect is not further studied here, but could shift threshold data and scaling relation if considered for the effective bunch length. For example, a 50% longer bunch, as found for bunches longer than 2 ps, will have an 2.5 times increased threshold current (see

below). Recent simulations by [3] include the effect of bunch lengthening by an inductive impedance, characterized by the normalized longitudinal impedance of $|Z_{\parallel}/n| = 0.2 \Omega$ to 0.35Ω [8], which fits well for bunches longer than 3 ps, but could be 10 times smaller for short bunches. A bunch lengthening, depending sensitive on the assumed value for $|Z_{\parallel}/n|$, can be estimated. As a preliminary result, the expected threshold current can be twice as large as the value derived from the CSR impedance only.

There is some uncertainty in the resulting lengthening effect of short bunches. For the following we will assume for bunches longer than 1 ps a lengthening by 50 %, indicated by the variable σ_z . For shorter bunches no lengthening is assumed and the zero current bunch length is applied, indicated by σ_0 . The zero current bunch length is additional dependent on the emitted radiation power by the insertion devices, which increases the energy spread of the beam. The strongest device is the 7 T multipole wiggler, which could lead to a 30 % increased naturale energy spread and to a bunch lengthening of the same amount. Bunch lengthening effects by the insertion devices are not considered.

The range of the hump around 2.5 ps is only visible in the simulation for the BESSY VSR threshold values. It is not so pronounced for the present BESSY II machine parameters. In the range of the hump the instability threshold becomes sensitive to the parameter β , the inverse of the product of synchrotron frequency f_s and the longitudinal damping time τ_z (8 ms for BESSY II), $\beta = 1/(2\pi f_s \tau_z)$ [9]. An increasing synchrotron frequency yields smaller β -values and a larger hump amplitude. The threshold current becomes reduced and scales like $\sqrt{\beta}$. With the present BESSY II low α optics, bunches of 2.5 ps length could be achieved at values of $f_s = 2.2$ kHz, yielding $\beta = 10 \times 10^{-3}$. For comparison, at BESSY VSR short bunches of 1.1 ps length, close to the critical area, are achieved at $f_s = 80$ kHz and $\beta = 0.25 \times 10^{-3}$, expecting a more pronounced hump. This parameter range of small β -values is presently not achievable at BESSY II operated at 1.7 GeV. The Metrology Light Source can be tuned to these small β -values and bursting thresholds clearly show the hump, [5], as predicted by the theory [9] and [10].

Based on the bunched beam model the relation between bunch length, threshold current and RF voltage is derived, [2],

$$(c\sigma_0)^{7/3} = (c^2 Z_0 I_b \rho^{1/3}) / (8\pi^2 \xi(\chi) V_{\text{rf}} f_{\text{rf}} f_{\text{rev}}) \propto I_b / V_{\text{rf}} \quad (2.2)$$

where $Z_0 = 377 \Omega$ is the free space impedance, for older versions of this scaling see [11] and [12]. Applying this relation for a fixed bunch length, the bunch current can be increased in proportion to the applied focusing voltage gradient. This proportionality is the underlying property for the BESSY VSR concept, where the current of short and stable bunches is enhanced in proportion with the upgraded

RF focusing. However, in the range of the hump, this simple scaling needs to be modified. Within the validity range of the scaling law, a simple rule of thumb can be applied, predicting that a two times longer bunch can store five times more current without loss of stability and a doubling of the bunch current will lead to a bunch lengthening of 35 %. The detection of any coherent bunch motion by the emitted THz radiation is extremely sensitive. The degrading of the beam quality starts at this point, but the beam can still be used to some extent beyond this point.

To derive the BESSY VSR performances as listed in Table 2.1 we proceed as follows. To predict the threshold we assume a bunch lengthening of 50 %, which is very likely an upper limit and changes the value of the bunch length from 1.1 ps to 1.7 ps, a conservative approach from the point of time resolved experiments and for the value of peak brilliance. To estimate the bunch current, we step back to a bunch length of 1.4 ps, the average between 1.1 ps and 1.7 ps, yielding less current compared to the value at 1.7 ps, again a conservative approach. The scaled current of these bunches vary in the range from 0.004 $\mu\text{A}/\text{kV}$ and 0.01 $\mu\text{A}/\text{kV}$ in Figure 2.2, depending on the simulation models and data points, the average will be 0.007 $\mu\text{A}/\text{kV}$, or, 0.8 mA per bunch.

Table 2.1: Bunch length and current threshold for the short bunches of BESSY VSR.

Optics	Bunch length σ_z/ps (rms)	Threshold current I_{th}/mA
User optics	1.7	0.8
Low α optics	0.3	0.04

These parameters of the short bunches can be compared with the corresponding values of the present low α optics to estimate the emitted THz power. The current value of 0.8 mA for the 1.7 ps long bunches is 20 times more, compared to the 0.04 mA at 3 ps of the low α optics. The expected THz power per bunch grows with the square of the current, if the bunch shape is fixed and even more enhanced if the bunches become shorter. Hence, at least 400 times more, nonbursting THz radiation power is emitted, see also Table 5.2.

The bunch length can be further manipulated by a change of the optics parameter α . The well established BESSY II low α optics can be combined with the BESSY VSR scheme. Short bunches of 300 fs length, see Table 2.5, are below the critical hump area. From Equation (2.2) the proportionality $\sigma_0^{7/3} \sim I_b/V_{\text{rf}}$ and a scaling parameter $\xi = 0.5$ are applied to derive a threshold current of 40 μA and for 150 bunches

an average current of 6 mA. These numbers are derived from scaling the present low α optics experience, where bunches of $\sigma_z = 3$ ps at $f_s = 1.75$ kHz and 1.5 MV voltage are stable up to 15 mA stored in 350 bunches (0.04 mA/bunch). The low α optics can be easily tuned to a “negative low α optics”, where the hump behaves completely differently or even could vanish and leads to a different threshold. This option is not further discussed here, but will be studied in the future.

2.2 Alternating Bunch Length Scheme

First ideas of a scheme to develop BESSY II into a variable electron pulse length storage ring have been presented in [11] and [13]. This section reproduces the basic concepts described in [13] with updated numbers and modifications according to the most recent developments.

From Equation (2.1), it follows that the bunch length $\sigma_0 \propto \sqrt{\alpha/V'_{\text{rf}}}$ remains constant, if the voltage gradient V'_{rf} and α are increased by the same factor. For a bunch length reduction by a factor of approximately 9 to get picosecond and sub picosecond bunches, an 80 times stronger gradient is required. To achieve this strong focusing, SC cavities operated in CW mode with high frequency and high electric field gradients in the order of 20 MV/m are required. For a consistent set of parameters for the BESSY II machine, two types of cavities are considered: energy replacement cavities and focusing cavities. The present $f_{\text{nc}} = 0.5$ GHz and $V_{\text{nc}} = 1.5$ MV cavities replenish the energy lost by the emitted synchrotron radiation and provide a gradient of $V'_{\text{nc}} = 2\pi \cdot 0.75$ MV GHz. This RF frequency defines the number of buckets to be 400. For the focusing cavities, there are several schemes possible.

Since the publication of [13], the preferred setup is the choice of the following two frequencies. The first one, the harmonic cavity, is chosen as $f_{\text{sc},1} = 1.5$ GHz ($f_{\text{sc},1} = n f_{\text{nc}}, n = 3$) and a voltage of $V_{\text{sc},1} = 20$ MV, a higher harmonics to 0.5 GHz, yielding a gradient of $V'_{\text{sc},1} = 2\pi \cdot 30$ MV GHz. The second one is chosen as $f_{\text{sc},2} = 1.75$ GHz ($f_{\text{sc},2} = (m + \frac{1}{2}) f_{\text{nc}}, m = 3$) and a voltage of $V_{\text{sc},2} = 17.14$ MV, a higher harmonics to 0.25 GHz, yieldings the same gradient of $V'_{\text{sc},2} = 2\pi \cdot 30$ MV GHz.

By labeling the buckets, or stable fixed points, from 1 to 400, the buckets are divided equally in a set of odd and even-labeled buckets.

The fields produced by the two SC cavity systems are adjusted with respect to phase and amplitude in such a way, that their temporal gradients $V'_{\text{sc},1}$ and $V'_{\text{sc},2}$ add up at even fixed points leading to an enhanced, strong focusing, and cancel at the odd fixed points. At even points, the SC cavities provide a combined gradient of

$V'_{\text{rf}} = 2\pi \cdot 60 \text{ MV GHz}$ which is 80 times higher than the gradient of the NC cavities, $V'_{\text{nc}} = 2\pi \cdot 0.75 \text{ MV GHz}$. The total focusing gradient at the even points is

$$V'_{\text{rf}}(t = 0) = 2\pi(f_{\text{nc}}V_{\text{nc}} + f_{\text{sc},1}V_{\text{sc},1} + f_{\text{sc},2}V_{\text{sc},2}) \quad (2.3)$$

and at the odd positions, where $f_{\text{sc},1}V_{\text{sc},1}(t = 2 \text{ ns}) + f_{\text{sc},2}V_{\text{sc},2}(t = 2 \text{ ns}) = 0$,

$$V'_{\text{rf}}(t = 2 \text{ ns}) = 2\pi f_{\text{nc}}V_{\text{nc}}. \quad (2.4)$$

As the temporal gradient V'_{rf} is proportional to the frequency, the amplitudes of the voltage have to be chosen in such a way that $|V_{\text{sc},1}/V_{\text{sc},2}| = f_{\text{sc},2}/f_{\text{sc},1}$ to ensure a complete cancellation. This temporal behavior of the involved cavity voltages leads to alternating longitudinal positions with short and long bunches, independent of the transverse beam optics. Figure 2.3 shows the voltages for the chosen cavities as a function of time. Short bunches are placed at longitudinal positions of even multiples of 2 ns, long bunches at odd multiples of 2 ns.

In addition, there is a second criterion of stability that needs to be satisfied in order to keep particles with larger oscillation amplitudes inside the focusing potential. The bucket has to have a significant momentum acceptance which means that the absolute value of the voltage of the sum potential should become large before it crosses the zero voltage point again at the neighboring unstable fixed points. This is achieved, if the sub harmonic cavity has a higher frequency than the harmonic cavity, i.e. $f_{\text{sc},2} > f_{\text{sc},1}$. The behavior is illustrated in Figure 2.4, for the BESSY VSR parameters in the left panel and a case with $f_{\text{sc},2} < f_{\text{sc},1}$ in the right panel, where the bucket is characterized by a very low RF acceptance.

As can be seen in Figure 2.3, there are more stable fixed points, namely where the sum voltage is zero and its gradient has the proper sign. However, only at multiples of $t = 2 \text{ ns}$ it is ensured that the voltages of all cavity systems vanish individually. At the other stable fixed points, the sum voltage vanishes, but the individual contributions, especially from the SC cavities, are large. Storing current in such a bucket could result in massive average power transfer from one cavity system to another which should be prevented.

Choice of Frequencies

The present choice of the harmonics of the NC cavities with $f_{\text{sc},1} = 1.5 \text{ GHz}$ and $f_{\text{sc},2} = 1.75 \text{ GHz}$ is a reasonable compromise between the following aspects. A set of SC cavity parameters at lower frequencies compared to the present solution satisfying all conditions mentioned above could be $f_{\text{sc},1} = 1 \text{ GHz}$ and $f_{\text{sc},2} = 1.25 \text{ GHz}$. In this case, the cavities become larger at the same focusing gradient and would no longer fit into one straight section of BESSY II or would require operation at an

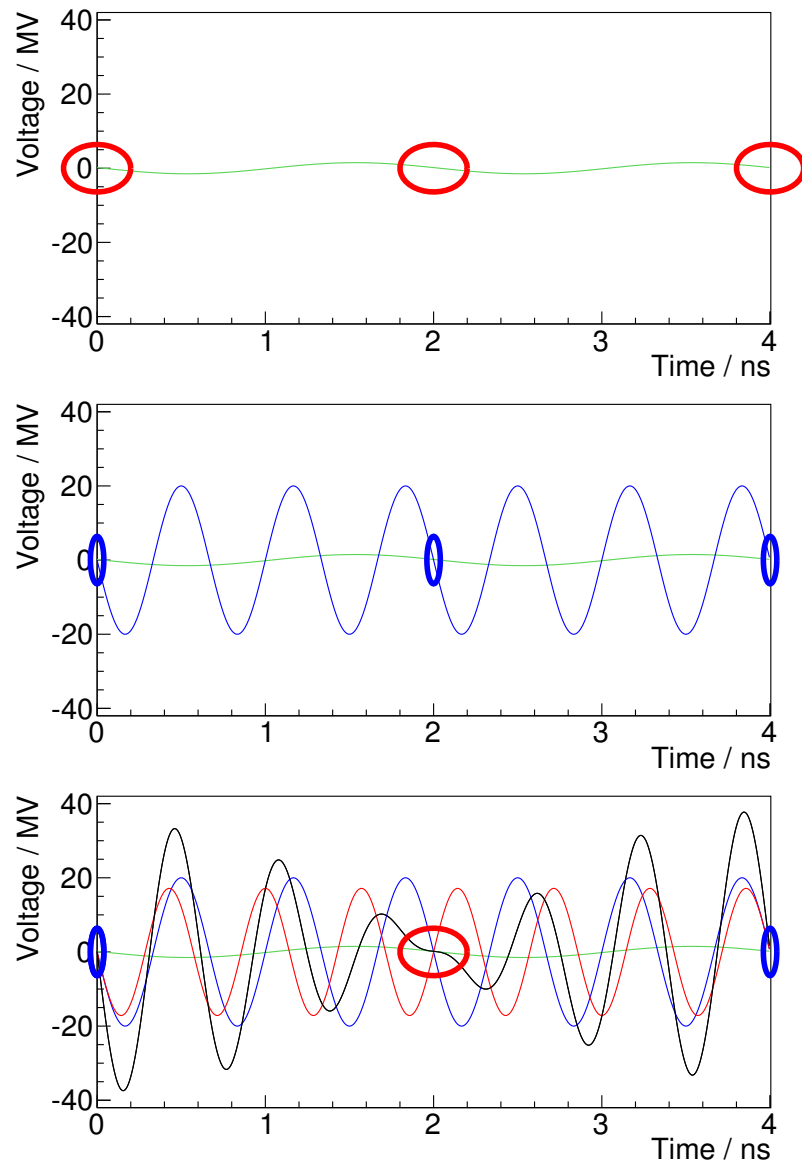


Figure 2.3: Voltages as a function of time of the 0.5 GHz, 1.5 GHz and 1.75 GHz cavity systems are shown in green, blue and red, respectively. The sum voltage is shown in black. Short bunches are placed at the longitudinal position $t = 0$ and $t = 4$ ns, long bunches are placed at $t = 2$ ns, indicated by blue and red ellipses respectively. Top: Only NC cavities. Center: NC cavities combined with the 1.5 GHz cavity system. Bottom: Full BESSY VSR setup with all three cavity systems.

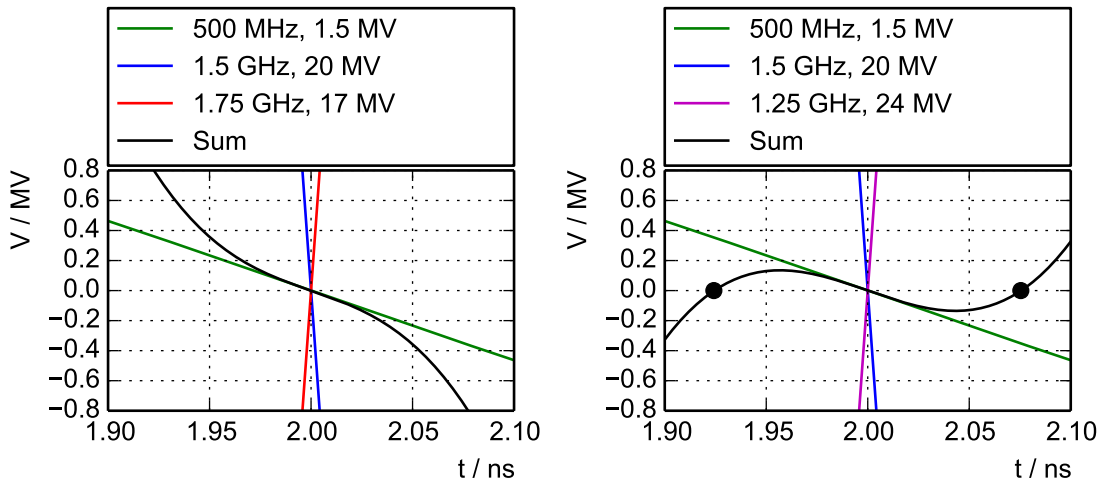


Figure 2.4: Voltages of the cavities in the close vicinity of the stable fix point of the long bunch. Left: BESSY VSR standard setup with $f_{sc,2} > f_{sc,1}$. Right: Hypothetical setup with $f_{sc,2} < f_{sc,1}$ which leads to limitation of the bucket by the additional unstable fixed points (black dots) and very low RF acceptance.

unreasonably high accelerating field. In the other case, with frequencies higher than the present ones, e.g., $f_{sc,1} = 2$ GHz and $f_{sc,2} = 2.25$ GHz, the structures become smaller. This raises the concern of increased excitation of higher order modes, leading to beam instabilities. Finally, technical aspects such as cryogenic losses, availability, scalability and maturity of presently available SC multi-cell cavities and RF generators favor the choice made for BESSY VSR.

2.3 Bucket Fill Pattern

The target fill pattern for BESSY VSR is mainly driven by user demands, which are motivated by means of beam separation, see Chapter 7.

Figure 2.5 shows the basic layout of the fill pattern intended for BESSY VSR operation. The total current stored corresponds to 300 mA. However, in contrast to BESSY II roughly only half the number of the buckets is available to store “standard-bunches” as discussed in Section 2.2. The major part of beam current is distributed to 150 buckets divided in two trains of 75 buckets each, i.e. the bunch current will approximately double compared to the present situation. Therefore, there are consequences for beam lifetime – see Section 2.4 and Chapter 9. Two gaps of 100 ns separate the two bunch trains to allow pulse picking of single bunches by a

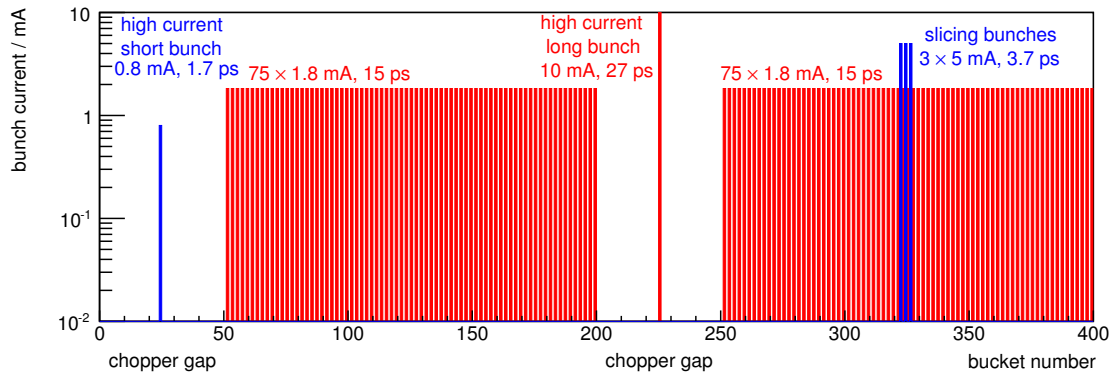


Figure 2.5: Intended fill pattern for BESSY VSR operation with short bunches (blue) and long bunches (red). Two chopper gaps are introduced to enable photon beam separation. Overall beam current is 300 mA.

mechanical chopper, see Section 7.1. In addition, three short bunches are populated with high current of about 3×5 mA for slicing experiments, see Section 1.4.

Figure 2.6 shows a slightly different fill pattern, which may be applied. Trains of short bunches are populated such to minimize the overall bunch current density. Therefore, beam lifetime is improved by about 10 %, as sketched in Section 2.4. In addition, this fill pattern supplies a large and adjustable amount of stable CSR in the THz range as well as short x-ray pulses with high repetition rate.

2.4 Touschek Lifetime

Manipulation of bunch current or bunch dimensions leads to a change of electron density. However, the electron density is an essential parameter for the scattering rate between electrons of the same bunch. Of particular interest is Touschek scattering [14], which is a major effect limiting the lifetime at most storage ring based synchrotron radiation sources. Within a single scattering process, significant transverse momentum may be transferred to the longitudinal plane. Therefore, the involved particles may be scattered from stable areas of the longitudinal phase space or scraped at apertures in dispersive sections.

The average beam lifetime of the BESSY II storage ring in standard operation is dominated by the Touschek effect [15]. However, one prerequisite for TopUp operation is to sustain an average lifetime of $\tau > 5$ h. In order to fight loss rate due to Touschek scattering, the beam is widened by noise in the vertical plane to

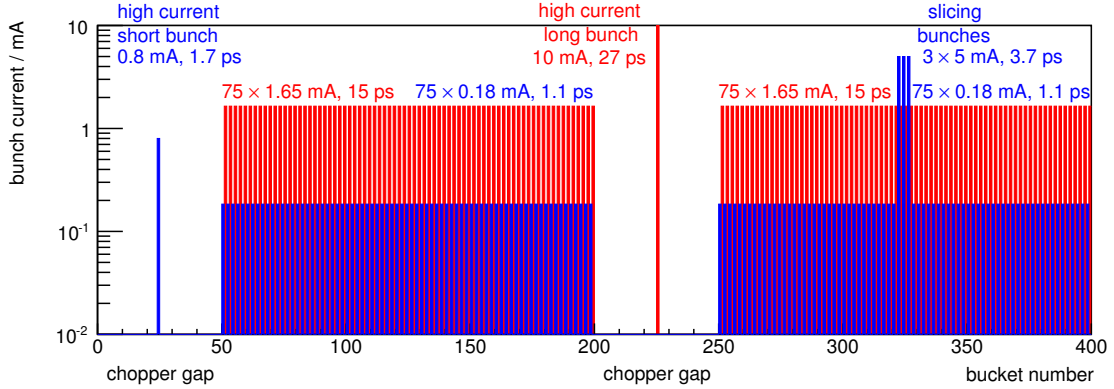


Figure 2.6: Possible fill pattern for BESSY VSR operation with short bunches (blue) and long bunches (red). Trains of short bunches are added to relax beam lifetime and to supply THz power as well as high repetition rate short x-ray pulses. Overall beam current is 300 mA.

relax the electron density to some extent at the cost of brilliance. Maintaining this TopUp condition will be a requirement for operation of BESSY VSR.

Predicting an absolute value for the expected Touschek lifetime is usually a difficult task afflicted with considerable uncertainty. It involves explicit knowledge and analysis of the bunch volume as well as apertures. These may vary over more than one order of magnitude as a function of the longitudinal position around the ring. However, one main premise of the BESSY VSR upgrade project is to preserve the transverse optics, which have evolved from a decade long optimization process. Therefore, a scaling of the loss rate due to Touschek effect seems to be the more suitable approach, which is given by [14]:

$$\tau^{-1} \propto \frac{N}{\sigma_z}, \quad (2.5)$$

where N is the number of electrons in the bunch and σ_z is the bunch length. The loss rate τ^{-1} will have to be analyzed on a bunch-by-bunch basis as BESSY VSR will feature a complex fill pattern, as beam loading determines the effective RF voltage for every single bunch, see Section 2.6.2, and bunch lengthening due to CSR occurs. The algorithm to estimate the scaled loss rate for every bunch can be sketched as follows:

1. determine Touschek loss rate for single bunch operation of BESSY II as a function of bunch length and bunch current
2. bunch currents are given through the BESSY VSR fill pattern, see Section 1.3

3. estimate bunch length while regarding beam loading and bunch lengthening, see Sections 2.1 and 2.6
4. calculate the ratio of current densities $(I_{\text{VSR}}/\sigma_{\text{VSR}})/(I_{\text{BII}}/\sigma_{\text{BII}})$ for individual bunches and apply the resulting factor to the Touschek loss rate of BESSY II to obtain the Touschek loss rate of BESSY VSR.

As an estimation the Touschek lifetime of BESSY VSR will be reduced by a factor of 3 ± 1.5 in the presently intended operation mode compared to BESSY II standard user operation. The large relative uncertainty is caused by the fact, that most of the buckets will be populated with currents at or above the bursting threshold. Therefore, the implications sketched in Section 2.1 apply with the corresponding uncertainties in bunch length and bunch current. A fill pattern with short bunch trains, as sketched in Figure 2.6, does feature a 10% increased lifetime compared to a fill pattern without short bunch trains – see Figure 2.5. Relative contributions of the different bunches to the overall loss rate is visualized in Figure 2.7. In general,

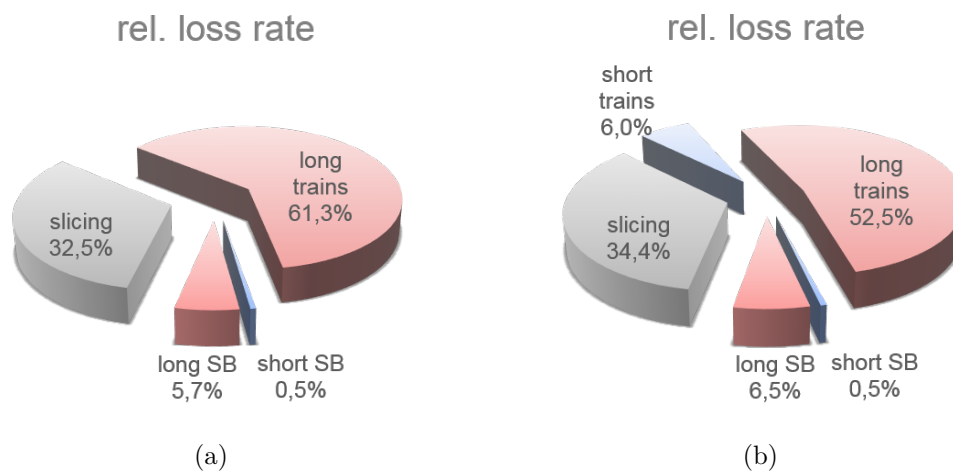


Figure 2.7: Relative contributions to the overall Touschek loss rate by different bunches. (a) For the fill pattern given in Figure 2.5 and (b) for the fill pattern in Figure 2.6.

the loss rate is dominated by the trains of long bunches, which generate more than half of the total lost electrons. The second largest contribution is contributed by the slicing bunches, which are placed in short buckets and populated with a current well above the bursting threshold. It is worth noting, that the short single bunch (SB) inside the gap as well as the trains of short bunch only generate a minor part of the losses.

As Touschek lifetime is expected to decrease, this suggests the assumption that the rate of intrabeam scattering may increase. Therefore, intrabeam scattering and its

consequences for the quality of the photon beam delivered to users will be a field of future studies.

2.5 RF Jitter

The ultimate bunch length in BESSY VSR will be as low as 300 fs rms, see Section 1.3. If the synchrotron radiation from those bunches is used for time-resolved measurements, it is essential that there is no longitudinal jitter that increases the bunch length or energy spread or apparent bunch length by introducing an uncertainty to the time of arrival.

Detailed studies published in [16] investigate the effects of amplitude and phase jitter in the RF system on the electron bunch by means of single particle tracking. It was concluded that phase jitter has a much stronger effect on the longitudinal phase space compared to amplitude jitter, thus the latter is neglected in the following discussion. The dominant effect of phase jitter is a modulation of the time of arrival, causing an effectively longer bunch. At reasonable jitter amplitudes, the bunch itself is neither elongated, nor increased in its energy spread.

If the synchrotron frequency of the bunches do not coincide with a strong line in the jitter spectrum, it is plausible to simply add the bunch length and the RF phase jitter in quadrature to obtain the effective bunch length.

Measurements at HZB [17] have demonstrated CW operation of a SC cavity at high fields with high phase and amplitude stability, see Figure 2.8. The integrated phase jitter corresponding to less than 50 fs rms at 1.5 GHz. This spectrum was used in particle tracking studies. The result of the tracking simulation is depicted in Figure 2.9 and summarized in Table 2.2 exemplarily for three representative values of nominal bunch length and two values of jitter strength.

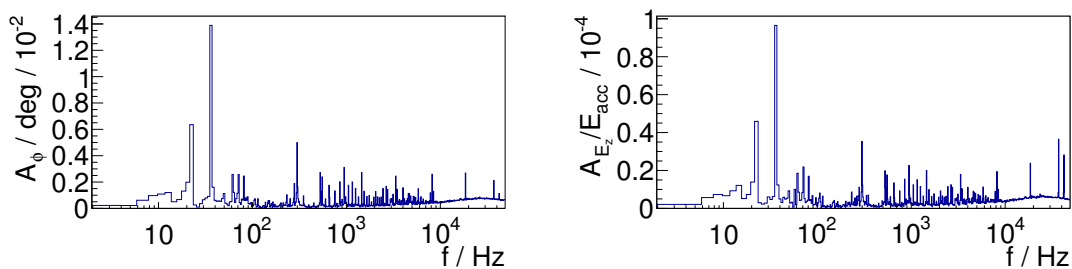


Figure 2.8: Measured noise spectrum of a TESLA cavity in CW operation [17]. Left panel: Amplitude of phase jitter A_ϕ . Right panel: Relative amplitude of voltage jitter A_{E_z}/E_{acc} .

It can be concluded, that the stability demonstrated in [17] is sufficient for all desired modes of operation in BESSY VSR. An effective lengthening of the long bunch is possible if a strong line of the jitter coincides with its synchrotron frequency, as it does in the example described here. However this is not harmful because the long bunch will not be used for timing experiments.

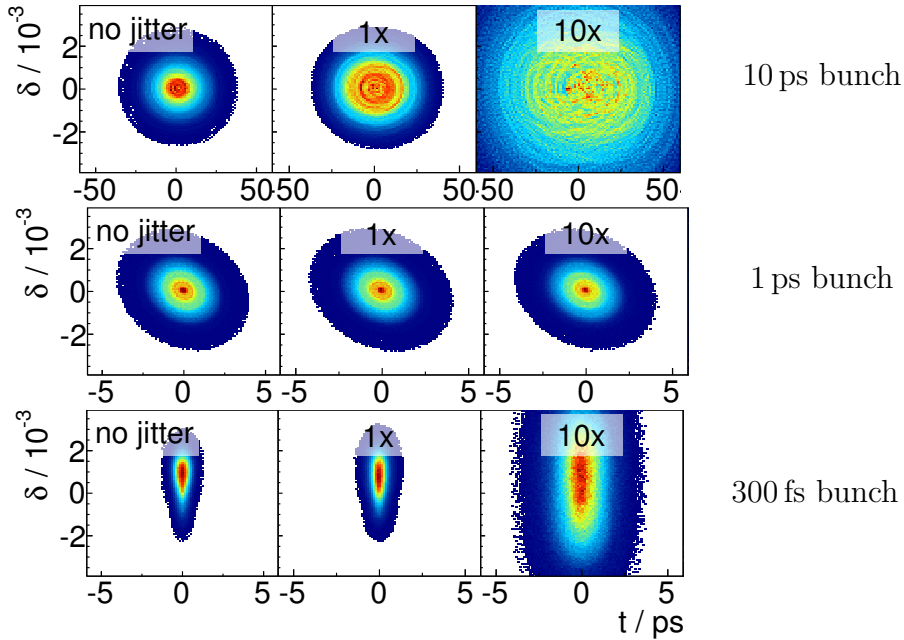


Figure 2.9: Effect of RF jitter on the effective longitudinal phase space distribution of bunches with nominal bunch length of 10 ps (top row), 1 ps (center row) and 300 fs (bottom row). Left column shows no jitter applied, center column with realistic phase jitter (c.f. Figure 2.8) and right column with tenfold enhanced jitter compared to the center column.

Some more words on the values of Table 2.2 are in order. Firstly, the numbers are subject to statistical fluctuations due to the finite number of turns. The relative size of the statistical uncertainty depends on the particular setup of the simulation, e.g. the synchrotron frequency. Both, the enhancement and the contra-intuitive fluctuation of the relative energy spread of the shortest bunch in Table 2.2 in the first two rows of data are subject to a combination of the use of a sub-optimal value for a parameter corresponding to integration steps in the tracking algorithm of ring magnets and the use of a non-ideal low- α lattice with potentially strong non-linearities in the higher order dependencies of tunes in all three planes. Those effects are understood and resolved by now, and do not change the statements drawn from the results of the simulations discussed here.

Table 2.2: Summary of simulation results. The rms relative energy spread δ_0 and the rms bunch length σ_z of the simulations depicted in Figure 2.9 are given.

Nominal bunch length	0.3 ps		1 ps		10 ps	
	$\frac{\sigma_z}{\text{ps}}$	$\frac{\delta_0}{10^{-4}}$	$\frac{\sigma_z}{\text{ps}}$	$\frac{\delta_0}{10^{-4}}$	$\frac{\sigma_z}{\text{ps}}$	$\frac{\delta_0}{10^{-4}}$
No jitter	0.33	8.5	1.0	7.1	9.8	6.9
Spectrum $\times 1$	0.34	8.0	1.0	7.0	13	9.3
Spectrum $\times 10$	1.0	19	1.0	7.0	31	26

2.6 Multi Bunch Effects

This section focuses on the effect of the impedances of the SC cavities that interact with the beam. The calculation of the impedance spectrum of the SC cavities is discussed in Chapter 3. Essentially, it is the sum over several sharply peaked resonator impedances which correspond to the fundamental and higher order modes (HOMs) of the cavity.

2.6.1 Coupled Bunch Instabilities

Narrow-band, i.e. high Q , resonators with a high impedance, such as the HOMs of a SC cavity, drive coupled bunch instabilities, a coherent motion of the bunches in the transverse or longitudinal plane.

A detailed study of coupled bunch instabilities for BESSY VSR is presented in [18]. This section will review some of its aspects and present updated results.

The strength of the instability is typically expressed as a growth rate. To judge whether an instability of certain strength poses a threat to beam stability, the growth rate has to be compared to the damping rate of the beam. The strongest damping is typically provided by active bunch-by-bunch feedback systems. The performance of the present bunch-by-bunch feedback of BESSY II has recently been evaluated for standard user settings [19]. The damping rate was found to be 4 ms^{-1} and 1.33 ms^{-1} in the transverse and longitudinal plane respectively. It exceeds the damping rate given by synchrotron radiation by more than 60 for the transverse plane 0.0625 ms^{-1} and by one order of magnitude for the longitudinal one 0.125 ms^{-1} .

Calculation of Coupled Bunch Instabilities (CBI)

In leading order, HOM driven coupled bunch motion can be described by bunches approximated by point charges performing dipole oscillations in the longitudinal or transverse planes. In this approximation, the bunches form a system of coupled harmonic oscillators with a driving term given by the wake fields induced by previous bunches in the HOM afflicted cavity. In the frequency domain, wake fields transform into impedances and the solutions can be discussed as small perturbations to the oscillation frequency.

Solutions to the equations of motion are called coupled bunch modes (CBMs). If the amplitude of oscillation of a CBM grows exponentially, the phenomenon is called coupled bunch instability (CBI). Derivations, both for the case of even fill and uneven fill are presented in [20] and [21] respectively. The growth rate τ^{-1} of mode μ with its complex angular synchrotron frequency Ω_μ is given by $\tau^{-1} = \text{Im}(\Omega_\mu - \omega_s)$, with ω_s the unperturbed synchrotron frequency. The case of even fill can readily be solved analytically and the relation of growth rate τ^{-1} to the sampled impedance Z at the frequency f can be expressed as:

$$\tau^{-1} = \frac{f_{\text{rev}} I}{2E/e} \times \begin{cases} \beta_{x,y} \text{Re}(Z_{\perp,x,y}(f)) & \text{transverse} \\ f \alpha \text{Re}(Z_{\parallel}(f))/f_s & \text{longitudinal} \end{cases} \quad (2.6)$$

with e the elementary charge and $\beta_{x,y}$ the values of the betatron functions at the position of the SC cavities. The longitudinal impedance Z_{\parallel} is defined as the quantity Z_0^{\parallel} in [20], namely the longitudinal impedance for the zeroth order transverse beam moment in the so called circuit definition of the shunt impedance². The transverse impedance $Z_{\perp,x,y}$ is defined as the horizontal and vertical component of the quantity Z_1^{\perp} in [20], namely the transverse impedance for the first order transverse beam moment in the circuit definition of the shunt impedance. All other parameters are explained in Table 1.1, together with the typical values that are used for the calculations in this section.

The synchrotron frequency of the short bunch is about one order of magnitude higher than for the long bunch. As a consequence, the coupling of long and short bunches is suppressed. In addition to the low current in short bunches, the growth rate of longitudinal CBI is reduced by the factor that the synchrotron frequency is higher, making the short bunches less prone to CBI, see Equation (2.6).

²Shunt impedance R_s^c in circuit definition: $R_s^c = V_{\text{acc}}^2/(2P_{\text{diss}})$ with V_{acc} the effective accelerating voltage that a particle traveling at the speed of light experiences at most, i.e. the cavity is phased on-crest, and P_{diss} the dissipated power. On resonance, the impedance equals the shunt impedance, $Z_{\parallel} = R_s^c$. Note that in most sections of this report, a different definition of the shunt impedance is used, namely the shunt impedance in the “effective accelerator convention” R_s with $R_s = 2R_s^c$.

According to Equation (2.6), the effectiveness of transverse impedances to drive transverse CBIs scales directly with the value of the beta function at the location of the SC cavities. For this reason, a so called low β straight is favored as the location for the cavities.

In all planes, the growth rates of CBIs depend primarily on the total (average) beam current stored in the long bunches. The fill pattern is typically a small correction to the expectations from even fill, unless the so called mode coupling is artificially provoked, which typically means a fill pattern where significantly less than 50% of the buckets are filled [22].

This study presents a comparison of recent HZB cavity designs, namely HZB1a and HZB2c, see Chapter 3, and one other design, namely the JLab HC cavity [23].

A convenient way to visualize cavity models with respect to CBI is a comparison of the longitudinal and transverse impedance spectrum with a threshold impedance given by the aforementioned damping rates of the present bunch by bunch feedback systems at BESSY II, calculated with the approximation given in Equation (2.6) and the parameters in Table 1.1 and a conservative number of $\beta_{x,y} = 4$ m. The results are shown in Figure 2.10 and Figure 2.11, where stability is given when the impedance lies below the threshold line. As a conservative approach, the quadrupole modes (r^4 scaling) are treated as dipole modes (r^2 scaling).

It can be seen that the model HZB2c shows an outstanding performance compared to other models with a maximum impedance that lies a factor of approximately 20 below the threshold line in both the transverse and the longitudinal plane. Note that this model is not a final one as the fundamental power coupler is not yet implemented and cross checks are ongoing, see Chapter 3. If those results are confirmed in future calculations and the addition of the fundamental power coupler has a minor impact, stability in BESSY VSR can be achieved with a significant safety margin.

The same pass band modes (SPMs) which are characterized by low shunt impedances but very high quality factors may have an impedance above the threshold line. However, their number is limited to four per cavity and their bandwidth is so small that a small detuning is sufficient to avoid their excitation.

If, for the argument's sake, it is supposed that the performance of HZB2c cannot be confirmed after production and we assume a cavity with a HOM spectrum comparable to HZB1a or the JLab HC cavity, a more detailed discussion of the results can be done. In the transverse plane, the following can be stated. Note that for the HZB1a cavity model shown in Figure 2.11, it is only due to the conservative treatment of the quadrupole modes that there are points above the present bunch-by-bunch feedback performance of BESSY II. Thus, the expected growth rates of transverse CBI seem to be in a regime where bunch-by-bunch feedback systems are

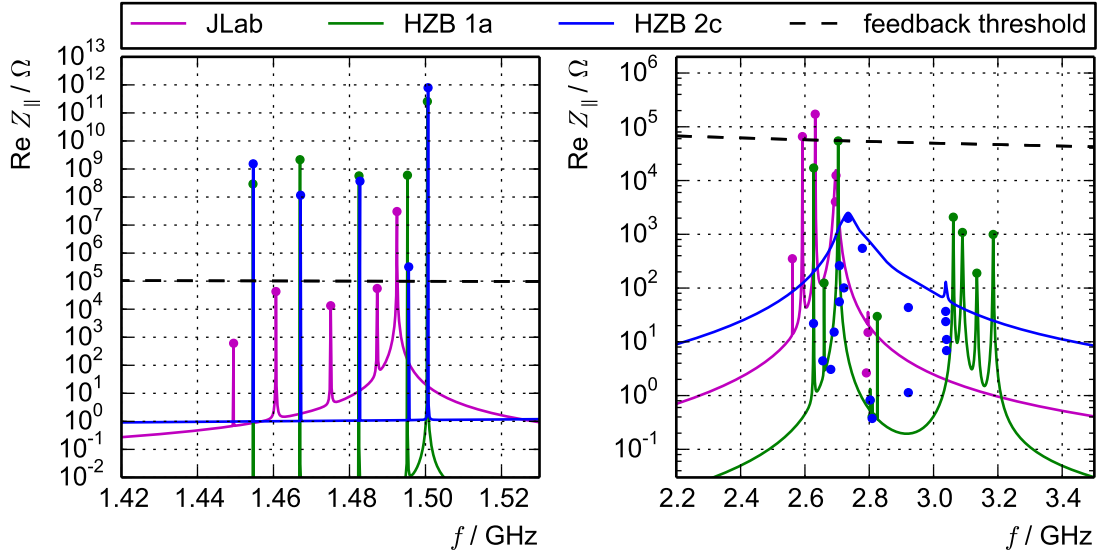


Figure 2.10: Comparison of longitudinal impedance of different HZB cavity models with the JLab HC model. The dashed line indicates the threshold given by the present feedback performance of BESSY II. Solid lines correspond to the sum over the Lorentzian functions of the HOMs while the dots depict their peak values. Left: Fundamental pass band. Right: Higher order modes.

capable of suppressing the instability. If necessary, improvements of the transverse feedback systems at BESSY II are possible with reasonable efforts, see Section 6.3. In the longitudinal plane, it can be seen that the model HZB1a is slightly above the threshold of the present bunch-by-bunch feedback performance of BESSY II. The impedance of the JLab HC cavity exceeds the threshold by approximately a factor of two. In such a case, the present bunch-by-bunch feedback performance of BESSY II would be insufficient, especially considering that for routine operation in the storage ring a significant safety margin between maximum performance and necessary performance is recommended. Potential upgrades of the longitudinal feedback systems are discussed in Section 6.3.

Further Notes

Further notes, valid for both the longitudinal and the transverse plane, need to be given. Firstly, the calculations did neither include an uncertainty of the quality factor nor of the normalized shunt impedance of the predicted HOMs. Secondly, it is assumed that there are no HOMs other than those given by the HOM spectrum.

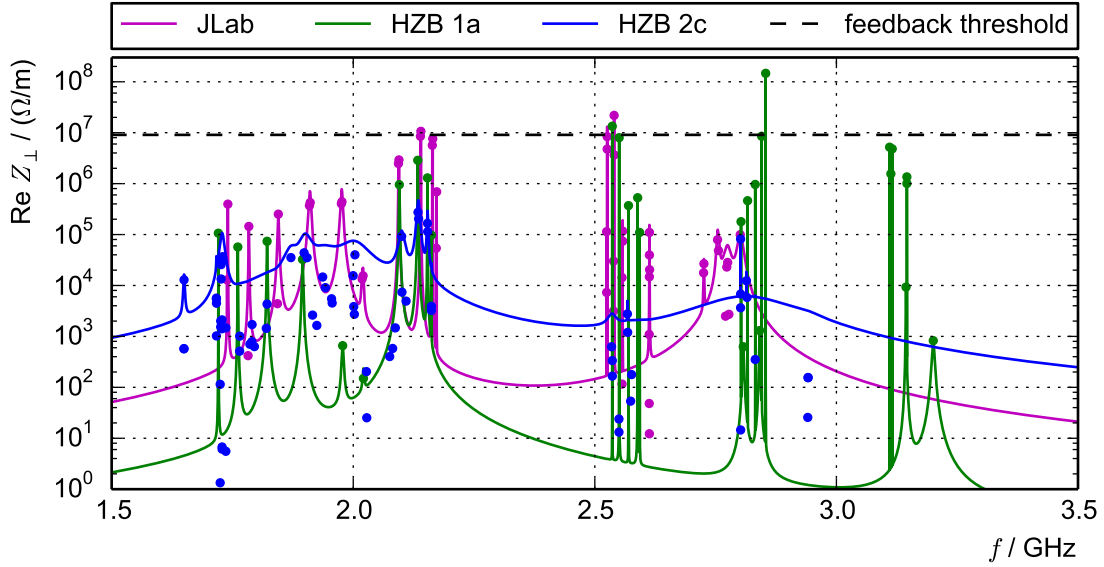


Figure 2.11: Comparison of transverse impedance of different HZB cavity models with the JLab HC model. The dashed line indicates the threshold given by the present feedback performance of BESSY II. Solid lines correspond to the sum over the Lorentzian functions of the HOMs while the dots depict their peak values.

Especially, it is assumed that there are no major contributions from HOMs above the limit of HOM calculations, which is typically around 3 GHz. The beam spectrum of a Gaussian bunch of length σ_z is Gaussian with an rms of $\sigma_f = 1/(2\pi\sigma_z)$. For a bunch length of $\sigma_z = 10$ ps one obtains $\sigma_f \approx 16$ GHz or $\Delta f_{\text{HWHM}} \approx 18.7$ GHz which means the effectiveness to drive an HOM halves at a frequency of 18.7 GHz compared to frequencies close to zero. Thirdly, the growth rate calculation was performed for one SC cavity only. The final BESSY VSR setup will consist of four SC cavities and the NC cavities. However, due to the frequency spread during fabrication, it is unlikely that the strongest HOMs will exactly add up. If both, the number of HOMs per cavity and their width are reasonably small, the over-all limit for stability will continue to be given by one, most critical, HOM if the number of cavities is increased.

2.6.2 Transient Beam Loading

If the fill pattern at BESSY VSR is uneven, e.g. if the bunch train is interrupted by gaps, the cavity systems interact with a non-constant current along the bunch train, which can be called transient beam loading. This section studies the effect

of transient beam loading from a beam dynamics point of view, focusing on the synchronous phase and effective length of the bunches. Further discussions on transient and average beam loading can be found in Chapter 3.

The beam loading causes the phases and amplitudes of all cavities to vary along the bunch train. Simulations show that for BESSY VSR this becomes a relatively large effect for the long bunches while the short bunches are much less strongly affected. The reason lies in the fact that long bunches in BESSY VSR are achieved by the cancellation of two large gradients, see Section 2.2, making it particularly sensitive to the momentary phases and amplitudes at the passage of the bunch. The result is a strong phase transient and a variation of the focusing gradient and, in turn, a variation of the bunch length and synchrotron frequency along the bunch train.

Most notably, no solution has been found where the average focusing strength of the long bunches could be significantly reduced compared to the present values of BESSY II. In other words, the majority of long bunches becomes shorter than desired which is of consequence for the question of Touschek life time, see Section 2.4.

Simulations for two different fill patterns are depicted in Figure 2.12 and Figure 2.13. Shown are optimized solutions with the attempt to minimize the over-all focusing gradient of the long bunches and to comply with the constraint of approximately zero net power transfer per turn for all SC cavities individually. The simulations are performed with a simplified tracking model. The NC cavities as well as the SC cavities are actively powered and controlled by a feedback loop. The feedback loop is programmed to be slow compared to bunch frequency (no change during a revolution period) but fast in terms of turn-to-turn adjustments. In terms of speed and power consumption, the simulated cavity feedback is not realistic. However, after a reasonable number of turns compared to the damping mechanisms, a self consistent equilibrium state is reached which clearly exhibits the features of the transient beam loading with an individual synchronous phase and length for each bunch. This equilibrium state is independent of the aforementioned feedback parameters.

The observed effect can be described in the following logic. The bunches perform beam loading on the cavities. As the SC cavities are operated at “zero crossing”, the beam loading is mostly a phase jump. The long bunch is located on opposite slopes for the 1.5 GHz cavity system and the 1.75 GHz cavity system. Thus, the phase jump caused by the bunch is of opposite sign. As a consequence, the 1.5 GHz cavity system and the 1.75 GHz cavity system obtain an increasingly large phase difference along the bunch train. The phase and amplitude of all cavity systems at the passage of each bunch is different. Hence, the resulting total cavity voltage has an individual shape for each bunch, having its zero crossing at different times for each bunch. This causes the phase transient. Furthermore, as the bunches are now

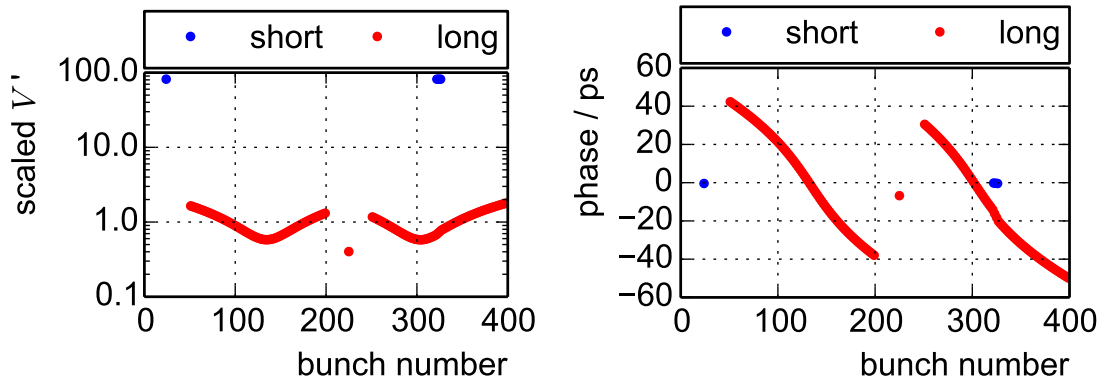


Figure 2.12: Calculations with the basic BESSY VSR fill pattern shown in Figure 2.5. Left: Focusing gradient, scaled to the nominal values of BESSY II of $V' = 2\pi \cdot 0.5 \text{ GHz} \cdot 1.5 \text{ MV}$. Right: Synchronous phase.

passing the cavity systems phases different from the nominal phase, the resulting cavity voltage is significantly different from the nominal values. The bunches end up at locations where the time derivative of the resulting voltage, i.e. the focusing gradient, is significantly different from the nominal value. The effect is especially large for the long bunches, causing most of the long bunches to be shorter than desired.

As mentioned before, the short bunches are less prone to the effect of small changes in the phases and amplitudes of the cavity systems. The phase transients are in the sub-ps regime, cf. Figure 2.14.

2.6.3 Robinson's Instability

Instabilities that arise from the interaction of the beam with the fundamental mode of a cavity are often referred to as Robinson's instability. There are two kinds of Robinson's instability.

Robinson's Instability of the First Kind

The Robinson's instability of the first kind, also known as "low intensity limit" or "ac Robinson's instability" is essentially a special case of the coupled bunch instabilities discussed earlier in this section. The fundamental mode of the cavity is a longitudinal resonator and behaves equivalently to any other longitudinal HOM. Its frequency is very close to a multiple of the bunch frequency, thus the corresponding

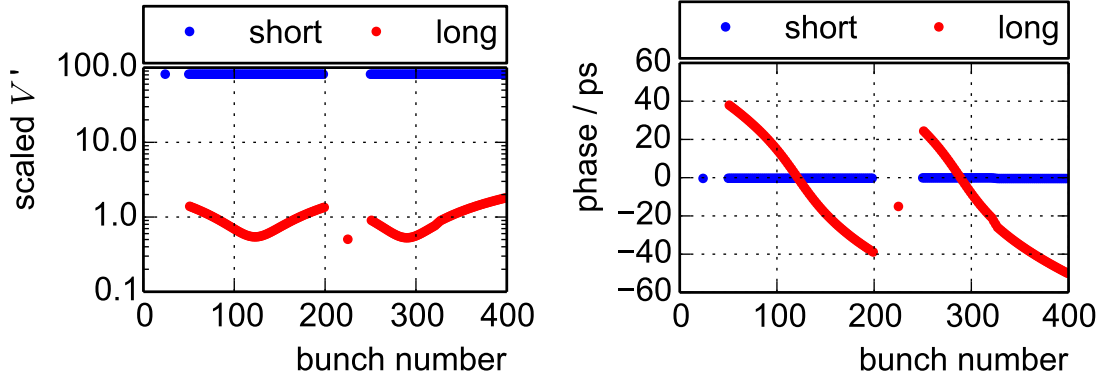


Figure 2.13: Calculations with the alternative BESSY VSR fill pattern shown in Figure 2.6. Left: Focusing gradient, scaled to the nominal values of BESSY II of $V' = 2\pi \cdot 0.5 \text{ GHz} \cdot 1.5 \text{ MV}$. Right: Synchronous phase.

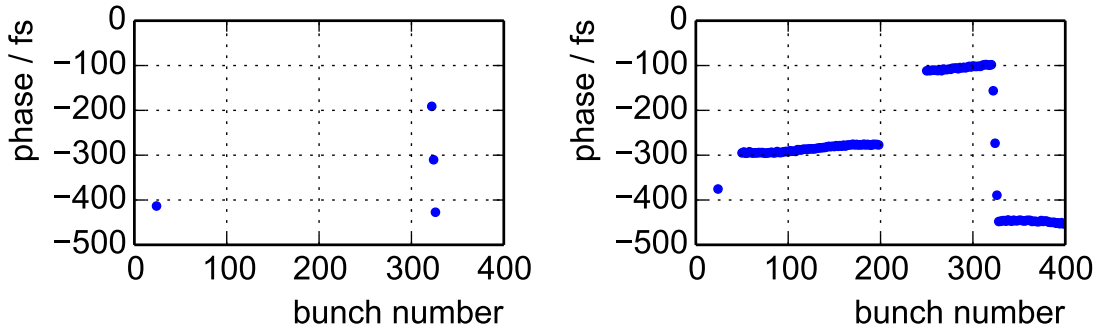


Figure 2.14: Synchronous phase of short bunches for the fill shown in Figure 2.5 (left) for the fill shown in Figure 2.6 (right).

coupled bunch mode is the mode number zero (all bunches oscillate in unison). The shunt impedance of the fundamental mode of a cavity is very large, consequently the corresponding instability is expected to be equally large.

For small complex frequency shifts, the growth rate of the instability can be approximately estimated by [21]

$$\tau^{-1} \approx \frac{f_{\text{rev}} I f_{\text{beam}} \alpha}{2(E/e) f_s} \text{Re} \left[Z_{\parallel}(f_{\text{beam}} + f_s) - Z_{\parallel}(f_{\text{beam}} - f_s) \right] \quad (2.7)$$

where f_{beam} is the harmonic of the beam frequency close to the fundamental mode, namely 1.5 GHz or 1.75 GHz. Basically, Equation (2.6) is evaluated at the frequencies of the positive and negative synchrotron side bands of the carrier signal close to the fundamental mode.

The real part of a resonator impedance is described by a Lorentzian peak which is a positive symmetric function around the resonance frequency. The sign of the growth rate in Equation (2.7) depends on the sign of the detuning $\Delta f = f_r - f_{\text{beam}}$ between the harmonic of the beam frequency f_{beam} and the fundamental mode of the cavity f_r . For BESSY II parameters, namely positive momentum compaction, the following general statement can be made:

$$\tau^{-1} = \begin{cases} < 0 & , \text{ if } \Delta f < 0 & \text{damped} \\ > 0 & , \text{ if } \Delta f > 0 & \text{anti-damped} \end{cases} \quad (2.8)$$

As described in Chapter 3, the values of Δf are quite strictly determined if R/Q and the accelerating voltage is fixed. In fact, the cavities providing a focusing gradient for the long bunches need to be operated on the Robinson damped side ($\Delta f < 0$) whilst the cavities providing a defocusing gradient for the long bunches need to be operated on the Robinson anti-damped side ($\Delta f > 0$).

Studies concerning the stability of the combined setup with 1.5 GHz cavities and 1.75 GHz cavities are discussed in Chapter 3, taking into account the low level RF feedback systems.

Robinson's Instability of the Second Kind

The Robinson's instability of the second kind, also known as "high intensity limit" or "dc Robinson's instability" is a criterion of phase stability. Violating the criterion will place the particle in an unstable potential well where no oscillation occurs [21]. The criterion can be calculated by knowledge of all cavity parameters including beam loading, synchronous phase and the cavity detuning. Equally to the Robinson's instability of the first kind, a change of the sign of the cavity detuning changes the outcome between stability and instability. More details are given in Section 3.6.

2.7 Low α Optics

The BESSY II storage ring provides synchrotron radiation in two different modes, bunches of 15 ps bunch length in the standard user mode and 3 ps short pulses in the low α mode. In the following the values of "zero current bunch length" will be used, i.e., 10 ps for the standard user mode and 2 ps in low α , not taking into account the bunch lengthening factor of 1.5 (see Section 2.1), since limits from single particle dynamics will be discussed.

For BESSY VSR it is planned to maintain the low α mode as an operating option aiming for shortest bunches in storage rings. As discussed in Section 1.3 and Section 2.1, the SC cavities will enhance the longitudinal focusing gradient by a factor of 80 allowing to store more current in short bunches and reducing the zero current bunch length by a factor of ≈ 9 , i.e., in the low α mode down to approximately 250 fs (rms) according to Equation (2.1). Table 2.3 compares lattice parameters, zero current bunch length σ_0 and bursting threshold current I_{th} of standard user mode and low α operation, as a basis for the following discussion.

Table 2.3: Comparison of lattice parameters, bunch length in the zero current limit σ_0 (rms) and the threshold bursting current I_{th} of standard user mode and low α operation.

	Standard	Low α
Emittance ϵ	5 nm rad	40 nm rad
Momentum comp. α	7.3×10^{-4}	3.5×10^{-5}
I_{th} at σ_0^{BII}	1.8 mA at 10 ps	0.045 mA at 2 ps
I_{th} at σ_0^{VSR} (short bunch)	0.8 mA at 1.1 ps	0.04 mA at 0.25 ps

Following these numbers the total BESSY VSR low α current stored in stable non-bursting bunches amounts to 13 mA, consisting of 150 bunches 2 ps long with a threshold current of 0.045 mA and another 150 bunches ≈ 300 fs long with a threshold current of 0.04 mA, taking into account single particle lengthening effects. If operating with currents at or below the bursting threshold, the Touschek loss rate will be smaller for the low α mode compared to the standard BESSY VSR mode. Additionally, it will be less sensitive to multi bunch effects as discussed in the previous Section 2.6. Beam loading will be reduced due to the lower current and in addition with the smaller momentum compaction factor α the growth rate of coupled bunch instabilities will be reduced at least by a factor of 50, see Equation (2.6).

It is also an option to operate the machine with higher currents in the bursting regime as it is already done in the present BESSY II low α mode on user demands. A current of 100 mA is stored, which is 7 times above the bursting threshold of 15 mA. The threshold currents and bunch length for BESSY VSR have been already listed in Table 1.2 and the bunch length scaling has been discussed in detail in Section 2.1. There, it has been pointed out that at threshold a bunch lengthening of 50% is taken into account due to the current dependent potential well distortion. Besides this multi particle effect, different single particle effects may also provide intrinsic bunch length limits becoming significant for the low α mode.

Although the present BESSY II low α optics can be used for BESSY VSR, an adapted optics have been developed increasing slightly the emittance, which is discussed in Section 2.7.1. In order to push for very short bunches in a storage ring with the BESSY VSR concept, relevant limiting single particle effects have been evaluated [24] and will be discussed in Section 2.7.2.

Multi particle effects may also limit the bunch length but are not discussed here. For example “intra beam scattering” of electrons within a bunch is a multi particle effect, which might introduce a lengthening. However, because of only few μA beam current in the low α optics, no lengthening effect is expected.

2.7.1 Low α Lattice

The low α optics used at BESSY II is discussed in detail in [25]. It provides an emittance of 30 nm rad and consists of 16 equal, completely symmetric DBA cells tuned to reduce the momentum compaction factor α by a factor of 20 from 7.3×10^{-4} to 3.5×10^{-5} . This is achieved by balancing the dispersion function in a way that its integral is reduced in the dipoles. In contrast to a standard DBA lattice the dispersion function is non-vanishing in the straight sections.

In order to avoid additional coupling effects between the horizontal and longitudinal plane in the straight section where the SC cavities will be installed for BESSY VSR, the 16-fold symmetry was broken and a dispersion free straight was introduced in the lattice. This modification increases the emittance to 40 nm rad. The optical functions for the adapted BESSY VSR low α lattice are shown in Figure 2.15.

Simulations have shown that the low α optics might be further improved reducing the emittance down to 5 nm rad. As a result all straight sections will have a low β function, which would hamper the injection. These studies are still in progress. However both optics, with and without dispersion in the SC cavities straight, are an option for BESSY VSR.

2.7.2 Bunch Length Limits

Different single particle effects may provide limitations for the achievable minimum bunch length. If these effects are independent of each other their contribution to the total width will add up quadratically. Two mechanisms, discussed in [26–28] drive the bunch lengthening:

- Longitudinal quantum radiation excitation and
- Horizontal-longitudinal coupling

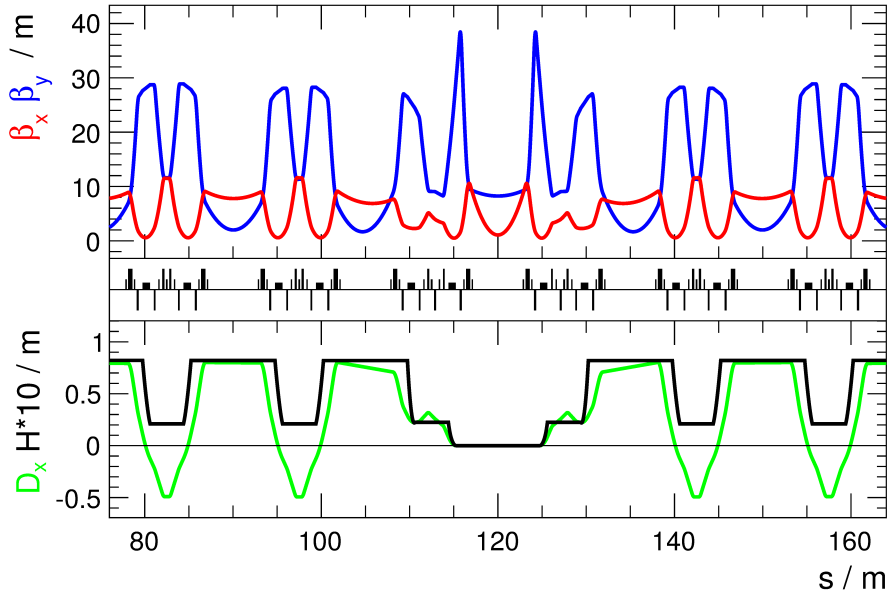


Figure 2.15: Optical functions of the adapted low α lattice for BESSY VSR. The dispersion D_x was tuned to zero in the straight where the SC cavities will be placed. The chromatic H function is a measure for a bunch length limit.

Longitudinal Quantum Radiation Excitation

The main idea of this limit [26] is based on the fact that the relative path length change $\Delta L/L_0$ of a radiating electron in a storage ring depends on the place where the photon emission took place. According to

$$\Delta L/L_0 = \alpha \Delta p/p_0 = \alpha \delta , \quad (2.9)$$

the path length for one revolution depends on the energy deviation δ and the momentum compaction α , which is defined for the global ring. For a radiating particle changing its energy, the partial momentum compaction $\bar{\alpha}$ becomes important and can be calculated for a storage ring by

$$\bar{\alpha} = \bar{\alpha}(s_i) = \frac{1}{L_0} \int_{s_i}^{L_0} \frac{D(s)}{\rho(s)} ds , \quad (2.10)$$

where L_0 is the ring circumference and s_i the point of photon emission. That means, when photon emission takes place the energy changes and the path lengthening depends on the new energy and the partial momentum compaction $\bar{\alpha}$ until a further photon is emitted. Where the photon emission takes place is a stochastic process provoking a smearing of the path length, i.e. a smearing in time. The

stochastic photon emission is a direct measure of the variance of the momentum compaction, named I_α defining the so called quantum radiation excitation bunch length limit σ_{re} . As a result of the radiation excitation, the bunch length cannot be reduced below [26]

$$\sigma_{\text{re}} = \frac{\delta_0 \sqrt{I_\alpha}}{f_0} \quad \text{with} \quad (2.11)$$

$$I_\alpha = \langle [\bar{\alpha}(s_i) - \langle \bar{\alpha} \rangle]^2 \rangle . \quad (2.12)$$

This intrinsic limit depends on the revolution frequency f_0 , the natural energy spread δ_0 and the variance of the momentum compaction factor I_α .

Table 2.4 shows the numbers for the variance of momentum compaction I_α and the associated bunch length limits at BESSY VSR when using a natural energy spread of $\delta_0 = 7 \times 10^{-4}$ and a revolution frequency of $f_0 = 1.25$ MHz.

Table 2.4: Variance of the momentum compaction I_α , the associated radiation excitation bunch length limit σ_{re} and zero current bunch length σ_0 , for standard and low α optics in BESSY VSR.

	Standard	Low α
Variance of mom. comp. I_α	$4.5 \cdot 10^{-8}$	$1.3 \cdot 10^{-8}$
Radiation excitation limit σ_{re}	0.12 ps	0.07 ps
Zero current bunch length σ_0	1.1 ps	0.25 ps

The radiation excitation bunch length limit was calculated to be $\sigma_{\text{re}} = 120$ fs for the standard user mode and $\sigma_{\text{re}} = 70$ fs for the low α mode, which is smaller than the zero current bunch length and therefore negligible. In low α operation this effect will increase the bunch length by only 4%.

Transverse Longitudinal Coupling

The zero current bunch length for ultra short bunches becomes additionally dependent on coupling effects between the horizontal and the longitudinal plane (and similar for the vertical plane), which can be distinguished in 1st order and higher order effects with respect to x, x' .

A 2nd order nonlinear effects was discussed in [28] pointing out that the path lengthening for one revolution ΔL_ξ is dependent on the betatron oscillation amplitude:

$$\Delta L_\xi = -2\pi \xi_x J_x . \quad (2.13)$$

It depends on the horizontal action $J_x = \epsilon/2$ of betatron motion and can be tuned by the chromaticity ξ_x . Using the emittance from Table 2.3 and the usual BESSY II chromaticity of $\xi_x \approx 3$ a bunch length limit of < 2 fs is expected and in comparison with the zero current bunch length of BESSY VSR insignificant.

A 1st order, linear path lengthening effect is generated when a particle with horizontal displacement is passing a dispersion producing section, e.g., dipole magnets [27]. Particle trajectories with different amplitudes and phases pass the dipole on different trajectories resulting in a longitudinal displacement (a rotation in $x - z$ plane) and another bunch length limit σ_H given by [27]

$$\sigma_H = \sqrt{\epsilon H}/c \quad \text{with} \quad (2.14)$$

$$H = H(s) = \gamma D^2 + 2\alpha D D' + \beta D'^2 . \quad (2.15)$$

H is the chromatic invariant function, which in turn depends on the optical Twiss functions γ, α, β and on the dispersion and its derivative D, D' . The coupling strength and consequently this bunch length limit is a local property depending on the emittance ϵ and the local H function. In case of a low α optics, the H function is typically non vanishing, as the dispersion, but it can be tuned to zero in few selected places by an appropriate optics. The H function is shown in Figure 2.15 for the adapted BESSY VSR low α lattice. It changes inside dipoles and stays constant between dipoles in the straight sections.

Using the adapted low α lattice the H function is 21 mm in the DBAs between the dipoles and nearly four times larger, 82 mm, in the straight sections where the IDs are placed. By means of Equation (2.14), the bunch length limit was calculated using an emittance of 40 nm. This limitation is then added up quadratically with the zero current bunch length of ≈ 250 fs yielding the effective bunch lengths σ_{eff} shown in Table 2.5.

Table 2.5: Bunch length limit from transverse longitudinal coupling and the effective bunch length.

	Trans. long. limit σ_H/fs	Effective bunch length $\sigma_{\text{eff}}/\text{fs}$
Cavity straight	0 fs	250 fs
Dipoles	100 fs	270 fs
ID straight	195 fs	320 fs

The effective “zero current bunch length” increases by 8% in the DBAs to 270 fs and by 28% in the straights to 320 fs. The tracking code elegant [29] was used to verify these numbers with long term tracking, showing excellent agreement with the analytical calculation. It seems feasible to reduce the horizontal-longitudinal coupling in one straight by changing the optics avoiding this limit. However, for this lattice, the residual bunch length given by limiting effects of coupling and radiation excitation would be 210 fs in the ID straights. By reducing the emittance for the low α lattice this limit may be further reduced.

In conclusion, BESSY VSR operated in the low α optics aims for shortest bunches in storage rings in a regime of a few hundred femtoseconds, where additional bunch length limiting effects have to be taken into account. For the current lattice, the effect given by radiation excitation provides a global limit of 70 fs. Another effect generated by transverse longitudinal coupling, gives a position dependent limit of 100 fs to 200 fs. This limit increase the zero current bunch length by nearly 30% in straight sections from 250 fs to 320 fs. For simplicity we set the zero current bunch length in the low α optics to 300 fs. Multi particle effects as the potential well distortion may induce a further lengthening, as discussed in Section 2.1.

2.8 Transparent Operation of the SC Cavities

From the beam dynamics point of view, transparent operation, i.e. “parking” of the SC cavities aims for two goals. Firstly, the influence of the cavities on the longitudinal phase space should be minimal to have the possibility to switch back to standard BESSY II operation. Secondly, other impedance effects, such as the effect of HOMs should be negligible. Therefore, the study is divided into two parts. First we discuss the interaction of the beam with the fundamental modes of the cavities and second the interaction of the beam with HOMs.

2.8.1 Fundamental Cavity Mode

If the number of individually tunable cavities of each frequency is an even number, the cavities can be tuned in such a way that they compensate each others fundamental mode. The imaginary part of the total impedance is then exactly zero at the beam frequency. Thus, there is no net focusing or defocusing that would influence the longitudinal phase space. The real part of the total impedance takes a small finite value, corresponding to the power dissipated in the cavities. An example illustrating this fundamental behavior is given in Figure 2.16. For a realistic parking scenario in BESSY VSR, numbers may vary. Especially, the cavities would

probably be detuned as much as possible to minimize the individual fields as well.

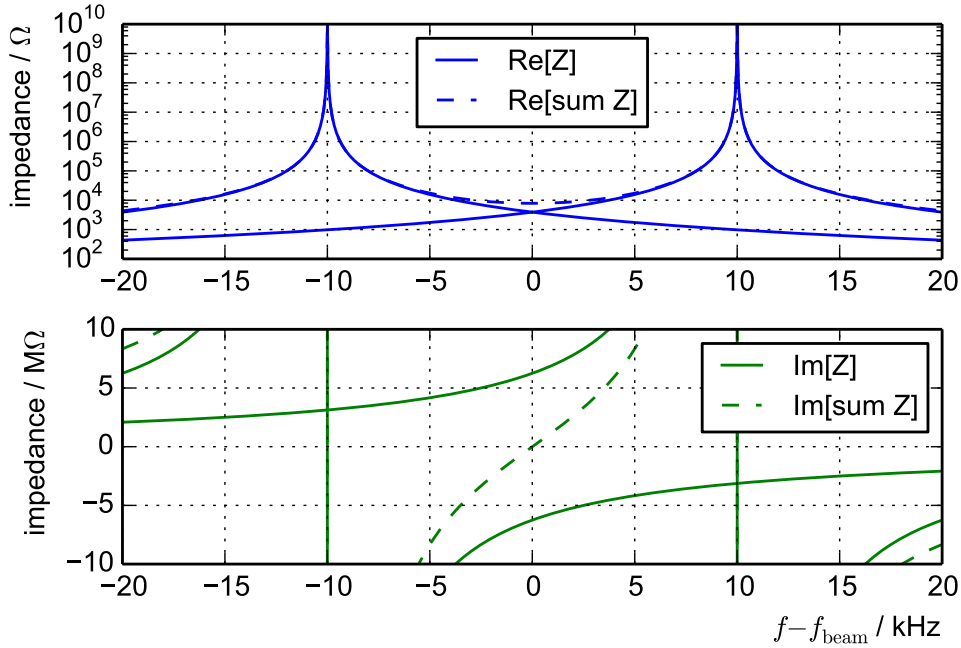


Figure 2.16: Depiction of the real (top) and imaginary part (bottom) of the impedances given by two 1.5 GHz cavities with a loaded quality factor $Q = 4 \cdot 10^7$ and $R_s^c/Q = 250 \Omega$ (circuit definition) tuned at plus and minus 10 kHz respectively.

If the number of individually tunable cavities of each frequency is an odd number, for example if only one cavity is brought into the ring, it is much more difficult to reduce the effect of the fundamental mode. In this case, one would try to detune the cavity as much as possible to minimize the induced voltage. Figure 2.17 shows the induced field of one cavity at 300 mA at different temperatures of the cavity and assuming a tuner range of ± 350 kHz. The temperature dependent frequency shift and change of quality factor is described in Section 3.2.4.

The calculation in Figure 2.17 was performed with the BESSY VSR hybrid fill pattern, a fill pattern with significant spectral components one and two revolution harmonics away from multiples of 250 MHz and 500 MHz respectively, owing to the fact that it exhibits two gaps. The beam spectrum in the vicinity of multiples of 500 MHz and odd multiples of 250 MHz is depicted in Figure 2.18. Notably, the fields induced by those spectral components oscillate at frequencies of the spectral components, causing potentially unwanted disturbance of the longitudinal phase

space along the bunch train. If a different fill pattern is chosen, the spectrum might significantly change. For example, a homogeneous fill exhibits no spectral components other than those at multiples of the bucket repetition frequency, which would lead to a situation where the solid lines in Figure 2.17 are the only remaining contributions to the induced voltages.

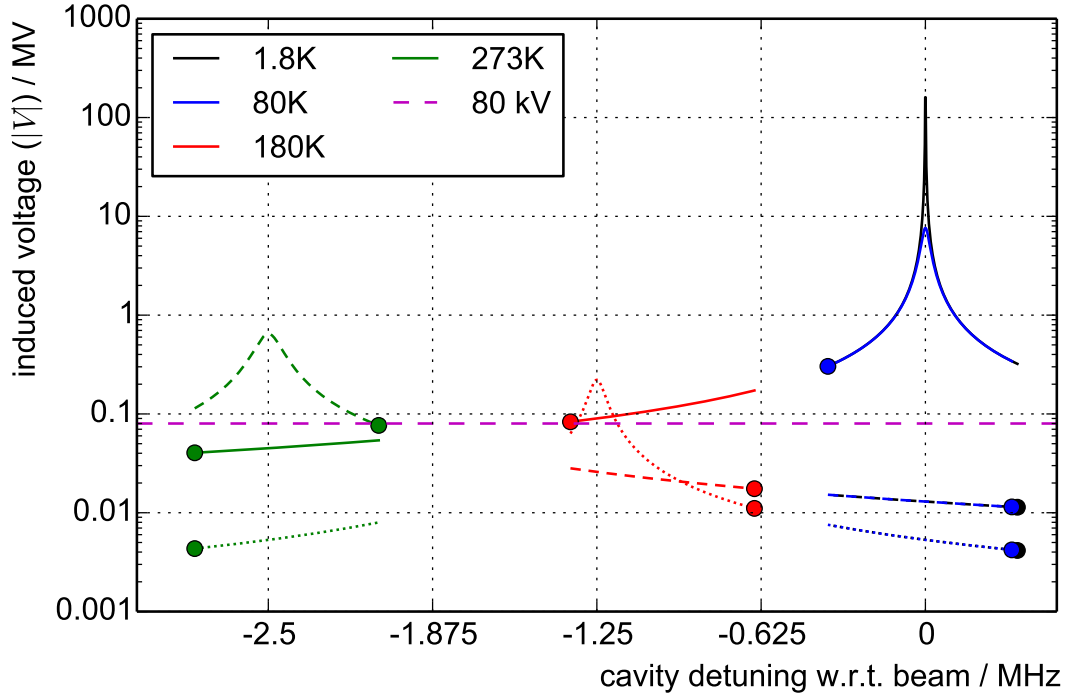


Figure 2.17: Induced fields of one parked 5-cell cavity at 300 mA with an assumed tuner range of ± 350 kHz at four different temperatures. The induced voltage is drawn individually for the corresponding components of the beam spectrum at frequencies $500 \text{ MHz} - h \cdot f_{\text{rev}}$ with $h = 0$ (solid line), $h = 1$ (dotted line) and $h = 2$ (dashed line). Each circular marker indicates the minimal induced field for a specific frequency and temperature.

In order to ensure that during parking the NC cavities dominate the longitudinal dynamics, an upper limit of the induced voltage of 80 kV is defined for any SC cavity. This limit corresponds to a maximum change of the bunch length of $\approx 10\%$ per cavity. Looking at Figure 2.17, the limit of 80 kV can not be fulfilled in a cold, superconducting state, where the induced voltage at 350 kHz detuning is still approximately 300 kV. At 180 K and 273 K, there is a tuning setting where the induced field of none of the frequency components is larger than about 80 kV.

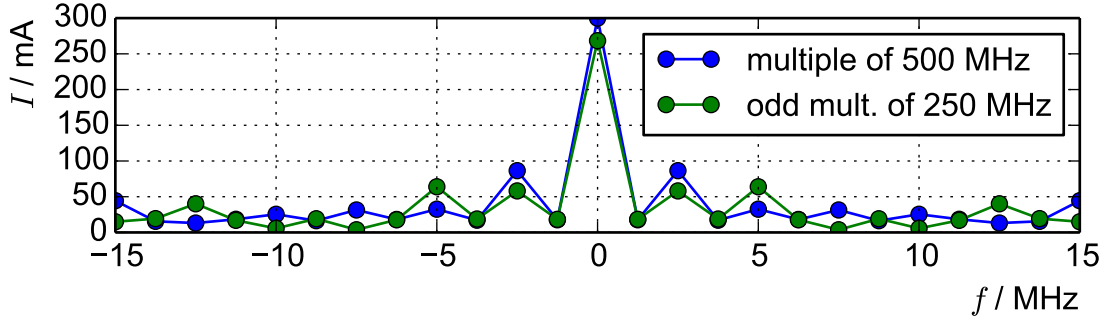


Figure 2.18: Beam spectrum in the vicinity of multiples of 500 MHz and odd multiples of 250 MHz for the default BESSY VSR hybrid fill pattern.

An alternative to the time consuming process of warming up the cavities is to utilize the existing 1.5 GHz NC Landau cavities to counter the induced fields of the cold SC cavities. A beam of 300 mA induces a total voltage of 225 kV in the Landau cavities, which provides an additional gradient for bunch shortening or lengthening. At BESSY II the focusing gradient of the NC 500 MHz cavities is reduced to $V'/(2\pi) = 0.4125 \text{ GHz MV}$ (55%), increasing the bunch length from 15 ps to 20 ps [30].

According to Figure 2.17, the induced voltage of one SC cavity with full detuning still yields 300 kV, only little more than the present Landau cavities. Thus, the focusing gradients can compensate each other almost completely, resulting in a gradient which affects the bunch length less than 10%.

If the cryomodule is equipped with only one SC 1.5 GHz cavity, it can also be operated like an additional Landau cavity providing a bunch shortening or lengthening with a voltage of up to 1/3 of the NC cavities, i.e., 500 kV. This gives a nearly zero slope for the total gradient at operation phase, leading to maximum lengthening and accordingly a maximum lifetime.

2.8.2 Higher Order Cavity Modes

If the number of individually tunable cavities of each frequency is an even number, the absolute value of detuning of each pair of cavities can be chosen quite freely within the limits of the tuner range. By this, one could try to find a tuning where the HOM excitation is minimal. However, this mitigation is limited by the fact that strongly damped HOM are of low quality factor, thus broad and therefore hard to avoid.

If the temperature of the cavities is increased, the HOM spectrum is significantly influenced, see Section 3.2.4 for details of this behavior. Most noticeably, the quality factor of the HOMs decreases with temperature, thus decreasing the shunt impedance, cf. Figure 2.19. However, strongly damped HOMs already exhibit a low quality factor at lowest temperatures which means little change with temperature is expected.

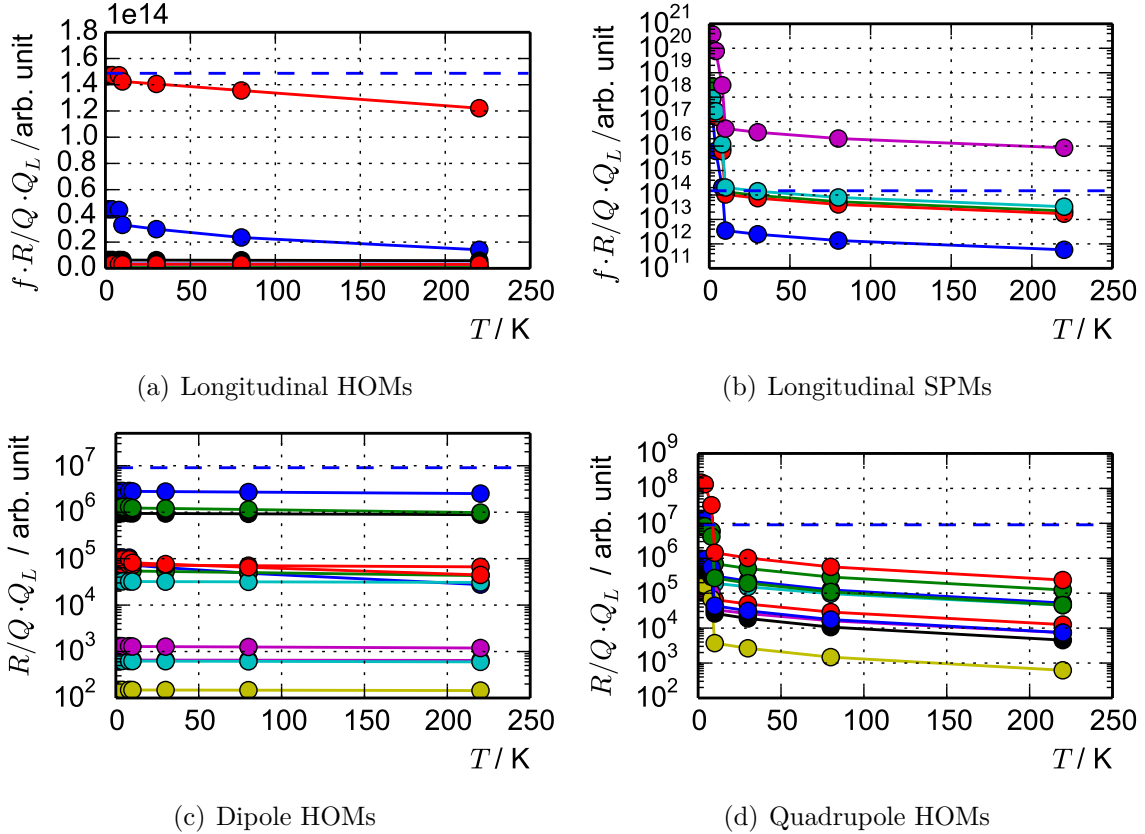


Figure 2.19: Shunt impedance of various higher order modes (cavity model HZB1a) as a function of cavity temperature. The dashed horizontal lines indicate the threshold defined by the bunch-by-bunch feedback of BESSY II, cf. Section 2.6. Note: As a conservative estimate, the quadrupole HOMs in (d) are interpreted as dipole modes, see text for details.

Figure 2.19(a) depicts the longitudinal HOMs. The decrease of the most harmful HOM is minor. This is because it is already damped strongly by the HOM dampers at the nominal temperature of 1.8 K. As this mode actually limits the over-all stability, the over-all gain by warm parking is little from an instabilities point of view.

Figure 2.19(b) depicts the fundamental pass band. As expected, the shunt impedance goes down strongly with the loss of superconductivity and the increase in temperature. At room temperature, the fundamental mode is still strong compared to the feedback threshold. This means, sufficient distance between a beam harmonic and the resonance frequency must be achieved by means of the tuner, which is pursued anyways to reduce the induced voltage, see Section 2.8.1. All other SPMs are then below the feedback threshold, which is important to know as their increased bandwidth increases the chance that they might be driven by the beam.

Figure 2.19(c) depicts the dipole modes. All modes are clearly below the threshold line and change little with temperature. This represents the fact that those modes are strongly damped, even at nominal operation temperature.

Figure 2.19(d) depicts the quadrupole modes (r^4 scaling) but treated as dipole modes (r^2 scaling) in terms of CBI. This is a conservative estimate and likely to be revised in the future. Those modes seem to be little damped at nominal operation temperature, thus the dependence with temperature is large. In normal conducting phase, this estimation predicts shunt impedances below the feedback threshold for the dipole instability.

The calculations shown in Figure 2.19 are performed with the model HZB1a, see Chapter 3 for details. As one can conclude from the figures, at room temperature all modes except the fundamental one are well below the required threshold. The more recent model HZB2c will certainly perform better due to its increased HOM damping.

2.9 Beam Injection

The injection at BESSY II takes place at full energy by means of a booster synchrotron that currently provides bunches with approximately 60 ps rms bunch length. Radiation safety requires an average injection efficiency of more than 90 % in order to operate in TopUp mode. The charge per injected bunch should be close to the maximum value of 0.4 nC so that the interval between injections is as long as possible and interruptions of the experiments by TopUp injections are reduced to the absolute minimum. At a beam lifetime of 6 h, one shot with 5 bunches every 180 s is necessary for an injected bunch charge of 0.4 nC. Experience shows that the TopUp conditions for BESSY II in user operation are fulfilled, especially maintaining an average injection efficiency in the order of 95 %. Preserving TopUp capability for BESSY VSR will be one of the major challenges.

In Table 2.6 some of the longitudinal parameters are collected which are relevant for the injection process. In the first row the longitudinal parameters of the current

Table 2.6: Longitudinal phase space characteristics of zero current bunches in synchrotron and storage ring.

	Bunch length σ_0/ps	Relative energy spread δ_0
BESSY II synchrotron		
$V_{\text{rf}} = 780 \text{ kV}$	58 (measured)	0.57×10^{-3}
$V_{\text{rf}} = 390 \text{ kV}$	88 (measured)	0.57×10^{-3}
BESSY II storage ring		
standard mode without 7 T-wiggler	10	0.7×10^{-3}
standard mode with 7 T-wiggler	15	1.0×10^{-3}
low α mode	2	0.7×10^{-3}
BESSY VSR		
standard mode	1.1	0.7×10^{-3}
low α mode	0.3	0.7×10^{-3}

BESSY II synchrotron are shown for two cavity voltages, V_{rf} . The second row contains these parameters for some of the operational modes of the storage ring. Bunch length and energy spread depend on the status of the 7 T-wiggler. In the low alpha mode bunches are shorter and even much shorter in the BESSY VSR mode as presented in the third row.

Presently, bunches delivered by the BESSY II synchrotron have the appropriate energy spread δ_0 , which is even slightly smaller than in the storage ring. However, the bunch length is mismatched and even more so for BESSY VSR. In case of an unmatched bunch length the injection efficiency suffers from two effects. Even if the beam is injected on-axis, so that the injected particles do not oscillate with large transverse amplitudes, after a quarter of the synchrotron period the energy spread of the injected bunch would be increased by the ratio of the bunch length of booster synchrotron and storage ring $\sigma_{\text{SYN}}/\sigma_{\text{SR}}$ (or the ratio of the bunch length of injected and stored beam).

With BESSY VSR this ratio becomes very large and the resulting energy spread will be larger than the energy acceptance of the ring, which is approximately $\delta_{\text{acc}} \sim 2.0\%$ to 2.5% . Therefore, the ratio of the bunch length in the synchrotron and storage ring should not exceed: $\sigma_{\text{SYN}}/\sigma_{\text{SR}} \sim 0.33 \cdot \delta_{\text{acc}}/\delta_0 < 8$. The factor 0.33 assures that almost all injected particles stay within the energy acceptance. In addition, the injection efficiency will suffer from the off-axis injection in case the

off-momentum transverse dynamic aperture is reduced. Usually, particles are lost more easily if they possess both a large oscillation amplitude and a large momentum offset at the same time.

Figure 2.20 shows a very recent measurement of the injection efficiency as a function of the bunch length ratio between synchrotron and storage ring. The experimental results support the above statement that both effects are important. The length of injected bunches should not exceed the bunch length in the storage ring by more than a factor of 8. Otherwise the injection efficiency will sharply drop below the 90 %-level.

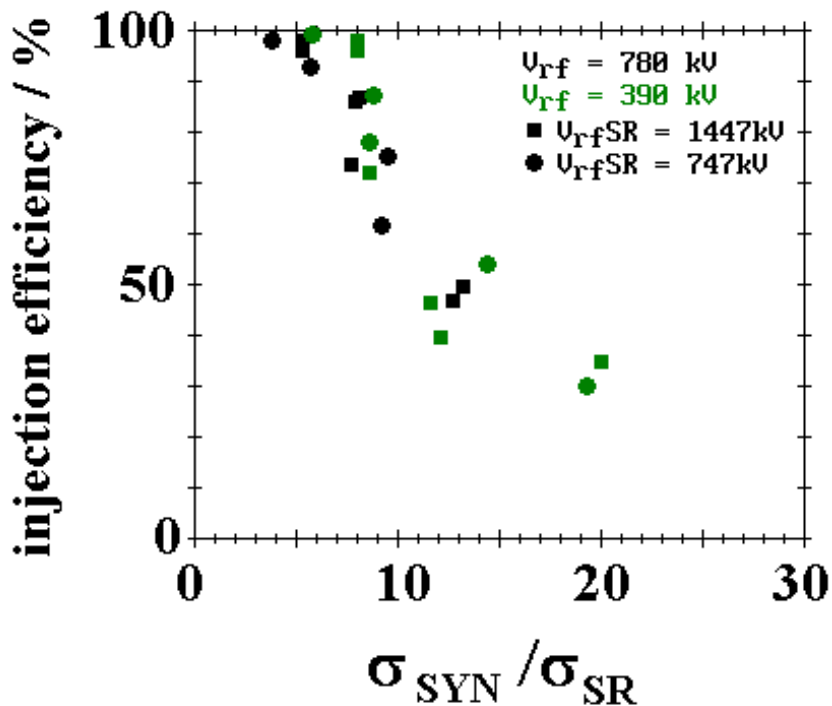


Figure 2.20: Injection efficiency as a function of the bunch length of the injected beam in relation to the bunch length in the storage ring. Bunch length variation in the storage ring by α -tuning and variation of the RF voltage and in the synchrotron by $V_{\text{rf}} = 390$ kV (green dots) and for $V_{\text{rf}} = 780$ kV in the synchrotron (black dots).

Ideally, a full energy linear accelerator providing picosecond bunches with sufficiently low energy spread (as for the MAX-IV project) would be the best choice as an injector into BESSY VSR. Cost and space requirements place this beyond the

current BESSY VSR proposal. In the following a few alternatives and mitigation strategies are discussed.

2.9.1 Ramping of the SC Cavities

The feasibility of a fast linear RF ramp for increasing the bunch length for injection has been studied from the beam dynamics point of view [16]. The cavities were modeled as kick-cavities with exact phase dependence without impedance, beam loading or generator model. The main concern is loss of halo particles due to an increased energy spread which is the consequence of a fast change of the longitudinal phase space when the SC cavities are ramped up. The inverse, a reduction in energy spread for fast down ramping of the cavities is also true but has no negative effect. Both mechanisms are shown in Figure 2.21 for a number of ramp velocities, where the ramping up starts at $t = 0$ ms and the ramping down at $t = 15$ ms. The investigation showed that if an increase of energy spread by a factor of two is assumed to be an acceptable limit, the SC cavities could be ramped up in as little as 10 ms.

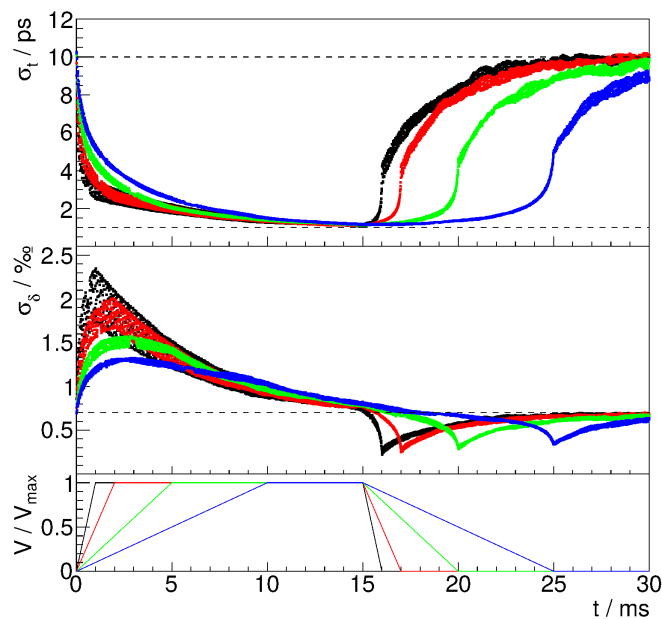


Figure 2.21: Bunch length (top), energy spread (center) and accelerating voltage (bottom) versus time for linear ramping of both SC cavity systems in 1 ms (black), 2 ms (red), 5 ms (green) and 10 ms (blue) [16].

However, ramping the cavities in a timescale of milliseconds seems to be impossible from an RF operations point of view due to the low power constraints, see Sec-

tion 3.6. Therefore, this method cannot provide high frequency TopUp injections but may serve as an option for experiments in decaying beam operation in early stages of the commissioning of BESSY VSR.

2.9.2 Short Bunches in the Booster Synchrotron

Without changing the circumference or the magnet lattice there are two possibilities to shorten bunches in the synchrotron which will be discussed briefly: low α operation and / or increasing the longitudinal gradient in the synchrotron.

The magnet lattice of the BESSY synchrotron is a missing magnet FODO-structure with 16-fold symmetry. By giving up this symmetry and with new and additional power supplies for the quadrupole magnets we could operate the synchrotron with a smaller momentum compaction factor than the current value of $\alpha \approx 0.033$. The optimization of this optics in terms of low emittance, injection and extraction of the beam needs improvements and these requirements might turn out to be impossible to meet. Moreover, if impedance issues of the vacuum chamber are ignored and only the shielded CSR interaction is taken into account the rough estimates presented in Table 2.7 indicate that the bunch length for stable acceleration of 0.4 nC per bunch has to be longer than 10 ps with the current capability of the RF system. The table also shows what could be achieved in terms of a stable beam in the synchrotron by a combination of increased RF gradient and reduced momentum compaction factor.

Table 2.7: Possible features of an upgraded BESSY II synchrotron providing short and stable bunches with a charge of 0.4 nC.

f_{rf}/GHz	V_{rf}/MV	mom. comp. α	σ_0/ps
0.5	0.5	$> 8.7 \times 10^{-4}$	> 10
3.0	2.0	$> 20 \times 10^{-4}$	> 3.1

Table 2.8 collects some of the features of the current BESSY synchrotron optics and the expected performance for an increased RF gradient to achieve bunch shortening. The emittance values quoted in parenthesis refer to the radiation equilibrium which would be reached on the down-ramp of the energy in the fast cycling booster synchrotron. Since we already extract the beam much earlier, on the up-ramp, the emittance is $\sim 30\%$ smaller, because the beam has not yet reached the equilibrium in the transverse dimensions. This value is quoted first. The transverse damping times are twice as long as in the longitudinal plane and the longitudinal equilibrium is reached already at earlier times.

Table 2.8: Features of the BESSY II synchrotron with the current optics and current working points ($Q_x = 5.9, Q_y = 3.39$) and longitudinal parameters with old and new RF system.

$\epsilon/\text{nm rad}$	$\alpha/10^{-2}$	V_{rf}/MV	f_{rf}/MHz	σ_0/ps	Comment
50(70.9)	3.31	0.5	500	62.2	with < 10 kW from old Klystron
50 (70.9)	3.31	1.0	500	44.0	with 38 kW from new solid-state-amplifier
50(70.9)	3.31	2.0	3000	12.7	new cavities and new RF power converter
50(70.9)	3.31	4.0	3000	9.0	new cavities and new RF power converter
50(70.9)	3.31	8.0	1500	9.0	superconducting RF

With the existing 500 MHz, 5-cell-cavity and the solid-state amplifier ($P = 38$ kW) the overall accelerating voltage can be doubled to 1 MV. This is still not enough and the bunch length would be a factor of 5 too long. Similar to the BESSY VSR case only the combination of a higher accelerating frequency and a higher accelerating voltage will deliver the desired short bunches. The required total gradient corresponds to 12 MV GHz. One realization could be a 3 GHz-standing-wave RF structures and suitable RF power sources.

In principle the White-circuits of the booster are working at 10 Hz. In TopUp mode the repetition rate is reduced administratively to 1 Hz in order to comply with radiation safety. This low duty cycle (100 ms/1 s) relaxes the demands on RF power and cavity cooling. A couple of straight sections with a length of up to 2 m are free to house the accelerating cavity structures.

There are a few issues with such a structure:

- An overall RF gradient of 12 MV GHz is required in order to reach the 7-fold reduction of the bunch length down to 9 ps. In Section 3.5 some of these issues with such an RF system are described in more detail.
- Most likely coupled bunch instabilities will occur due to excited HOMs in the cavities. Longitudinal instability of that type is also observed with the 5cell-500 MHz-cavity today. Fighting the instability will require bunch-by-bunch feedback systems. Space for suitable transverse or longitudinal kickers

is available in the synchrotron. In case a feedback system against coupled bunch modes cannot be realized a single bunch has to be accelerated in the synchrotron. The permanent injection of only a single bunch will lead to shorter injection intervals as of today.

- The installation of a 3 GHz-cavity string will reduce the available transverse acceptance of the synchrotron. This could potentially have an impact on the injection and extraction process. Such an aperture reduction should be mimicked by mechanical scrapers and investigated experimentally. The scrapers need to be installed in the synchrotron in the location foreseen for the cavity string.
- Once the aperture limitations turn out to be acceptable the installation of a similar cavity-string for test purposes could be considered. The more closely this cavity comes to the final design the better.

Conclusion

At the moment, the increase of RF gradient seems to be the best approach to efficiently inject into the short bunches foreseen for BESSY VSR and still be compatible with the radiation safety requirements for TopUp operation. In addition, a reduction of the momentum compaction factor in the synchrotron may be applied. TopUp injections into the short bunches of the BESSY VSR low α mode seem to be impossible without a dedicated LINAC. However, TopUp may not be needed in this operation mode as beam lifetime is expected to be large.

References

- [1] A. Chao and J. Gareyte. “Scaling Law for Bunch Lengthening in SPEAR II”. In: *Particle Accelerators* 25 (1990), pp. 229–234 (cit. on p. 30).
- [2] Y. Cai. “Theory of Microwave Instability and Coherent Synchrotron Radiation in Electron Storage Rings”. In: *Proceedings of IPAC* (2011), p. 3774 (cit. on pp. 30–34).
- [3] P. Kuske. *Private Communications*. Jan. 2015 (cit. on pp. 30, 32, 34).
- [4] P. Kuske. “Calculation of Longitudinal Instability Threshold Currents for Single Bunches”. In: *Proceedings of ICAP2012 THSDC3* (2012), pp. 267–269 (cit. on pp. 30, 32).

-
- [5] M. Ries. “Nonlinear Momentum Compaction and Coherent Synchrotron Radiation at the Metrology Light Source”. PhD thesis. Humboldt-Universität zu Berlin, 2013 (cit. on pp. 30, 32, 34).
- [6] B. Zotter. *Potential-Well Bunch Lengthening*. Tech. rep. CERN-SPS-81-14-DI. 1981 (cit. on p. 32).
- [7] J. Feikes et al. “Sub-Picosecond Electron Bunches in the BESSY Storage Ring”. In: *Proceedings of EPAC 2004* (2004), pp. 1954–1956 (cit. on p. 33).
- [8] P. Kuske. *Longitudinal Stability of Short Bunches at BESSY*. Conference Website. Talk at ICFA Mini-Workshop on „Frontiers of Short Bunches in Storage Rings“ INFN-LNF. Nov. 2005 (cit. on p. 34).
- [9] K. L. F. Bane, Y. Cai, and G. Stupakov. “Threshold studies of the microwave instability in electron storage rings”. In: *Phys. Rev. ST Accel. Beams* 13 (10 Oct. 2010), p. 104402. URL: <http://link.aps.org/doi/10.1103/PhysRevSTAB.13.104402> (cit. on p. 34).
- [10] P. Kuske. “CSR-driven Longitudinal Single Bunch Instability Thresholds”. In: *Proceedings of IPAC2013* (2013), pp. 2041–2043 (cit. on p. 34).
- [11] J. Feikes, P. Kuske, and G. Wuestefeld. “Towards Sub-picoseconds Electron Bunches: Upgrading Ideas for BESSY II”. In: *Proceedings of EPAC2006* (2006), pp. 157–159 (cit. on pp. 34, 36).
- [12] G. Wüstefeld et al. “Coherent THz Measurements at the Metrology Light Source”. In: *Proceedings of IPAC2010 WEPEA015* (2010), pp. 2508–2510 (cit. on p. 34).
- [13] G. Wüstefeld et al. “Simultaneous long and short electron bunches in the BESSY II storage ring”. In: *Proceedings of IPAC2011 THPC014* (2011), pp. 2936–2938 (cit. on p. 36).
- [14] A. Piwinski. *The Touschek effect in strong focusing storage rings*. Tech. rep. DESY-98-179. 1998 (cit. on pp. 40, 41).
- [15] K. Ott. “Radiation Protection Issues of the TopUp Operation of BESSY”. In: *Proc. 7th Intern. Workshop on Radiation Safety at Synchrotron Radiation Facilities* (2013) (cit. on p. 40).
- [16] M. Ruprecht et al. “Single Particle Tracking for Simultaneous Long and Short Electron Bunches in the BESSY II Storage Ring”. In: *Proceedings of IPAC2013 WEOAB101* (2013), pp. 2038–2040 (cit. on pp. 43, 67).
- [17] A. Neumann et al. “CW Measurements of Cornell LLRF System at HoBi-CaT”. In: *Proceedings of SRF2011 MOPO067* (2011), pp. 262–266 (cit. on pp. 43, 44).
- [18] M. Ruprecht et al. “Analysis of Coupled Bunch Instabilities in BESSY-VSR”. In: *Proceedings of IPAC2014 TUPRI043* (2014), pp. 1659–1661 (cit. on p. 45).

- [19] A. Schällicke et al. “Status and Performance of Bunch-by-bunch Feedback at BESSY II and MLS”. In: *Proceedings of IPAC2014* TUPRI072 (2014), pp. 1733–1735 (cit. on p. 45).
- [20] A. W. Chao. *Physics of Collective Beam Instabilities in High Energy Accelerators (Wiley Series in Beam Physics and Accelerator Technology)*. 1st ed. Wiley-VCH, Jan. 1993 (cit. on p. 46).
- [21] K. Y. Ng. *Physics of Intensity Dependent Beam Instabilities*. World Scientific Publishing Company, Dec. 2005 (cit. on pp. 46, 52, 53).
- [22] M. Wang, P. Chou, and A. Chao. “Study of uneven fills to cure the coupled-bunch instability in SRRC”. In: *Proceedings of PAC2001* 3 (2001), pp. 1981–1983 (cit. on p. 47).
- [23] F. Marhauser. *JLab High Current Cryomodule Development*. Conference Website. Proceedings of ERL2009. 2009. URL: http://accelconf.web.cern.ch/AccelConf/ERL2009/talks/wg307_talk.pdf (cit. on p. 47).
- [24] P. Goslawski et al. “The low- α lattice and bunch length limits at BESSY-VSR”. In: *Proceedings of IPAC2014* MOPRP058 (2014), pp. 216–218 (cit. on p. 55).
- [25] J. Feikes et al. “Compressed Electron bunches for THz generation - Operating BESSY II in a dedicated low alpha mode”. In: *Proceedings of EPAC 2004* (2004), pp. 2290–2292 (cit. on p. 55).
- [26] Y. Shoji. “Longitudinal radiation excitation in an electron storage ring”. In: *Physical Review E* 54.5 (1996), R4556 (cit. on pp. 55–57).
- [27] Y. Shoji. “Bunch lengthening by a betatron motion 5 in quasi-isochronous storage rings”. In: *Physical Review Special Topics - Accelerators and Beams* 7 (2004), p. 090703 (cit. on pp. 55, 58).
- [28] Y. Shoji. “Dependence of average path length betatron motion in a storage ring”. In: *Physical Review Special Topics - Accelerators and Beams* 8 (2005), p. 094001 (cit. on pp. 55, 57).
- [29] M. Borland. *elegant*. Advanced Photon Source LS-287. Sept. 2000 (cit. on p. 59).
- [30] W. Anders and P. Kuske. “HOM Damped NC Passive Harmonic Cavities at BESSY”. In: *Proceedings of the 2003 Particle Accelerator Conference* (2003), pp. 1186–1188 (cit. on p. 62).

3 Superconducting RF Systems

The BESSY VSR proposal places highest demands on the operation and design of the superconducting radio frequency (SRF) cavities pushing the limits to new frontiers when comparing to existing projects and running particle accelerators. The two higher harmonics systems will have to supply a high continuous wave (CW) voltage, therefore experiencing high peak fields and interact with a high current beam, which includes transients by one or more clearing gaps and some sets of single bunches to cover the needs of a modern synchrotron based light source and user facility. For example the BESSY VSR cavities will operate at an order of magnitude higher voltage than the fundamental SOLEIL cavities while accelerating a similar average beam current [1]. The same holds true for higher harmonic SRF systems as presented in [2] or as they are in use at SLS and ELETTRA [3]. Proposals for Super B-factories also discussed the layout of RF systems for high current storage rings including uneven fill patterns. Also here, as discussed in e.g. [4], the required gap voltage per cavity is smaller and huge RF power installations were foreseen. For those the effect of transient beam loading and also Robinson instabilities could be tackled by artificially reducing the cavity shunt impedance R/Q which is not an option for an SRF system operating at high CW field level.

The RF design thus has to allow strong higher order mode (HOM) propagation and following damping to mitigate transverse and longitudinal coupled bunch motions. But it also needs to minimize the RF losses and peak fields on the superconductor's surface to avoid the danger of quenches, local heating and field emission to name a few. Especially local heating and thus the possibility of reaching the limit of stable stratified helium heat flow, poses the danger of additional microphonics and thus trip of the field by Lorentz-force detuning coupled ponderomotive instabilities. This effect was e.g. observed with a superconducting RF photo-injector cavity [5].

From the operations point of view any excitation of the same pass band modes (SPM) of the fundamental mode's passband has to be suppressed as they are of similar loaded quality factor as the accelerating π mode and may strongly contribute to a longitudinal beam instability. Due to the zero-crossing operation there is a strong reactive beam loading contribution by the 300 mA long pulse beam and the detuning of the cavity has to be kept close to the optimum in order to allow operation at less than 10 kW. Any deviation from this steady state detuning by

beam transients of the gap, bunch current decay and by the TopUp mode refilling of the machine has to be taken into account to determine the cavity working point.

Table 3.1 summarizes the RF properties of the BESSY VSR scheme for the two higher harmonic cavity (HHC) systems.

Table 3.1: Required SRF cavity parameters of the higher harmonic systems for a factor of nine reduction in bunch length and assuming an even filling of the high current long pulse buckets.

Parameter	Expected value
RF frequencies	1.5 GHz, 1.75 GHz
Voltage at 1.5 GHz	20.0 MV
Voltage at 1.75 GHz	17.14 MV
Mean acc. field at 1.5 GHz	20.0 MV/m
Mean acc. field at 1.75 GHz	20.0 MV/m
Cell number at 1.5 GHz	2×5 cell
Cell number at 1.75 GHz	2×5 cell
$I_{\text{avg. beam}}$	300 mA
Cavity detuning for beam loading at even filled buckets	−11.25 kHz for 1.5 GHz 15.3 kHz for 1.75 GHz
Avg. P_{forward} per cavity (1.5 GHz, 1.75 GHz)	1.49 kW, 1.0 kW
Q_{loaded}	$5 \cdot 10^7$
R/Q per cell $\text{TM}_{010,\pi}$	$\geq 100 \Omega$
ϕ_{acc}	$90^\circ, -90^\circ$

Here the parameters¹ are given assuming a constant filling of the ring without clearance gap. For the more complex bunch patterns envisaged for BESSY VSR the optimum tuning angle was determined by means of RF simulations shown in Section 3.6. This is even more important, as it is intended to keep the capital investment costs as low as possible, to remain within the ≤ 10 kW fundamental power level allowing the usage of existing solid state RF sources and power couplers.

¹Throughout this Chapter the effective accelerator convention for the normalized shunt impedance is used: $R/Q = (V_0 T_r)^2 / (\omega U)$, with V_0 the integrated on-axis voltage, T_r the transit time factor for a $\beta = v/c \approx 1$ particle, ω the angular frequency and U the stored energy within the resonator as given in [6] p. 43 Equation (2.55). The impedance Z is usually given in circuit definition as in Chapter 2.

Outline of this Chapter

To cover all aspects for the SRF system, this chapter is arranged in six Sections. First an overview of the required SRF parameters is given (Section 3.1) including aspects as optimum bath temperature of the helium system, followed by the Section describing the RF design process of the cavities, especially with emphasis on the damping of the HOMs (Section 3.2). Sections 3.3 and 3.4 describe the needed ancillary components and the module design. Here, the tuning system and high power RF coupler are of major importance as their designs set the boundary conditions for the operating conditions. The module design has to take care of housing the mechanically complex cavity and HOM damping into a rather limited available space of 4.0m including the cold to warm transitions and means to minimize the deterioration of the cavity surface quality by the dirty storage ring environment. Section 3.5 shows possible solutions and parameters for the RF sources which can be utilized for this proposal. Finally Section 3.6 tackles most of the operational aspects for the HHC systems and a possible layout for a low level RF control system (LLRF).

3.1 SRF Parameters

For this project, two different higher harmonics SRF cavities will be developed in order to accomplish bunch compression operating at zero crossing. Specifically, 3rd and 3.5rd harmonics were chosen with 1.5 GHz and 1.75 GHz. As it was previously pointed out, one of the main restrictive topics about the cavity design is CW operation with high accelerating field of $E_{\text{acc}} = 20 \text{ MV/m}$. This fact forces the design to be extremely careful with the geometry of the cavity cell shape in order to ensure acceptable field limits on the Nb surface that could potentially lead to discharges or quenching (see Table 3.2). In addition, the beam current is high, $I_{\text{beam}} = 300 \text{ mA}$, and thus, HOM damping becomes a key issue. The HOM damper section has to be accurately defined so the maximum amount of HOM power can be damped. A final cavity design must ensure stable beam operation, avoiding couple bunch instabilities excited by HOMs, which has been studied in detail and is presented in Chapter 2. Possible “parking” scenarios for the HHC must be also considered when a failure occurs (e.g. tuner failure) or when no BESSY VSR operation but normal storage ring operation is desired.

Due to the zero crossing operation of BESSY VSR close to zero net beam loading is expected. Thus weak RF coupling and therefore high external quality factors can be used ($Q_{\text{ext}} \geq 5 \times 10^7$) with relatively low power requirements $P \leq 10 \text{ kW}$, see Section 3.6. When parking the cavity at increased temperature, a change in the

coupling factor for the fundamental power coupler could be needed so the impedance can be changed.

Low power requirements allows us to make use of a coupler concept similar to the Cornell 60 kW power coupler [7] which is attractive because its coupling can be adjusted. This fact will leave some additional power reserve for future upgrades. Thus, such a coupler represents an advantage compared to standard waveguide approaches since coupling can be changed in a way that the impedance for the fundamental π -TM₀₁₀ mode will not compromise the parking mode. Nevertheless for design convenience we have started by considering fixed coupling waveguide power couplers that will be then replaced by the Cornell-type coaxial couplers. Table 3.2 shows a summary of the target RF design parameters.

Table 3.2: RF design parameters.

Parameter	Target value
E_{acc}	20 MV/m
I_{beam}	≤ 300 mA
$E_{\text{pk}}/E_{\text{acc}}$	≤ 2.3
$B_{\text{pk}}/E_{\text{acc}}$	≤ 5.3 mT / (MV/m)
R/Q	≥ 100 Ω
K for TM ₀₁₀	≥ 3 %
μ_{ff} for TM ₀₁₀	≥ 97 %

The space available for the installation in the ring defines the number of cavities and the number of cells per cavity. For BESSY VSR, the usage of one low β straight section is foreseen. As a consequence, modules are restricted to a total length of 4 m. An optimum choice of real estate gradient and limited field level led to a choice of two five cell cavities each (1.5 GHz, 1.75 GHz). A higher number of cells increases the probability of trapped higher order modes within the inner cells.

In order to determine the suitable operation temperature the dynamic cryogenic losses have been calculated using the cavity parameters reported in Table 3.3, where the RF power dissipation P_{diss} in the cavity walls for the fundamental π -TM₀₁₀ mode is given by:

$$P_{\text{diss}} = \frac{(V_{\text{acc}})^2}{Q_0 \cdot R/Q} . \quad (3.1)$$

To compute the cryo-losses at different temperatures it is important to determine the Q_0 for any of those possible operation points. Thus, the Q_0 factor can be evaluated by means of the expression relating the geometry factor G , the R_{BCS} resistance

(proportional to the frequency and temperature) and the residual resistance R_{res} (material properties and cool down conditions [8]). Since G remains constant for the operating mode, the set of different values for Q_0 at different temperatures can be easily evaluated:

$$Q_0 = \frac{G}{R_{\text{BCS}} + R_{\text{res}}} . \quad (3.2)$$

In order to obtain realistic values of R_{BCS} for different cold temperatures and frequencies, the code SHRIMP [9] has been used. Field emission effects are included by accounting for $R_{\text{res}} = 23 \text{ n}\Omega$. This value is extracted from experimental data on 5-cell SRF cavities developed at JLab [10]. Figure 3.1 depicts the evolution of the unloaded quality factor Q_0 for the π -TM₀₁₀ mode at the two harmonic frequencies (1.5 GHz, 1.75 GHz) for a possible superconducting temperature range.

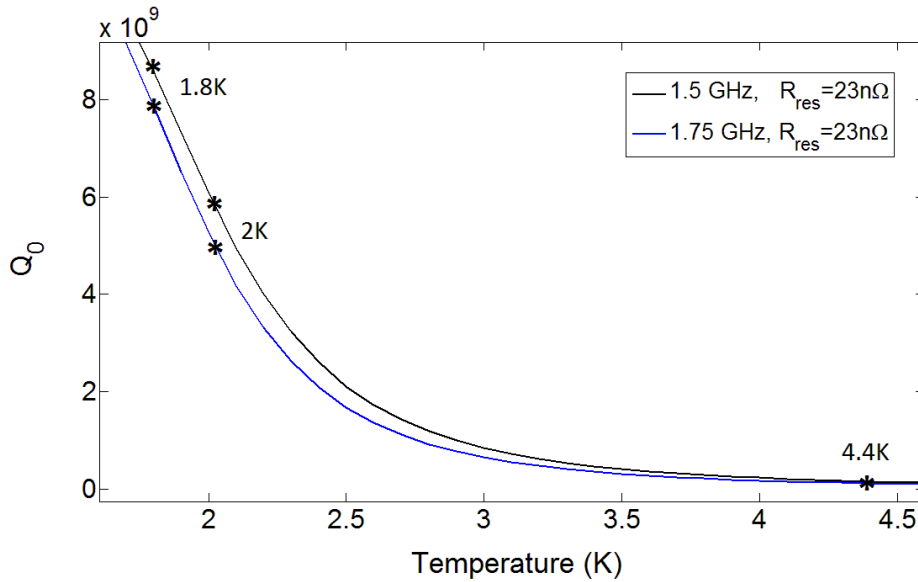


Figure 3.1: Evolution of the unloaded quality factor Q_0 with temperature for the two operating frequencies. An effective residual resistance of $R_{\text{res}} = 23 \text{ n}\Omega$ accounts for field emission [10].

Currently the project cryo capabilities allows a maximum of 35 W dynamic load per cavity at 1.8 K. Table 3.3 shows a compilation of the main RF parameters with the expected Q_0 and dynamic load per cavity at the two possible operating temperatures. Both temperatures, 1.8 K and 2 K, would be feasible with respect to the dynamic losses. Nevertheless, the fact of having higher unloaded quality factors for the 1.8 K case offers more stable behavior, since operation at lower pressure reduces the microphonics detuning. Since the preparatory phase operation will run at higher temperature of 4.4 K the Q_0 is also stated leading to a maximum

achievable accelerating field of 3.52 MV/m at dynamic losses of 35 W (no field emission considered).

Table 3.3: Compilation of SRF parameters for the expected number of cells and cavities at the two high harmonic frequencies (1.5 GHz, 1.75 GHz). (*) The values R/Q and G for 1.75 GHz cavity have been assumed to be equal to the 1.5 GHz one for calculations (not yet calculated).

Cavity parameter	1.5 GHz	1.75 GHz
Frequency	1.5 GHz	1.75 GHz
Number of cells	5	5
Number of cavities	2	2
Voltage	20.0 MV	17.14 MV
Accelerating field	20.0 MV/m	20.0 MV/m
Cavity length	0.5 m	0.43 m
(R/Q)	525 Ω	525 Ω *
G	280 Ω	280 Ω *
Q_0 at E_{acc} ($R_{\text{res}} = 23 \text{ n}\Omega$)		
@1.8 K	8.56e9	7.86e9
@2.0 K	6.1e9	5.2e9
@4.4 K	1.66e8	1.26e8
Dynamic losses per cavity		
@1.8 K ($R_{\text{res}} = 23 \text{ n}\Omega$)	22.3 W	17.8 W
@2.0 K ($R_{\text{res}} = 23 \text{ n}\Omega$)	31.2 W	26.9 W
Total gradient	60.0 MV GHz	
Module electrical length	1.86 m	

3.2 Cavity Design

The cavity design is currently focused on fulfilling the requirements for the 1.5 GHz five cell high harmonic cavity. Once this step is completed, the conclusions obtained will be used on scaling the model to the second frequency (1.75 GHz). Although a higher frequency is needed in this case no major modifications are expected. Nevertheless, the same design steps as for the 1.5 GHz case will be repeated. The design procedure is divided in the following phases.

- Mid-Cell design. Parametric studies of the optimum mid-cell geometry accomplishing the RF specifications depicted in Table 3.2. Special attention devoted to RF parameters: R/Q , G , E_{pk}/E_{acc} , B_{pk}/E_{acc} and coupling factor K .
- Full five-cell design with end-cells tuning to obtain field flatness.
- End-Group design. HOMs couplers and power coupler studies for damping and loading.
- If needed steps one and two are repeated to perform minor adjustments.

3.2.1 Mid-Cell Design

The current mid-cell design presented in this sections takes as starting point designs from Cornell [11] and JLab [12]. As it was previously pointed out damping higher order modes is an important issue when designing an SRF cavity and in particular for the BESSY VSR project this aspect plays a crucial role. Thus it is vital to ensure a proper damping and avoiding trapped modes inside the structure. A general indicator of how easy the modes can be propagated along the structure is the coupling factor K , characterizing the electromagnetic coupling between adjacent cells. K is determined by the cell geometry, especially the diameter of the iris. The coupling factor is defined by

$$K (\%) = 2 \frac{f_\pi - f_0}{f_\pi + f_0} \cdot 100 , \quad (3.3)$$

where f_π and f_0 represent the resonance frequency for the π and 0 modes respectively. In our design the iris diameter has been increased to $\varnothing = 71.34$ mm. This value is slightly larger than in JLab and Cornell models in order to obtain a higher cell to cell coupling factor for the fundamental mode as shown in Table 3.4 [13]. This increase allows the most probable trapped modes to propagate more efficiently through coupling from the inner cells to the outer ones. A final set of mid-cell parameters fulfilling specifications has been obtained by performing

parametric 2D/3D electromagnetic calculations in Comsol Multiphysics [14] with the main figures of merit (R/Q , G , E_{pk}/E_{acc} and B_{pk}/E_{acc}) as design goal. Comsol Multiphysics was chosen due to the possibility to perform fast electromagnetic 2D/3D calculations. Results have been validated with SUPERFISH [15]. Figure 3.2 shows the cell geometry for the two base models used with the fundamental π - TM_{010} excited and can be compared to the mid-cell layout for the HZB design depicted in Figure 3.3. As it can be observed the cell-shape obtained with enlarged iris represents a transition in terms of roundness of the equator between the Cornell and the JLab models.

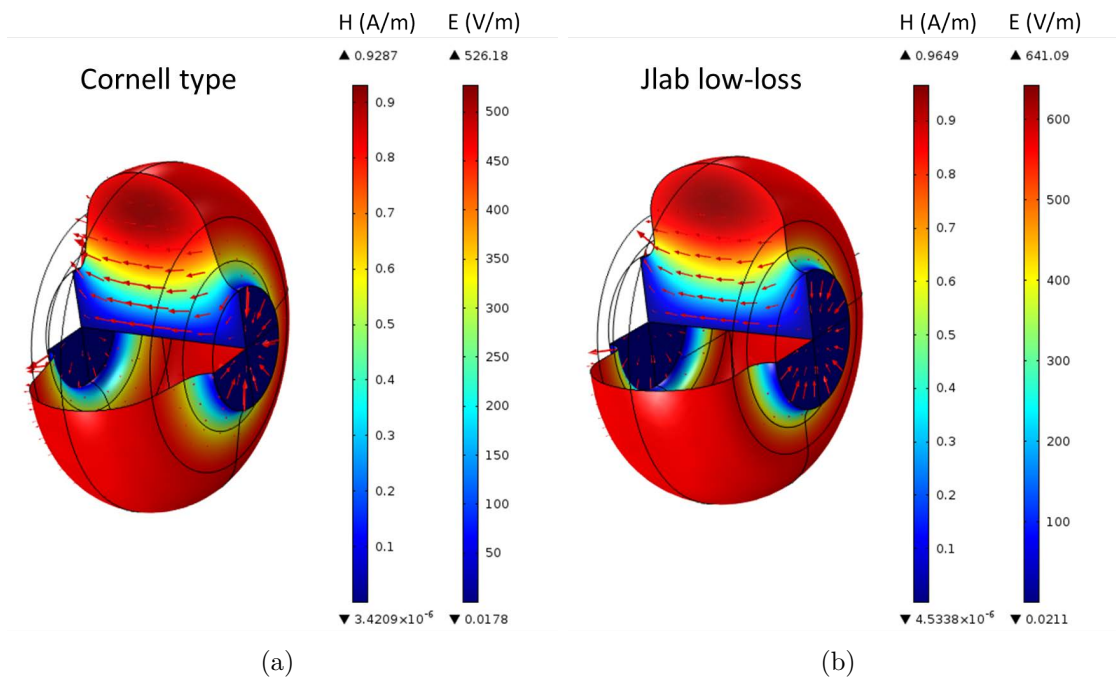


Figure 3.2: Electric field (vector) and magnetic field (solid) for the π - TM_{010} on the base mid-cell models. (a) Cornell mid-cell design, (b) JLab low loss design.

A comparison of the results obtained on the HZB mid-cell design with the characteristic parameters for the JLab and Cornell models are depicted in Table 3.4. As it can be seen all the target RF specifications are fulfilled with a significant improvement of the coupling factor K in comparison to the base models.

In conclusion, the mid-cell geometry obtained represents a good candidate as a base model for the whole five-cell cavity design.

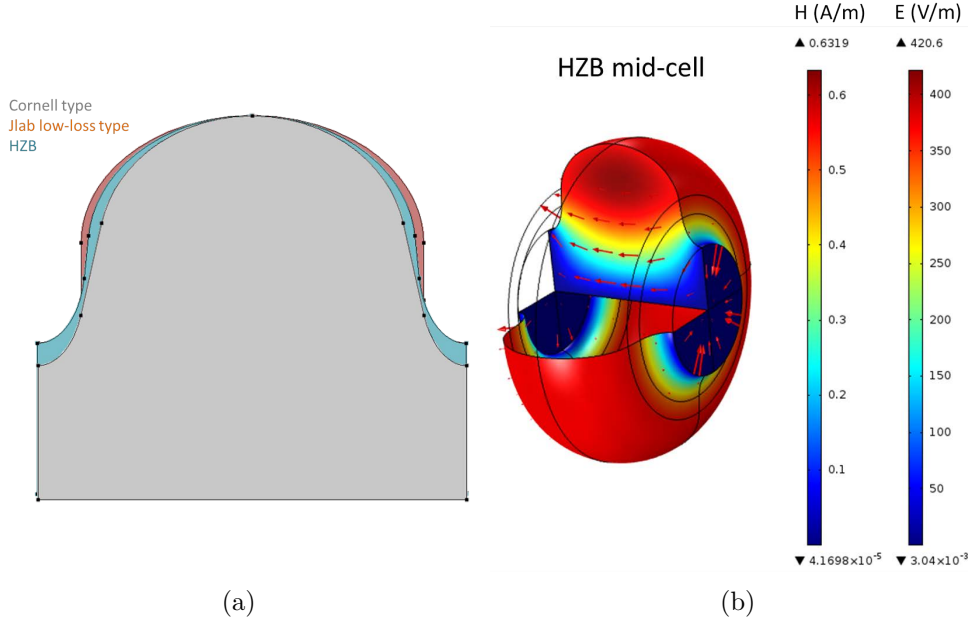


Figure 3.3: (a) Comparison between different base-model mid-cell and the HZB base layout. (b) Electric field representation for the π -TM₀₁₀ mode for the HZB mid-cell layout.

Table 3.4: Comparison between RF design goal parameters for the Cornell, JLab and BESSY VSR mid-cells models.

Parameter	Cornell	JLab	HZB
E_{pk}/E_{acc}	2.06	2.43	2.29
$(B_{pk}/E_{acc})/(\text{mT}/(\text{MV}/\text{m}))$	4.66	3.95	4.18
$(R/Q)/\Omega$	110	104.4	100.7
G/Ω	271.13	277.2	280.05
K for π -TM ₀₁₀ in %	2.01	2.01	3.3
Iris \varnothing /mm	62	68	71

3.2.2 Five-Cell 1.5 GHz Cavity

Once the optimum geometry for the mid-cell was found, the next step was to find the correct five-cell cavity geometry ensuring again fulfillment of the RF specifications (E_{pk}/E_{acc} , B_{pk}/E_{acc} , R/Q , and K) stated in Table 3.2 and maximizing field

flatness μ_{ff} . Field flatness in a mid-cell SRF cavity gives an overall view of how homogeneously the accelerating field is distributed from cell to cell and has an important effect not only on the net accelerating voltage. Therefore, it represents a key aspect in the design and is characterized by:

$$\mu_{\text{ff}} = \left(1 - \frac{E_{0,\text{max}} - E_{0,\text{min}}}{\frac{1}{N} \sum_{i=1}^N E_{0,i}} \right) 100 \%,$$

where the on-axis fields $E_{0,\text{max}}$ and $E_{0,\text{min}}$ are computed for the TM_{010} monopole mode. Thus, in order to successfully complete the design of the five-cell cavity we made use of the mid-cell geometry proposed in the previous section. The center-cell geometry was then replicated five times and the end-cells parametrized so fine geometry tuning can be made. Full 3D eigenmode analysis of the five cell model has been iteratively performed in Comsol Multiphysics [14], Ansoft HFSS [16] and CST Microwave Studio [17] and a final prototype candidate was found fulfilling the specifications with maximum performance. These three software tools were used in parallel for comparison of the results and validation of the solver accuracy for different mesh sizes.

Table 3.5 shows a compilation of the final RF values obtained after the parametric study. As it can be inferred, all the specifications are fulfilled and the design is ready to step into the next phase: The design of the end-groups including couplers for HOM damping and loading. A view of the field flatness is depicted in Figure 3.4 by plotting the longitudinal on axis field for the fundamental π -mode.

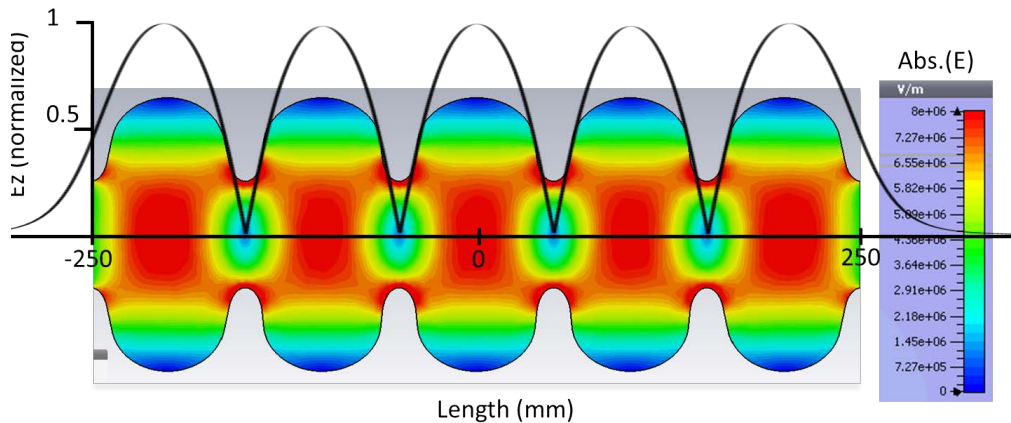


Figure 3.4: Layout of the final geometry after end-cell tuning. Field flatness is depicted giving a value of 98.2%.

Table 3.5: RF achieved specifications after end-cells re-design for the HZB five-cell cavity prototype.

Cavity parameter	Design goal	HZB
E_{pk}/E_{acc}	≤ 2.3	2.29
B_{pk}/E_{acc}	$\leq 5.3 \text{ mT}/(\text{MV}/\text{m})$	$4.4 \text{ mT}/(\text{MV}/\text{m})$
R/Q	$\geq 500 \Omega$	525Ω
K for π -TM ₀₁₀	$\geq 3\%$	3.3%
μ_{ff} for π -TM ₀₁₀	$\geq 97\%$	98.2%

3.2.3 Modal Spectrum, End-groups and HOM absorbers

As it was previously pointed out, high order modes represent a main issue for beam stability and thus they must be damped as much as possible. In order to properly damp higher order modes, many techniques can be used [18] such as beam pipe loads, coaxial coupler dampers or waveguide dampers. This latest have been selected because of the power capabilities, ability to damp HOMs and the natural cutoff to avoid leakage of the fundamental mode. In addition, the distance between ferrite loads and the cavity is large and thus the risk of dust contamination is reduced. To this end, a Y-shape waveguide system for HOM damping has been studied. Both end-groups are identical with 3 waveguides each (120° separation) and shifted 60° with respect to each other in order to cover for all possible HOM polarizations.

Two different waveguide damping schemes are presented. The first one consists on designing the beam pipe radius equal to the cavity iris (design termed in the following as HZB1) and the second one uses a transition in the beam pipe to a larger radius (termed as HZB2). The reason to establish a difference between the two approaches relies on the beam pipe cutoff frequency. In the first approach (HZB1), the cutoff frequency for the beam pipe is chosen to lay above the first dipole band (2.46 GHz). This design should in principle ensure minimum power from the fundamental accelerating mode (TM₀₁₀) to be lost by leakage on the dampers but might imply a worse HOM damping behavior. For the second scheme, the beam pipe diameter is enlarged so the first dipole band can also be propagated ($f_{\text{cutoff}} = 1.67 \text{ GHz}$).

In addition, two different scenarios have been considered for both designs: In the first case, waveguide HOM dampers with standard dimensions of $H = W/2$ ($44 \text{ mm} \times 88 \text{ mm}$) are used (standard waveguide) and in the second case the height of the waveguide is slightly increased ($H = 60 \text{ mm}$) (tuned waveguide). The reason

for this two different waveguide sizes relies on the different H field orientations on the damping regions and the desired frequency cutoffs as it is explained in [19]. In all the models, the standard waveguide length from beam pipe to load is set to 200 mm. Figure 3.5 depicts a layout of the full cavity with waveguide loaded end-groups attached and tuned waveguides. In order to offer a better visualization of the results presented for the different models a description of the model with the naming code is showed in Table 3.6.

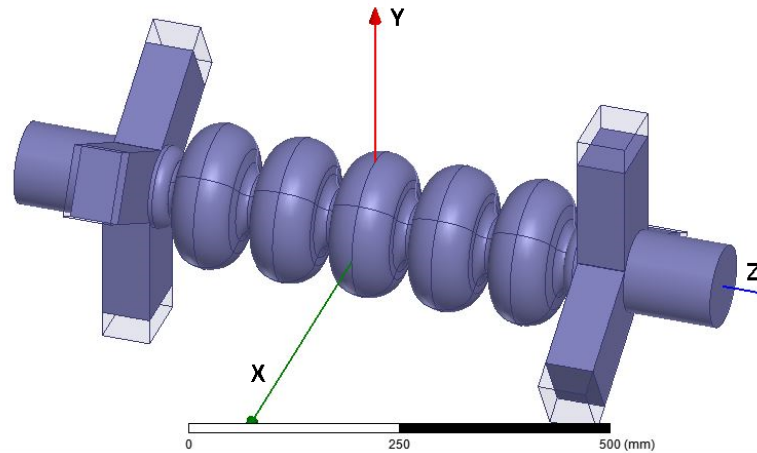


Figure 3.5: HZB five cell cavity with enlarged beam pipe design with end-groups attached (HZB2b).

Table 3.6: Naming code for the different models.

Design name	Beam-pipe \varnothing	Waveguides	Length
HZB1	71.34 mm	none	—
HZB1a	71.34 mm	standard WG	200 mm
HZB1b	71.34 mm	tuned WG	200 mm
HZB2	105.2 mm	none	—
HZB2a	105.2 mm	standard WG	200 mm
HZB2b	105.2 mm	tuned WG	200 mm
HZB2c	106.5 mm	tuned WG	400 mm
HZB3	71.34 mm (extension 104 mm)	standard WG	200 mm

As it can be inferred from Figure 3.6, a good damping level can be obtained by these techniques for higher order modes. In the case of the two HZB1 type models

the damping of the modes such as TE_{011} and TM_{211} improves considerably (Q_{ext} reduces) when switching from a standard waveguide to the tuned waveguide design (HZB1a to HZB1b). Also, damping for the TE_{211} quadrupole mode (2.5 GHz band) is slightly improved. Nevertheless, the TM_{011} monopole mode which seems to be a limiting band for stability reasons (see Chapter 2) cannot be improved by this technique.

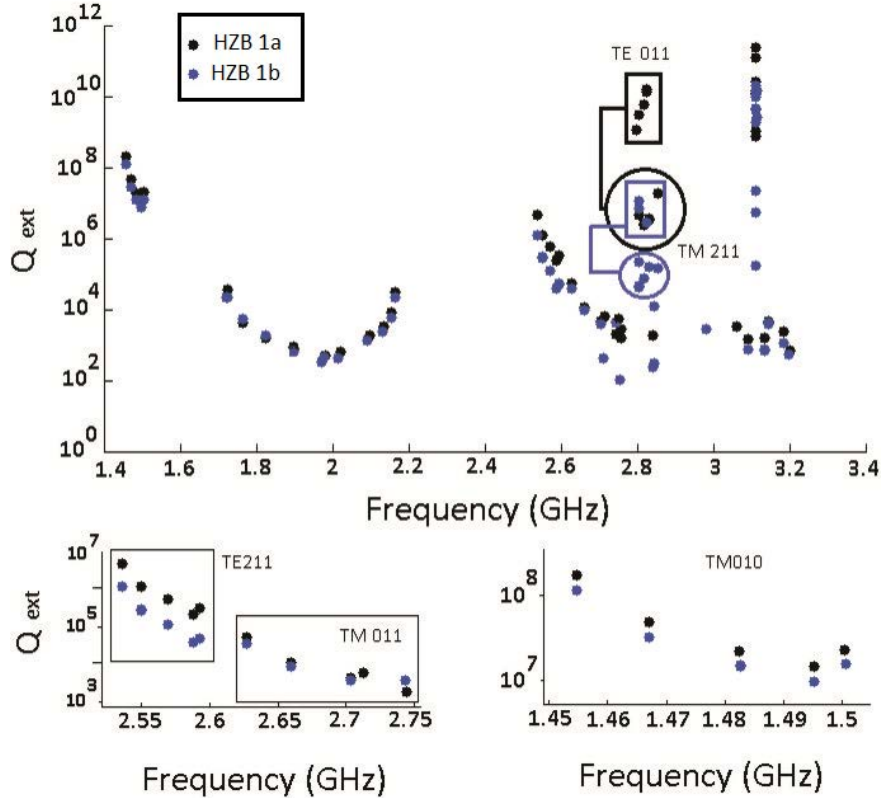


Figure 3.6: Mode spectrum for the HZB five-cell design. Comparison of the HZB1a and HZB1b designs.

On the other hand as shown in Figure 3.7, enlarging the diameter from $\varnothing = 71.34\text{mm}$ to $\varnothing = 105\text{mm}$ as in the bERLinPro case [20], represents a significant improvement (HZB2). All the bands experience a significant drop in their Q_{ext} , and especially the TE_{211} (2.5 GHz band) quadrupole mode. At the same time, the limiting TM_{011} monopole mode (2.6 GHz band) damping is slightly increased when compared to the HZB1 models. A comparison between the two enlarged beam pipe models (HZB2a and HZB2b) and a standard beam pipe approach (HZB1a) is depicted on Figure 3.7. The HZB2 models show a better performance regarding higher order bands.

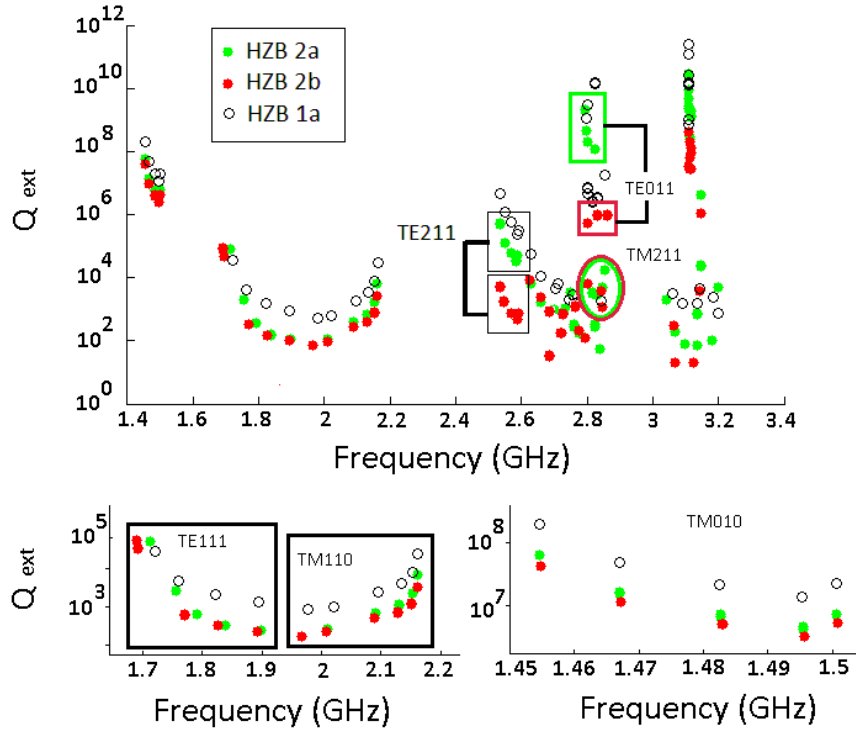


Figure 3.7: Modal spectrum for the HZB five-cell design. Comparison of the enlarged beam pipe models HZB2a and HZB2b with the HZB1a model.

Taking a closer look to the fundamental band, the present design has a clear limitation regarding the maximum achievable $Q_{\text{ext}} = 1 \times 10^8$. This fact is attributed to the short length of the waveguide dampers which in these designs has been set to 200 mm from the beam pipe border to the load in order to save space into the module. As it is following described, short damper lengths will result into a significant decrease of the Q_{ext} for the fundamental band due to leakage into the damping waveguides and thus reaching the loads. A view of this TM_{010} energy leakage is depicted in Figure 3.8. As it can be observed, the relatively big dimensions of the iris allow the fundamental mode to spread out of the cavity end-cell into the waveguide dampers and thus affects the Q_{ext} value. In order to optimize the amount of power dissipated by the load and after discussions with F. Marhauser from JLab the decision of increasing the waveguide length to 400 mm was taken. This length is still admissible and will not give any major obstacle for the cryomodule design. Thus a new optimization procedure of the model was done by increasing the waveguide damper length to 400 mm and slightly tuning the dimensions of the waveguide dampers and their distance to the cavity obtaining very promising results (see Figure 3.10). This design is termed as HZB2c.

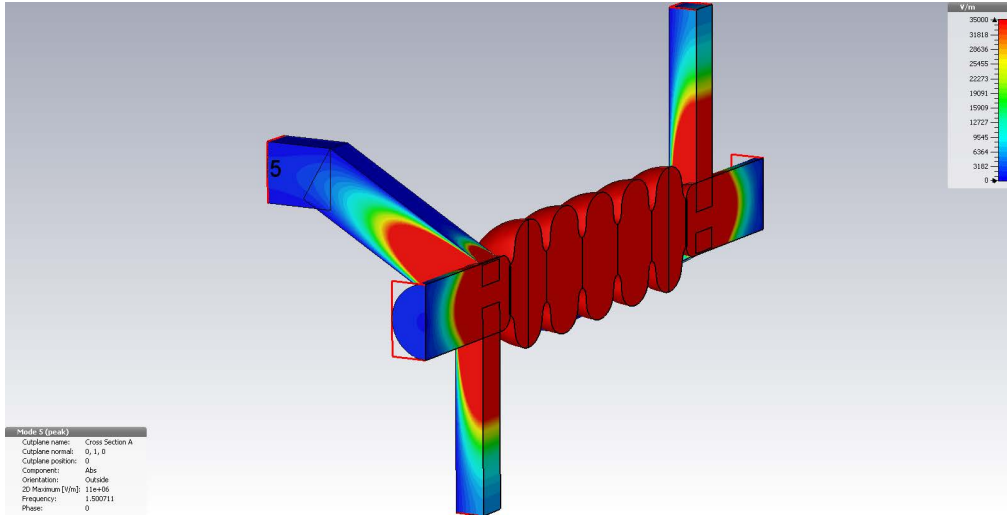


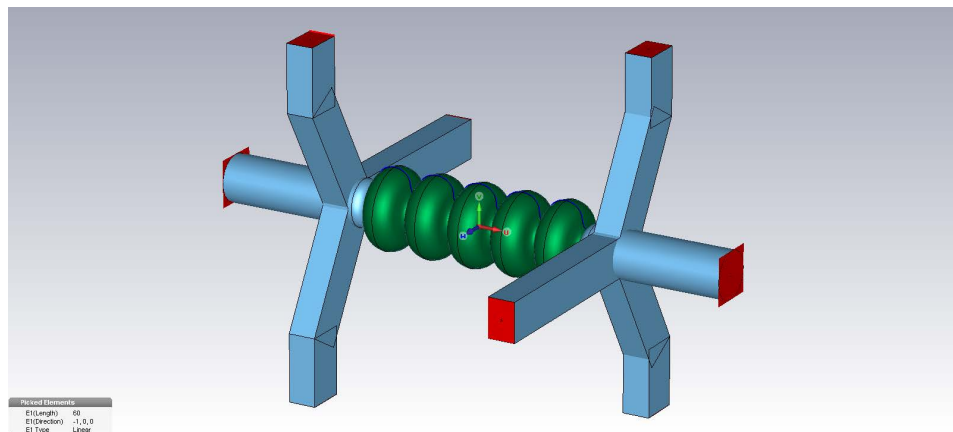
Figure 3.8: View of the effective energy leakage for the TM_{011} π -mode through the damping section when enlarged beam pipe is placed in the vicinity of end-cell iris.

Figure 3.9 shows a layout of the optimized HZB2c geometry with increased length of the waveguide dampers, tuned end-groups and tuned beam pipe diameter. The new design HZB2c increases the isolation for the fundamental band while keeping an excellent performance when extracting excited higher order modes, shown in Figure 3.9 (b, c).

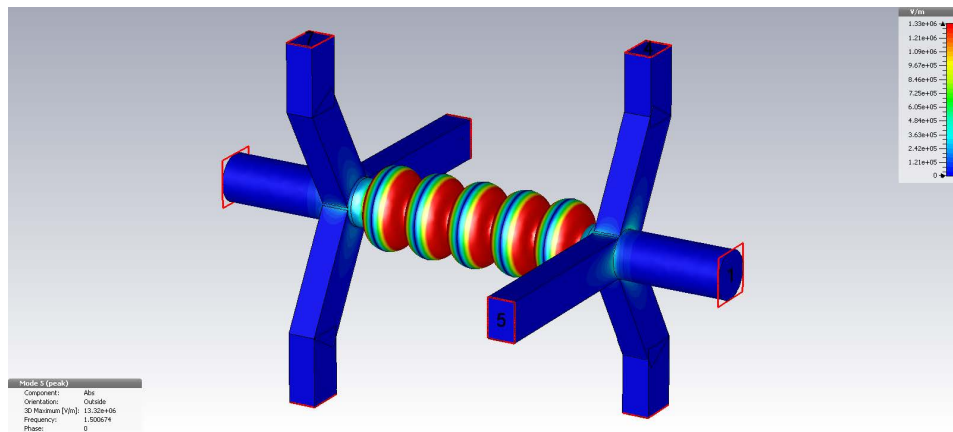
Nevertheless, the Q_{ext} value obtained for the fundamental π -mode ($Q_{\text{ext}} = 4 \times 10^9$) is still slightly below the expected value ($Q_{\text{ext}} \geq 1 \times 10^{10}$). It is possible that the reason of this low value is not because of physical reasons such as leakage but attributed to computational problems in CST [17] when solving modes below the beam pipe cutoff. In order to clear this issue, the same model was calculated in HFSS [16] and results cross-checked giving a value of $Q_{\text{ext}} = 8 \times 10^{10}$ for the π - TM_{010} mode. All the solved modes above the beam pipe cutoff show similar results for Q_{ext} and R/Q both in CST and HFSS. Therefore the model can be assumed to exhibit high isolation values for the fundamental band within the desired limits.

In addition, the new model exhibits high performance when damping higher order modes, as depicted in Figure 3.10. By slightly increasing the beam pipe diameter of the HZB2c model, the beam pipe cutoff is reduced to 1.65 GHz increasing damping for the first dipole band TE_{111} with respect to the HZB2b model. Also Q_{ext} for the dangerous TM_{011} monopole mode remains controlled exhibiting low values (≤ 70). On the other hand the TM_{211} band shows some increase with respect to the HZB2b but still remains under reasonable limits.

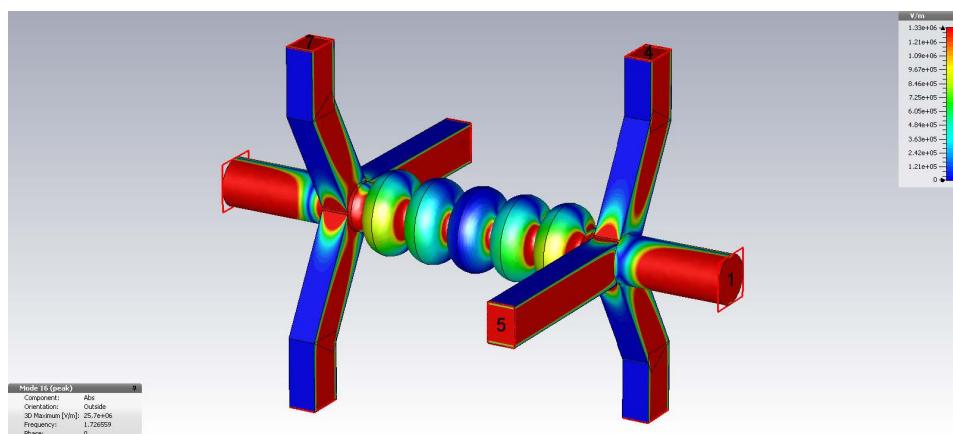
3 Superconducting RF Systems



(a)



(b)



(c)

Figure 3.9: Layout of the HZB2c design with enlarged beam pipe, tuned waveguides and longer waveguide dampers. General layout (a), $TM_{010}-\pi$ mode (b) and TE_{111} dipole HOM (c).

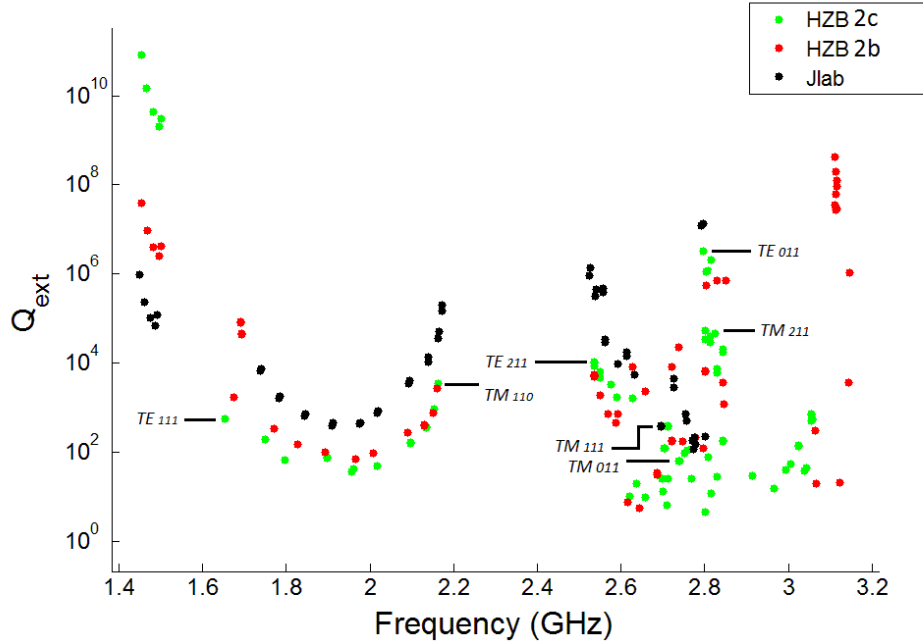


Figure 3.10: Mode spectrum for HZB2c design compared to the previous HZB2b and JLab model.

Although Q_{ext} shows a good damping performance we need to analyze the factor $R/Q \cdot Q_{\text{ext}}$ in order to get a realistic view of how good the model is in terms of beam stability, see Figure 3.11. When computing coupled bunch instability thresholds, the highest $R/Q \cdot Q_{\text{ext}}$ value of all modes is the one defining the final performance. For that reason it is crucial to be able to keep this factor as low as possible for every modal band and below the feedback threshold ($\sim 10^5$ for monopole modes, $\sim 10^7$ for dipole and quadrupole modes ...). Notice that R/Q is always referred in this section to $(R/Q)_{\parallel}$, since it is extracted from the integrated on axis longitudinal field for monopoles and off-axis field for non-monopoles. For a better comparison with the JLab model the $R/Q \cdot Q_{\text{ext}}$ values are depicted in Figure 3.11, where a 5 mm offset is considered for non-monopole modes.

Nevertheless, these values do not make a statement regarding the ratio to the feedback threshold. To do so, non-monopole modes must be normalized considering the offset factor and their natural transverse component. This is done by applying the Panofsky–Wenzel theorem relating V_{\parallel} and V_{\perp} by:

$$V_{\perp} = \frac{-ic}{\omega r^m} \cdot m V_{\parallel} , \quad (3.4)$$

where $m = 1$ for dipoles and $m = 2$ for quadrupoles. As it is shown in Figure 3.11(b) there is a significant improvement in model HZB2c with respect to the previous ones.

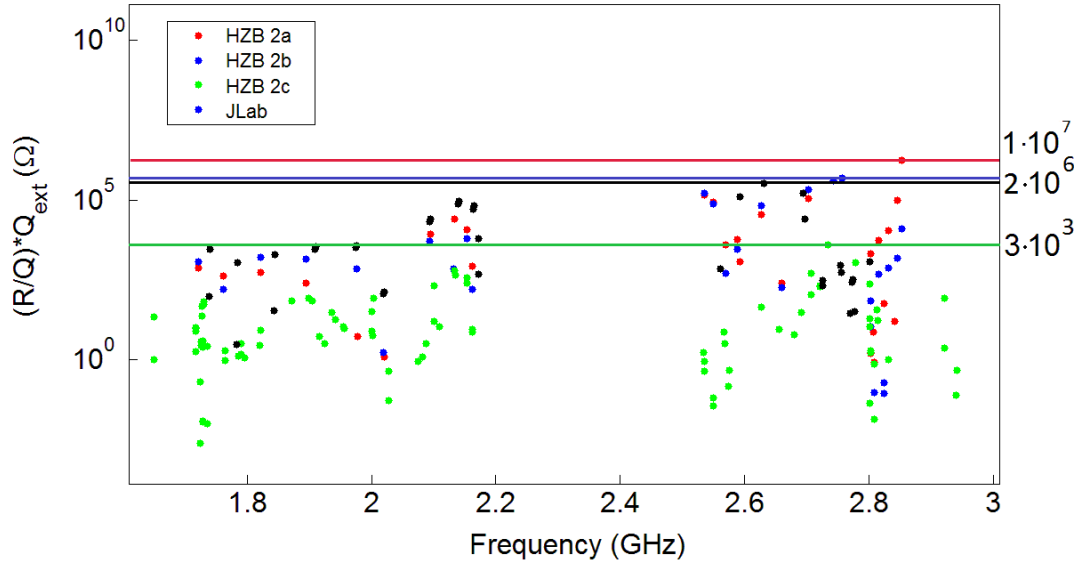


Figure 3.11: Comparison of the $R/Q \cdot Q_{\text{ext}}$ for the models HZB2a, HZB2b, HZB2c and the JLab design. Continuous lines show the maximum HOM value for every model. For non-monopole modes a 5 mm offset is considered.

Table 3.7 summarizes the maximum values of $R/Q \cdot Q_{\text{ext}}$ obtained for the modal bands below 3 GHz.

Table 3.7: Maximum $R/Q \cdot Q_{\text{ext}}$ values for most of the HOM bands below 3 GHz for the HZB2c model. For non-monopole modes a 5 mm offset is considered.

Mode	$(R/Q \cdot Q_{\text{ext}})/\Omega$	Frequency f/GHz
TE ₁₁₁	66	1.72
TM ₁₁₀	610	2.13
TE ₂₁₁	7.4	2.56
TM ₀₁₁	3×10^2	2.73
TE ₀₁₁	3×10^3	2.79
TM ₂₁₁	10	2.8

To confirm the obtained results the modal spectrum up to 3 GHz was used to compute couple bunch instability thresholds (see Chapter 2). $R/Q \cdot Q_{\text{ext}}$ calculations

were done assuming the worst case scenario where the polarization angle for every mode was checked in order to extract the longitudinal field at its maximum (see Figure 3.12). Then fields were extracted and processed in MATLAB and results cross-checked with the CST post-processing tool with very good agreement. Also, the same model was validated in HFSS [16] by computing and comparing field patterns, Q_{ext} and R/Q for different modes (monopole, dipole and quadrupole) with CST (see Figure 3.13).

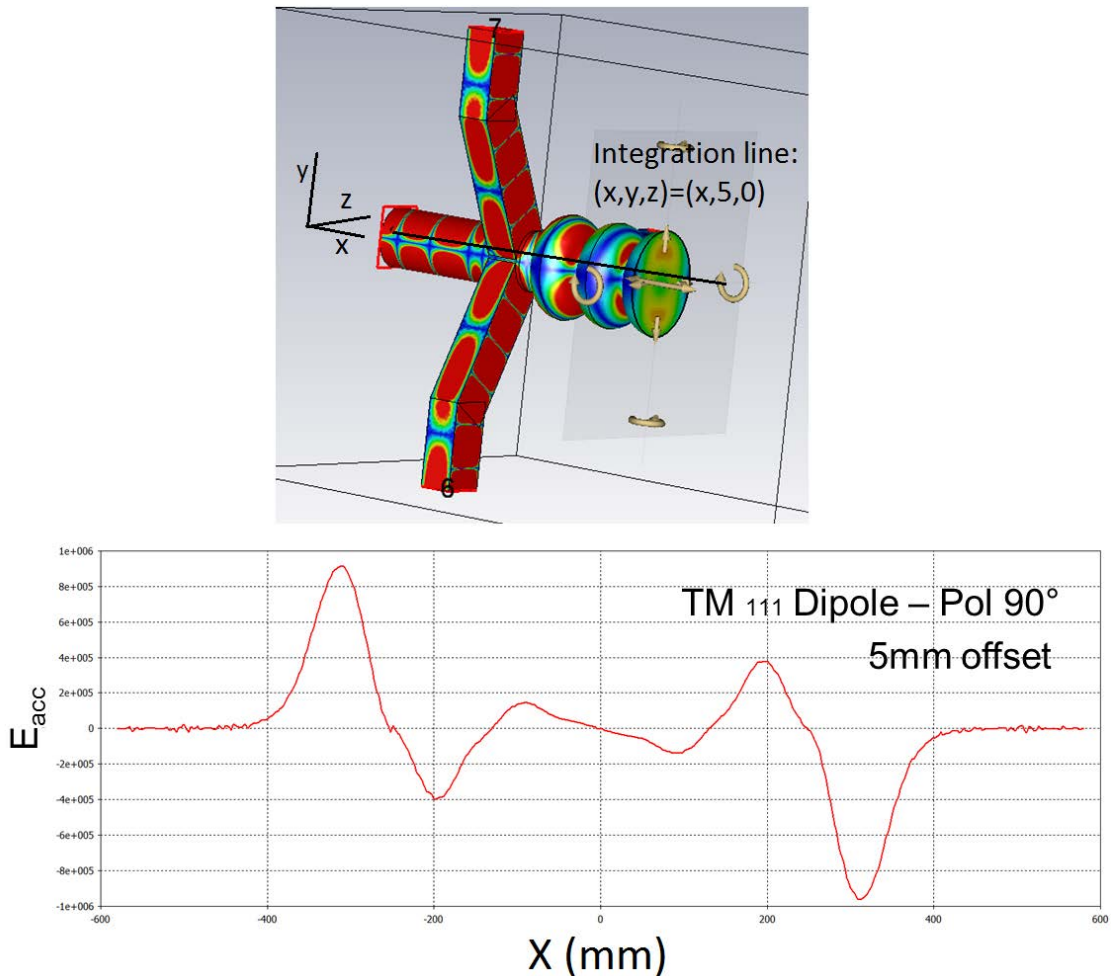


Figure 3.12: Analysis of a mode polarization to export fields for R/Q calculations.

In conclusion, the model HZB2c represents a good candidate to become a final cavity prototype as it has been confirmed by beam instability computations. Moreover and even when the present design waveguide dampers length is feasible, further optimizations studies have been done in order to minimize the waveguide length and distance to the end-cell iris and thus save space inside the module. Thus, to

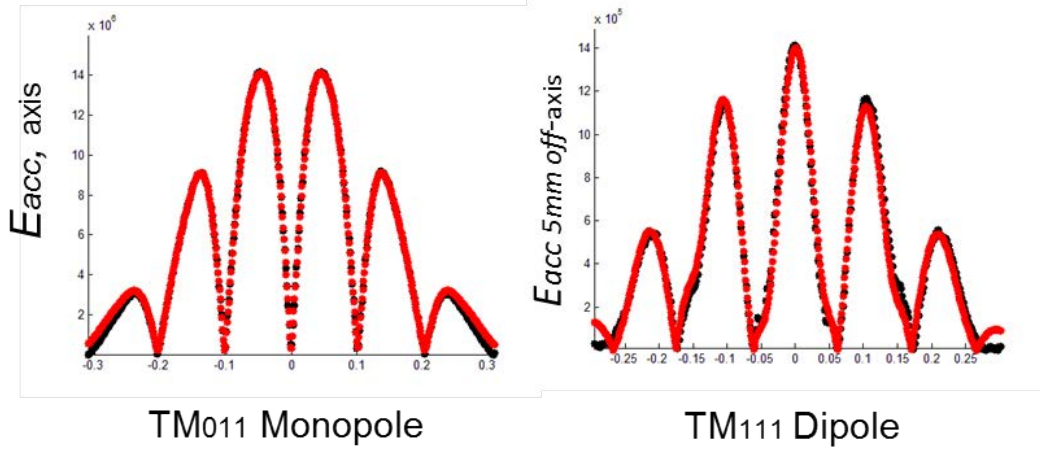


Figure 3.13: Comparison of the computed E_{acc} for two of the calculated modes (TM₀₁₁, monopole and TM₁₁₁, dipole) both in HFSS (black) and CST (red).

have a broader view of the leaking phenomena parametric studies regarding the distance between the end-cells and the Y-shape damping waveguide groups have been performed as shown in Figure 3.14.

It was demonstrated that the quality factor can be increased by sufficiently lengthening the waveguides to reduce the energy leakage ($Q_{ext} = 1 \times 10^9$ for $l = 300$ mm), see Figure 3.14(c). Also, the distance from the end-cells to the damping section plays an important role. Thus, if we want to reduce the distance from beam pipe to flanges and save space in the module we must optimize these two parameters. To this end, the end-group shape has been modified in order to obtain higher confinement of the fundamental mode while keeping HOM damping levels and reduced dimensions.

The resulting layout is depicted in Figure 3.15 and named HZB3. The technique used consists of implementing a first short 20 mm section of standard beam pipe ($\varnothing_{iris} = 71.34$ mm) followed by an enlarged beam pipe transition to dampers ($\varnothing = 104$ mm). The use of the short standard beam pipe sections serves as stopper for some amount of leakage due to the lower cutoff, while the wider beam pipe sections recovers the HOMs and transports them to the dampers. In this case, the length of the waveguide dampers can be reduced to the original 200 mm and the Y-section damper can be placed 30 mm away from the iris (measured from iris end to waveguide wall).

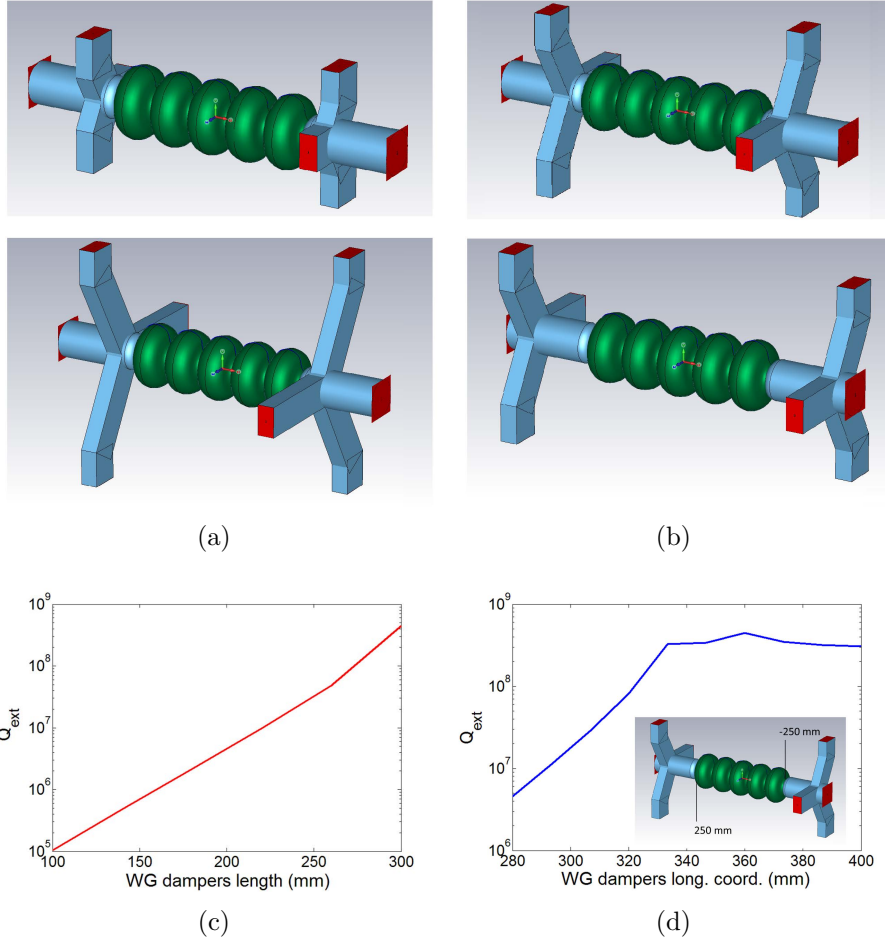


Figure 3.14: Parametric studies of the leaking TM_{010} mode for different layouts. (a) Variation of the length of the waveguide and (b) variation of the longitudinal position of the waveguide damper. (c) Results for the π -mode extracted from (a). (d) Results for the π -mode extracted from (b).

As it is depicted in Figure 3.16, the Q_{ext} for the whole fundamental band is increased by two orders of magnitude compared to the previous designs for the same waveguide length (200 mm). HOM damping also shows in general a good performance. Improvements of this design are currently under development which will allow to improve HOM damping by modifying the section of the dampers.

As described, all the results previously shown have been computed considering 6 HOM waveguide couplers in the cases where the isolation of the fundamental mode was under study. As it was introduced at the beginning of this chapter, this was only done for design convenience when finding the suitable geometry. Nevertheless,

since an adjustable coupler will improve the capabilities of the system, the next step is to implement a new coupler design similar to the Cornell Injector 60 kW Power couplers [7]. This design is currently under study and requires some extra calculations to determine coupler kicks and further effects.

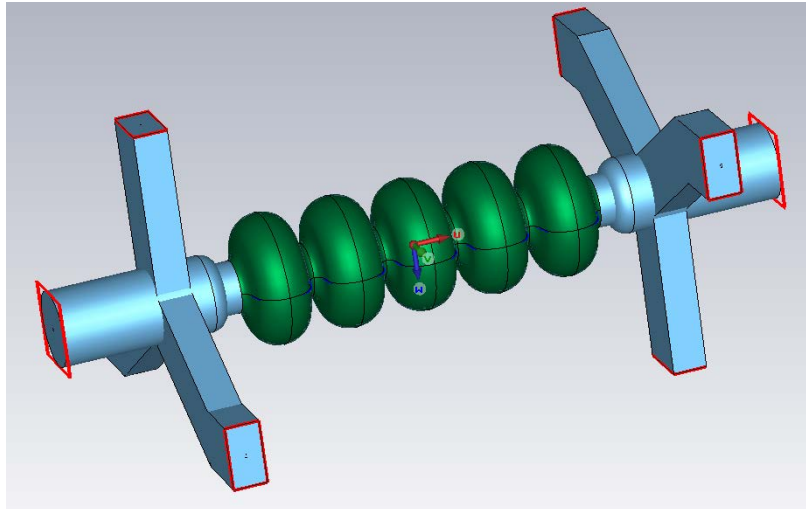


Figure 3.15: Five cell cavity design (HZB3) with end-groups attached for reduced damping of the TM_{010} mode.

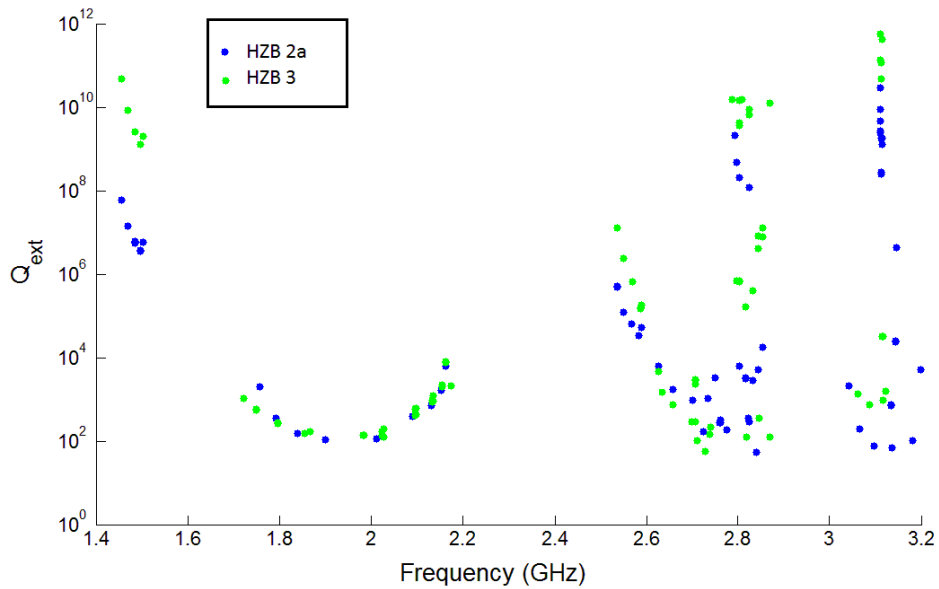


Figure 3.16: Comparison between HZB3 and HZB2a. Isolation for fundamental band is raised to similar values as in the HZB2a for shorter waveguides (200 mm).

3.2.4 Transparent operation

System failures such as RF source or cryogenic plant failure must be considered when designing the SRF cavities. Thus, it is essential that in case of failure the BESSY VSR cavities can be “parked” so that it is transparent for standard BESSY II operation without necessitating its removal. To do so, the cavity has to be provided with the ability to be detuned enough so minimum cavity beam interaction is obtained. As it is well known mechanical tuners are not able to cover for wide frequency shifts ($\simeq 350$ kHz) while temperature rise can lead to higher frequency displacements. Thus, the frequency variation as a consequence of a temperature rise for the fundamental $TM_{010}-\pi$ mode and HOMs must be evaluated. In consequence, the frequency shifting in the cavity due to thermal shrinkage has been evaluated for different temperatures from 1.8 K to room temperature by performing eigenmode simulations in Comsol Multiphysics [14]. To do so, experimental thermal expansion coefficients have been extracted from a material properties review published by Fermilab [21].

In general, a temperature rise first induces a positive frequency shift due to helium pressure ($\simeq 100$ Hz/mbar). Nevertheless, when further increasing the temperature mechanical expansion dominates the frequency shifting. As explained, since the mechanical tuners do not offer a sufficiently broad band frequency range temperature can be used for this purpose while using the tuners to perform fine tuning around the new resonance frequencies. A total frequency shift of -2.43 MHz is expected when moving from cold state (1.8 K) to room temperature. As a consequence the cavity voltage drops when moving away from the driving frequency.

Figure 3.17 shows the effect of the temperature variation on the resonance curves. The voltage envelope for every temperature case is represented in the maximum frequency tuning-range allowed by the mechanical tuners ($\simeq 350$ kHz). The used Q_L values come as a result on the quality factor analysis as it is later shown. Thus, we use the Breit-Wigner distribution as the dependence of the cavity field amplitude and phase where I_g represents the generator current and Z_1 the loaded impedance:

$$V_{\Delta(\omega)} = \frac{Z_1 I_g}{\sqrt{1 + \tan^2 \Phi}} \quad (3.5)$$

$$\tan \Phi = 2 Q_L \frac{\Delta\omega}{\omega_0} \quad (3.6)$$

In addition to the frequency of the modes, another important aspect to be evaluated is the mode impedance, which is proportional to the R/Q and the loaded quality factor Q_L . Therefore the evolution of the loaded quality factor Q_L from 1.8 K to room temperature has been carefully computed up to a frequency of 3 GHz.

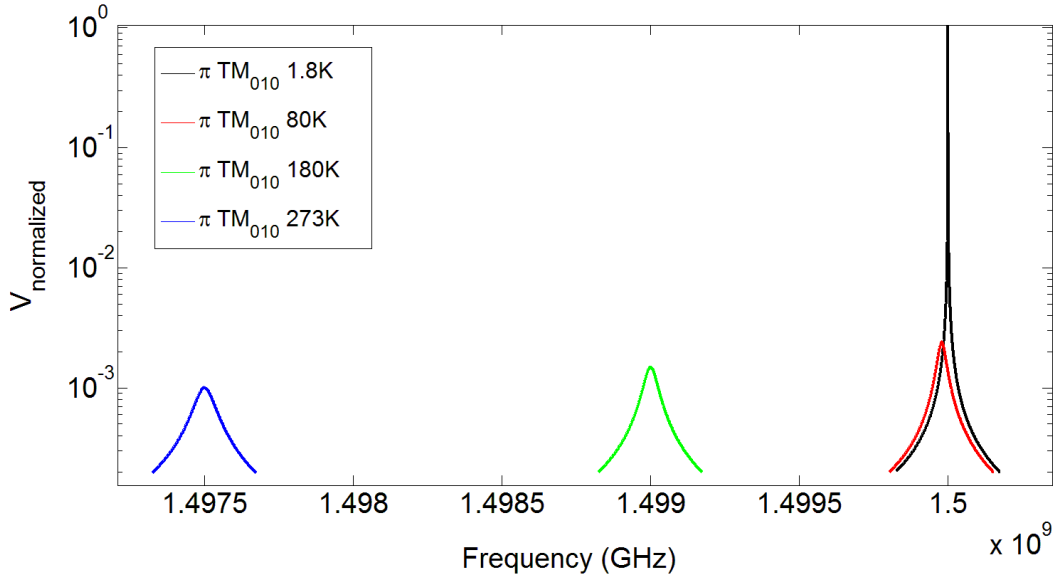


Figure 3.17: Normalized cavity voltage spectrum drop due to temperature with an assumed mechanical tuner range of ± 350 kHz.

Above T_c the same set of parameters have been calculated for the non-superconducting state. As it is known, Q_0 is no longer characterized by the R_{BCS} but the surface resistance R_S as a function of the electric conductivity and the skin depth.

$$R_S = \frac{1}{\sigma(T) \delta(T)} \quad (3.7)$$

In this case, the correspondent conductivity values for the Niobium at different temperatures have also extracted from [21].

Also, all the HOM impedance values have been calculated for both superconducting and normal conducting states up to room temperature. These results are used to compute beam instabilities for the HZB1a model. Figure 3.18 shows the impedance values for all the π -modes up to 3 GHz in the superconducting state. All these depicted parameters by themselves do not make a definitive statement of how stable parking will be but the impedance value and the evolution of the loaded Q can help in visualizing the possibility of an eventual problem. Thus, all these parameters were used as input to compute more complex beam stability studies (Chapter 2).

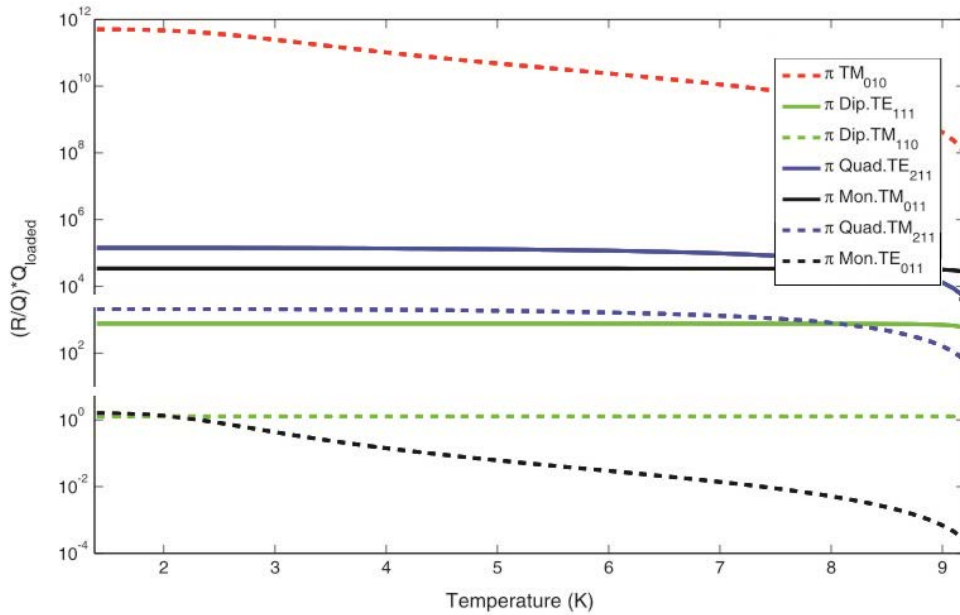


Figure 3.18: Computed loaded impedances for different temperatures.

3.3 Cryomodule Design

BESSY VSR will be accomplished using a single cryomodule that will contain 4 SRF cavities, two operating at 1.5 GHz and two operating at 1.75 GHz. A schematic of the module layout is shown in Figure 3.19.

The module design has been chosen to make the best use of the available low β straight section in the ring, where there is in total 4.6 m of space for installation of the SRF cavities. The module concept is 4.0 m long and the critical beamline components occupying this space are the four cavities, two RF shielded gate valves and 7 bellows sections. The overall cavity and cryomodule parameters can be found in Table 3.8.

The module design is based on the bERLinPro cryomodule concept where 3 unique cryomodules are being built based on the Cornell Injector module[22, 23]. This cryomodule design utilizes a 300 mm helium gas return pipe for support and alignment of the cavities and has been demonstrated as a robust and reliable design in operation at Cornell. It is also the design the engineering staff at HZB are familiar with, thus providing synergy between bERLinPro and BESSY VSR and allowing BESSY VSR to leverage the experience and lessons learned from the bERLinPro project since the first bERLinPro cryomodule will go into operation in 2016.

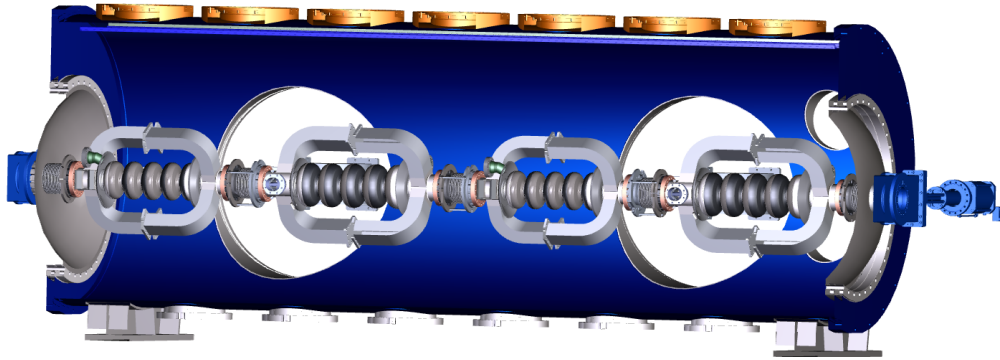


Figure 3.19: The BESSY VSR cryomodule design concept showing the 1.5 GHz and 1.75 GHz SRF cavities along with bellows that will be utilized to accommodate thermal expansion and contraction.

The BESSY VSR cryomodule will utilize only helium as the cooling media for the cavities, thermal intercepts and shields. The reason for this is based on the fact that a new cryogenic plant must be purchased for the BESSY VSR phase and it will be ordered optimized for cooling of the module. Table 3.9 provides a list of the cooling media, temperature and use in the BESSY VSR module. More information on the cryogenic system is found in Chapter 4.

The choice of operating temperature for the SRF cavities has been described in detail in Section 3.1. In summary operation at 1.8 K provides the best balance between cavity performance and cost efficiency when a new cryogenic system is being considered. By operating at 1.8 K versus 2.0 K there is an improvement in the operating unloaded quality factor Q_0 of approximately a factor of 2, thus resulting in approximately the same factor of 2 decrease in the dynamic heat load into the helium system. In addition the microphonic noise is reduced as the pressure is reduced from 30 mbar to 18 mbar, providing a more stable operating environment.

3.3.1 Cryomodule Components for Preparatory Phase

As previously mentioned, the preparatory phase will be carried out using only a limited number of components in comparison to the final BESSY VSR setup. For the SRF systems and the cryomodule this means only 2 SRF cavities will be installed in the module, thus reducing the total number of components that are necessary, which in turn reduces the cost and risk. The plan is to install two 1.5 GHz cavities to allow for measurement of the performance of two cavities in the module and more importantly in the BESSY II storage ring. This will also serve as a demonstration of all the ancillary components required for the cavities, which will reduce the uncertainty going into the BESSY VSR phase.

Table 3.8: The SRF cavity and cryomodule parameters to gauge the efficient use of the accelerating space.

Cavity parameter	1.5 GHz Cavity	1.75 GHz Cavity
Frequency	1.5 GHz	1.75 GHz
Cavity active length	0.5 m	0.43 m
Accelerating gradient	20.0 MV/m	20.00 MV/m
Accelerating voltage	10.0 MV	8.57 MV
Number of cavities	2	2
Total accelerating voltage	20.0 MV	17.14 MV
Total accelerating voltage of cryomodule		37.14 MV
Total active cavity length		1.86 m
Cryomodule length		4.0 m
Real estate gradient		9.29 MV/m
(Total Acc. Voltage / Cryomodule Length)		

The module itself will be identical to what will be used for the BESSY VSR phase, unless a problem is found. After the preparatory phase has concluded the module will be retrofitted with two additional cavities and the necessary ancillary components to serve for BESSY VSR phase.

The largest difference in the two phases in terms of operations will be the fact that the preparatory phase will be carried out at 4.4 K using the existing BESSY II cryogenic infrastructure with limited modifications. This will mean significantly reduced performance, as mentioned in Section 1.5, but will still allow for the key demonstration of the BESSY VSR concept as well as the critical technical validation of the module design.

Additionally, as the cryomodule test facility will not be ready in time for commissioning of the preparatory phase cryomodule, the current plan is to use the bERLinPro accelerator hall for the cryomodule commissioning. This will in any case allow for the cryomodule testing to take place independent of BESSY II operations.

Table 3.9: A list of cryogenics which will be used in the BESSY VSR cryomodule.

Item to be cooled	Media
SRF cavities	1.8 K liquid helium
Bellows between cavities	3 bar 5 K helium
Fundamental power coupler cavity flange	3 bar 5 K helium
Fundamental power coupler transition to room temperature	50 K helium gas
Thermal shield	50 K helium gas
Thermal transition between end cavity and gate valve	3 bar 5 K and 50 K helium gas

3.3.2 Cryomodule Components for Final BESSY VSR Setup

In the final BESSY VSR setup of the project the complete 4 cavity module will be constructed and tested in the new cryomodule test facility before relocation to the BESSY II storage ring. The facility will allow for commissioning of the module at 1.8 K, albeit powering only one cavity at a time. Once the module is certified for operation it will be moved into position in the storage ring, and the preparatory phase module will be rebuilt with 4 cavities to serve as a critical spare in the event a problem develops with the module in the ring. Having a fully assembled and tested spare module will allow for rapid replacement of the module in the ring should a problem arise during operation. It will also allow for testing of the spare module in the test facility if there are any additional diagnostic experiments which need to be carried out to understand behavior which is seen in the ring, but where there is no opportunity to investigate the cause. In addition to the testing facility housing the critical spare module, it will also house spare RF transmitters for both the 1.5 GHz and 1.75 GHz RF system, along with spare LLRF components. More details on this can be found in Section 3.5.

3.4 Ancillary Components

The main ancillary components required for the BESSY VSR cryomodule are the cavity tuning system, the RF input power couplers, the higher order mode (HOM)

absorbers, the magnetic and thermal shields as well as the RF shielded bellows and gate valves.

The tuning system required for these cavities is planned to be a Cornell style blade tuner, similar to what has been employed in the bERLinPro project. This style of tuner is relatively compact and is a well proven design based on the DESY/INFN design but with a modified piezo actuator assembly [24–26] which has been extensively characterized by Helmholtz-Zentrum Berlin. Additionally no extra space is required to mount the tuner at the end of the cavity, such as with an end lever tuner. The helium vessel for both the 1.5 GHz and 1.75 GHz cavities will be produced with a bellows section in the middle of the helium vessel, and it is around this bellows that the tuner will act to compress or lengthen the cavity. In this design, the mechanical tuner is integrated with piezoelectric actuators to allow for fine tuning and microphonics compensation. The challenge with the integration of this tuner is positioning it such that it does not interfere with the magnetic shield which must go directly adjacent to the cavity; nor with the HOM loads which will be positioned around the cavity to best utilize the space available in the cryomodule, similar to the Jefferson Lab (JLab) high current cavity design[27]. A model of the JLab waveguide configuration is shown in Figure 3.20 for reference.

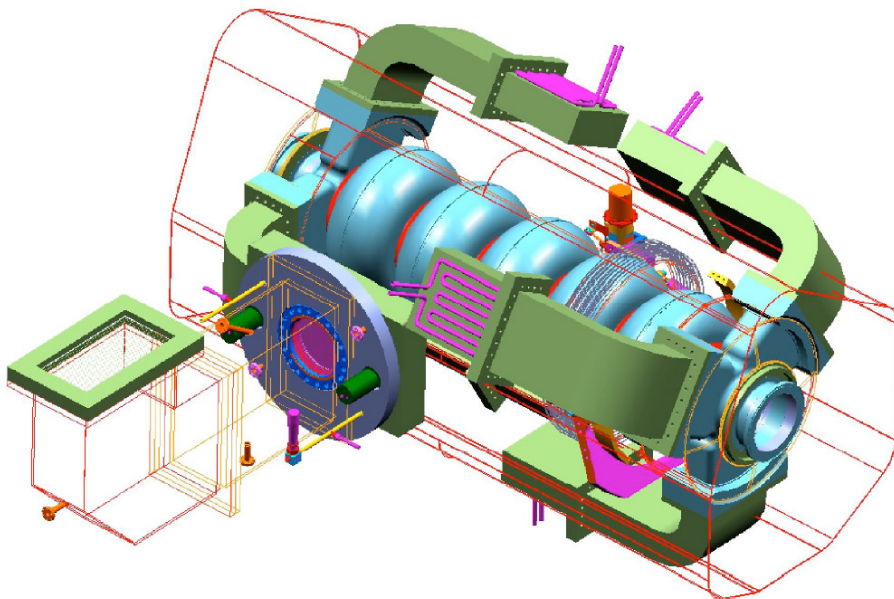


Figure 3.20: The JLab high current waveguide damped cavity design. The blue section will be maintained at 1.8 K and heat intercepts will be placed along the bent section of waveguide before the HOM absorber, shown with the magenta cooling tubes.

A model of Cornell style blade tuner is shown in Figure 3.21 so the reader can visualize installation of the tuner around the cavity shown above.

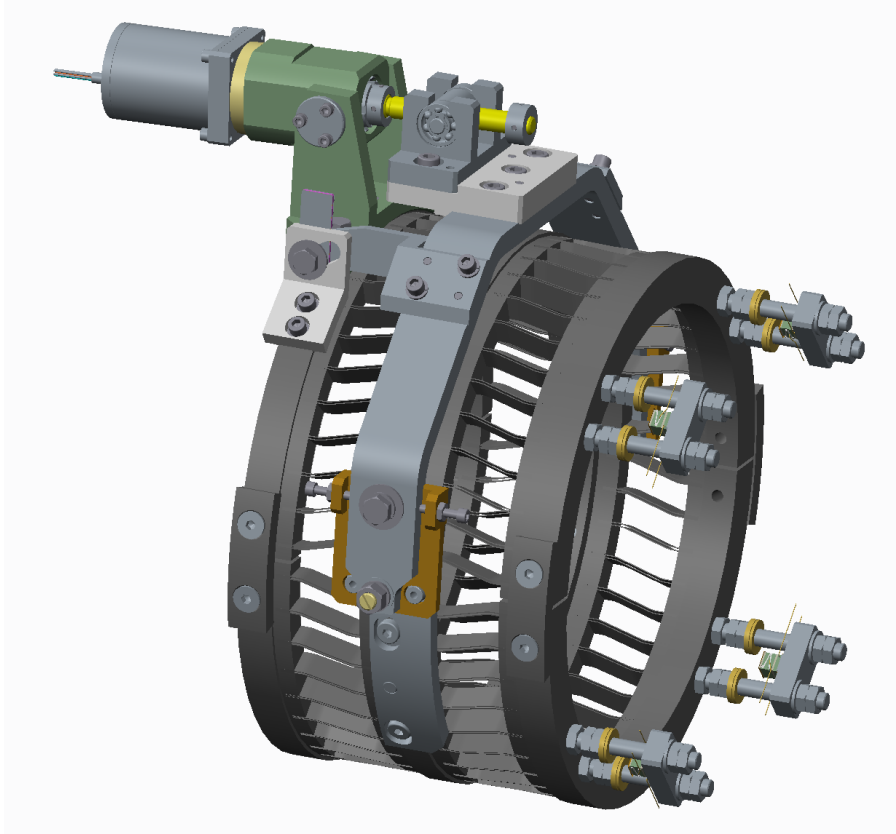


Figure 3.21: The Cornell style blade tuner.

The RF input power couplers for both the 1.5 GHz and 1.75 GHz cavities will be based on the design by Cornell University which has successfully been demonstrated at 1.3 GHz up to 60 kW CW input power[7, 28]. The Cornell style coupler is a variable coupling coaxial coupler which can provide a change in Q_{ext} for the coupler of approximately one order of magnitude, allowing for the optimum coupling range to be chosen based on the operating conditions of the machine, as well as to allow for safe parking of the cavities above T_c when the cavities operation is not required. The coupler design will have to be modified for operation at 1.5 GHz and 1.75 GHz and thorough simulations carried out on the design prior to fabrication of the couplers. Figure 3.22 shows the Cornell input coupler design.

The higher order mode (HOM) absorbers that will be used for the BESSY VSR cavities are based on a design by Jefferson Laboratory, and is designed to handle hundreds of watts of power dissipation in each absorber[29]. The HOM loads will

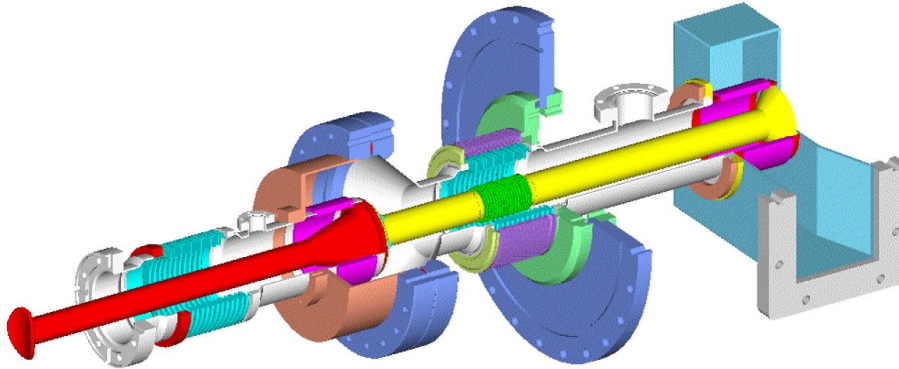


Figure 3.22: The Cornell RF input coupler.

be attached to waveguide ports on the cavity, as described above and shown in Figure 3.20, and will be arranged around the cavity in such a manner that they will intercept all of the different polarizations of the HOMs. The HOM absorber itself is designed to be water cooled due to the high power handling capability and the anticipated HOM power that will be encountered in BESSY VSR.

There are several reasons to use waveguide HOM absorbers instead of beamline absorbers in this application. The risk of particulate contamination is reduced with the beamline absorber further from the cavity and not in direct line of sight to the cavity. There is also no possibility of problems associated with electrostatic charge buildup on the absorber as the electron beam does not “see” the absorber material. Additionally, beamline absorbers must be cryogenically cooled in order to reduce the static heat leak into the SRF cavity, while the waveguide absorber can be water cooled due to the distance between it and the cavity. Due to the anticipated power level cryogenic cooling of a beamline absorber would be challenging as well as extremely expensive to implement if even possible. This results in significant cost savings as well as risk reduction by reducing the demands on the cryogenic system. Finally the waveguide absorber allows the cavities to be placed closer together, thus improving the packing factor and the so called real estate gradient of overall accelerating gradient per meter of space utilized. Most importantly in the case of BESSY VSR it allows for the module to be designed to fit into the low β straight section which is available for the module.

The magnetic shielding that will be employed in this module will consist of an inner and outer shield. The inner shield will be designed to go adjacent to the cavity and helium vessel and will be located inside of the aforementioned blade tuner. This will be a cold shield designed and annealed for operation at less than 10 K, the anticipated temperature of the shield in poor thermal contact with the

helium vessel. There are a great number of challenges in engineering this shield to properly cover the cavity, taking into account the large number of discontinuities introduced by the HOM waveguide ports. Horizontal testing of the cavities in the horizontal test cryostat HoBiCaT will be critical in understanding the design and building confidence that the cavity performance is adequate and the cavity Q_0 can be maintained.

The second magnetic shield will be a 50 K designed shield that will be located just to the outside of the HOM loads, but still in close proximity to the cavity. With a dual shield design the earth's stray field should be reduced below 5 μ T at the cavity surface, more than adequate to attain the desired operating quality factor for the BESSY VSR project. In addition to the two main shields, local shielding will be placed around known problem components, specifically the motor on the tuner.

The 50 K thermal shield for the module will be a liquid helium cooled copper shield located near the outer edge of the cryomodule. The shield will be designed to have the cooling channels laser welded directly to the shield mass to improve the heat transfer and thus the cooling efficiency of the shield. The shield plays an active role in intercepting the heat loads from the fundamental power couplers as they are the most direct link of the 1.8 K cavity to the 300 K exterior environment, an important consideration in the design as this can have a very significant effect on the overall 5 K and 1.8 K cryogenic budgets if this heat load is not properly managed.

The final two components of note in the module are the bellows between the cavities and the RF shielded gate valves that will be used to isolate the module from beam-line. The bellows will be of similar design to what is currently used in BESSY II, a copper plated bellows with RF shield on the inside to avoid heating of the bellows from the wall currents of the 300 mA recirculating electron beam. The technical challenges here are ensuring the bellows can move freely without generating any particulate matter while also being designed to handle the thermal load introduced by the beam. Both criteria are critical to the performance of the SRF cavities and place very stringent demands on the quality of the fabricated parts.

The RF shielded gate valves will be a commercial product and a proven design already in use in BESSY II and several other electron accelerators around the world. The key to the RF shielded gate valve is ensuring the valve body does not heat up due to the close proximity to the cavities at the beginning and end of the module as well as due to the wake fields from the 300 mA beam. This will be simulated in ANSYS[®] to ensure no additional cooling is necessary on the valve body, as well to better understand the impedance this configuration introduces.

3.5 RF Systems

In this section the RF power components such as transmitters, circulators and waveguides are discussed while the amplitude and phase control loops as well as RF power requirements are discussed in Section 3.6.

3.5.1 RF Transmitters

Each cavity will be powered by an individual transmitter so that individual phase and amplitude control is possible. The required power level for each transmitter is 16 kW as discussed in Section 3.6 including losses in the RF distribution. The RF power overhead is primarily required for microphonics compensation.

There are two options to generate this power: electron tube based amplifiers or solid state amplifiers. At 1.5 GHz frequency there are 13 kW klystrons used at CEBAF [30]. At 1.75 GHz no klystron is on the market. It has to be developed by scaling a similar tube. An alternative choice is the use of solid state transmitters. At a frequency of 1.3 GHz they are well established and already in use at ELBE accelerator [31] and at HZB at the HoBiCaT test facility, see Figure 3.23.



Figure 3.23: Solid state transmitter (1.3 GHz 15 kW) at the HoBiCaT test facility of the HZB.

For higher frequencies the transistor efficiency decreases and more transistors will be needed, but transmitters for 1.5 GHz and 1.75 GHz can be developed for a reasonable price. Solid state amplifiers have the great advantage that the noise generated by the transmitter is very low, which helps meet the high stability demands for BESSY VSR. Figure 3.24 shows the amplitude and phase noise of the operational HZB 1.3 GHz 15 kW transmitter. There is only minor noise added by the power transmitter to the noise of the driving source.

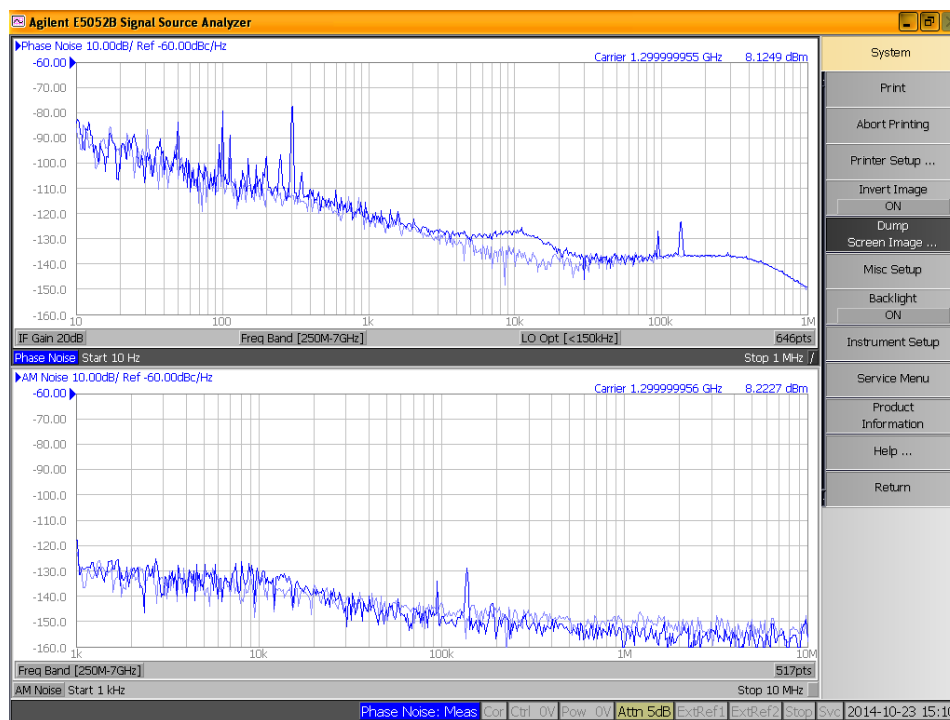


Figure 3.24: Phase (upper) and amplitude (lower) noise of a solid state transmitter 1.3 GHz 15 kW. The light blue line is the noise of the master generator, dark blue the output of the transmitter

3.5.2 RF Transmission Lines

At the required power level only waveguides can be used. Whether a single power circulator in the output line or distributed circulators in the transmitter are a better choice will be evaluated by the costs; either is possible and state of the art.

3.5.3 RF System for the Booster Synchrotron

In order to produce shorter bunches in the booster synchrotron for efficient injection into the short bunches of the storage ring a new RF system at a frequency of 3 GHz delivering 4 MV accelerating peak voltage is proposed, see Table 2.7.

3 GHz Cavity for the Booster Synchrotron

The RF system of the booster is operated in long pulse mode. The accelerating cycle is 45 ms and the de-accelerating cycle the same. The repetition rate is 1 Hz (restricted by radiation protection). At this frequency only travelling wave structures are developed, optimized for short pulse application. There is a NC standing wave structure at 2.45 GHz and a scaled version at 4.9 GHz by University of Mainz available [32], see Figure 3.25 that would fit when scaled to the right frequency.

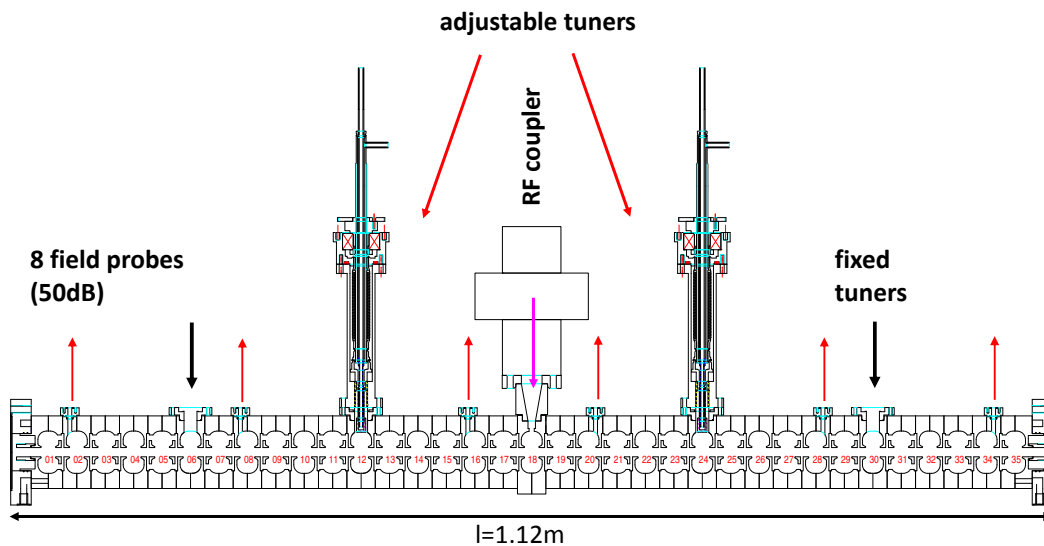


Figure 3.25: 4.9 GHz standing wave RF structure from University Mainz [32].

3 GHz Transmitter for the Booster Synchrotron

To achieve a peak voltage of 4 MV and using scaled University Mainz cavity structures the required total power level at the cavities is 69 kW when using two cavity structures or 46 kW when using three cavities. 30% power has to be added for losses in the waveguides and circulators. A klystron developed for a frequency of

2.45 GHz and 50 kW power level exists [33]. This klystron needs to be scaled in frequency. Alternately the use of solid state technology is an option. But at a frequency of 3 GHz each transistor can only deliver 30 W to 40 W of power compared to 150 W to 250 W in L-band. To build a transmitter of some 10 kW power a high number of transistors is needed. Due to the fact that the technology for solid state amplifiers is strongly progressing and the prices are slightly falling, the final setup of the RF system for the booster meaning the choice of transmitter technology and the choice of the number of installed structures will be made by optimizing the price at the time when the budget is available.

3.6 RF Control and LLRF, Microphonics

The task of the low level RF field control (LLRF) is to maintain a stable amplitude and phase of the longitudinally focusing $\text{TM}_{010-\pi}$ mode of the higher harmonics cavities with respect to a reference given by a multiple of the beam revolution period $\omega_{\text{rf}} = \nu\omega_0$.

On the one hand this means to deal with the challenge to operate a high loaded Q SRF cavity in CW mode. Typical error sources contributing to cavity field amplitude and phase jitter are microphonics detuning and the coupling of the Lorentz force detuning to any deviation in field amplitude. Other noise sources include phase noise from the RF source and the reference distribution system. Those noise sources have been studied in detail at various labs including the work done at HZB's HoBiCaTcavity test facility [23, 34]. Using Cornell's LLRF system it was demonstrated that operation at high Q_L of 5×10^7 to 2×10^8 is feasible achieving residual phase errors of $\leq 0.01^\circ - 0.02^\circ$ and a relative amplitude jitter of 1×10^{-4} or even lower [35]. The peak detuning measured at that time at E_{acc} of 12 MV/m was 15 Hz. At 20 MV/m probably a larger peak detuning will be observed by the increased Lorentz force detuning. The measured jitter data were also used for the single particle dynamics shown in Section 2.5. This part of field control is still a challenge, especially in the case of strong microphonics, but seems to be manageable.

On the other hand, the synchronous phase of the HHC is set to zero-crossing and the cavity experiences a mainly reactive beam-loading. This leads to an additional in quadrature cavity voltage, resulting in a phase shift [36] of the RF voltage. In steady state this can be easily compensated by the correct amount of cavity tuning and phase adjustment, but in the case of BESSY VSR there will be one or two gaps within the bunch train and also several single bunches contributing to a transient beam loading effect. Thus the induced beam loading voltage cannot any longer

be considered as constant [37]. The shifted optimum detuning has to be carefully determined by RF simulation assisted calculations.

Each beam gap comes with a repetition rate of 1.25 MHz. Even if enough power overhead to compensate for the full beam transient was available, this gap width of $\Delta T_{\text{gap}} = 200$ ns would be far beyond the bandwidth of any LLRF loops. It will be detected by the high sampling rates offered by modern digital signal processing (DSP) systems, but the loop gain will be small due to needed suppression of the other passband modes and the need to avoid feedback instability.

By the zero crossing synchronous phase the optimum cavity coupling β_c is in theory unity, which is not feasible for a high Q_0 resonator with a sub-hertz bandwidth. Therefore the fundamental mode's external Q is chosen to adapt the bandwidth to the expected peak detuning as:

$$Q_{\text{ext,opt}} = \frac{1}{2} \frac{f_{\text{rf}}}{\Delta f_{\text{peak}}} \quad (3.8)$$

which is a direct consequence of Equation (3.11) to minimize the required power. Assuming that the transient beam loading and tuning to compensate for Robinson instability can be controlled, a loaded Q of 5×10^7 seems within reach allowing operation at the few kW level at a peak detuning of 15 Hz.

As already discussed in Chapter 2 the LLRF feedback system cannot be considered as a standalone system only compensating unwanted modulations of the accelerating voltage in the cavity gap. In a storage ring a bunched beam performs several damped motions in both longitudinal and transverse planes, as ,e.g., the coupling of the bunch's synchronous phase and energy via the synchrotron oscillations. The voltage V_{br} excited by the beam's image current I_{im} in the cavity depends linearly on the cavity's shunt impedance R_{shunt} and is on resonance given by:

$$V_{\text{br}} = \frac{I_{\text{im}} R_{\text{shunt}}}{(1 + \beta_c)}. \quad (3.9)$$

Here, β_c is the coupling between the cavity and the external RF source and the effective loaded shunt impedance is given by $R_L = R_{\text{shunt}} / (1 + \beta_c)$. Any beam induced voltage, if not compensated for by extra generator voltage, alters the restoring potential which is available to achieve a phase stable synchrotron motion. By detuning the cavity the excited voltage is reduced according to the relationship

$$\begin{aligned} \tilde{V}_b &= \tilde{I}_{\text{im}} \frac{R_L}{1 - iQ_L \left(\frac{\omega_r}{\omega_{\text{rf}}} - \frac{\omega_{\text{rf}}}{\omega_r} \right)} \\ &= \tilde{I}_{\text{im}} \underbrace{R_L \cos \psi e^{i\psi}}_{\tilde{Z}_{\text{cav}}}, \end{aligned} \quad (3.10)$$

with the tuning angle ψ for small $\Delta\omega^2$ given by $\tan \psi = 2Q_L\Delta\omega/\omega_r$. Optimum detuning is obtained when the sum of the ψ shifted beam loading induced and generator voltage add up to the desired cavity voltage at the desired synchronous phase with respect to the beam at minimum required generator power. The needed forward power at a given coupling β_c for a cavity voltage V_{cav} and synchronous phase ϕ_{acc} , can be derived from the beam and generators phasor relation to [37]:

$$P_f = \frac{V_{\text{cav}}^2}{R_L} \frac{\beta_c + 1}{8\beta_c} \left\{ \left(1 + \frac{2R_L I_{b0}}{V_{\text{cav}}} \cos \phi_{\text{acc}} \right)^2 + \left(\tan \psi + \frac{2R_L I_{b0}}{V_{\text{cav}}} \sin \phi_{\text{acc}} \right)^2 \right\}$$

Here, ϕ_{acc} is ± 90 degree at zero crossing. For SC cavities with $\beta_c \gg 1$:

$$P_f \approx \frac{V_{\text{cav}}^2}{\frac{R}{Q} Q_L} \frac{1}{4} \left\{ \underbrace{\left(1 + \frac{\frac{R}{Q} Q_L I_{b0}}{V_{\text{cav}}} \cos \phi_{\text{acc}} \right)^2}_{\text{resistive}} + \underbrace{\left(\frac{\Delta f}{f_{1/2}} + \frac{\frac{R}{Q} Q_L I_{b0}}{V_{\text{cav}}} \sin \phi_{\text{acc}} \right)^2}_{\text{reactive}} \right\}. \quad (3.11)$$

Here the approximation was used, that for short Gaussian bunches the image currents Fourier component at the cavity's RF is twice the DC beam current ($I_{\text{im}} = 2I_{b0}$). The cavity 3 dB half-bandwidth is given by $f_{1/2} = f_{\text{rf}}/(2Q_L)$. Compensating for the beam loading means to detune the cavity so that the reactive term vanishes:

$$\Delta f = -\frac{R}{Q} \frac{f_{\text{rf}} I_{b0}}{2V_{\text{cav}}} \sin \phi_{\text{acc}} \quad (3.12)$$

Ramping of Cavities and Injection Issues

Figure 3.26 shows the dependence of the required detuning for a given beam current and cavity impedance versus the cavity voltage. The BESSY VSR working point is depicted by the blue circle, the dashed brown curve shows an alternative with reduced R/Q and beam current. Generally, the ramping of the HHC with the beam being stored requires a tuning of the order of tens to hundreds of kHz, that only a coarse tuner system will be able to cover that range. E.g. reducing the cavity voltage from 10 MV down to 600 kV demands a tuning by about 176 kHz. Typical tuning systems cover a range of ± 350 kHz with a stepper motor based system and in addition only 1 kHz to 2 kHz using fast piezo based systems [23]. The solid linear curves depict the required forward power at optimum detuning for different loaded Q_L . To stay within the 10 kW level $Q_L \geq 5 \times 10^6$ is required. As discussed later, this will already limit the range of impedance reduction for the beam and has a direct influence on the level of the Robinson instability threshold.

²Small detuning with respect to the radio frequency or $\omega_{\text{rf}}/\omega_r \approx 1$. $\Delta\omega = \omega_r - \omega_{\text{rf}}$. Here, ω_r is the cavity resonant frequency.

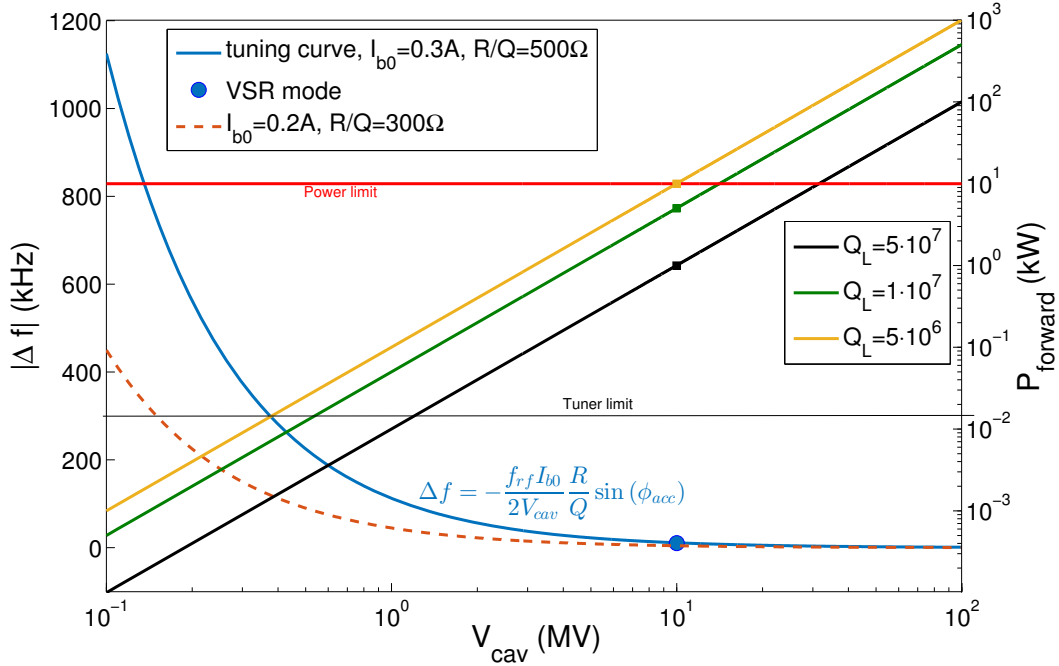


Figure 3.26: The blue line depicts the required detuning at zero-crossing operation for the 1.5 GHz system versus the cavity voltage. The BESSY VSR working point is shown by the blue circle. The yellow, green and black solid lines denote the required forward power at the coupler for different coupling strengths or Q_L at optimum detuning. The solid horizontal lines give an estimates of the upper tuner and power source limits. The dashed brown curve shows the tuning for a lower beam current, lower R/Q scenario.

For injection into the short buckets using the existing booster synchrotron the HHCs have to be ramped down in field as the bunches from the booster need to be injected in rather standard long buckets for high injection efficiency (see Section 2.9.1). During that process the cavity still experience the high reactive beam loading of the main long bucket beam. The coarse tuner will need rather order of minutes for tuning the cavity for the minimum acceptable field limit. The fast piezo tuner does not offer the needed tuning range. Thus the fraction of dark time for short pulse users may reach the order of 50%. As shown in Figure 3.27 a deviation from the optimum tuning is not a choice as well, because it would mean to foresee a huge power overhead of the order of hundreds of kW (out of the range of this plot). A third possibility might be artificially reducing the impedance and beam current as given by the dashed brown line of Figure 3.26. This would reduce the reactive

beam loading and such the required tuning. Reducing the R/Q by a factor of two and the beam current to 200 mA still require a range only covered by slow coarse tuning systems. Further, such a low impedance superconducting cavity will quite probably operate at 20 MV/m close to or even above its quench limit.

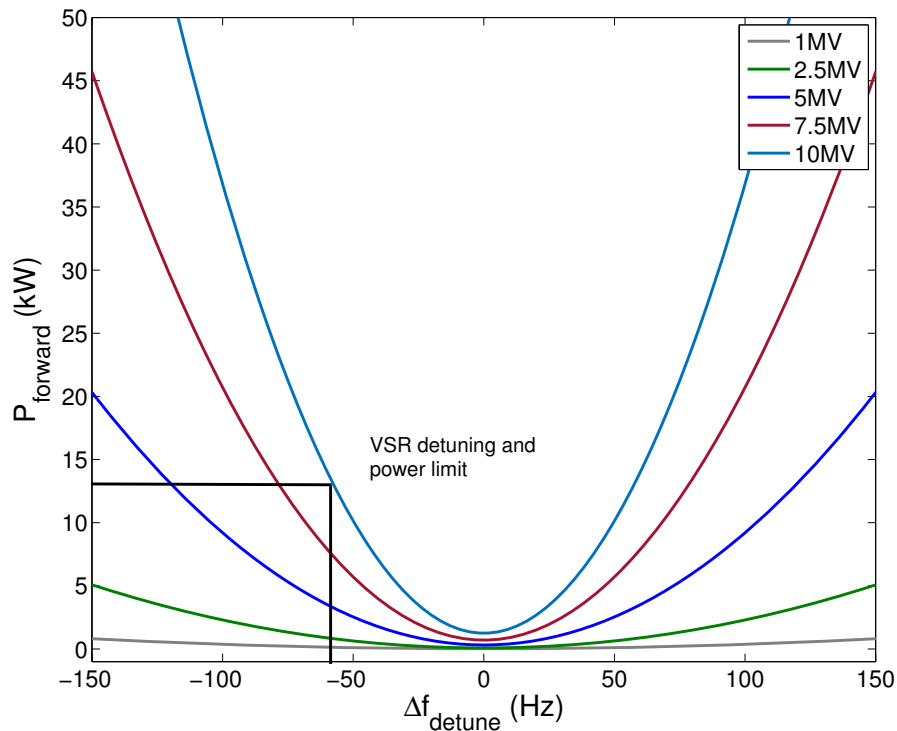


Figure 3.27: For different cavity voltages at and below the BESSY VSR design voltage the required forward power is plotted against a deviation of the cavity tuning away from the optimum tuning. Here a Q_L of 5×10^7 was assumed.

Summing up, with the existing synchrotron TopUp injection into the short buckets or even only an injection a few times per hour to compensate the decay mode is not feasible with the given boundaries. Besides the power overhead needed to compensate for detuning deviation while ramping the field level and thus the necessity for high power couplers and transmitters, a high tuning duty cycle increases the risk for tuner mechanics failure and even cavity leakage by mechanical stress. Further, to prohibit a runaway of the beam induced cavity fields the tuning curve vs. voltage has to be tracked to high precision during e.g. a ramping of the field level while the beam is already stored or vice versa. Any deviation has to be compensated by large amount of RF power, an investment not foreseen for this project. A fast

ramping of the cavity fields under full beam loading as e.g. by the top up operation and being mostly a question of short bunch Touschek lifetime is nearly impossible within the envisaged boundary conditions of a SRF low power operation.

Choice of Required Forward Power

As given in Figure 3.27 at the operating cavity voltage of 10 MV and 300 mA beam current a deviation from the optimum detuning of 58 Hz leads to a required power of 13 kW. To keep capital cost as low as possible, we aim to limit the power overhead to as low as possible without posing too much risk on the final stability of the BESSY VSR mode of operation. Thus, the required forward power of 16 kW, resulting in about 13 kW available power at the coupler after subtraction of transmission line losses, is given by the following assumptions:

- Measured peak detuning levels of CW operated cavities are between 15 Hz to 20 Hz. Those measurements were done at intermediate field levels between 10 MV/m to 12 MV/m. At higher fields increased microphonics by higher RF losses in the helium bath and ponderomotive instabilities may be expected. An overhead of about a factor of three should leave enough safety margin, especially taking into account that other effects contribute as well.
- The detuning overhead of 58 Hz at 10 MV cavity voltage allows a beam current deviation of 1.55 mA which can be given by non properly synchronized TopUp injection events or a mis-calibrated beam current measurement. The latter might be compensated by the tuning algorithm anyway.

As we decided to use the Cornell 60 kW power coupler design (see Section 3.2.2 and Section 3.4), there is still head room to later upgrade the existing solid state amplifiers.

Robinson Stability and High Intensity Beams

A critical limit for high intensity beam operation is given by the DC and AC Robinson stability criteria as explained in [38]. The AC instability results from the interaction of the beam's synchrotron sidebands with the cavity impedance. In an above transition machine like an electron ring damping of synchrotron oscillation occurs if an e.g. lower momentum particle having a higher revolution frequency sees a lower detuning angle ψ and thus gains more energy than the synchronous particle. This is true for the condition:

$$\begin{cases} \psi > 0 & \text{or } \omega > \omega_{RF} & \text{below transition} \\ \psi < 0 & \text{or } \omega < \omega_{RF} & \text{above transition} \end{cases}$$

This criterion is obviously not satisfied for the 1.75 GHz system which operates for the long pulses at $\pi/2$ thus requiring $\psi > 0$ in order to satisfy the minimum power requirement by Equation (3.11). In the DC case, matters are even more severe because the restoring potential does not even exist. This means that any extra accelerating voltage imposed by perturbed phasing due to the beam loading voltage has to be compensated such by the RF and proper tuning that the stable potential is still maintained. This is satisfied if:

$$\frac{V_{\text{br}}}{V_{\text{cav}}} < \frac{\cos \phi_{\text{acc}}}{\sin \psi \cos \psi} \begin{cases} \psi > 0 \text{ or } \omega > \omega_{\text{RF}} & \text{below transition} \\ \psi < 0 \text{ or } \omega < \omega_{\text{RF}} & \text{above transition} \end{cases} \quad (3.13)$$

This is again not the case for the 1.75 GHz system. Figure 3.28 shows the stability criterion from Equation (3.13) for the 1.5 GHz cavity for two different couplings. A

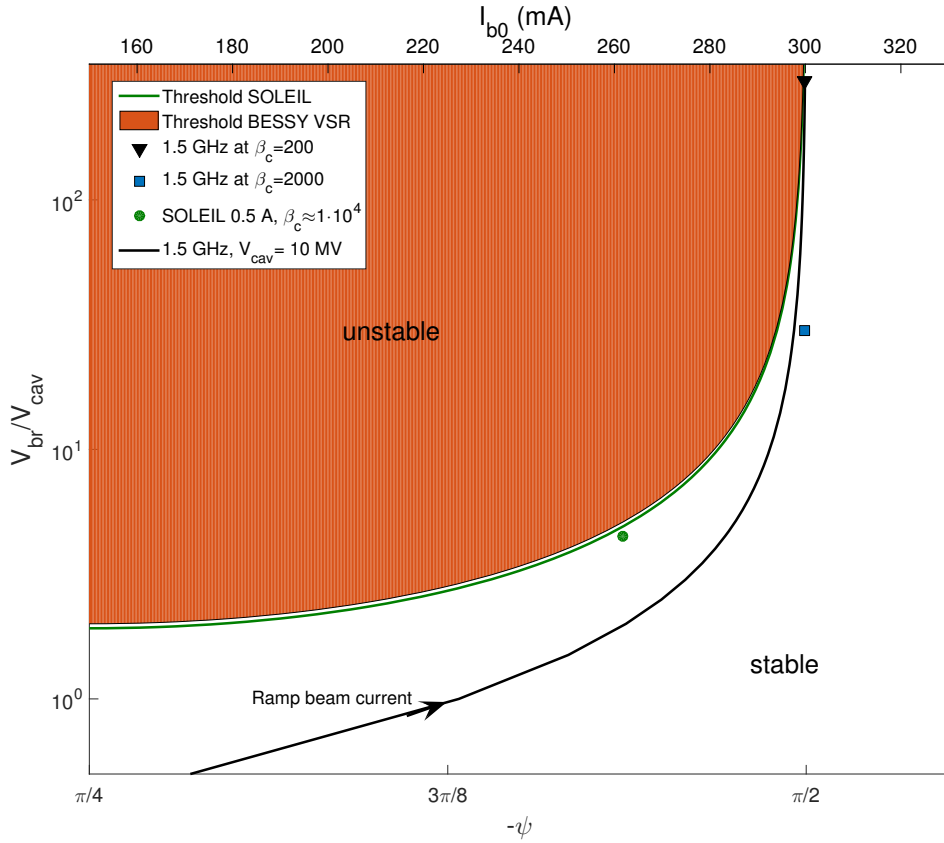


Figure 3.28: Threshold limit of beam current for the 1.5 GHz system according to the DC Robinson stability criterion at two different cavity couplings β_c versus tuning angle ψ . The black line denotes the beam injection into a 10 MV cavity assuming optimum detuning. For a comparison the SOLEIL fundamental system is shown.

stronger coupling reduces the cavity impedance and hence V_{br} . This would increase the stability margin to the threshold limit, but as mentioned above that would have to be paid for by a factor of ten increase in RF power. Also it has to be checked whether the ramping of the cavities while the beam is already present can be done in a stable way or if the beam has to be injected into already fully powered cavities, as it is shown by the solid black line. Here, also an optimum tuning with respect to the beam current was assumed. Nevertheless, RF feedback methods, like direct RF feedback, amplitude and phase control and tuning loops also change the impedance the beam couples to [39, 40]. In case of direct RF feedback and amplitude/phase control the stability threshold scales by $1 + G$ with G being the loop gain. But it can already be stated, that a passive operation of the 1.75 GHz system alone is unstable as it violates the Robinson criteria. The 1.5 GHz system alone can be operated as a passive harmonic system in BESSY II. The combined system of all frequencies is stable again, as there is a cancellation of the unstable regime by the 3rd harmonic system, but it needs to be studied how robust this combined system is to any perturbation.

However, to evaluate the impact of the LLRF feedback system and gain on the effective impedance experienced by the beam, one not only needs to consider the synchrotron sidebands. The non-uniform beam filling further complicates the situation. Transient beam loading by a complex beam pattern including ion clearing gaps and single bunches for different user applications further deviates the bunched beam Fourier components, adding contributions at the gap's revolution frequency. Thus the beam threshold current has to be analyzed in frequency domain (Laplace domain) to consider the variable loop gain as a function of sideband frequency. Also the optimum tuning is additionally influenced by the gap as it induces a phase variation across the bunch train and thus different voltages experienced by the bunches within the train.

Summing up, a frequency domain analysis of the LLRF-cavity system is mandatory to determine the loaded impedance and gain at the sidebands and finally the DC and AC Robinson instability thresholds. Also the correct detuning has to be determined by simulations. A starting point was estimated by Equation (3.12) by composing the beam into the long and short pulse components which have different phasing for the 1.75 GHz cavity. An approach to study this problem by combined LLRF-cavity and longitudinal beam dynamics simulation will be presented in the following sub-section.

3.6.1 Combined LLRF-Cavity Beam Dynamics Simulations

To test the BESSY VSR operation from the cavity point of view a combined RF cavity, LLRF feedback and longitudinal beam dynamics simulation was started

based on the well known LCR circuit model to describe the cavity field envelope of the fundamental mode evolving under given perturbations, like e.g. microphonics, tuning, Lorentz-force detuning, phase noise, feedback loop delay times to name a few. An overview is given in Figure 3.29.

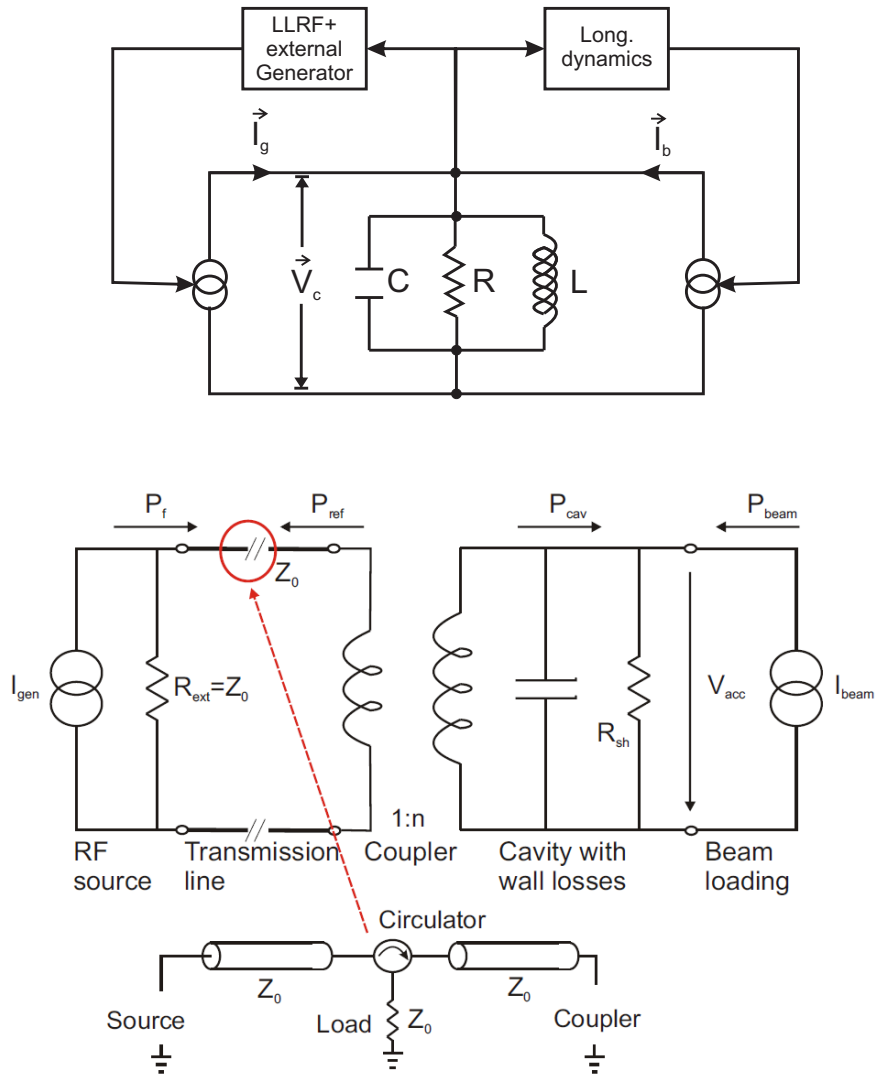


Figure 3.29: LCR circuit model for an accelerating cavity including an RF generator with a feedback system and the longitudinal beam dynamics for the synchrotron oscillations. Here, for the cavity also modeling of the various cavity detuning sources are included. The lower figure displays the full LCR model in more detail.

The lower subfigure depicts the LCR circuit for the cavity impedance as well as the transformer to model the coupling of an external load by the RF generator. This model is extended by several detuning and error sources as described in [41] and features a second order mechanical model. Different LLRF feedback schemes can be implemented for the RF loop and the tuning loop. This model was further extended, as demonstrated in the upper subfigure, by a beam creator for the foreseen bunch pattern including charge and injection jitter and also the longitudinal dynamics for the storage ring.

In Figure 3.30 the outcome of a long-term simulation of about ten thousand turns is shown. An operation of both HHC systems in active mode was possible with about one kW of forward power in steady state by operating the bunch train in a quasi zero-crossing operation, that at the end only one bunch experiences a real zero-crossing gradient, which will lead to variations of the synchronous phase and voltage gradient across the train and thus of the bunch length as discussed in Section 2.6.

The upper plot depicts the variation of the cavity RF phase of the 1.5 GHz structure and the resulting variation of the gap voltage, as the tuning is constant. The color coded circles show the relative energy deviations of the macro-particle bunches.

Table 3.10 summarizes the simulation parameters and the outcome of the simulation regarding the field stability and the gap induced phase transients across the train. First simulation show stable solutions, but more detailed studies are ongoing. Not included so far (but implemented in the code) was, except the Lorentz-force detuning, the microphonics detuning and its compensation as those time domain based calculations are very time consuming. The time scales range from ns beam macro particles up to ms regime regarding damping time constants of the second order mechanical system.

But first short term simulations already showed that precise microphonics control by piezos is mandatory to keep the loop within the limit of the available forward power. The latter being especially important to avoid Lorentz-force induced ponderomotive field oscillations or decay, which would immediately lead to unstable synchrotron oscillations. Further, a more realistic fill pattern with individual current levels within the buckets to account for injection charge jitter and the decay and refilling process of the TopUp mode (see e.g. Figure 7.2) needs to be implemented.

Recently, the fundamental 500 MHz system, quantum excitation and synchrotron radiation losses per turn were included, so that finally these simulations can be compared to the outcome of the tracking studies discussed within Chapter 2. First attempts show again a stable behavior, but those simulations are still under study. Also, a more detailed analysis of beam decay and its compensation by the tuning

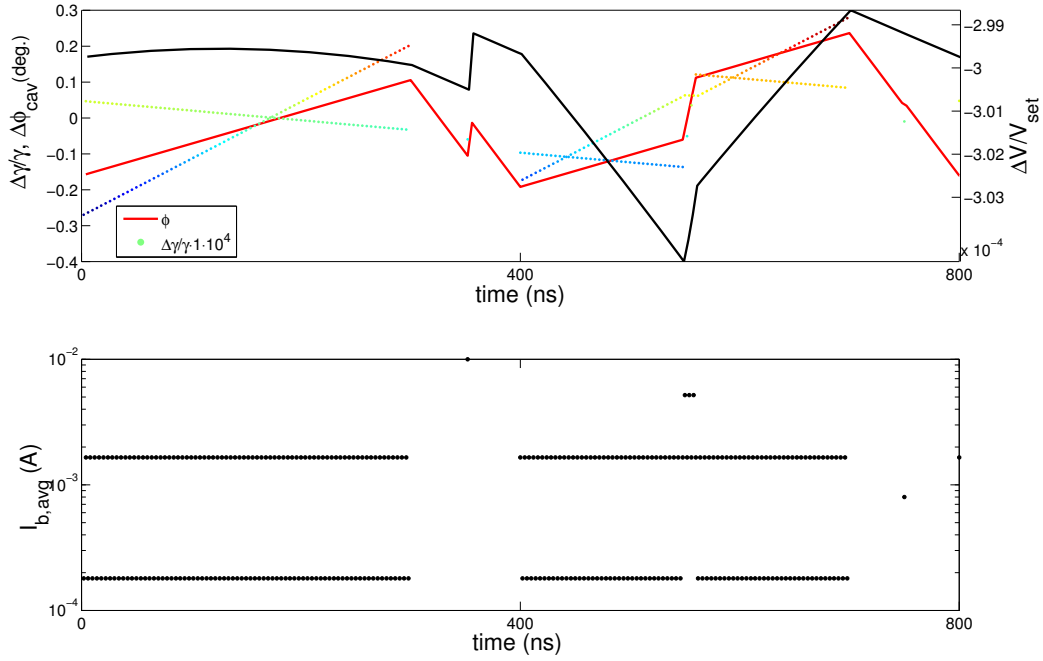


Figure 3.30: The upper plot shows the transient in the cavity voltage (black) and RF phase (red) for the 1.5 GHz cavity. The color coded scatter plot shows the relative energy deviation operating both RF systems using the fill pattern depicted below. Each cavity is operated at Q_L of 5×10^7 and the LLRF settings described within the text. Longitudinal beam dynamics are included.

loop as well as the handling of additional beam transients by the TopUp injection will be performed.

A further topic is to determine optimum loop parameters and the stability margin and maximum gain to avoid the unstable Robinson regimes. An example of the influence of loop gain on the longitudinal stability is presented in Figure 3.31. It shows the longitudinal phase space of the same set up of both HHC operated with active feedback loops but different loop gains. As can be seen a low loop gain leads to the expected onset of the DC Robinson instability. Similar simulations also need to be done for injection phase errors.

Table 3.10: Parameters set and simulation results obtained by LLRF-cavity-beam dynamics simulations. The sampling time was 1 ns. The obtained detuning for minimum power includes Lorentz force detuning. The simulation ran for 10000 turns. Here, only one cavity per frequency was simulated.

Parameter	Simulation value
HHC	
RF frequencies	1.5 GHz, 1.75 GHz
Voltage at 1.5 GHz	10 MV
Voltage at 1.75 GHz	8.7 MV
Mean acc. field at 1.5 GHz	20.0 MV/m
Mean acc. field at 1.75 GHz	20.0 MV/m
Q_L	5×10^7
R/Q TM ₀₁₀ - π	500 Ω
ϕ_{acc}	90, -90°
LLRF loop	
Feedback gain K_P	3500
Loop filter f_{cutoff}	50 kHz
Loop latency τ_{loop}	800 ns
Long. beam dynamics	
α	7.3×10^{-4}
τ_{rad}	8 ms
Results	
Δf for 2 nd bunch	-11.26 kHz
Pattern at 1.5 GHz, 1.75 GHz	9.969 kHz
Average P_f per cavity (1.5 GHz, 1.75 GHz)	1.07 kW, 1.12 kW
$\Delta\phi_{\text{RF}}$ by gap	$\pm 0.2^\circ$
$\Delta V_{\text{cav}}/V_{\text{set}}$	3×10^{-4}
$\Delta\gamma/\gamma$ across train (long bunch)	$2.8 \times 10^{-4} - 3.2 \times 10^{-4}$
$\Delta\gamma/\gamma$ across train (short bunch)	$2.6 \times 10^{-4} - 3.4 \times 10^{-4}$

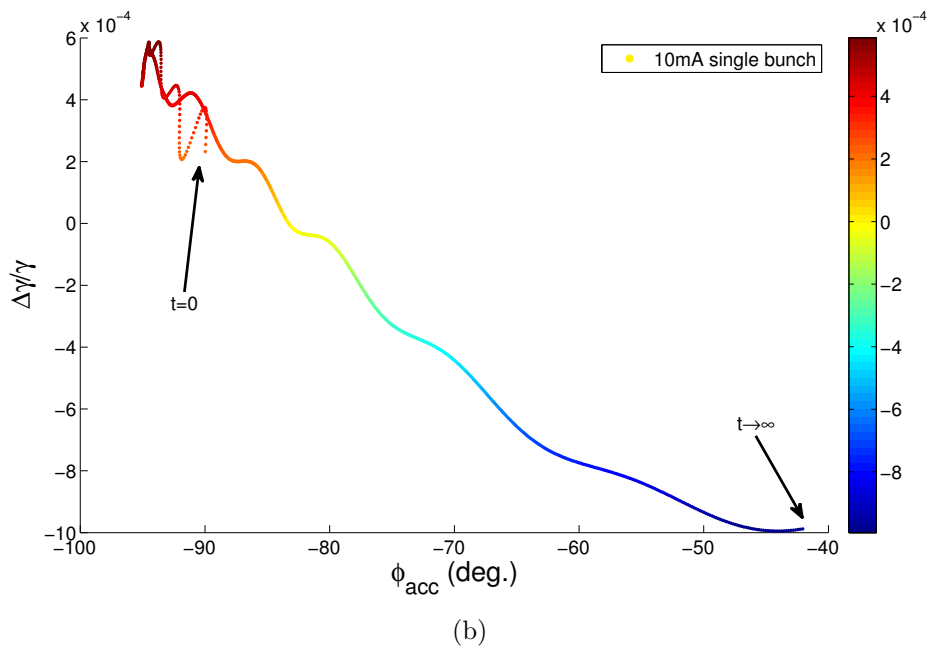
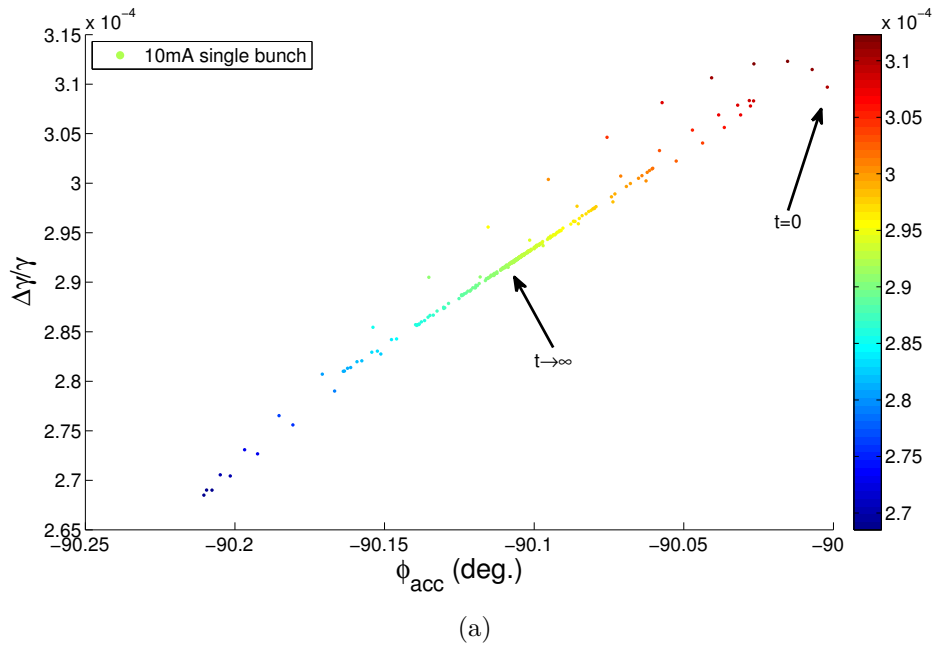


Figure 3.31: Longitudinal phase space for the high current long pulse bunch for high gain case of $K_P = 3000$ (a) and $K_P = 30$ (b). While the high gain case damps to a stable steady state solution, for the low gain case the bunch experiences a DC Robinson decay. The color code denotes the energy deviation from the reference particle without scaling.

3.6.2 A Generic LLRF System

Within the L-band regime modern digital LLRF control systems mostly rely on the analog down-conversion by mixing with a shifted local oscillator frequency (LO) in order to sample the field components at an intermediate frequency signal (IF) to still obtain the needed bit resolution. Modern digital LLRF systems operate at IFs of 20 MHz to 80 MHz using four times oversampling or odd sampling techniques to determine the field's amplitude and phase information acquired via in-phase and in-quadrature (IQ) sampling.

The signal conditioning takes place in an analog front-end system down-converting the different probe signals as forward, reflected and transmitted power to the IF which are then digitized and decomposed into the I and Q components. Those signals are used to reconstruct the current field vector, compare it to reference and wanted set point value and feed back an amplified and/or integrated difference signal to the RF source in order to minimize the field deviation by a counter modulation of the forward signal.

This process has to be fast and is usually programmed within an field programmable gate array environment to keep the system latency small to allow for high gain operation without the danger of control loop instabilities. The only additional features of those loops are filtering, mainly to avoid excitation of the neighboring passband modes and feed-forward and set point tables to cover special modes of operation, as e.g. to ramp the field. Current systems reach an ADC to DAC time delay of 600 ns [42].

The field components are also processed on a slower time scale on any other kind of digital signal processing (DSP) board to calculate the cavity tuning and to implement detuning compensation schemes to suppress microphonics in CW mode, counteract ponderomotive Lorentz-force detuning and to detect cavity field trips. Further bundling all available cavity signals, as e.g. vacuum and temperature sensor information, once can program a state machine like system in order to control the cavity within the BESSY VSR scheme and to perform quench detection and other exception handling.

Because of the need for precise tuning, microphonics has to be recorded as well as the beam current to track the needed tuning angle and remain within the tight power margin of 13 kW. The system will foresee different loops as already discussed within this Section:

1. Fast LLRF loop with high sampling rate and high gain IQ control including filtering of the neighboring $4/5\pi$ passband mode, proportional integral control of the field variations

2. Direct RF feedback loop including comb filter to reduce all $1/5\pi - 4/5\pi$ passband mode's impedances
3. Beam current and cavity voltage tuning loop using the motor tuner for coarse tuning and the piezo tuner for fine adjustment of optimum tuning
4. Microphonics and Lorentz-force detuning compensation loop recording deviation of the set tuning angle with time and deviations from field set point and currently measured field level
5. Feedforward signal triggered by TopUp injection to reduce beam induced transient
6. Measurement of HOM excitation by recording the signals for given dipole modes in the HOM waveguide dampers to allow reconstruction of the beam position and detect for coupled bunch instabilities

It has to be assured that no unwanted cross-talk within these loops or to the beam based feedback schemes occurs.

Feedback Stability and Gain Margin

A first glance at analyzing the LLRF system was done by calculating the open loop transfer function in the Laplace domain including the complete TM_{010} passband as reported in e.g. [43]. The transfer function of the loop contains the continuous description of the cavity passband for the on resonance case with the Laplace transform $F(s) = \int_0^\infty f(t)e^{-st}dt$ with $s = \delta + i \cdot \omega$:

$$\begin{aligned}
 H_\pi(s) &= \frac{1}{1 + \frac{s}{\omega_{1/2}}} \\
 H_{(n/5)\pi}(s) &\stackrel{n \neq 5}{=} (-1)^{n+1} 2 \sin^2 \left(\frac{n\pi}{10} \right) \frac{\omega_{1/2} (s + \omega_{1/2})}{\Delta\omega_n^2 + (s + \omega_{1/2})^2} \\
 H_{\text{cav}}(s) &= \sum_{n=1}^5 H_{(n/5)\pi}(s). \tag{3.14}
 \end{aligned}$$

Here $\Delta\omega_n = 2\pi (f_{(n/5)\pi} - f_\pi)$ for a system tuned to π -resonance and $\omega_{1/2} = 2 \sin^2 \left(\frac{n\pi}{10} \right) \frac{\pi f_{n/5\pi}}{Q_{L,\pi}}$. The \sin^2 term accounts for the field level of the individual passband mode in the end-cell coupling to the power coupler. The RF transmitter's

low pass behavior ($3\text{ dB cutoff} = f_{3\text{dB}}$), the loop delay τ_{loop} and the loop gain K_P are modeled as:

$$\begin{aligned} H_{\text{kly}}(s) &= \frac{1}{1 + \frac{s}{2\pi f_{3\text{dB}}}} \quad \text{similar to a cavity} \\ H_{\text{delay}}(s) &= e^{-s\tau_{\text{loop}}} \\ H_{\text{P-gain}}(s) &= K_P \quad \text{for the complete loop gain} \end{aligned} \quad (3.15)$$

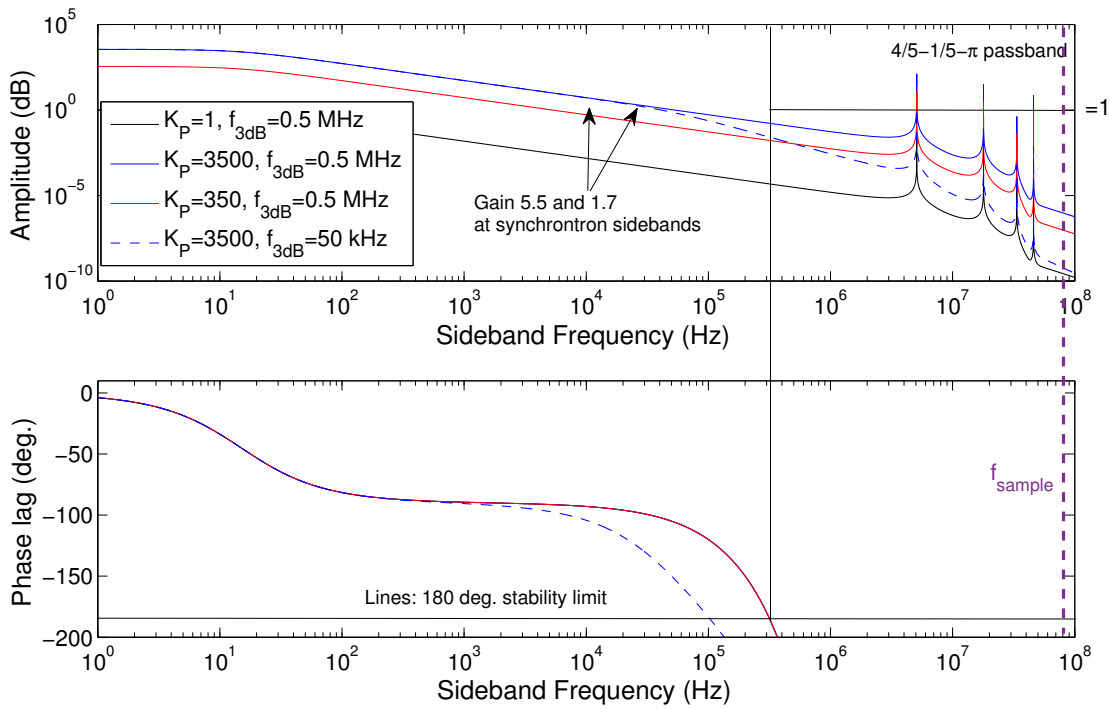


Figure 3.32: Bode plot of the continuous open loop transfer function of a tuned 5-cell cavity including loop delay of 800 ns, RF transmitter bandwidth, proportional feedback gain and first order low pass filtering. The solid black lines denote the π phase shifted unity gain stability limit, the vertical dashed lines the expected sampling rate.

To investigate the stability margin of the total transfer function the frequency sideband is analyzed by propagating a modulation signal through the complete chain given by the product of the sub-components. The outcome is then plotted in amplitude and phase response as given in Figure 3.32 for various feedback gains,

filter settings and control loop delays. The passband parameters were taken from the calculations presented in Section 3.2. The parameters used for the simulations shown in the previous Section 3.6.1 are given by the dashed blue curve. Instability can be determined roughly by the error frequency at which a phase shift of more than 180 degree occurs with a minimum gain of one. This leads to an increase of the unwanted modulation rather than damping. The maximum stable gain here is about $K_P = 7000$, leaving a margin of a factor of two, 3500 should achieve a stable solution for $Q_L = 5 \times 10^7$. This was also demonstrated in simulation, but there without modeling of the closest passband mode, which will be done in future studies.

On the one hand in order to damp the $4/5\pi$ mode a low pass filtering is mandatory, if not a more sophisticated notch filter based system, as a general low pass reduces the bandwidth of the whole loop. On the other hand, for BESSY VSR there are major components within the beam spectrum and thus transient beam loading at the revolution frequency. Compensating for the beam transient with high gain leads to high peak power level above the envisaged power limit. In contrast a high damping of the synchrotron sidebands is favorable, as to reduce the impedance for the Robinson instability. Thus, there needs to be a rather steep slope for frequencies beyond the synchrotron sidebands. This topic needs to be analyzed further and a complete frequency domain analysis as given in [44] will be a useful tool.

LLRF System Parameters

It is already envisaged for the ERL project bERLinPro [45] to use microTCA based LLRF hardware components which were developed by DESY for the European XFEL [46]. Except for the reactive beam loading requirements the cavities for bERLinPro face similar CW operation stability requirements as for the BESSY VSR project. The same type of hardware extended by additional loops can be used for the HHC systems as well. A listing of the LLRF system parameters of DESY's microTCA is given in Table 3.11.

Table 3.11: LLRF system parameters for a mTCA based system.

Parameter	Range
IF	54 MHz
Sampling rate	81.25 MHz
Bit resolution	16 bit at 125 MSamples/s
Phase resolution	0.0015°
ADC to DAC latency	≈ 600 ns
Short term noise stability ADC	≤ 10 fs (10 Hz to 1.0 MHz)
Downconverter RF bandwidth	700 MHz up to 4.0 GHz
Downconverter modulation bandwidth	50 MHz
Short term noise stability Downconverter	≤ 4 fs (10 Hz to 1.0 MHz)
Piezo driver bandwidth	50 kHz at 0.1 μF

References

- [1] P. Marchand et al. “Operational Experience with the SOLEIL Superconducting RF System”. In: *Proceedings of SRF2013* WEP56 (2014), pp. 627–631 (cit. on p. 73).
- [2] J. M. Byrd et al. “Transient beam loading effects in harmonic rf systems for light sources”. In: *Physical Review Special Topics - Accelerators and Beams* 5 (2002), p. 092001. URL: <http://link.aps.org/doi/10.1103/PhysRevSTAB.5.092001> (cit. on p. 73).
- [3] P. Marchand. “Superconducting RF Cavities for Synchrotron Light Sources”. In: *Proceedings of EPAC2004* MOYCH03 (2004), pp. 21–25 (cit. on p. 73).
- [4] D. Teytelman. “Beam-Loading Compensation for SUPER B-Factories”. In: *Proceedings of PAC2005* TOAC002 (2005), pp. 154–158 (cit. on p. 73).
- [5] A. Neumann et al. “Towards a 100mA Superconducting RF Photoinjector for bERLinPro”. In: *Proceedings of SRF2013* MOIOB02 (2013), pp. 42–49 (cit. on p. 73).
- [6] T. P. Wangler. *RF Linear Accelerators*. 2nd. Weinheim, Germany: Wiley-VCH, 2008 (cit. on p. 74).
- [7] V. Veshcherevich et al. “A High Power CW Input Coupler for Cornell ERL Injector Cavities”. In: *Proceedings of SRF2003* THP38 (2003), pp. 722–725 (cit. on pp. 76, 94, 102).

- [8] J.-M. Vogt, O. Kugeler, and J. Knobloch. “Impact of cool-down conditions at T_c on the superconducting rf cavity quality factor”. In: *Phys. Rev. ST Accel. Beams* 16 (10 Oct. 2013), p. 102002. URL: <http://link.aps.org/doi/10.1103/PhysRevSTAB.16.102002> (cit. on p. 77).
- [9] J. Halbritter. “Comparison between measured and calculated RF losses in the superconducting state”. In: *Zeitschrift für Physik* 238.5 (1970), pp. 466–476. URL: <http://dx.doi.org/10.1007/BF01409429> (cit. on p. 77).
- [10] F. Marhauser et al. “Status and Test Results of high Current 5-Cell SRF Cavities developed at JLAB”. In: *Proceedings of EPAC2008 MOPP140* (2008), pp. 886–888 (cit. on p. 77).
- [11] N. Valles et al. “Seven-cell cavity optimization for Cornell’s energy recovery linac”. In: *Proceedings of SRF2009 THPPO08* (2009), pp. 538–542 (cit. on p. 79).
- [12] R. Rimmer et al. “Recent progress on high current SRF cavities at JLAB”. In: *Proceedings of IPAC2010 WEPEC076* (2010), pp. 3052–3054 (cit. on p. 79).
- [13] J. Sekutowicz et al. “Design of a low loss SRF cavity for the ILC”. In: *Proceedings of PAC2005 TPPT056* (2005), pp. 3342–3344 (cit. on p. 79).
- [14] COMSOL Inc. *Multiphysics*. URL: www.comsol.com (cit. on pp. 80, 82, 95).
- [15] K. Halbach and R. Holsinger. “SUPERFISH - a Computer Program for Evaluation of RF Cavities with Cylindrical Symmetry”. In: *Particle Accelerators* 7 (1976), pp. 213–222 (cit. on p. 80).
- [16] ANSYS Inc. *ANSYS HFSS*. URL: www.ansys.com (cit. on pp. 82, 87, 91).
- [17] CST – Computer Simulation Technology AG. *Microwave Studio*. URL: www.cst.com (cit. on pp. 82, 87).
- [18] R. Rimmer et al. *Waveguide HOM damping studies at JLab*. Conference Agenda. International Workshop on HOM Damping in Superconducting RF Cavities. 2010. URL: http://www.lns.cornell.edu/Events/HOM10/rsrc/LEPP/Events/HOM10/Agenda/TA1_Rimmer.pdf (cit. on p. 83).
- [19] A. Velez et al. “BESSY VSR 1.5 GHz Cavity Design and Considerations on Waveguide Damping”. In: *Proceedings of LINAC2014 MOPP071* (2014), p. 221 (cit. on p. 84).
- [20] A. Neumann et al. “Results and performance simulations of the main Linac Design for BerlinPro”. In: *Proceedings of LINAC2012 MOPB067* (2012), pp. 333–335 (cit. on p. 85).
- [21] F. T. Note. “Material Properties for Engineering Analyses of SRF Cavities”. In: *5500.000-ES-371110* (2011) (cit. on pp. 95, 96).

-
- [22] M. Liepe et al. “Status of the Cornell ERL Injector Cryomodule”. In: *Proceedings of LINAC2010* TU303 (2010), pp. 382–386 (cit. on p. 97).
- [23] O. Kugeler et al. “Adapting TESLA technology for future cw light sources using HoBiCaT”. In: *Review of Scientific Instruments* 81.7, 074701 (2010), p. 074701. URL: <http://scitation.aip.org/content/aip/journal/rsi/81/7/10.1063/1.3443561> (cit. on pp. 97, 108, 110).
- [24] A. Bosotti et al. “Full Characterization of the Piezo Blade Tuner for Superconducting RF Cavities”. In: *Proceedings of EPAC2008* MOPP120 (2008), pp. 838–840 (cit. on p. 101).
- [25] H. Kaiser. “New Approaches to Tuning of TESLA Resonators”. In: *Proceedings of SRF1999* TUP043 (1999), pp. 324–327 (cit. on p. 101).
- [26] Z. Conway and M. Liepe. “Fast Piezoelectric Actuator Control of Microphonics in the CW Cornell ERL Injector Cryomodule”. In: *Proceedings of PAC2009* TU5PFP043 (2009), pp. 918–920 (cit. on p. 101).
- [27] R. Rimmer et al. “Concepts for the JLab Ampere-Class CW Cryomodule”. In: *Proceedings of PAC2005* RPPE063 (2005), pp. 3588–3590 (cit. on p. 101).
- [28] V. Veshcherevich et al. “Design of High Power Input Coupler for Cornell ERL Injector Cavities”. In: *Proceedings of SRF2005* THP54 (2005), pp. 590–592 (cit. on p. 102).
- [29] F. Marhauser. *Narrowband and Broadband Impedance Budget of the 1497 Mhz HOM-Damped Five Cell High Current Cavity*. Tech. rep. JLab-TN-08-002. Newport News, Virginia: Thomas Jefferson National Laboratory, Accelerator Ops, R&D, 2008 (cit. on p. 102).
- [30] R. Nelson and A. Kimber. “RF Power Upgrade for CEBAF at Jefferson Laboratory”. In: *Proceedings of 2011 PAC, New York, THOCS4* (2011), p. 2127 (cit. on p. 105).
- [31] H. Buettig et al. “Operation of a 10kW@1.3 GHz Solid State Amplifier at the Superconducting Linac ELBE”. In: *Proc. of the 6th Workshop on CW and High Average Power RF, Barcelona* (2010) (cit. on p. 105).
- [32] A. Jankowiak. *The MAMI C Upgrade Project*. Conference Website. 20th Students Workshop on Electromagnetic Interactions, Bosen. 2003. URL: <http://wwwa1.kph.uni-mainz.de/Bosen/archive/talks/2003/lectures/Jankowiak.pdf> (cit. on p. 107).
- [33] Communications & Power Industries LLC. *Product Specification VKS-7960M Klystron Amplifier*. URL: <http://www.cpii.com> (cit. on p. 108).

- [34] A. Neumann et al. “Analysis and active compensation of microphonics in continuous wave narrow-bandwidth superconducting cavities”. In: *Phys. Rev. ST Accel. Beams* 13 (8 Aug. 2010), p. 082001. URL: <http://link.aps.org/doi/10.1103/PhysRevSTAB.13.082001> (cit. on p. 108).
- [35] A. Neumann et al. “CW Measurements of Cornell LLRF System at HoBi-CaT”. In: *Proceedings of SRF2011* MOPO067 (2011), pp. 262–266 (cit. on p. 108).
- [36] D. Boussard. “Beam Loading”. In: ed. by S. Turner. CAS-CERN Accelerator School: 5th Advanced Accelerator Physics Course, Rhodes, Greece, 20 Sep-1 Oct 1993: Proceedings. 2. 1995 (cit. on p. 108).
- [37] P. Wilson. “Fundamental-mode rf design in e+ e- storage ring factories”. In: *Frontiers of Particle Beams: Factories with e+ e- Rings*. Ed. by M. Dienes et al. Vol. 425. Lecture Notes in Physics. Springer Berlin Heidelberg, 1994, pp. 293–311. URL: http://dx.doi.org/10.1007/3540565884_16 (cit. on pp. 109, 110).
- [38] K. Y. Ng. *Physics of Intensity Dependent Beam Instabilities*. World Scientific Publishing Company, Dec. 2005 (cit. on p. 113).
- [39] T.-S. F. Wang. “Synchrotron Beam-Loading Stability with a Higher RF Harmonic”. In: *Proceedings of PAC1993* (1993), pp. 3500–3502 (cit. on p. 115).
- [40] A. Mosnier, F. Orsini, and B. Phung. “Analysis of the heavily Beam-loaded SOLEIL RF System”. In: *Proceedings of EPAC1998* WEP28G (1998), pp. 1720–1722 (cit. on p. 115).
- [41] A. Neumann and J. Knobloch. “Cavity and linac RF and detuning control simulations”. In: *Proceedings of SRF2007* WEP56 (2014), pp. 627–631 (cit. on p. 117).
- [42] H. Schlarb. *Private communications*. 2014 (cit. on p. 121).
- [43] E. Vogel. “High gain proportional rf control stability at TESLA cavities”. In: *Phys. Rev. ST Accel. Beams* 10 (5 May 2007), p. 052001. URL: <http://link.aps.org/doi/10.1103/PhysRevSTAB.10.052001> (cit. on p. 122).
- [44] S. Heifets and D. Teytelman. “Effect of coupled-bunch modes on the longitudinal feedback system”. In: *Phys. Rev. ST Accel. Beams* 10 (1 Jan. 2007), p. 012804. URL: <http://link.aps.org/doi/10.1103/PhysRevSTAB.10.012804> (cit. on p. 124).
- [45] J. Knobloch. “BERLinPro—addressing the challenges of modern ERLs (a status report)”. In: *Beam Dynamics Newsletter No. 58*. Ed. by W. Chou and E. Métral. Vol. 58. IDFA Beam Dynamics Newsletter. Springer Berlin Heidelberg, 2012, pp. 118–131. URL: <http://www-bd.fnal.gov/icfabd/Newsletter58.pdf> (cit. on p. 124).

- [46] J. Branlard et al. “The European XFEL LLRF System”. In: *Proceedings of IPAC2012* MOOAC01 (2012), pp. 55–57 (cit. on p. 124).

4 Cryogenics

In total, 4 cavities must be cooled with liquid helium to 1.8 K. This temperature can be achieved by operating liquid helium at a sub atmospheric pressure of 16 mbar using a set of cold and warm vacuum pumps. Three temperature levels are used in the module: 1.8 K for cooling the SC cavities, 5 K for thermal intercepts and 50 K for thermal intercepts and the thermal radiation shield of the module. Furthermore the cryogenic plant has to provide LHe for the weekly filling of the superconducting wave length shifter magnets (WLS) installed at BESSY II.

The basic components of the cryogenic installation are:

- a coldbox hosting:
 - a helium refrigerator to produce LHe out of pressurized warm gaseous helium (GHe)
 - cold compressors (cc)
- a set of warm vacuum pumps
- a set of helium compressors
- a helium dewar to store liquid helium
- a helium buffer to store GHe at medium pressure (2 bara to 12 bara) at room temperature
- cryogenic transfer lines
- and a valve box

In Figure 4.1 the layout of the cryogenic system is shown. The components will be discussed in the following section.

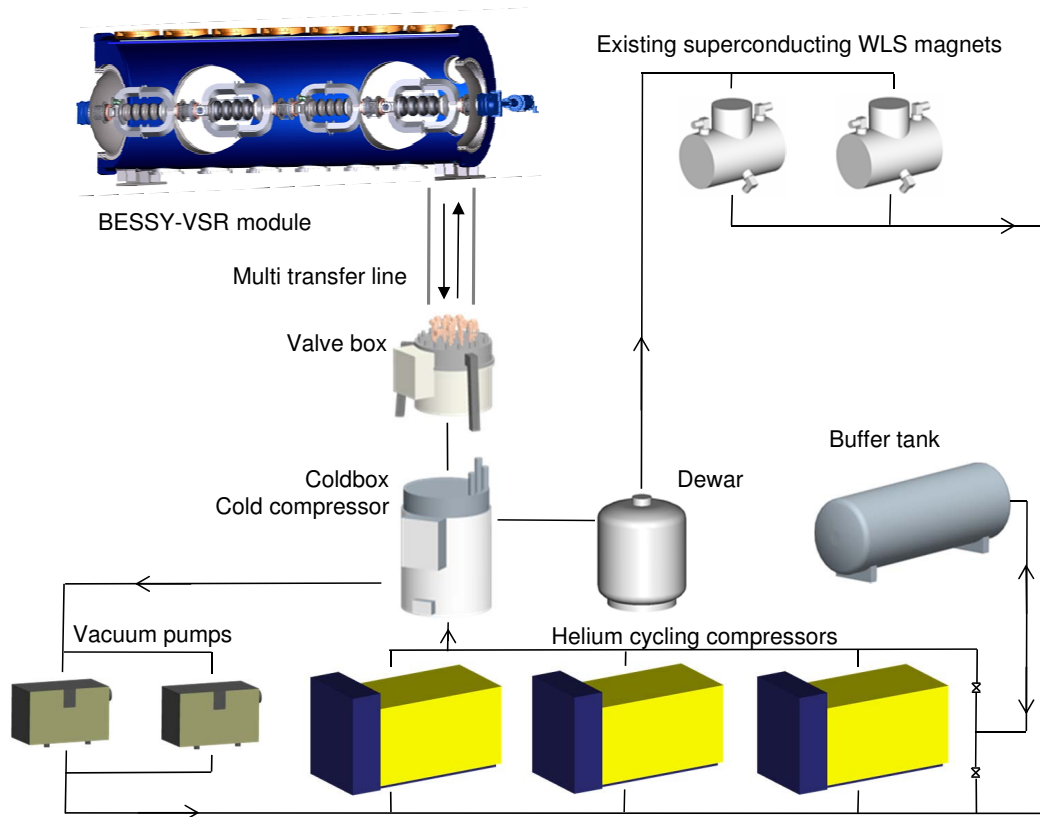


Figure 4.1: Layout of the cryogenic system for the BESSY VSR cryomodule.

4.1 Cryogenic Loads

The cryogenic installation has to serve the losses of the SC cavity module and has to deliver the helium for refilling the SC wave length shifter magnets installed in the BESSY II storage ring. The cryogenic loads are given by the losses of:

- the SC cavities,
- heat conduction from the room temperature HOM loads,
- the fundamental power couplers,
- the thermal transitions of the beam pipe at the end of the module,
- the thermal shield,
- and the transferlines including the valve box.

Values are taken from calculations assuming a gradient of 20 MV/m for all cavities and $Q_0 = 8 \times 10^9$ at 1.5 GHz and $Q_0 = 7 \times 10^9$ for the cavities at 1.75 GHz. The Q values are related on specifications of CEBAF [1] including expected losses due to field emission.

The estimated cryogenic loads based upon [2–7] are listed in Table 4.1. The HOM power is dumped in water cooled absorbers at 300 K not included in this table.

Table 4.1: Cryogenic loads for the BESSY VSR SRF installation.

Heat leaks in Watt Load	1.8 K		5 K		50 K	
	static	dynamic	static	dynamic	static	dynamic
Components						
4×Cornell Coupler	0.2	1	7	8	10	40
2×1.5 GHz cavity		48				
2×1.75 GHz cavity		40				
20×HOM dampers	40		40		200	
4×Beampipe	2		4		20	
Cryomodule	10		60		200	
Total cryomodule	52	89	111	8	430	40
Cryo distribution	5	0	45	0	550	0
Total cryoload	57	89	156	8	980	40
	146		164		1020	

4.2 Cryogenic Plant

For BESSY VSR the cryogenic plant has to cover three temperature levels to be cooled in the module:

- 1.8 K for cooling the cavities
- 5 K for thermal intercepts at the beam pipe, the RF couplers and the HOM dampers
- 50 K for thermal intercepts and a thermal shield of the module and the transfer-lines

The required capacity of the coldbox is dominated by the power level at 1.8K temperature. Additional an overhead of 50 % is foreseen for a total 1.8K capacity of 220 W. A modified version of the coldbox L700 used for the bERLinPro project fits to the requirements. In Figure 4.2 the coldbox type L700 is shown using three turbines and two compressors.



Figure 4.2: The coldbox L700 for bERLinPro currently installed at the HZB "Schwerlasthalle". The coldbox including the three turbines is seen in the foreground and the two compressors (yellow) in the background.

The coldbox will provide 5 K and 50 K helium. There will be a short transferline to a valve box and the helium dewar. Due to space restrictions in the tunnel, there will be no dedicated cryogenic feedbox at the module. The heat exchanger for subcooling of the helium will be located in the valve box. There will be a 14 m long multi transfer line to the cavity module (see Figure 4.3).

To produce helium with a temperature of 1.8K vacuum pumps are required to pump down the gas phase in the cavity vessels to a pressure of 16 mbar. There are two choices that are at this time available at roughly the same cost: One choice is to warm up the helium and use conventional warm vacuum pumps and the other possibility is to use one cold compressor located in the coldbox giving a compression factor of four and warm up in a heat exchanger recovering the "cold energy". The subsequent final compression then uses conventional vacuum pumps. Both methods are viable solutions and a final decision will be made when ordering the cryoplant.

Cryogenic Installation in the BESSY II Building

To reduce cryogenic losses and to keep the costs low, the coldbox should be placed close to the cryomodule but outside of the radiation area of the accelerator tunnel. Due to the fact that the piping at room temperature is less expensive compared to cold transfer lines, the compressors and warm vacuum pumps can be located in quite a distance if necessary. This is useful with respect to storage ring operation since both units are noisy and cause vibrations.

With respect to these criteria, the coldbox will be placed in the experimental area close to the radiation wall next to the straight where the module is installed, see Figure 4.4.

A radiation protection concrete plate covers the ceiling opening straight above the module. This plate will be lifted and a new labyrinth will be constructed for the passage of the cryoline, see Figure 4.3. While the coldbox and the He-dewar are located at ground level, the valve box will be located on top of the storage ring ceiling but close to the coldbox.

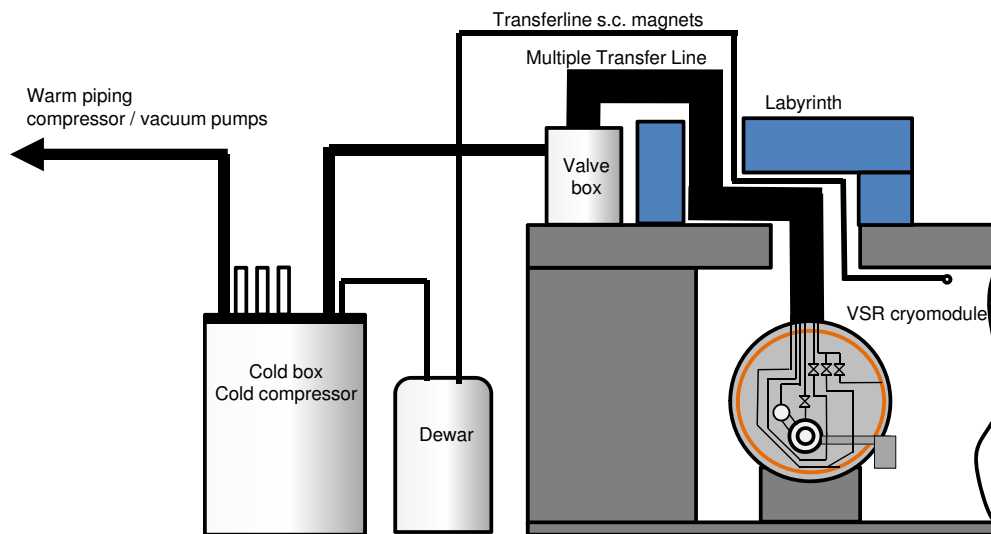


Figure 4.3: Layout of the cryogenic installation.

4.3 Cryogenic Transferlines

The main criteria for the design of the cryogenic lines are the space restrictions given by the existing accelerator tunnel and fast disconnection of the cryolines from the

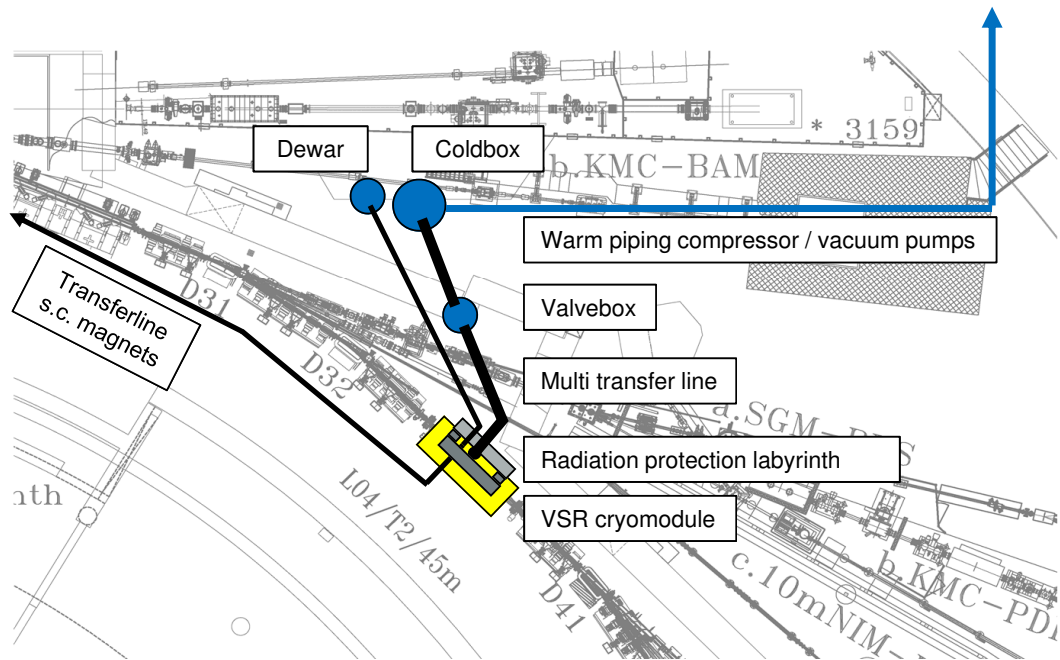


Figure 4.4: Topview of the cryogenic installation. The BESSY VSR cryomodule is shown in yellow, the cryo-transferlines in black and the cryo plant components in blue.

module in case of removal of the module. The connection of the cryo module to the cryogenic line will be from the top. To provide maximum accessibility the interface is located directly below the ceiling on the radiation labyrinth exit. A rigid multi transferline for seven media will be used to connect the cryogenic plant and valve box to the cryomodule. The Joule Thompson valve will be located in the module. By using a vacuum barrier between the cryoline and the cavity module and flanges at the connection of the cryoline to the module the time for disconnecting the module in case of trouble is minimized.

4.4 Cryogenics for Preparatory Phase

For the preparatory phase a cost effective solution is planned. This can be realized by mostly using existing cryogenic infrastructure of BESSY II. The cavities will be cooled at a temperature level of 4.4 K by using the existing cryo plant TCF50 currently in use for WLS filling. Due to the high temperature level the Q_0 values of the cavities will be poor and operation will be possible only at reduced voltage. The capacity of the TCF50 cryoplant is 120 W. Subtracting losses on the cryolines

and thermal intercepts 80 W is available to cool the cavities. Assuming realistic Q_0 values including field emission of $Q_0 = 1.6 \times 10^8$ for the 1.5 GHz cavity a field gradient of 3.5 MV/m can be realized. The cryogenic piping will be done by using flexible cryolines by NEXANS.

4.5 Warm Operation of SC Cavities

In case of loss of operability, it is essential to detune the cavities. If it is not possible to stay cold on helium temperatures, the cavities will be warmed up, but machine operation must be able to continue in standard BESSY II mode without the SC cavities affecting the beam. Warm cavities will have Q_0 values of about 10.000 or less. The induced voltage by the beam will result in heating of the cavity walls on the order of 1 kW, even if the cavity is detuned. To cool the cavity walls in warm operation, the He-vessel will be flooded with He-gas at 300 K cooled by a separate compressor system.

References

- [1] J. Hogan et al. “Overview and Lessons learned of the Jefferson Lab Cryomodule Production for the CEBAF 12 GeV Upgrade”. In: *Proceedings of PAC2013 WEZAA2* (2013), p. 749 (cit. on p. 133).
- [2] R. Hicks and E. Daly. *Thermal Analysis of a 13 kW Waveguide for the 12 GeV Upgrade Cryomodule*. Tech. rep. JLAB-TN-02-040. JLAB, 2002 (cit. on p. 133).
- [3] C. Reece et al. “Performance of CEBAF Prototype Cryomodule RENESCENCE”. In: *Proceedings of SRF2007, Beijing* WEP32 (2007), p. 540 (cit. on p. 133).
- [4] M. Liepe et al. “The Cornell ERL Superconducting 2-Cell Injector Cavity String and Test Cryomodule”. In: *Proceedings of PAC2007, Albuquerque* THOAKI02 (2007), p. 2572 (cit. on p. 133).
- [5] E. Chojnacki et al. “Cryogenic Heat Load of the Cornell ERL Main Linac Cryomodule”. In: *Proceedings of SRF2009, Berlin* THPPO034 (2009), p. 638 (cit. on p. 133).
- [6] V. Veshcherevich and S. Belomestnykh. “Input Coupler for Main Linac of Cornell ERL”. In: *Proceedings of SRF2009* THPPO009 (2009), p. 543 (cit. on p. 133).

- [7] S. Noguchi et al. “Present Status of Superconducting Cavity System for cERL Injector Linac at KEK”. In: *Proceedings of IPAC2010, Kyoto* WEPEC024 (2010), p. 2944 (cit. on p. 133).

5 Machine Integration

An overview of the straight section with the designated cryogenic module is presented in Figure 5.1. All of the vacuum parts between the upstream storage ring magnets and the cryogenic module and in downstream direction after the cryogenic module and the storage ring magnets have to be reworked. It is assumed that for a successful operation of BESSY VSR average vacuum pressure values in the low 10^{-10} mbar range are sufficient, following the XFEL specification. Therefore, a bake-out of the complete section to reduce water partial pressure and material outgassing rates is planned.

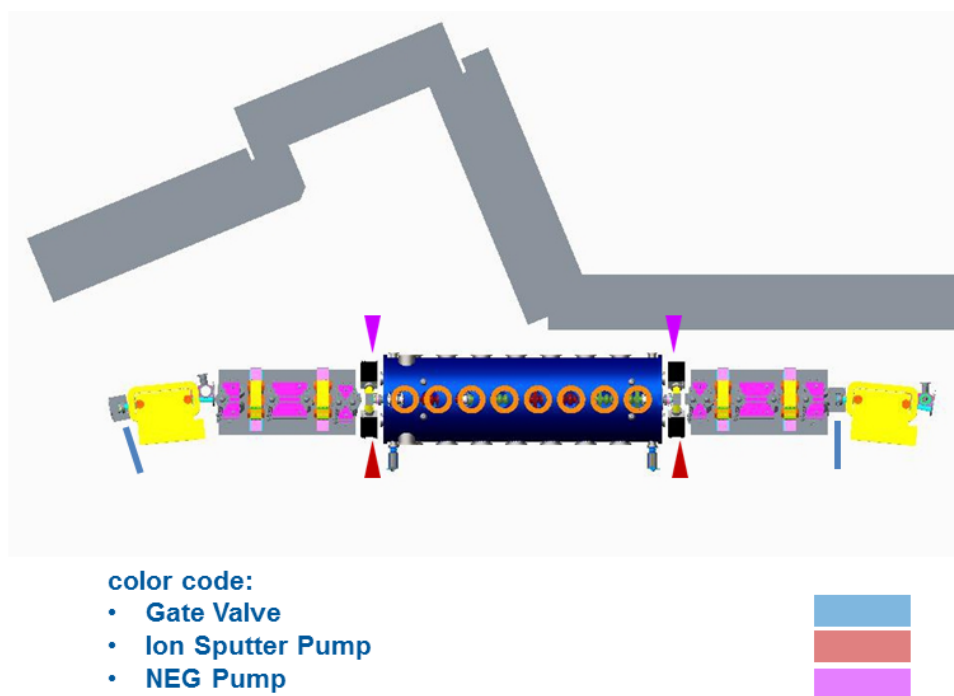


Figure 5.1: Top view of the 4.6 m long BESSY VSR straight with installed cryomodule of 4 m.

5.1 Module Integration in Storage Ring

To realize the particle free vacuum system all vacuum chambers 10 m before and 10 m behind the cryogenic module have to be dismantled for a special cleaning procedure or replaced by new components. The existing cable trays have to be removed and installed in another way. For the particle free installation of all vacuum parts and the cryogenic module itself, a portable cleanroom area is required. Sufficient free space at the beginning and at the end of the cryogenic module straight section for vacuum ion pumps and tapering has to be reserved. First assumptions amounted to 300 mm each for both sides. The total length of the straight section amounts to 4.6 m, allowing for ca. 4 m length for the cryomodule.

5.2 Vacuum System

For the separation of the cryogenic module from the storage ring, additional radio-frequency-shielded all-metal gate valves are mandatory. They will be arranged in front of the bending magnets which will be close to the cryogenic module, to keep the free installation space in the BESSY VSR straight section as long as possible. The vacuum sector will be equipped with three cold cathode gauges for monitoring the vacuum pressure, which are connected to the vacuum interlock system.

To improve the pumping speed in the reserved sections before and after the cryogenic module ion pumps with internal NEG cartridges seem to be recommendable. They will boost the moderate ion pump pumping speed by some orders of magnitude without extended space requirements. Tests at the NEG supplier have shown that a special NEG cartridge model with zero particle emissions during activation will be available shortly. The pumping ports for the ion pumps also incorporate vacuum gauges and all-metal cross-angle valves which are used for roughing and venting. The tapering from the magnet cross section to the superconducting cavity cross section will also be done at this place. Dry turbo molecular pumps will be used for roughing and during bake-out. This procedure should be established with permanent connected pump carts, which in addition are equipped with dry and oil-free diaphragm pumps, a vacuum control and a venting system. The pump carts can be connected via flexible hoses to the cross angle valves which are installed in each vacuum sector. These pump carts following a well proven DESY/XFEL design allow for very slow venting and pumping of the vacuum system, so that existing particles do not move. Figure 5.2 shows a schematic overview of the pumping system.

First prototypes of these carts are already under construction and will be soon ready for testing and tuning. In order to avoid a particle transport into the cryo-

genic module, the dry nitrogen flow rate during the venting process must not exceed the limit of 50 mbar l/s. This value has been tested and approved by cryogenic manufacturers (Research Instruments) and operators of similar cryogenic devices. In the same way, it is very important to reduce the average vacuum pressure below 1.0×10^{-10} mbar in the region of 5 m before and after the cryogenic module, to keep the superconducting device free from the residual storage ring vacuum. This requirements follows the specification for XFEL and Flash vacuum systems. Therefore the adjacent old vacuum chambers through the magnets 5 m before and after the module have to be replaced by new ones of stainless steel, coated with NEG material for a better distributed pumping. All ConFlat flanges will be commonly built using standard stainless steel material (316LN). The investments costs for adapting the vacuum system to BESSY VSR requirements amount to 860 k€.

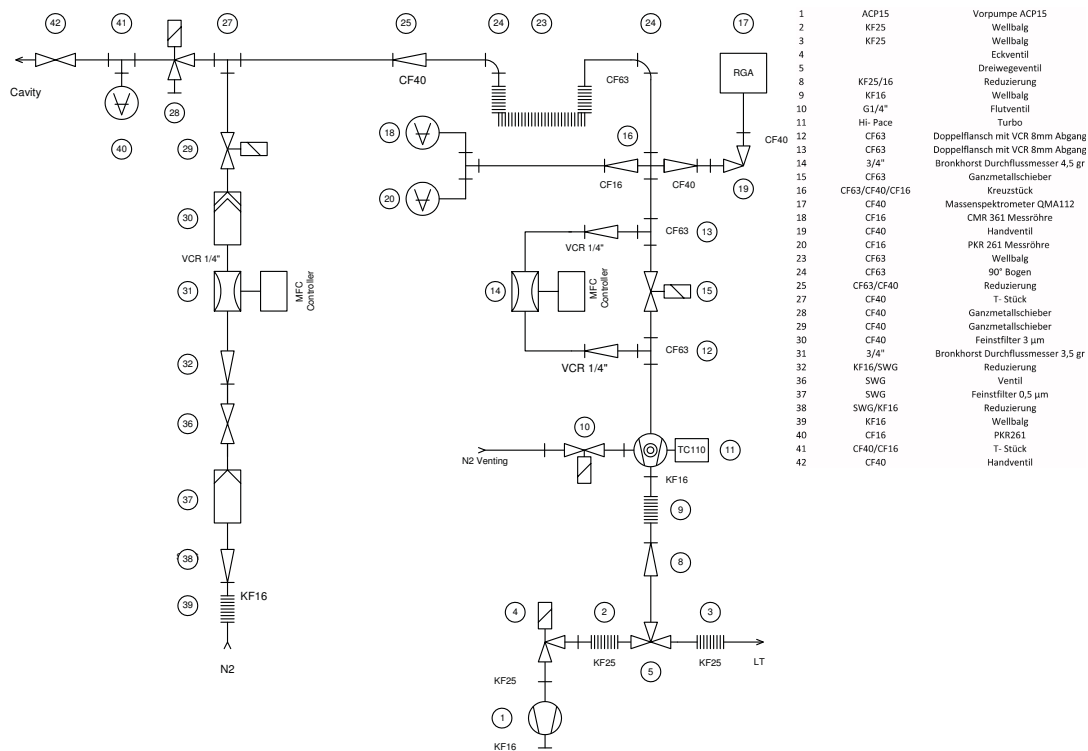


Figure 5.2: Particle free pump cart design by RI Research Instruments.

Pressure Profile for BESSY VSR Operation

With respect to the vacuum requirements listed above a calculation of the expected pressure profiles has been essential. Therefore, all already known BESSY VSR

boundary conditions like storage ring cross sections, pumping sizes and types, tube lengths and thermal desorption rates were determined and first fundamental vacuum calculations have been done, presented in the Figure 5.3. The three coloured curves for different cases are showing that the addressed design changes with additional pumps in the BESSY VSR straight are well placed reducing the pressure below 1.0×10^{-10} mbar. However, it would be recommended to add more pumping speed (NEG coating) to the neighbouring storage ring straights, to achieve on a higher pressure reserve for operating the storage ring at 300 mA with different high bunch charges and fill patterns. The additional electron stimulated desorption in the dipole chambers will affect the pressure profile in the BESSY VSR region, as well. Further investigations will be required with respect to the continuous scientific and technical developments of BESSY VSR and also for the real operation case.

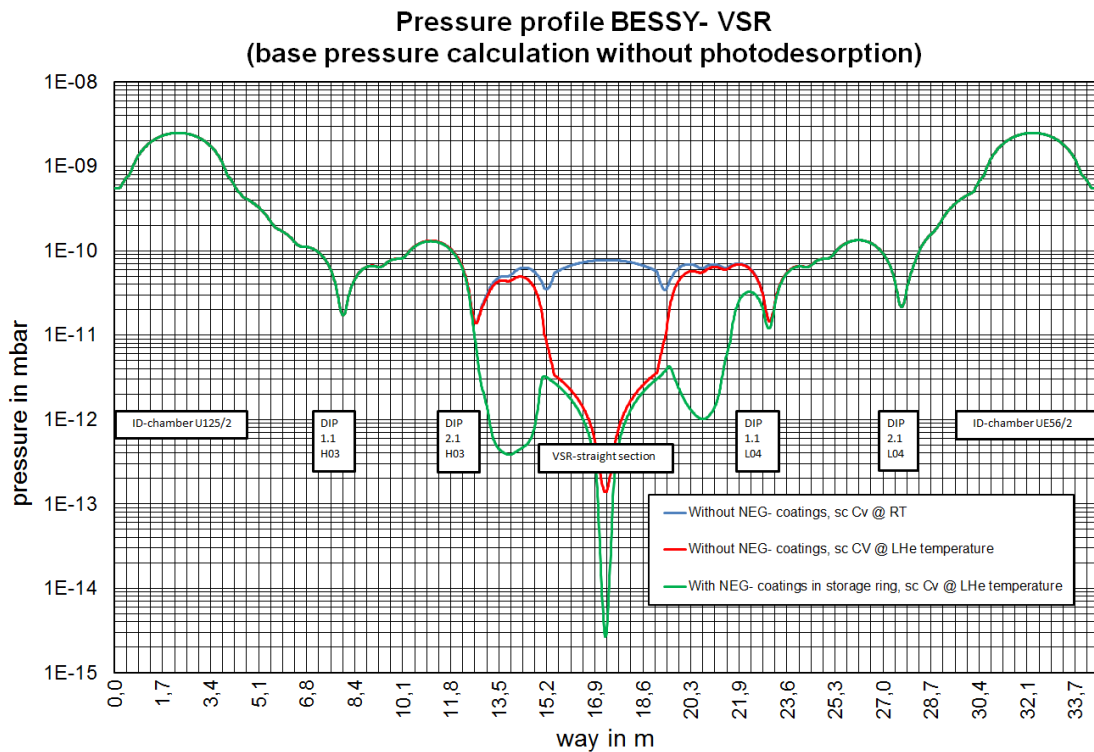


Figure 5.3: Pressure profile calculated for different scenarios in the BESSY VSR straight. The text boxes, ID-chamber, DIP-bending magnets are placed at their correct position within the BESSY II ring.

Survey and Alignment of Machine Parts and BESSY VSR Components

To align the components of the machine a geodetic network is necessary. The coordinates of the components with reference to the electron path/ photon path have to be transformed into the geodetic network coordinate system. Therefore, the alignments of the components have to be measured relative to the designed electron path.

Network The fundamental geodetic network consists of magnetic nests for laser tracker targets with a typical diameter of 1.55 inch. They are placed on the concrete wall, floor and ceiling of the accelerator hall and of the equipment hall. The network is measured using a laser tracker and a digital level. To obtain final coordinates for the network points, all measurements are processed using least-square adjustment software.

Fiducial Alignment To adjust the components of the machine with respect to the geodetic network, all mechanical parts have to be equipped with bore holes with a specific diameter, in which an adapter for the laser tracker references is placed.

Equipment and Accuracy The available survey equipment consists of a Leica AT901-B laser tracker and a Leica DNA03 digital level. Under stable environmental conditions and a maximum distance of 40 m, the uncertainty of a coordinate measured with the laser tracker is $\pm 15 \mu\text{m} \pm 6 \mu\text{m}/\text{m}$. Within a volume of $2.5 \text{ m} \times 5 \text{ m} \times 10 \text{ m}$ an accuracy of $\pm 10 \mu\text{m} \pm 5 \mu\text{m}/\text{m}$ is achievable. These specifications are stated in units of maximum permission error (MPE). Typical results are around half of the MPE. The digital level is specified with a standard deviation of 0.3 mm/km double leveling using an invar staff.

5.3 Impedance Upgrade

The traveling electron bunch interacting with the surrounding vacuum chamber induces electro-magnetic fields. The effect depends critically on the single-bunch charge, the bunch length and the impedance of the vacuum components. Trapped modes can trigger coupled-bunch-instabilities, induce impedance heating which in turn can degrade the vacuum level, and cause fatigue stress and may finally lead to a vacuum leak.

For a beam with a given charge distribution $\rho(t)$ and its Fourier transform

$$\tilde{\rho}(\omega) = \frac{1}{\sqrt{2\pi}} \int_{-\infty}^{\infty} dt e^{-i\omega t} \rho(t) \quad (5.1)$$

the energy loss can be expressed as [1]

$$\Delta E = \frac{1}{\sqrt{2\pi}} \int_{-\infty}^{\infty} d\omega |\tilde{\rho}(\omega)|^2 \operatorname{Re} Z^{\parallel}(\omega) \quad (5.2)$$

where $Z^{\parallel}(\omega)$ is the longitudinal impedance of the vacuum component.

In Figure 5.4 the frequency spectrum for standard BESSY II fill pattern and for a BESSY VSR scenario are shown. For the standard mode the Fourier spectrum is

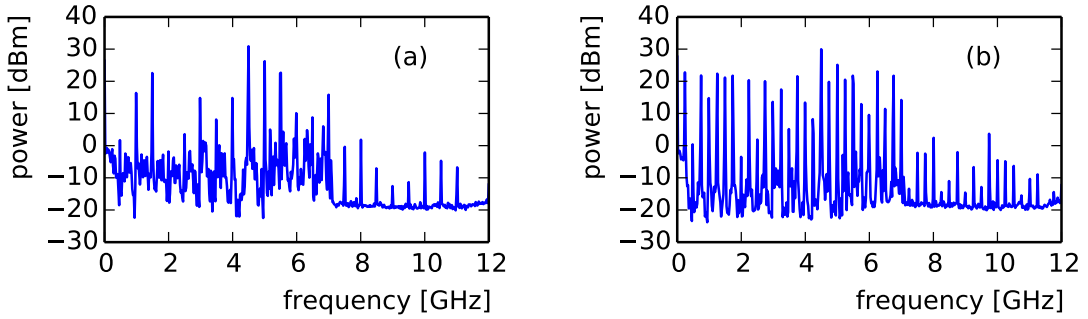


Figure 5.4: Bunch spectrum as measured at a stripline monitor. (a) For Standard BESSY II fill pattern with 300 mA. (b) A 270 mA BESSY VSR-like fill pattern with every second bucket filled and 200 ns gap. The amplitude of the 500 MHz line is reduced in both plots, due to the geometry of the pickup. The jump at 7 GHz is a measurement artefact.

dominated by harmonics of 500 MHz. For BESSY VSR also harmonics of 250 MHz are pronounced. Both, higher bunch current and shorter bunch length lead to an increase in energy loss. For quantitative statements the impedance needs to be taken into account.

Resistive Wake

For a given bunch charge Q and bunch length σ_z the total power losses P_{res} in the vacuum chamber due to resistive wake field can be estimate by [1]

$$P_{\text{res}} = \frac{\Gamma\left(\frac{3}{4}\right)}{4\pi^2\sqrt{2}} \frac{c^2 Q^2 \sqrt{Z_0 \rho}}{r(c\sigma_z)^{3/2}} \quad (5.3)$$

provided the bunch length $c\sigma_z \gg \chi^{1/3}r$ with $\chi = \rho/Z_0r$, where $Z_0 = 376.7\Omega$ is the vacuum impedance, ρ is the resistivity of the vacuum chamber material (for stainless steel $\rho = 0.71\mu\Omega\text{m}$) and r is the vacuum chamber radius.

In Table 5.1 a comparison of the power losses due to resistive wake for standard BESSY II operation and a BESSY VSR fill pattern is given. The estimated power loss of BESSY VSR exceeds the corresponding value for standard operation by more than a factor four, dominated by the short high-current (slicing) bunches, but are well below 10 kW. Thus, no problems are expected due to resistive wake losses.

Table 5.1: Comparison of power loss due to resistive wake for standard BESSY II operation and a BESSY VSR scenario.

Name	No.	Bunch charge [nC]	σ_z [ps]	Total current [mA]	P_{res} [W]	Relative contrib.
Standard mode						
camshaft	1	3.2	25	4	29	2.5%
slicing	3	3.2	25	12	88	7.4%
multi-bunch	300	0.757	15	284	1064	90.1%
				300	1181	
BESSY VSR mode						
short	1	0.64	1.7	0.8	66	1.3%
long	1	8.01	27	10.0	163	3.1%
slicing	3	4.00	3.7	15.0	2406	46.3%
long-MB	150	1.32	15	247.2	1605	30.9%
short-MB	150	0.14	1.1	27.0	962	18.5%
				300	5201	

On the other hand these numbers illustrate the impedance dependence on the bunch length, and indicate possible problems with geometrical wake impedances of the short high-current bunches (cf. following sections).

CSR-Wake

The CSR-power emitted by a single bunch with N electrons moving in free space on a circle with radius $R = 4.35\text{m}$ (BESSY II dipole bending radius) is given by [2]:

$$P_{\text{coh}}^{\text{free-space}}[\text{W}] = 2.42 \times 10^{-20} \frac{N^2}{R^{2/3}[\text{m}] \cdot (c\sigma_z)^{4/3}[\text{m}]}, \quad (5.4)$$

where σ_z is the rms-bunch length. The radiated power is related to the energy loss of the N particles due to the interaction with their own radiation fields created in the dipole magnets. In reality the bunch is not moving on a circle in the storage ring. Most of the time the bunch is not radiating at all and the emitted power is reduced by the ratio of the total dipole magnet length, $2\pi R$, and the circumference of the ring, which is 240 m in the BESSY II ring. With the BESSY II parameters the equation simplifies to:

$$P_{\text{coh}}^{\text{free-space}}[\text{kW}] = 2.013 \cdot \frac{Q^2[\text{nC}]}{\sigma_z^{4/3}[\text{ps}]}. \quad (5.5)$$

The above given steady-state result has to be further corrected. When the bunch enters the dipole the radiation field will build up slowly and reach its steady-state value only more than half way through the BESSY II dipole. This depends on the bunch length and is characterized by the slippage length [3]. In order to approach the steady-state CSR field in the BESSY II dipole the bunch length should be shorter than 1 mm which is the case for the short BESSY VSR bunches. After the bunch has left the dipole magnet the interaction will continue since the electrons still move in the radiation field. According to M. Borland [4] this field decays with the overtaking length (closely related to the slippage length) given by: $L_0 = (24 \cdot c\sigma_z \cdot R^2)^{1/3}$. Usually the slow build-up of the interaction is more than compensated for by the slow decay of the high field finally created in the dipole magnet. With the short bunches the distance between dipoles is large compared to the overtaking length so that interference effects between dipoles can be ignored. This correction is named transient correction and given in Table 5.2 (trans.).

An additional correction is needed due to the presence of the nearby metallic vacuum chamber, which has the potential to shield or suppress part of the electromagnetic fields of the moving electron bunch. The impact of a simplified model for the chamber in the form of two perfectly conducting parallel plates has been estimated in the frequency domain.

The result is identical to Bane's time domain calculation and shown in Figure 5.5 together with Bane's Gaussian approximation [5]. The shielding correction factor as presented in Table 5.2 (shield.) is based on a direct calculation in frequency domain.

Applying both corrections discussed above the total CSR power $P_{\text{coh}}^{\text{total}}$ has been evaluated for the various bunches and is presented in Table 5.2, as well as the incoherent and coherent energy loss.

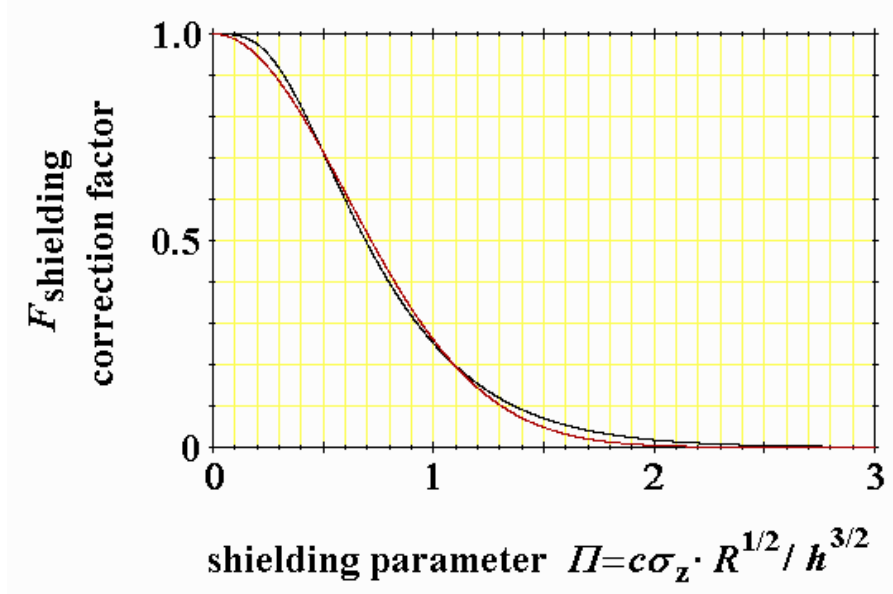


Figure 5.5: The correction factor for the shielding of a Gaussian bunch radiating between conducting plates separated by the distance $2h$ as a function of the shielding parameter Π . Note that in the rest of the study h is defined differently and as the distance of the plates. The black line is the result of the frequency domain calculation performed for this study and the red line is Bane's Gaussian approximation given by $e^{-(\Pi-\Pi/0.742)}$.

The energy loss U_0 , of each electron due incoherent synchrotron radiation is given by:

$$U_0[\text{keV}] = 88.5 \cdot \frac{E^4[\text{GeV}]}{R[\text{m}]} = 88.5 \cdot \frac{1.72^4}{4.35} = 178. \quad (5.6)$$

The additional energy loss due to the coherent radiation U_{coh} , can be obtained from:

$$U_{\text{coh}}[\text{keV}] = P_{\text{coh}}^{\text{total}}[\text{W}] / I_{\text{total}}[\text{mA}]. \quad (5.7)$$

The CSR-power emitted by the long bunches is small and can be neglected. The most worrisome contributions come from the many short and low intensity bunches and the three lengthened but high intensity slicing bunches. In case of trouble the current in these bunches can be adjusted to an acceptable level. The emitted power of incoherent synchrotron radiation P_{incoh} is approx. 50 kW and the additional contributions from the coherent radiation of shorter bunches with BESSY VSR and the power losses due to the resistive wake will increase this value by up to 18 kW. The higher energy loss per turn has to be compensated for by the RF-system.

Table 5.2: Energy loss and CSR-power corrected by transient and shielding factors for the short bunches at BESSY VSR.

Bunch length σ_z/ps	Bunch charge Q/nC	No.	CSR power steady-state $P_{\text{coh}}^{\text{free}}/\text{kW}$	Correction trans.	shield.	CSR power total $P_{\text{coh}}^{\text{total}}/\text{kW}$	Energy loss $E_{\text{loss}}/\text{keV}$
Short bunches in BESSY VSR mode							
1.1	0.4	1	0.284	1.281	0.919	0.334	668 + 178
1.7	0.64	1	0.406	1.325	0.759	0.409	511 + 178
1.1	0.144	150	5.51	1.281	0.919	6.49	240 + 178
Slicing bunches in BESSY VSR mode							
3.7	4.0	3	16.9	1.50	0.252	6.38	425 + 178
Ultra short bunches in BESSY VSR low α mode							
0.3	0.04	1	0.016	1.19	0.999	0.0191	382 + 178
0.4	0.04	1	0.011	1.21	0.997	0.0132	264 + 178
0.4	0.04	150	1.64	1.21	0.997	1.98	264 + 178
Short bunches in today's BESSY II low α mode							
2.4	0.034	350	0.253	1.38	0.546	0.191	12.7 + 178
3.0	0.034	350	0.188	1.38	0.389	0.101	6.71 + 178
3.6	0.034	350	0.148	1.38	0.268	0.0546	3.63 + 178

This is not really a challenge for the existing 500 MHz-RF-system since the 7 T-wiggler and the two 7 T-WLS produce an incoherent power loss of ≈ 50 kW, and the 7 T-wiggler will not be in operation with BESSY VSR. For BESSY VSR the bunch length dependent energy loss per turn and the corresponding shifts of the synchrotron phases are more critical and deserve further studies.

Impedance Budget

The impedance caused by geometrical wake of individual vacuum components can be studied with discretization computer codes (e.g. [6, 7]). The costs of impedance calculations increases drastically with the complexity of the geometry and in particular with the upper frequency limit of the simulation. The memory consumption increases with the third power while CPU time increases with the fourth power of the frequency limit. Thus, with currently available computer power, this kind

of calculations are very time consuming if extended beyond the range of a few 10 GHz.

In recent years, extensive impedances studies have been performed for a number of machines, see [8, 9]. But for the BESSY II storage ring such calculations are not available yet. In context of BESSY VSR numerical impedance calculations will be performed at least for the most important components.

Table 5.3 gives an overview of vacuum components in the BESSY II storage ring.

Critical components include all dipole chambers (due to the high number of ports), bellows, scrapers, collimators. Also the impedance effect of the new in-vacuum undulator should be studied in detail. On the other hand many components are already equipped with powerful cooling system due to the high intensity synchrotron radiation, which could mitigate impedance heating.

Temperature Monitoring

The final answer to impedance effects can only be determined using the beam. In particular the short high-current (slicing) bunches will sample uncharted territory. It is therefore essential to allow in-situ temperature monitoring of vacuum components. i.e. the system should be able to take measurements in the storage ring bunker during beam operation.

Currently, temperature monitoring is performed by a number of PT100 temperature sensors. These measurements give valuable information about the temperature change with current, but are limited to specific locations. In addition measurements with an IR-camera on a tri-pod allowed a more detailed analysis of critical components.

For BESSY VSR it is important to improve the temperature monitoring system in order to quickly evaluate the effect of the short bunches on vacuum components. The system should be able to map at least one complete sector. This could be achieved by moveable IR-camera, e.g. mounted on a rail system.

Summary

General impedance effects have been taken into account in the design phase of BESSY II [10], but there is very little quantitative knowledge about the impedance of individual vacuum components. It is recommended to perform a similar study like for the bERLinPro project [9]. At the same time a temperature monitoring

Table 5.3: Overview of vacuum components in the BESSY II storage ring with the status of impedance calculations, where *status R* indicates components where a detailed analysis is highly recommended.

Vacuum component	Number	Status
Bends (12 vacuum elements)		
Dipol chamber DIP 1.1	16	R
Dipol chamber DIP 2.1	16	R
Valve	2x8 + 4*	
Bellow	2x16	R
other	7	
ID-Straights		
Undulator chamber	13	
In-vacuum undulator	1	R
Feedback & Diagnostics		
Diagnostics kicker	1	
Power stripline (Knockout, TFB)	2	
Diagnostics stripline	3	
Long. feedback cavity	1	
Fluorescent screen (FOM)	5	
Beam position monitor (BPM)	7x16	
Current Monitor	2	
Injection and RF		
Septum	1	R
Inj. Kicker	4	R
Landaus (ferrit damper)	4	
Other vacuum elements		
Flange	≈240	
Scraper	1	R
Collimator	1	R

*The installation of four new vacuum valves is scheduled for the 2015 shut-down.

system should be developed. Both simulation and in particular measurements may lead to the identification of critical components.

In case of the observation of drastic heat-up vacuum, counter measures need to be

taken. These should include

- cooling improvements,
- installation of a temperature controlled heating system (to minimize thermal stress),
- or may require redesign and replacement of the vacuum components.

Table 5.4 gives summary of the costs. Note that the costs for impedance related hardware changes represents a rough estimate only.

Table 5.4: Summary of costs associated with impedance upgrade.

Item	Amount	Costs
Simulation		
Licence for CST STUDIO SUITE	2 x 2year	40 k€
<ul style="list-style-type: none"> • Wakefield Solver 		
Temperature Monitoring		
IR Camera	1	30 k€
automotive system	1	ca. 50 k€
Hardware changes		
impedance upgrade		ca. 150 k€
Sum		ca. 270 k€

5.4 Installations, Run-In, Dark Times, Precautions

Installation of novel devices, that change the characteristics of the user facility BESSY II drastically the way BESSY VSR does, require substantial risk considerations and realistic planning. A balance has to be found between overcautious long dark times, and a schedule, that tries to minimize the total out of service time. A conservative long shutdown allows for diligent commissioning, and if necessary, for last minute corrective actions. In an overambitious short shutdown, unforeseen problems or accidents might in the end need more than the saved time, or even worse, it can mean a big and painful impact on user routine operation.

5.4.1 Operation Constraints for Hardware Implementation

Several operating conditions specific for BESSY II put serious constraints on the different phases of the BESSY VSR implementation. Or from a different perspective, at least within tight limits, they allow to take advantage of a smart distribution of scheduled user beamtime, shifting higher risk operation modes to a later point in time.

On the average BESSY II fulfills the user demands for beamtime offering between some 3300 h/y and 4300 h/y of hybrid multibunch (MB), typically 400 h/y of single bunch (SB) and 270 h/y of low alpha mode, generating short pulses or stable coherent THz radiation in alternating 12 h shifts. Typically total no-beam outage times are well below 200 h/y, thus the source BESSY II is known for its very high availability.

It can be foreseen, that with the advancement of puls picking methods the demand for true SB operation will be reduced, low alpha will remain within specific BESSY VSR operation modes.

The hybrid multibunch mode features true single bunch TopUp injection. The even MB filling serves the average user community. A high current, low emittance camshaft bunch in a 100 ns gap allows for pump probe experiments and pulse picking with the chopper wheel, several high current bunches serve the fs-slicing experiment. The latter shares undulator and beamtime with a non-slicing set-up, i.e., during certain shifts, no slicing bunches need to be offered. In addition one slightly isolated bunch can be resonantly excited for pulse picking, all at the same time.

At BESSY II an over-booking factor around 2, more than 40 usable beamlines and a sophisticated beamtime distribution, for each semester approved by the scientific advisory committee, in units of 8 h shifts, several days, weeks or several weeks puts pressure on minimized periods of unplanned beam outage.

Radiation protection prescribes an injection efficiency $>90\%$ in the 4 h average (Chapter 9). Within limits, these very tight constraints can be mitigated by relaxing certain beam parameters, like beam intensity, i.e. total current and bunch current in the desired fill pattern (see 2.7). Maybe also operation modes with intermittent time slots of certain less ambitious cavity settings, i.e. lower gradient and not so short bunches, combined with a tailored TopUp refill pattern (e.g. several minutes decay, sequence of refill shots) become interesting.

5.4.2 Installation, Commissioning in the Preparatory Phase

Installation of the cryomodule with equipped only with two 1.5 GHz cavities will be a more or less straightforward shutdown activity, since techniques involved are well known and mastered.

In terms of a raw sketch the installations in autumn 2018 will require sequential phases (only “dark” shutdown weeks are considered)

Preparatory work: The cryo module needs to be equipped with both cavities, tested (1.8 K, full field), fully conditioned, ready for integration. Necessary connections have to be installed in a preceding shutdown: 4 K Nexans pipes, 300 K He-gas cooling, electrical cabling (motor controller, control system, diagnostics)

Put cryo module in place (2 w): Remove cold MPW, dismantle beamline and frontend, enhance radiation protection wall, re-adjust labyrinth at feed-through on top, insert and align cryo module

Cooldown (1 w): Cool shield, module, test 300 K cooling system

Conditioning (1 w): Personal interlock system has to be set, apply full field to both cavities and test and tune LLRF

Beam based tuning (3 w): Establish proper power and phases, for all combinations of the two cold/warm SRF cavities and the 4 NC cavities, for park positions and bunch lengthening, adjust BBFB for various fill pattern and beam currents.

A minimum of 7 weeks user dark time is needed to enable preparatory phase at all. Further post shutdown commissioning has to be combined with user operation, in the beginning possibly with slightly degraded beam conditions.

As an isolated activity of breaking the vacuum, the cryo module installation probably requires minimal beam scrubbing. First priority of further machine development then aims at the establishment of the best achievable transparency of this novel device. A safe park positions have to be found for all operating temperatures (warm, cold/SC, see Section 2.8). It has to be characterized, if and how the existing 4 NC 3rd harmonic cavities can contribute to a proper control of the remaining effects of the “parked” SRF cavity on the beam while maintaining the lengthening required for the lifetime constraints of TopUp operation.

Subject of further studies then will be the bunch lengthening and shortening options accessible by all 1.5 GHz cavities. Acquired data and conclusions from this combined cavity tuning will be important for the next steps towards the BESSY VSR parameter space.

5.4.3 Installation, Commissioning of the Booster Synchrotron Cavity

Installation of the bunch shortening cavity in the booster (see Section 3.5) requires 6 weeks of shutdown in 2019. Preparing work (wave guides, cabling) can be the side activity of a small preceding shutdown (2-3 weeks). If all systems function properly, one week of commissioning could be sufficient to come back to stable acceleration, extraction and finally injection of high current bunches with high injection efficiency. In summary another 7 weeks of user dark time result.

5.4.4 Installation, Commissioning of Final BESSY VSR

Final installations in 2020 will require long sequential phases (assessable in weeks)

Clean vacuum chamber (11 w): Some 15m of vacuum chamber up- and downstream of the cryo module has to be replaced (Section 5.2)

Multiple cryo line (2 w): This transfer line has to be welded down, the labyrinth has to be reorganized, the cryo plant needs commissioning (see Chapter 4)

Cryo module in, cooling (3 w): The preparatory phase module has to go out, the new module will be inserted, old connectors have to be removed, new lines attached, cooldown completed

Conditioning (3 w): Personal interlock system has to be set, apply full field at all cavities, LLRF has to be tested and tuned

Beam based tuning (3 w): Proper power and phases, for all combinations of the four cold/warm SRF cavities and the 4 copper cavities, for park positions and bunch lengthening, have to be established. BBFB for various fill pattern and beam currents has to be adjusted.

Dependent on the feasibility to interlace these activities a minimum of 12–20 weeks user dark time is needed to modify BESSY II for BESSY VSR.

Operational experience will rapidly show, how well design parameters can be met. Prospects concerning improved tuning capabilities could become feasible with additional space. Some space will be possibly regained by making the old 3rd harmonic copper cavities and 3 out of 4 NC 500 MHz accelerating cavities dispensable. This is subject to future upgrade options (see Chapter 12).

5.4.5 Precautional Measures

Big cold masses at other light sources (SC RF), also at BESSY II (SC MPW) have shown that lengthy, maybe frequent warm-up procedures [11, 12] can significantly impede operations. At the affected ring sector big cryo pumps are switched off, fading vacuum conditions, limit stability and lifetime.

Experiences with fundamental mode SC cavities vary, even with the same type of cavity [13]. As countermeasure to the adverse effects on beam availability and stability Diamond plans to add two normal conducting cavities of the BESSY II fundamental mode type to the remaining two SC cavities [14, 15], in place of the middle 3rd SC cavity, resembling a hybrid RF straight section. This remedy is not available for BESSY VSR.

Different scenarios of a slow or event based degradation of SRF cavities or cryo module might require a fast removal from the ring and external repair. Any provision to allow for a fast disassembling or exchange of the still cold cryo module has to be foreseen to allow for continuation of standard user mode.

Valves that allow to seal the SRF vacuum as well as the remaining storage ring are required. A vacuum barrier between the cryoline and the cavity module, and flanges at the connection of the cryoline to the module are foreseen, to allow for controlled heating in preparation of a rapid disconnect (see Chapter 4). Then, as the cryo module is removed from the ring, the prepared replacement unit has to be available and in place.

Even then, minimal mandatory warming up requires 1 day, removal and mounting of the replacement unit another day. Then 2 days of cool down are needed, followed by 1-2 days of conditioning. In summary, even under optimal conditions a full week of dark time will result from any situation requiring the replacement of a faulty cryo module.

References

- [1] A. W. Chao. *Physics of Collective Beam Instabilities in High Energy Accelerators (Wiley Series in Beam Physics and Accelerator Technology)*. 1st ed. Wiley-VCH, Jan. 1993 (cit. on p. 144).
- [2] S. Krinsky. “Coherent Synchrotron Radiation”. In: ed. by A. W. Chao, K. H. Mess, and F. Zimmermann. 2nd edition. *Handbook of Accelerator Physics and Engineering*. 2013. Chap. 3.1.7, pp. 227–229 (cit. on p. 145).

- [3] E. L. Saldin, E. A. Schneidmiller, and M. V. Yurkov. “On the coherent radiation of an electron bunch moving in an arc of a circle”. In: *Nucl. Instrum. Methods Phys. Res., Sect. A* A398 (1997), pp. 373–394 (cit. on p. 146).
- [4] M. Borland. “Simple method for particle tracking with coherent synchrotron radiation”. In: *Phys. Rev. ST Accel. Beams* 4 (7 July 2001), p. 070701. URL: <http://link.aps.org/doi/10.1103/PhysRevSTAB.4.070701> (cit. on p. 146).
- [5] K. L. F. Bane and P. Emma. *Estimates of Power Radiated by the Beam in Bends of LCLS-II*. Tech. rep. SLAC-PUB-15864. Dec. 2013 (cit. on p. 146).
- [6] CST – Computer Simulation Technology AG. *Microwave Studio*. URL: www.cst.com (cit. on p. 148).
- [7] W. Bruns. *The GdfidL Electromagnetic Field Simulator*. URL: <http://www.gdfidl.de> (cit. on p. 148).
- [8] G. Skripka et al. “Transverse Beam Instabilities in the MAX IV 3 GeV ring”. In: *Proceedings of IPAC2014 TUPRI053* (2014), pp. 1689–1691 (cit. on p. 149).
- [9] H.-W. Glock (Compaec e.G.) *Abschlussbericht: Strahlerregte Felder in den warmen Komponenten von bERLinPro*. Tech. rep. 2015 (cit. on p. 149).
- [10] S. Khan. “Beam impedance study for the BESSY-II storage ring”. In: *Proceedings of PAC1997 2* (May 1997), pp. 1703–1705 (cit. on p. 149).
- [11] P. Gu et al. “Management for the Long-Term Reliability of the Diamond Superconducting RF Cavities”. In: *Proceedings of SRF2013 MOP059* (2013), pp. 255–2578. URL: <http://accelconf.web.cern.ch/AccelConf/SRF2013/papers/mop059.pdf> (cit. on p. 155).
- [12] *Workshop on the Operation of CESR Design 500 MHz Cavities*. Conference Website. 2011. URL: <http://www.diamond.ac.uk/Home/Events/2011/cesr.html> (cit. on p. 155).
- [13] M. R. F. Jensen. “Operational Experience with SRF Cavities for Light Sources”. In: *Proceedings of SRF2011 MOIOB05* (2011). SRF2011, pp. 27–31. URL: <http://accelconf.web.cern.ch/AccelConf/SRF2011/papers/moiob05.pdf> (cit. on p. 155).
- [14] R. Bartolini. “Diamond Light Source status”. In: (). URL: <http://www.diamond.ac.uk/Home/Events/2011/cesr.html> (cit. on p. 155).
- [15] R. Bartolini. *Diamond Light Source status*. Conference Website. ESLS XXII Workshop. Nov. 2014. URL: http://www.esrf.eu/files/live/sites/www/files/events/conferences/XXII%20ESLS/BARTOLINI_2014_11_25_ESLS_RB1.ppt (cit. on p. 155).

6 Beam Diagnostics

6.1 Required Information

Commissioning and operation of BESSY VSR requires an upgrade of machine diagnostics. There will be new beam parameters used as a figure of merit as well as existing parameters in new ranges. Two main tasks will have to be accomplished. On the one hand, beam diagnostics is needed for machine commissioning as well as development. In particular, this involves understanding the injection process as well as combining BESSY VSR and low- α to generate short pulses in the sub-ps range. On the other hand, a set of non-invasive diagnostic techniques is needed to ensure long-term quality and stability of the photon beam delivered to users.

Table 6.1 shows beam and radiation parameters, which are intended to be measured for the commissioning and/or operation of BESSY VSR. An exceptional feature of measuring these parameters is given by the fact, that parameters have to be measured on a bunch-by-bunch basis due to the complex fill pattern – see Section 2.3.

It should be noted that mechanical stability of beamline elements such as mirrors or optical tables can become an issue when using very short bunches. Therefore, the corresponding vibration measurements should be projected.

6.2 Diagnostic Beamline

A beamline for photon diagnostics is foreseen for BESSY VSR. This beamline should offer the possibility to operate a streak camera, THz detectors and spectrometers as well as additional space for tests and development of new diagnostic techniques. It is intended to operate the beamline over the full project range of BESSY VSR – during commissioning as well as user operation.

Table 6.1: Beam parameters to be measured for BESSY VSR.

Parameter	Measurement techniques
Instantaneous bunch length	Streak camera THz spectroscopy
Average bunch length	Streak camera Slicing THz spectroscopy
Longitudinal jitter	Streak camera Bunch-by-bunch BPM / stripline Slicing
Transverse jitter	Bunch-by-bunch BPM / stripline Source point imaging Quadrant diodes
Transverse source size	Source point imaging Streak camera
THz power	Schottky diodes
THz spectrum	Bolometers Schottky diodes FTIR

6.2.1 General Setup

The use of bending magnet radiation seems to be necessary, as the demand for user time at insertion devices is notoriously high. In addition, the injection process is of particular interest. Therefore, the beamline should be able to operate with closed beam shutters – see Chapter 9. At the time of writing this study, the only acceptable solution fulfilling all these demands is to use an out-of-plane beamline. Therefore, a vertical mirror is applied to achieve a 90° reflection just behind a bending magnet. This mirror should be as close to the dipole magnet as possible to maximize acceptance of radiation in the THz range. A new opening in the radiation shielding is needed, which will be covered by a labyrinth of additional shielding material. Beamlines of this kind are already well established at BESSY II, such as the IR and THz beamline.

Figure 6.1(a) shows possible positions of the diagnostic beamline along the BESSY II storage ring, which are given by green markers. The red marker indicates the posi-

tion of the superconducting RF cavity system. Positions next to the cavity system would be favorable in terms of being able to detect beam parameters directly in the vicinity of these new and strong elements. However, space requirement by the cryogenic system may hamper the setup of a diagnostic beamline at those positions – see Chapter 4. Figure 6.1(b) shows a platform based beamline setup at the example of the IR beamline at BESSY II. It should be noted, that the beamline with all optical elements and detectors is placed on the concrete part of the radiation shielding for reasons of mechanical stability. Setting up the beamline would require roughly one year, starting with the decision of position. The required reconstruction work will be carried out in regularly scheduled shutdowns and will not lead to additional downtime.

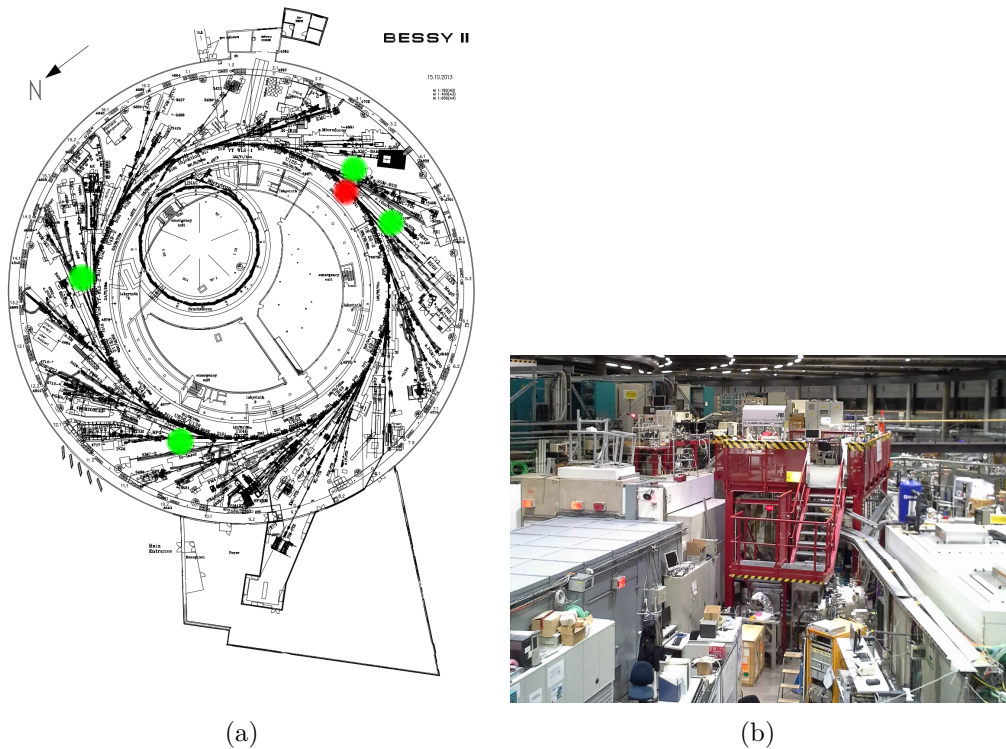


Figure 6.1: Possible positions of a diagnostic beamline (a). Green markers indicate the position along the storage ring, whereas the red marker indicates the position of the superconducting RF cavities system. A platform based solution (b) can be chosen similar to the IR beamline at BESSY II.

Using at least $2 \times 90^\circ$ reflections, restricts the available wavelength range to the lower photon energy part of the synchrotron radiation spectrum of BESSY II. The

use of technologies like multi-layer mirrors will have to be explored to evaluate possible application of higher photon energies in the range of hundreds of eV.

Table 6.2 shows estimated costs for the setup of a diagnostic beamline.

Table 6.2: Projected costs of a diagnostic beamline and equipment for BESSY VSR.

Item	Costs
Baseline costs (platform & radiation shielding)	100 k€
Photon beamline	200 k€
Standard diagnostic equipment (oscilloscope, spectrum analyzer ...)	100 k€
Streak camera (including optical elements)	300 k€
Dipole chamber with dedicated THz port (front & back port)	100 k€
Schottky diodes, bolometer & accessories	100k€
Bunch resolved beam position	30k€
Bunch resolved source point imaging	to be estimated
Sum	930 k€

6.2.2 Bunch Length Diagnostics

A well established technique of measuring the bunch length in electron storage rings is the use of streak cameras. The bunch length regime that can be covered using the streak camera technique in general is about $\sigma \approx 1 \text{ ps} \dots 100 \text{ ps}$. At present, there is already a streak camera in operation at BESSY II, which has a resolution of about $\sigma \approx 2 \text{ ps}$.

It is necessary to distinguish between two different kinds of operation of a streak camera:

1. synchroscan,
2. single streak.

The synchroscan mode is well established at electron storage rings and makes use of the highly repetitive radiation patterns. Therefore, requirements in terms of photon flux are quite relaxed and can be countered by longer acquisition times. However, this technique only reveals information about the average bunch length. Fast oscillations or jittering of the electron beam may increase the measured bunch length. In contrast, the single streak technique is based on the measurement of the bunch length of individual bunches in a single pass. Therefore, enough photons emitted by the bunch and accepted by the beamline are needed, which amount to roughly 100 . . . 1000 photons. Commercially available single streak cameras are able to resolve an instantaneous bunch length of about $\sigma \approx 100$ fs. Simulations to determine whether this technique is possible at all, require a more progressed project state with detailed knowledge of beamline position and geometry. This level of resolution imposes tight demands on the signal/trigger distribution system, as well as the mechanical stability of the beamline, which will be necessary for BESSY VSR operation in any case. However, single streak cameras are prone to a quite large trigger jitter, which is orders of magnitude larger. Therefore, jitter and oscillations may not be resolved by this technique.

An alternative method to extract the bunch length for short bunches in the picosecond to sub-picosecond range is the detection and analysis of coherent synchrotron radiation in the THz range. This technique is already established at BESSY II [1]. Recent developments in Schottky diode detectors may allow efficient monitoring of bunch-by-bunch THz spectra and stability.

Complementing to machine diagnostics to determine sub-picosecond bunch lengths and stability, user experiments can contribute significantly. E.g. the slicing experiment may probe the bunch length by adjusting the phase between laser and bunch.

6.2.3 Source Size Diagnostics

BESSY II is operating pinhole monitor systems to measure transverse beam dimensions [2]. However, the complex fill pattern of BESSY VSR as given in Section 2.3 indicates the need to determine this information on a bunch-by-bunch scale.

One way of measuring a bunch-resolved source size could be to make use of fast optical gates in the hundreds-of-picoseconds range. However, the required optical gates are well established in the visible range only.

Table 6.3 shows the calculated resolution limits for bending magnet radiation following [3]. Compared with BESSY II source point size as given in Section 1.3, the use of UV or VIS radiation seems to be of limited applicability. In addition to diffraction, the depth-of-field effect may limit resolution which can be avoided by

reduction of the acceptance angle [4]. Further studies to extract bunch-resolved transverse beam dimensions using source point imaging techniques are ongoing.

Table 6.3: Source point imaging – resolution limit in the vertical plane for bending magnet radiation.

Wavelength/nm	Diffraction limit/ μm
13.5	3
200	16
550	30

As an alternative approach, streak cameras can be used to monitor the bunch-resolved bunch dimension in one plane. However, this technique is more commonly used for proof-of-principle measurement or injection studies in contrast to long-term, high resolution monitoring.

6.3 Digital Feedback System

Storage Ring

Since 2013 a digital bunch-by-bunch feedback system is in operation in the BESSY II storage ring. This system has proven to be a powerful tool for the mitigation of coupled-bunch instabilities in all three planes, and also provides valuable diagnostics capabilities [5].

A temporal resolution of approximately 100 fs was achieved in the longitudinal plane, which can be utilized for longitudinal jitter analysis of short bunches in BESSY VSR.

For BESSY VSR the power of the currently installed system is believed to be sufficient, but in particular in the longitudinal plane the system will be upgraded in order to provide enough operational head room. Recently new state-of-the-art amplifiers have been acquired. These include two 250 W broadband amplifiers (9 kHz to 250 MHz) for the transverse plane, and one 200 W RF-amplifier (0.8 GHz to 3 GHz) for the longitudinal plane. Commissioning is ongoing and will be completed by mid 2015. For the transverse plane this provides an easy upgrade plan: With a second pair of 250 W broadband amplifiers, and utilizing the free stripes of the stripline kicker, the system power can be doubled. In the longitudinal plane a

factor two in kicker amplitude would require an amplifier power upgrade of factor four. This is possible but expensive. Therefore at least one additional longitudinal feedback cavity will be installed.

In general the damping times achievable with the longitudinal bunch-by-bunch feedback system is limited by the synchrotron frequency. Additional improvements of the performance may be possible by alternative feedback designs utilizing a different pickup-schemes, which is subject of current research.

Booster Synchrotron

In the moment the booster synchrotron is operated without bunch-by-bunch feedback. Longitudinal instabilities exist and contribute approximately with 70 ps to the bunch length at extraction (see Figure 6.2). This jitter is not acceptable for the reliable injection into short bunches. Thus, the installation of longitudinal bunch-by-bunch feedback is needed. In addition the installation of a full 3D system (as in the storage ring) is recommended, both to provide bunch-by-bunch/turn by turn diagnostics and to mitigate possible transversal multi-bunch instabilities that may arise in future operation modes of the booster.

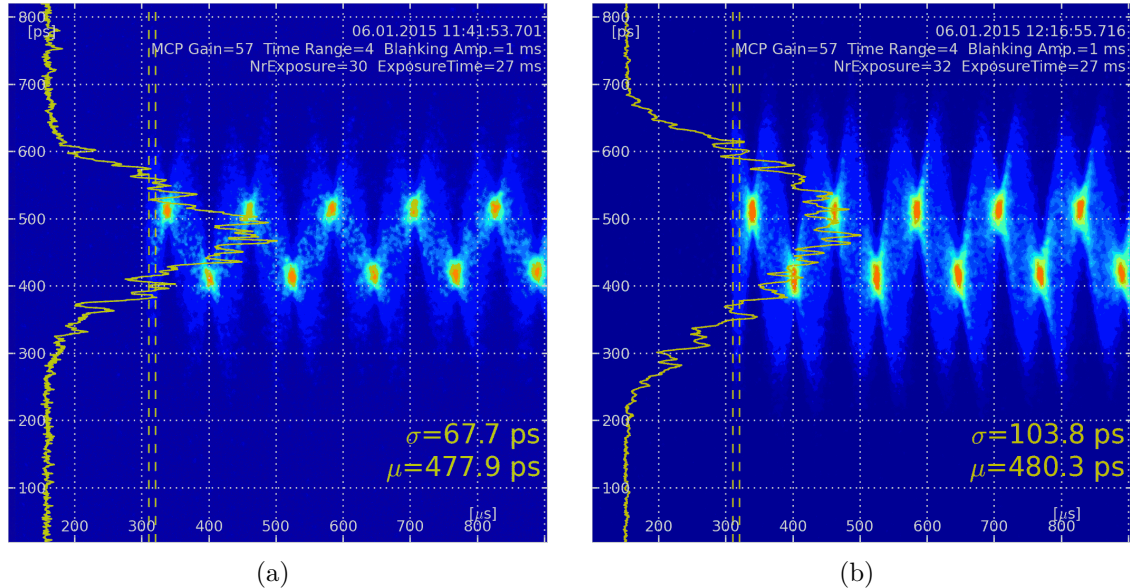


Figure 6.2: Streak camera measurements of the injection process (a) single-bunch injection, (b) four-bunch injection. Coupled-bunch instabilities lead to an effective bunch lengthening of approximately 70 ps.

Table 6.4 gives a summary of the costs for upgrading the digital feedback systems.

Table 6.4: Summary of costs associated with digital feedback upgrade. These costs include an upgrade of the existing bunch-by-bunch feedback system in the storage ring, and the installation of a dedicated system in the booster synchrotron.

Item	Amount	Costs
Storage ring		
250 W broad band amplifier (transverse plane)	2	45 k€
Longitudinal kicker cavity	1	50 k€
200 W 0.8 GHz to 3 GHz amplifier (longitudinal plane)	1	65 k€
Vacuum chamber modification		ca. 15 k€
Experimental bunch-by-bunch feedback processor	1	70 k€
Sum		245 k€
Synchrotron		
Digital bunch-by-bunch feedback processors (e.g. Dimtel iGp12)	3	200 k€
250 W broad band amplifier (transverse plane)	2	45 k€
Longitudinal kicker cavity	1	50 k€
200 W 0.8 GHz to 3 GHz amplifier (longitudinal plane)	1	65 k€
Vacuum chamber modification		ca. 15 k€
Sum		375 k€
Total sum		620 k€

In order to achieve a better beam alignment and orbit stability for BESSY VSR an upgrade to a digital BPM system is necessary. A rough estimate for upgrading BESSY II's BPM system shows that the investment costs amount to 1700 k€.

References

- [1] J. Feikes et al. "Sub-Picosecond Electron Bunches in the BESSY Storage Ring". In: *Proceedings of EPAC 2004* (2004), pp. 1954–1956 (cit. on p. 161).

- [2] K. Holldack, J. Feikes, and W. B. Peatman. “Source size and emittance monitoring on BESSY II”. In: *Nuclear Instruments and Methods in Physics Research Section A: Accelerators, Spectrometers, Detectors and Associated Equipment* 467–468, Part 1 (2001). 7th Int.Conf. on Synchrotron Radiation Instrumentation, pp. 235–238. URL: <http://www.sciencedirect.com/science/article/pii/S0168900201005551> (cit. on p. 161).
- [3] A. Hofmann and F. Méot. “Optical resolution of beam cross-section measurements by means of synchrotron radiation”. In: *Nuclear Instruments and Methods in Physics Research* 203.1–3 (1982), pp. 483–493. URL: <http://www.sciencedirect.com/science/article/pii/0167508782906639> (cit. on p. 161).
- [4] W. Cheng. “Synchrotron Light Monitor System for NSLS-II”. In: *Proceedings of BIW10 TUPSM110* (2010), pp. 478–482 (cit. on p. 162).
- [5] A. Schälicke et al. “Status and Performance of Bunch-by-bunch Feedback at BESSY II and MLS”. In: *Proceedings of IPAC2014 TUPRI072* (2014), pp. 1733–1735 (cit. on p. 162).

7 Bunch Separation Schemes

The light emitted by long bunches has to be separated from the short light pulses to allow for efficient use of the characteristics. Several techniques are at hand to achieve that goal. On the one hand temporal separation, either by electronic means and gated detection – not further discussed here, or by a fast spinning chopper wheel which blanks out the unwanted long light pulses and which will be presented in Section 7.1. Both techniques require a gap of ~ 50 ns on both sides of the short bunch in order to be applicable. Or, on the other hand, spatial separation of the short bunch from the rest by so called “resonant pulse picking”, successfully demonstrated at BESSY II and described in detail in Section 7.2. Spatial separation by transverse deflecting structures is covered in Section 7.3. Finally, Section 7.4 presents the technique of creating transverse resonance islands which can be populated at will for each individual bunch and can also be used for spatial separation of bunches. The latter techniques do not require long gaps around the bunch being separated. This is a clear advantage over the chopper wheel because the 100 ns long gap produces phase transients which reduce the life time (see Section 2.6).

7.1 Chopper Systems

Anticipating the BESSY VSR fill pattern with variable bunch length we have proven the workability of a MHz (turn-by-turn) mechanical chopper system to pick single (camshaft) X-ray pulses of variable pulse length out of the different multibunch pulse trains as foreseen for the BESSY VSR upgrade. This device (FZJ/MPI/HZB-development) is a unique high-tech gadget compared to conventional kHz-choppers [1, 2] as it must withstand strong centrifugal forces owing to a high orbital speed of triple sound velocity. After recent tests we demonstrated - by an elaborate interplay between mechanical precision, a fast phase locked electronic feedback control and a high performance X-ray beamline - that only pulses of 1.25 MHz repetition rate may pass the chopper mimicking a single bunch mode X-ray emission at preserved peak brilliance. This system may facilitate all single bunch applications as usually performed in the regular but rare single bunch accelerator mode. It will be installed in beamlines that are unfeasible to benefit from other pulse picking techniques (see

[3, 4]). The first prototype has been recently implemented in the PM4 - beamline, a Plane Grating Monochromator (PGM) on a dipole source.

The system as depicted in Figure 7.1 consists of a specially designed in-vacuum chopper wheel rotating with 0.998 kHz angular frequency. The wheel needs to

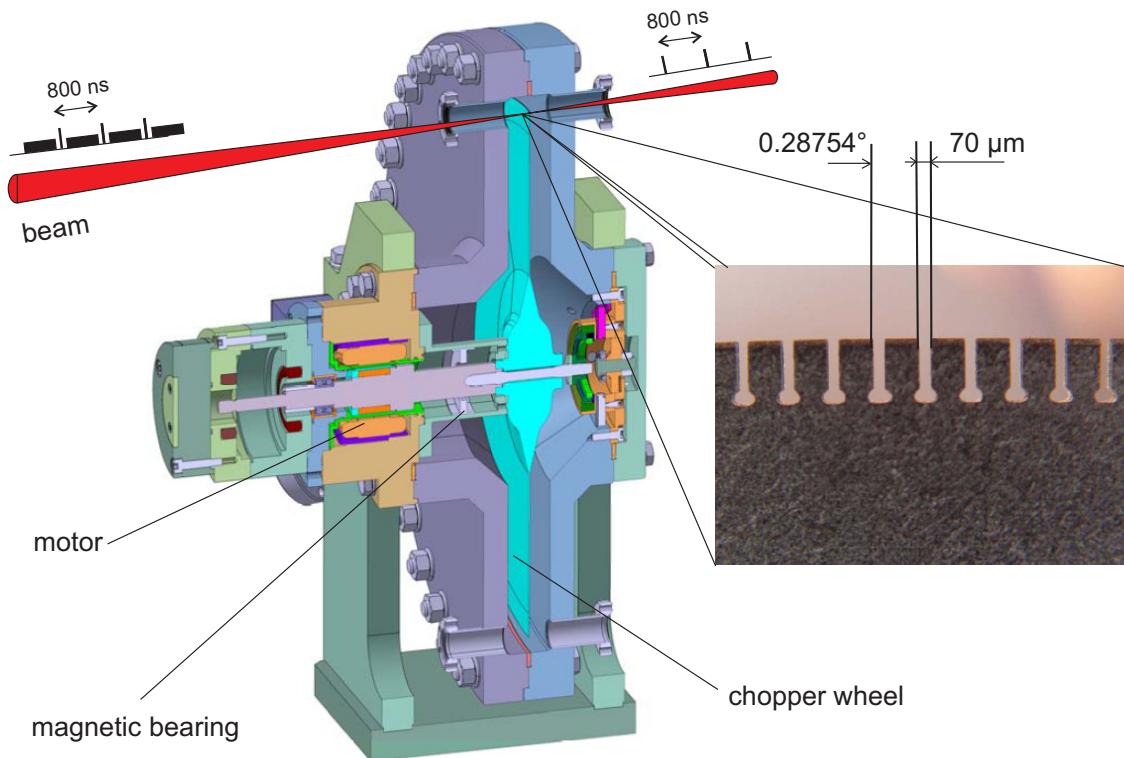


Figure 7.1: Optical layout and mechanical assembly drawing of the MHz light chopper system. A specially designed wheel (light blue) with radially decreasing thickness (minimum 0.5 mm) is driven by a mechanism as widely used for magnetically pivoted turbo-molecular pumps. After passing a variable entrance slit (here 70 μm) the incident focused light beam (flaming red) is passing the set of wire-eroded chopper slits at the outer edge of the wheel. The patterns close to the beam (red) depict a temporal pattern as emitted by the source and after the chopper, respectively indicating that only a single X-ray pulse at 1.25 MHz (800 ns) is being passed through the slits.

be operated in vacuum by magnetic bearings and capable of withstanding high centrifugal forces. Pulses are picked by 1252 high precision slits of 70 μm width in the outer edge of the wheel corresponding to a temporal opening window of the

chopper of 70 ns at 1060 m/s orbital speed and 998 Hz rotation frequency. The chopper needs a beamline with intermediate focus and was successfully tested in a dedicated setup on a dipole magnet beamline at BESSY II [5]. The device was placed in the intermediate focus after the first mirror (toroidal mirror at 6° grazing incidence, 12° total horizontal deflection, Gold coating) that produces a 1:1 image of the source 24 m behind the electron beam at a beam height of 1.4 m. After that mirror the beam is a white beam (50 eV to 1 keV) limited at high photon energies by the mirror's reflectivity cut-off and at low energies by a $2\ \mu\text{m}$ thick Aluminum filter in front of the detector (APD-Avalanche Photodiode, Hamamatsu-2381) as used 1 m behind the chopper.

Using this setup we have successfully proven the workability of the MHz mechanical chopper system by using it to pick single pink X-ray pulses of 50 ps pulse length (FWHM) out of the regular multibunch pulse train in the BESSY II storage ring as confirmed by Figure 7.2.

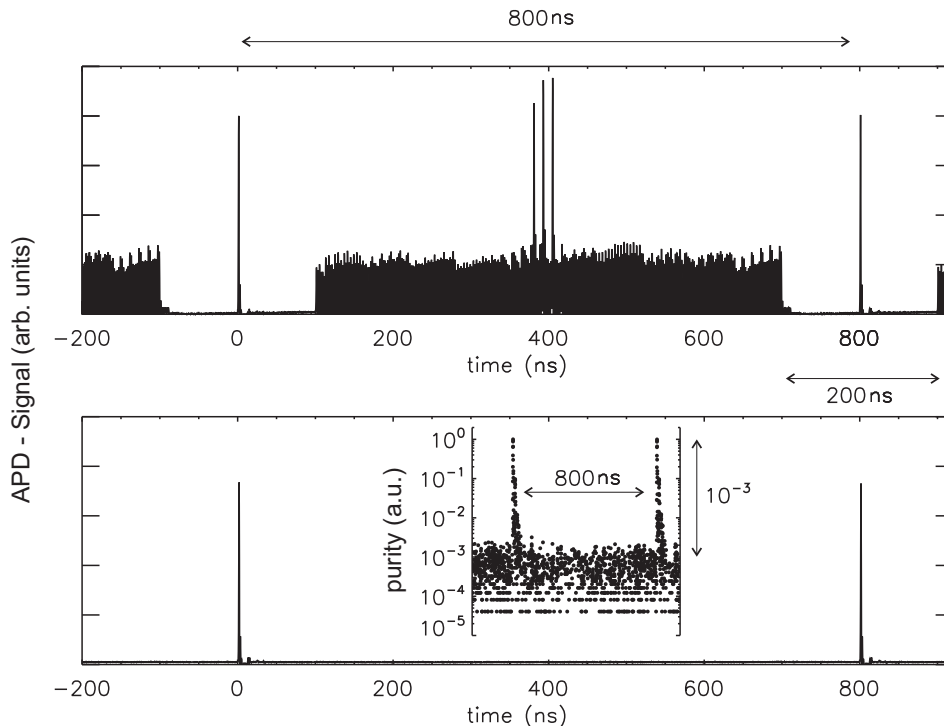


Figure 7.2: X-ray signal behind the chopper with the chopper at rest (upper plot) and with the chopper slit phase-locked to the bunch clock and at a phase value that keeps the opening window symmetrical to the camshaft bunch (lower plot). To confirm the high purity, the same waveform is plotted at logarithmic y-scale in the inset.

The inset Figure 7.2 clearly demonstrates that a single bunch pattern of extraordi-

nary purity serves the experiment. The temporal opening window of the device is given by the convolution of two $70\ \mu\text{m}$ slits, one of them placed 10 cm upstream of the chopper and the chopper slit itself. At the current beamline this convolution is $150\ \mu\text{m}$ wide, sufficient to pick pulses out of a 200 ns clearing gap in BESSY II's fill pattern. However, at beamlines with smaller intermediate focus, the ultimate limit as given by the $70\ \mu\text{m}$ wide chopper slits and their orbital velocity of 1060 m/s is 70 ns.

The chopper technique, currently optimized for an ion clearing gap of 200 ns, needs to be adapted to the envisaged BESSY VSR fill pattern with a gap of only 100 ns. The investment costs for upgrading the chopper system are summarized in Table 7.1.

Table 7.1: Estimation of costs for adapting the MHz chopper system to a 100 ns ion clearing gap.

Sub-100 ns MHz-chopper	Costs/k€	Remarks
Modified prototype for dipoles	210	Final BESSY VSR phase, sub-50 micron slitted wheel
Controls, data acquisition	105	
Adapted slit unit	65	Modification of the PGM
New prototype for IDs	210	Final BESSY VSR phase
Controls, data acquisition	105	
Exit slit modification	90	Monochromator modifications
Total costs:	785 k€	

7.2 Incoherent Excitation

Everything we know nowadays about novel materials and the underlying processes defining them we know thanks to studies at contemporary synchrotron facilities like BESSY II. Here, relativistic electrons in a storage ring are employed to generate very brilliant and partly coherent light pulses from the THz to the X-ray regime in undulators and other devices. However, most of the techniques used at Synchrotron

Facilities are very "photon hungry" and demand ever brighter light pulses to conduct innovative experiments. In the soft and tender X-ray range these applications will be certainly covered by diffraction limited light sources very soon. The general greed for stronger light pulses does, however, not really meet the requirements of one of the most important techniques in material science: Photoelectron spectroscopy. Physicists and chemists have been using it for decades to study molecules, gases and surfaces of solids. However, if too many photons hit a surface at the same time, space charge effects of the emitted electrons deteriorate the results. Owing to these limits, certain material parameters stay hidden in such cases. Thus, a tailored temporal pattern of X-ray pulses is mandatory to move things forward in surface physics at Synchrotrons, especially when dynamics on the picosecond and even sub-picosecond timescale is supposed to be addressed.

Our novel method [3] is capable of picking single pulses out of a conventional pulse train as usually emitted from synchrotron facilities. We managed to apply this for the first time to time-of-flight electron spectroscopy based on modern instruments as developed at BESSY II within a joint Lab with Uppsala University, Sweden [6]. The pulse picking technique as depicted in Figure 7.3 is based on a quasi resonant magnetic excitation of transverse oscillations in one specific relativistic electron bunch that - like all others - generates a radiation cone within an undulator. The selective excitation leads to an enlargement of the radiation cone. Employing a detour ("bump") in the electron beam path, the regular radiation and the radiation from the excited electrons can be easily separated and only pulses from the latter arrive - once per revolution - at the experiment as confirmed by Figure 7.4.

Thus, the arrival time difference (800 ns) of subsequent pulses is now perfectly accommodated for modern high resolution time-of-flight spectrometers. The development of the Pulse Picking by Resonant Excitation (PPRE) was science driven by our user community working with single bunch techniques. They demand more beamtime to improve studies on e.g. graphene, topological insulators and other hot topics in material science like the current debates about high Tc-Superconductors, magnetic ordering phenomena and catalytic surface effects for energy storage. Moreover, with pulse picking techniques at hand, we are now well prepared for our future light source with variable pulse lengths: BESSY VSR, where users will appreciate pulse selection on demand to readily switch from high brightness to ultrashort pulses according to their individual needs.

We have proven the feasibility of the method with ARTOF-time-of-flight spectrometers at different undulators and beamlines as well as in BESSY II's regular user mode. We could certainly benefit from long year experiences with emittance manipulation. The small kicks of typically $\sim 0.1 \mu\text{rad}$ per bunch passage add up and lead to a 3 times horizontally blown-up bunch. Thanks to accelerator developments in the past, we are capable of even picking ultrashort pulses out of the bunch trains

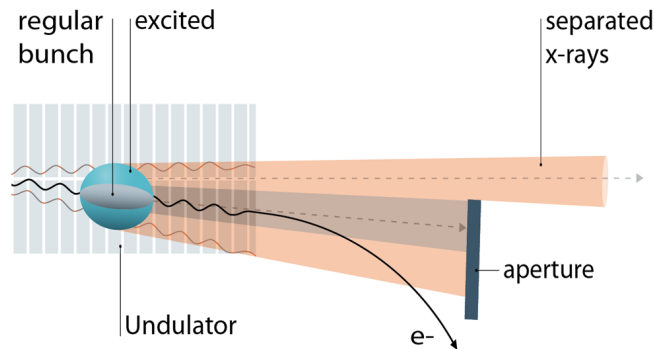


Figure 7.3: Undulator light (grey) emitted from the regular electrons in the bunch train (2 ns distance) is dumped into an aperture. In regular operation, the bump is turned off and the non-excited bunches (grey ellipse) emit undulator radiation on-axis. With the bump turned on, this radiation is emitted off-axis and hits the knife edge being dumped there and only a part of the radiation (orange) from one resonantly excited (blue ellipse) bunch can enter the beamline after travelling on-axis and thus, preserving the circular polarization degree $(S3/S0) = 0.7$ to 0.9 as available from elliptical undulators.

in low-alpha operation, a special operation mode of BESSY II. At last, the users can, already right now, individually switch - within minutes - between high static flux and the single pulse without touching any settings at their instruments and the sample. At BESSY VSR the two pulses in the 2 clearing gaps can be selected on demand by just changing a delay in the timing system that controls the bunch excitation and the devices which are utilized at the experiment for electronic gating or time-correlated counting, respectively.

7.3 Transverse Deflecting Structure

Separation with a transverse deflecting structure is very similar to the separation by incoherent excitation. The emittance increase by the quasi resonant excitation of a particular bunch requires only a very modest strength of the transverse kicker, however, has the disadvantage that only a rather small fraction of the light emitted by the bunch can be utilized in the experiments. In nearly all cases, and as long as the emitted light is not diffraction limited, the required angle for full separation depends on the emittance of the electron beam. With dedicated and advanced techniques the kick applied to the desired bunch can be made considerably larger.

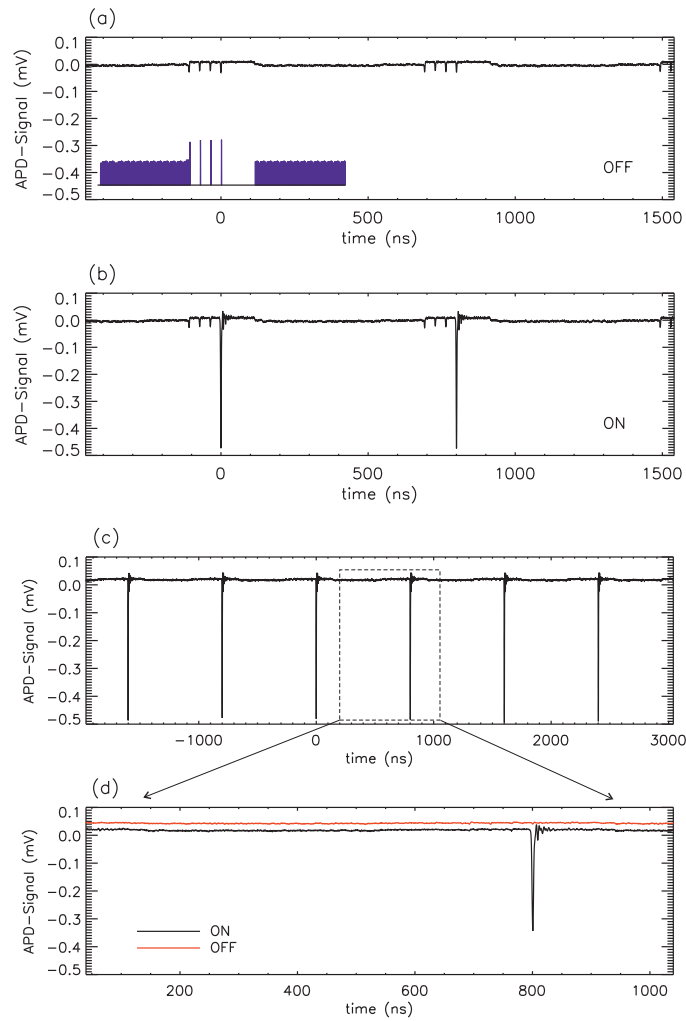


Figure 7.4: X-ray signals at different excitation conditions. Signals measured with an avalanche photodiode behind the exit slit of the UE56/1 beamline at a photon energy of 1200 eV for different situations: (a) Normal hybrid mode with four camshaft bunches of 36 ns distance in an ion clearing gap of 200 ns. The blue inset in (a) shows the fill pattern. A weak resonant excitation of one camshaft bunch out of 4 in (b) leads already to one order of magnitude higher signal from that bunch. At even stronger excitation in (c) a real stationary turn-by-turn repetition (shown by larger timescale) of the picked bunch at 800 ns (1.25 MHz) remains even though the excitation is performed only at 190 kHz excitation frequency. A close up of the single bunch signal, depicted in (d) shows the result if the excitation is switched OFF and ON, respectively. The comparison between the black and the red curve (shifted for clarity) reveals that a signal contribution from multi-bunches is not detectable at all, even with a signal-to-noise limit $> 10^3$.

If the kick would be on the order of one mrad the light emitted by the long and short bunches can be completely separated in the horizontal plane so that the full intensity of the short pulse would be available.

The ALS [4] was the first facility to develop the so called pseudo-single-bunch operational mode, a bunch separation scheme based on a fast transverse deflecting stripline kicker, which is also suitable for BESSY VSR. The basic idea is shown in Figure 7.5 [7]. The kicks are applied in the vertical direction where the emittance of the electron beam is sufficiently small so that the radiation is diffraction limited and full separation of a single bunch is easier. If the bunch is kicked on every revolution, the bunch will circulate on a stable closed orbit vertically shifted with respect to the other bunches.

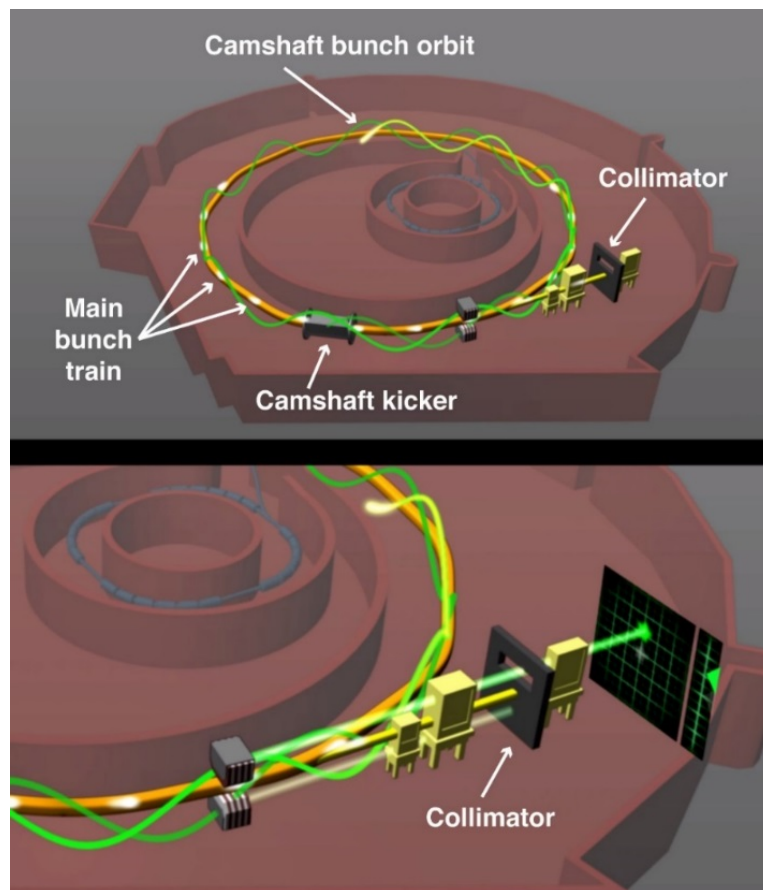
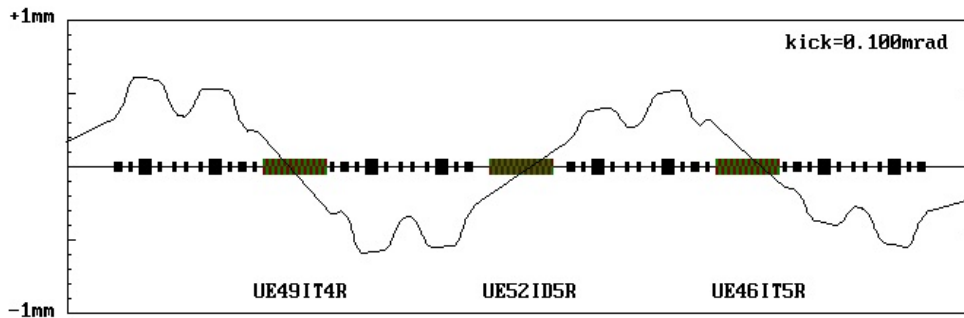
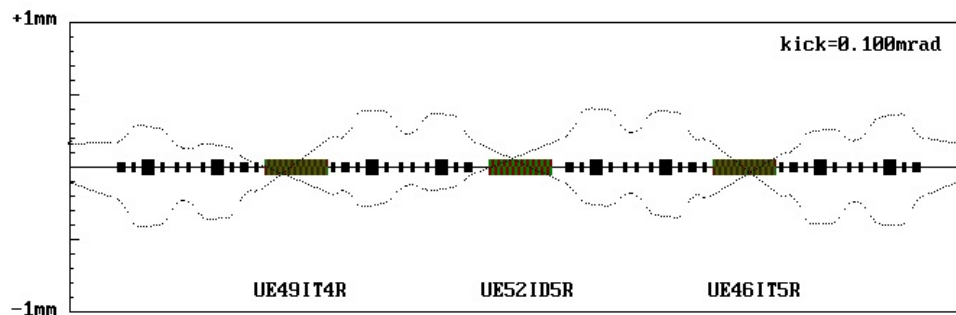


Figure 7.5: Creation of a pseudo-single-bunch from a multi-bunch fill pattern at the ALS. The bunch in the gap is kicked vertically on every revolution and because of the displaced orbit the light emitted by that bunch can be separated by a collimator from the rest of the radiation [7].

As depicted in Figure 7.5 a strategically placed collimator in the beamline can suppress the unwanted radiation. The source point conditions depend on the relative position of the beamline and the location of the kicker magnet. This is shown in Figure 7.6 for a section of the BESSY II ring and a position of the stripline kicker in front of the BAM WLS, space currently occupied by the four normal conducting 1.5 GHz-Landau cavities.



(a)



(b)

Figure 7.6: One- (a) and two-turn (b) closed orbits from a 100 μ rad vertical kick at BESSY II. The repetition rate of short light pulses would be 1.25 MHz or 0.625 MHz. If the beam is kicked on every second revolution the strength of the kick should be $K_{n=2} = K_1 \frac{\sin(n\pi Q)}{\sin(\pi Q)}$ in order to produce a similar orbit shift.

If the kicker produces a kick of 100 μ rad every 800 ns the solid orbit offset is obtained and if a kick is applied every second turn then the dotted orbit distortion would be created. Shifted orbits, closed after 2 or even 3 turns, would offer opportunities to catch the right radiation on nearly all beamlines, however, at a reduced repetition frequency and with a suitable strength of the kicker magnet. The strong kicks at these repetition rates can be produced with state of the art stripline [8] and

electronics designs [9]. Rise and fall time of these pulses would be below 10 ns so that a total gap of only 20 ns would be required, much shorter than needed for the chopper wheel. With a suitable 4-kicker DC-bump the orbit of the displaced bunch must be brought back to the on-axis design orbit. This will usually include position and angle of the beam and, in case of a shifted orbit closing after 1 turn, full separation might be possible on a few beamlines only. The opening cone of the radiation will be determined by the characteristics of the undulator rather than the emittance of the electron beam. The vertical emittance is small enough to produce diffraction limited radiation up to a few keV photon energy.

The actual vertical tune at BESSY II with a value of 6.74 is very close to the fourth order resonance. It would be straight forward to apply the kick-and-cancel scheme demonstrated at the ALS. In this scheme the beam would be kicked and 2 turns later kicked again. The second kick ideally removes all the transverse momentum of the bunch and the bunch travels for 2 turns on a shifted orbit compared to the rest of the beam. This would allow for freely adjustable repetition frequencies of the light pulses from ms to μ s time intervals.

The pseudo-single-bunch technique can also be applied in the horizontal plane. The emittance is much larger and considerably larger kicks on the order of one mrad are required to fully separate the short light pulses from the light emitted by the long bunches. Due to the elliptical shape of the vacuum chamber with a typical aspect ratio of two it is much easier to produce the necessary vertical kicks.

For the BESSY VSR fill pattern of the storage ring there is an alternative to the broad band stripline kicker namely a resonant transverse deflecting cavity structure working at an uneven multiple of 250 MHz. In such a cavity the deflecting field changes direction every 2 ns and bunches stored in even buckets (short bunches) could be spatially separated from bunches in the uneven buckets (long bunches), the buckets created by the combined 1.5 GHz and 1.75 GHz cavity-systems 2 ns apart. For example, short bunches would be kicked to one side and the long bunches to the other. With a static transverse field the desired type of radiation could be guided through the beamline and onto the sample. This would not lead to a perfect separation due to the planned filling pattern which foresees to include a couple of short bunches for slicing with a charge as high as possible. It would nevertheless relax the requirements for an additional chopper or for gating the detector. For the APS-crabbing scheme an appropriate superconducting cavity has been developed. The operating frequency of 2.8 GHz, close to the 2.75 GHz cavity which we would need [10]. This cavity has produced a peak deflecting voltage of 2 MV. If this cavity would be installed at BESSY II the beam could be separated with a total angle of ~ 2.3 mrad, which is at least one order of magnitude larger than needed for the vertical separation of short and long bunches. This bunch separation scheme will be studied in details within the BESSY VSR project.

7.4 Resonance Island Buckets

Nonlinear beam dynamics may enable storage rings to operate with multiple beams simultaneously. A separation of electron beams in space or angle yields an intrinsic separation of photon beams, which may be exploited by users through means of apertures or imaging. Storage of multiple electron beams can be achieved by introducing additional buckets to the phase space in at least one plane. Main advantages of this beam separation technique are the use of static magnetic fields, a limited impact on emittance and most important: separated beams are supplied to all user ports simultaneously – bending magnet and ID beamlines alike. No new hardware and only marginal detuning of the well established beam optics will be required for implementation. However, applicability for high current user operation at large scale synchrotron light sources operating under TopUp conditions still has to be shown.

In the transverse plane, additional buckets are well known and described in the vicinity of resonances [11]. Therefore, these buckets are named “resonance island buckets”. A single known application of these buckets is slow extraction applied at CERN [12]. However, resonance island buckets are not yet exploited for the storage of multiple beams at synchrotron radiation sources. Usually, only moderate changes to the transverse beam optics are required to approach some resonance near the established working point. Therefore, this technique is compatible with the BESSY VSR objective to preserve the transverse beam optics. Most of the experimental techniques and results in the following section were obtained at the MLS [13–15] and are now in the process of being transferred to the BESSY II storage ring.

BESSY VSR operation with resonance islands buckets is investigated around horizontal resonances. Figure 7.7 shows examples of particle tracking results in the horizontal plane near the resonances $\Delta Q_x = 1/2$ (a), $\Delta Q_x = 1/3$ (b) and $\Delta Q_x = 1/4$ (c), which have been verified experimentally. The number of islands in phase space is determined by the resonance approached. The stable area is strongly dependent on the distance to the resonance, i.e. quadrupoles, as well as the tuning of nonlinear elements, i.e. sextupoles. Island bucket acceptance has to be maximized, while preserving sufficient acceptance of the “core beam”. In addition, it is desirable to achieve an “embracing bucket”, which surrounds core and islands buckets. Particles lost from core or islands are then still trapped on closed trajectories and have a high probability to be damped back to core or island. Therefore, particle redistribution from core to island and vice versa is possible e.g. by resonant excitation at core or island bucket tunes using fast kickers such as the ones used for bunch-by-bunch feedbacks.

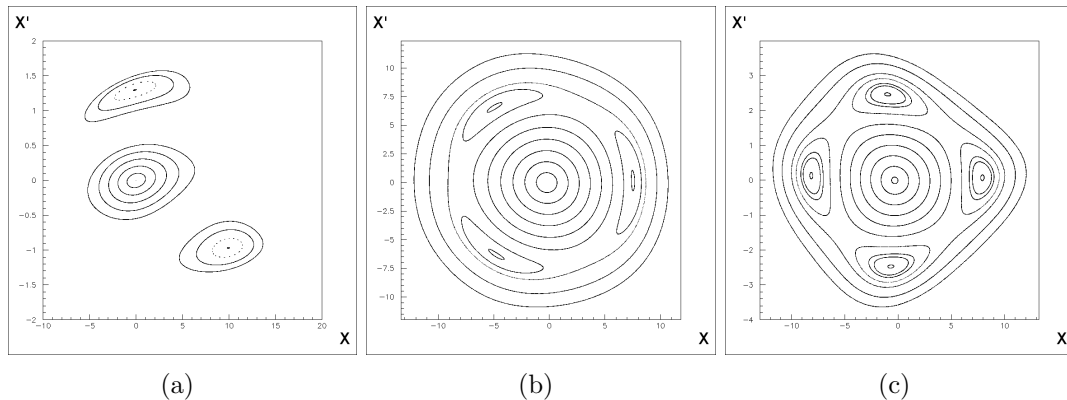


Figure 7.7: Particle tracking results shown for resonance island bucket operation near $\Delta Q_x = 1/2$ (a), $\Delta Q_x = 1/3$ (b) and $\Delta Q_x = 1/4$ (c). The corresponding area of island bucket acceptance is strongly dependent on the setting of nonlinear elements – in particular elements such as harmonic sextupoles or octupoles.

Figure 7.8 shows source point images of island bucket operation at the MLS (a) and BESSY II (b). Skew quadrupoles were applied introducing coupling between horizontal and vertical plane for reasons of visualization. At the MLS, it is possible to store the maximum current of $I \approx 200$ mA inside the island buckets at a lifetime of $\tau > 3$ h. Active bunch-by-bunch feedback was operational to counteract longitudinal coupled bunch instabilities. Particle redistribution between island and core bucket was demonstrated by means of narrow band excitation using existing hardware of the bunch-by-bunch feedback system. Diffusion rates for particles leaving core or island buckets were reduced to a bearable level for stable long term operation and bunch as well as bucket selective phase space cleaning. Island bucket population for a single bunch was shown while operating a homogeneous multi bunch fill as core beam. Arbitrary core or island bucket population could be switched on an on-demand and bunch-selective basis.

The required techniques are now applied to BESSY II to achieve a comparable degree of usability. At the time of writing this study, the storable current in $\Delta Q_x = 1/3$ island buckets at BESSY II is about $I \approx 100$ mA. However, more boundary conditions apply such as the ability to inject to core buckets and lifetime restrictions for TopUp capability.

As electrons stored in island buckets are separated in space and in angle, the photon beams generated by these electrons will be separated too. It depends on the exact user beamline geometry whether a separation in space or angle is desirable. However, resonance island buckets may fulfill both demands. Figure 7.9 shows the separation of radiation cones at user ports of the MLS, where (a) corresponds to

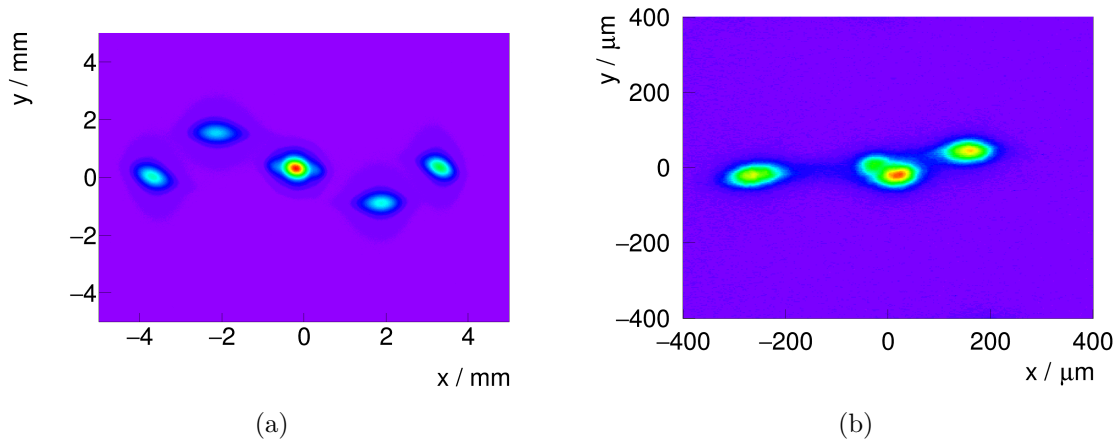


Figure 7.8: Source point images in the xy -plane for resonance island buckets in operation at (a) the MLS (1/4 resonance) and at (b) BESSY II (1/3 resonance).

a bending magnet beamline and (b) to an insertion device beamline. Users may selectively accept radiation from one bucket type only. Additional separation may be achieved by applying coupling between horizontal and vertical plane. However, this may interfere with beamline geometry requirements.

A very distinct feature of transverse island buckets is the possibility of user operation with repetition rates of sub-harmonic of the revolution time. This mode of operation will be discussed for the example of operation near $\Delta Q_x = 1/3$ corresponding to Fig. 7.7(b). A particle with 6D coordinates of the island bucket fixed point for $X' = 0$ as initial value will “jump” to a fixed point of another island in the next turn. Whether the “jump” occurs clockwise or counterclockwise in phase space depends on the interplay between linear and nonlinear elements. Therefore, if only one of the islands is populated, the resulting pulse structure would be characterized by a repetition rate of $f_{\text{rev}}/3$. This unique characteristic could be exploited by users such as time-of-flight (TOF) experiments. Peak brilliance is conserved. In the given example, users could exclusively apply radiation from the same single bunch every third turn, i.e. with a repetition rate of $f_{\text{rev}}/3 = 417$ kHz, without the need for dedicated single bunch operation shifts.

Conclusion

The separation of the short from the long light pulses can be achieved at BESSY II with a couple of approaches which already have successfully demonstrated the de-

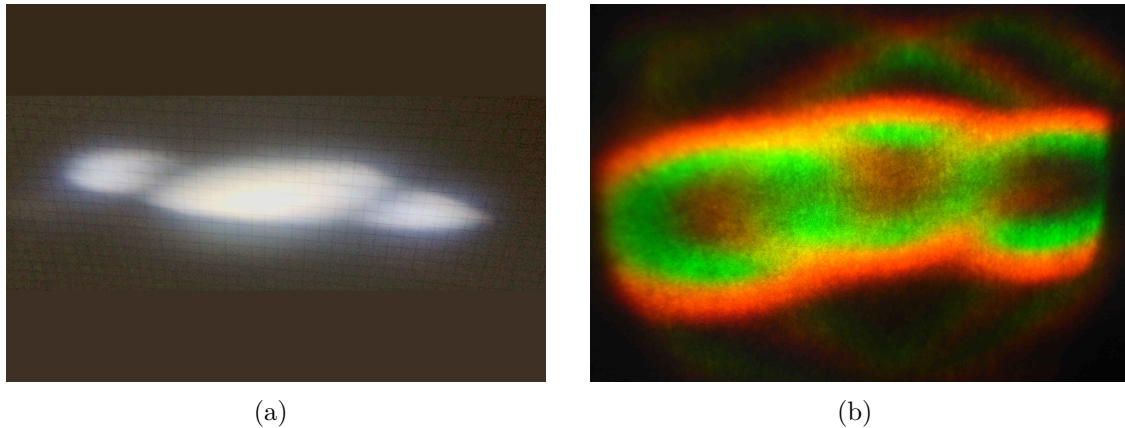


Figure 7.9: Spatial separation of radiation power from resonance island bucket operation at selected user ports. Bending magnet radiation (a) as well as undulator radiation are shown (b).

sired performance. For the time being, the chopper wheel is first choice for the separation in the beamlines in order to get the full intensity of the light pulse. In case lower intensities are sufficient or desired, the resonant pulse picking will be employed in order, for example, not to destroy delicate samples. The other techniques mentioned, like selectively forcing the short bunch on a different orbit or the creation of resonance islands and their selective population, will be optimized and tried out in the near future.

A rough cost estimate for a vertical bunch separation scheme with a resonant kicker shows that 500 k€ would be needed for its implementation into the BESSY II storage ring. The stripline kicker requires ~ 150 k€ and the 1.25 MHz, 3 kV high voltage pulse generators are estimated to cost ~ 350 k€. The quoted price is for 2 kickers and 4 generators so that enough spare parts are included in order to guarantee a continuous mode of operation.

References

- [1] M. Cammarata et al. “Chopper system for time resolved experiments with synchrotron radiation”. In: *Review of Scientific Instruments* 80.1, 015101 (2009), p. 015101. URL: <http://scitation.aip.org/content/aip/journal/rsi/80/1/10.1063/1.3036983> (cit. on p. 167).
- [2] M. Gembicky, S. Adachi, and P. Coppens. “A kHz heat-load shutter for white-beam experiments at synchrotron sources”. In: *Journal of Synchrotron Radiation* 14 (2007), pp. 295–296 (cit. on p. 167).

-
- [3] K. Holldack et al. “Single bunch X-ray pulses on demand from a multi-bunch synchrotron radiation source”. In: *Nature Communications* 5 (2014), p. 4010 (cit. on pp. 168, 171).
- [4] C. Sun et al. “Pseudo-Single-Bunch with Adjustable Frequency: A New Operation Mode for Synchrotron Light Sources”. In: *Phys. Rev. Lett.* 109 (Dec. 2012). 2012, p. 264801. URL: <http://link.aps.org/doi/10.1103/PhysRevLett.109.264801> (cit. on pp. 168, 174).
- [5] G. Reichardt et al. “Adaption of the BESSY I-3m normal incidence monochromators to the BESSY II source”. In: *Nuclear Instruments and Methods in Physics research A* 467.1 (2001), pp. 458–461 (cit. on p. 169).
- [6] R. Ovsyannikov et al. “Principles and operation of a new type of electron spectrometer - ArTOF”. In: *Journal of Electron Spectroscopy and Related Phenomena* 191 (2013), pp. 92–103 (cit. on p. 171).
- [7] URL: <http://www-als.lbl.gov/index.php/holding/855-pseudo-single-bunch-expands-experimental-scope-.html> (cit. on p. 174).
- [8] D. Alesini et al. “Design, test, and operation of new tapered stripline injection kickers for the e^+e^- collider DAΦNE”. In: *Phys. Rev. ST Accel. Beams* 13 (11 Nov. 2010), p. 111002. URL: <http://link.aps.org/doi/10.1103/PhysRevSTAB.13.111002> (cit. on p. 175).
- [9] FID GmbH. URL: <http://www.fidtechnology.com/> (cit. on p. 176).
- [10] Z. Conway et al. “Development and Test Results of a Quasi-waveguide Multi-cell Resonator”. In: *Proceedings of IPAC2014* WEPRI050 (2014), pp. 2595–2597 (cit. on p. 176).
- [11] C. J. A. Corsten. “Resonance and Coupling Effects in Circular Accelerators”. PhD thesis. Eindhoven University of Technology, 1982 (cit. on p. 177).
- [12] R. Capii and M. Giovannozzi. “Multiturn extraction and injection by means of adiabatic capture in stable islands of phase space”. In: *Phys. Rev. ST Accel. Beams* 7 (2 Feb. 2004), p. 024001. URL: <http://link.aps.org/doi/10.1103/PhysRevSTAB.7.024001> (cit. on p. 177).
- [13] J. Feikes et al. “Metrology Light Source: The first electron storage ring optimized for generating coherent THz radiation”. In: *Phys. Rev. ST Accel. Beams* 14.3 (Mar. 2011), p. 030705. URL: <http://link.aps.org/doi/10.1103/PhysRevSTAB.14.030705> (cit. on p. 177).
- [14] P. Goslawski et al. *Bunch Separation with Resonance Island Buckets*. Conference Website. ESLS XXII Workshop. Nov. 2014. URL: http://www.esrf.eu/files/live/sites/www/files/events/conferences/XXII%20ESLS/GOSLAWSKI_RI.pdf (cit. on p. 177).

- [15] M. Ries et al. “Transverse Resonance Islands for Simultaneous Multi Beam Storage at the MLS”. In: *Proceedings of IPAC2015* to be published (May 2015) (cit. on p. 177).

8 Beamlines, Endstations and Experiments

8.1 Photon Beams

Novel scientific fields open up through the combination of the BESSY VSR source properties with unique experimental capabilities. This requires - in addition to the performance of the accelerator itself - a thorough optimization of the facility starting from radiation generation, the selection and synchronization of individual bunches at MHz rates, as well as dedicated experimental infrastructure. Since BESSY VSR stores simultaneously long and short bunches, optimized undulators are required to generate with high efficiency and minimum bunch elongation the BESSY VSR radiation with variable polarization in the soft and tender X-ray range of BESSY II.

To achieve this goal, optimized radiators are employed as radiation source that allow one to extract soft and tender X-ray pulses from the stored BESSY VSR bunch patterns using low undulator harmonics at full polarization control. Some of existing conventional APPLE II-type undulators (e.g UE56) should be replaced by short period small gap in-vacuum undulators (e.g UE30) allowing for overcompensating losses in flux when operating BESSY VSR at low momentum compaction factor for sub-ps applications. It is part of the conceptual design that BESSY VSR preserves the Average Brilliance B_A of BESSY II undulators as illustrated by Table 8.1. As an example, the maximum brilliance values for the UE49 - an important undulator used for X-ray microscopy and other photon hungry applications (PEEM, SMART, RICXS) - are given and compared to predicted values at BESSY VSR according to the planned fill pattern (Figure 2.5). The peak brilliance provided by the individual bunches in a multiple fill is given by $B_P = B_A / (n_B f_{\text{rev}} \sigma_z)$, where f_{rev} is the revolution frequency, n_B the number of bunches and σ_z the bunch length in longitudinal phase space. The table nicely depicts that the peak brilliance of almost all bunches in the fill is of the order of 10^{22} meaning that any time resolved application at BESSY VSR (X-ray pump-probe, STXM etc.) can be performed always at the same peak brilliance regardless which pulse is picked out. Particularly surprising is the fact that the peak brilliance of BESSY VSR is an order of magnitude higher

Table 8.1: Photon beam properties at BESSY VSR compared to different modes of BESSY II. Brilliance values refer to the UE49 undulator in planar mode at the BESSY II design emittance of 5 nm rad and 2% coupling.

Facility	Peak brilliance ph/s/mrad ² /mm ² /0.1 %BW	Average brilliance (multi bunch curr.)	Number of bunches	Pulse duration ps (rms)
BESSY II				
standard	6.1e21	4e19 (300 mA)	350	15
low α	1.9e20	2.5e17 (15 mA)	350	3
BESSY VSR				
total	varying	4e19 (300 mA)	varying	varying
std. long pulses	1.2e22	3.3e19 (248 mA)	150	15
std. short pulses	1.7e22	3.6e18 (27 mA)	150	1.1
long camshaft	3.95e22	1.3e18 (10 mA)	1	27
short camshaft	5.1e22	1e17 (0.8 mA)	1	1.7
low α	2.2e21	1.2e17 (7.5 mA)	150	0.3

than at BESSY II albeit much lower than at FELs but at up to 500 MHz repetition rate. When approaching very short bunches combining BESSY VSR and the low alpha mode, losses in emittance are partly compensated by the upcoming in-vacuum undulators which will deliver up to an order of magnitude higher Brilliance than the UE49. It is further remarkable that Femtoslicing benefits by a factor of 4 if performed in BESSY VSR since it is performed on compressed bunches [1]. Another intriguing aspect of slicing at VSR is the potential emission of laser-induced THz pulses with up to μJ pulse energy at MV/cm field strength and tunable sub-ps pulse length.

8.2 Timing and Synchronization

The bunch separation between the long and short bunches and sub-sets of the BESSY VSR fill pattern requires both the implementation of pulse-picking capabilities (see Chapter 7) and the associated diagnostics and controls at individual beamlines for user's switch-ability. This requires the implementation of the synchronized timing signals to relay the bunch information to each experimental sta-

tion and beamline. So far the 500 MHz has been only available as an analogue RF signal. In order to achieve a sub-ps synchronization level a distributed optical timing distribution based on fiber links is mandatory. First prototypes have been recently successfully tested at selected beamlines. Based on this information our MHz Chopper systems will be implemented within the exit slit positions of the individual beamlines which requires adaption of slit units and refocusing optics. An estimation of costs for upgrading beamlines with optical timing distribution and optical components is given in Table 8.2. Also electronic pulse picking through sep-

Table 8.2: Costs for upgrading user beamlines with optical timing distribution and optical components.

X-ray diagnostics and timing	Costs/k€	Remarks
Optical timing distribution	210	13 k€/section, 1 st project year
X-ray diagnostics beamline		Replaces 3mNIM, 2nd project year
Front-end	250	
Mirror chamber	90	
Mirror (toroid, 1 m)	40	
Vacuum (pipes, pumps, gauges)	50	5 k€/m
Radiation protection	10	Depends on energy range
Media support	10	
Controls+ Data acquisition	105	Oscilloscope, digi- tal boxcar, spec- trum analyzer
X-ray diagnostics in ID beamlines	420	30 k€/section, 2 nd and 3 rd project year
Total costs:	1175 k€	

aration by gating of fast detectors, as currently only available at a few endstations, has to be implemented in the framework of upgrades of the beamline's control and data acquisition systems.

8.3 Endstations and Experiments

To exploit the time structure of BESSY VSR in addition to the static operation, excitation through femtosecond light pulses in the eV and meV range need to be delivered and synchronized at MHz repetition rates to the electron bunches. To this end, suitable synchronized lasers and e.g. optical parametric amplifier systems need to be located in close proximity to BESSY VSR beamlines for individual experiments. Safe operation requires protective housing and interlock measures as well as active feedbacks for the transport lines. In addition, in-coupling and diagnostics for X-ray optical spatial and temporal overlap is required.

The data acquisition of beam parameters and experimental signals need to distinguish the different temporal sub-patterns within BESSY VSR. This can be achieved through fast digitizers, integrators and time-correlated pulse-counting detection. Alike fast camera and delay line detection require time stamps that allow unambiguous assignment of measurements to the X-ray pulse arrival time. Dedicated experimental stations will cover the full range of spectroscopic and diffraction probes that the soft and tender X-ray regime provides. Here, dedicated X-ray detectors that are fast enough but insensitive to the excitation pulses are required. Many experiences with all of these components have been gained within the past 10 years with fs-X-ray-science at BESSY II [1]. As estimated in this paper, BESSY VSR will deliver through time-slicing techniques also monochromatic X-ray pulses below 100 fs at kHz repetition rate exceeding a flux 10^8 ph/s/0.1 %BW, about 2 orders of magnitude more in comparison to now. Here, a factor of 4 results from the bunch compression in BESSY VSR and a further factor of 25 is gained by combining a higher laser repetition rate of 50 kHz with the new in-vacuum radiator UE30 being currently (2015) under construction.

Spectroscopy of electrons and charged particles will benefit at BESSY VSR through the time of flight detection capabilities [2] utilizing the temporally well defined pulses at high repetition rate. Thus, highly efficient detection will allow to push the space charge limited resolving power below the meV energy scale. In addition, low dose detection on radiation sensitive materials becomes feasible and the simultaneous angular distributions resulting e.g. from electron diffraction can be combined with chemical selectivity. Complete experiments that detect the full quantum state of the matter under investigation through the control of incident radiation and the parameters of the emitted messenger particles in coincidence detection will strongly benefit from the well in time defined synchrotron bunches at high repetition rate. For driven states of matter, the exposure to driving fields synchronized to the MHz bunch structure will allow to sweep at a high duty cycle through the parameter space. Similarly scanning probe techniques, i.e. X-ray microscopy [3], will benefit

from the fast MHz repetition rate to combine picosecond timescales with X-ray microscopic information.

References

- [1] K. Holldack et al. “FemtoSpeX: a versatile optical pump-soft X-ray probe facility with 100 fs X-ray pulses of variable polarization”. In: *Journal of Synchrotron Radiation* 21.5 (2014), pp. 1090–1104 (cit. on pp. 184, 186).
- [2] R. Ovsyannikov et al. “Principles and operation of a new type of electron spectrometer - ArTOF”. In: *Journal of Electron Spectroscopy and Related Phenomena* 191 (2013), pp. 92–103 (cit. on p. 186).
- [3] A. Bisig et al. “Correlation between spin structure oscillations and domain wall velocities”. In: *Nature Communications* 4 (2013), p. 2328 (cit. on p. 186).

9 Radiation Protection Issues of BESSY VSR

The shielding requirement of synchrotron light sources is defined by the numbers of electrons injected per year. Every injected electron will be lost at the vacuum system of the accelerator, either during injection or later caused by collisions with rest gas molecules, Touschek or intra beam scattering. The losses are expressed as injection efficiency and life time and can be controlled by an interlock system to keep the overall electron losses below a given limit. This method has its limitations where the life time is reduced drastically as it is the case at diffraction limited storage rings (DLSR) with their strongly reduced transversal emittance. The TopUp operation is of course no method to compensate such reduced life times because the increased number of injected electrons can increase the annual dose even beyond the possibility to get an operation license from the authorities. For existing storage rings an appropriate increase of the shielding wall thickness is no option. A tenth value layer of ordinary concrete is 45 cm for both γ and giant resonance neutron radiation and even 1.1 m for high energy neutrons. In comparison with DLSR the VSR method offers the possibility to keep the life time constant, by distributing the electrons among the longer and shorter buckets and by the excitation of the beam. From the radiation safety point of view an upgrade program like BESSY VSR has considerable advantages in comparison with the transformation to a DLSR.

9.1 Electron Loss Limitation

The shielding walls of BESSY require to keep the number of injected electrons per year on the same value of $2 \times 10^{15} \text{ e}^-/\text{a}$ as it is the case now, summarised in Table 9.1.

As can be seen in Table 9.1 the number of stored electrons has increased by a factor 3.2 when the injection mode was changed from the decay to the TopUp mode. To keep the overall number of injected electrons constant the injection efficiency had to be increased from 30 % to 90 %. A further increase of the injection efficiency is

Table 9.1: Overview of BESSY annual electron losses.

Mode	Decay		TopUp	
	250 days/a		250 days/a	6000 h/a
Operation time	250 days/a		250 days/a	6000 h/a
Injections	3/day	750/a	2880/day	720000/a
Injected current	150 mA/inj.	112.5 A/a	0.5 mA/inj.	360 A/a
Injected charge		9e-5 C/a		2.88e-4 C/a
Efficiency		30 %		90 %
Injected electrons	5.62e14/a	1.9e15/a	1.8e15/a	2.0e15/a

not possible, so the electron losses of the BESSY VSR mode must also be limited to $2 \times 10^{15} e^-/a$.

The TopUp interlock systems blocks the extraction from the synchrotron booster if the life time is < 5 h at a stored current of 300 mA in the storage ring. This corresponds to injection shots which increase the ring current by 0.5 mA every 30 seconds. The most important measure to limit electron losses is the 90 % injection efficiency which is controlled every injection shot. The average 90 % injection efficiency must be held over a 4 h block. If not, the lower efficiency is compensated by switching to the decay mode during a penalty time. If the injection efficiency is < 60 % the TopUp operation is stopped immediately.

Further measures to control the electron losses are the interlock monitored limit of the maximum injection frequency of 0.1 Hz and the maximum charge limit of the linac with 2 nC/shot.

Besides the losses due to regular operation it is also possible that instabilities of the beam increase the numbers of stochastic beam dumps.

9.2 Life Time

The increase of the stored current of 0.5 mA added every 30 seconds by TopUp injections corresponds to a lifetime $\tau = 5$ h, for $\Delta I = 0.5$ mA, $I_0 = 300$ mA and $t = 30$ s calculated with Equation (9.1).

$$\tau = -t / \ln((I_0 - \Delta I) / I_0) \quad (9.1)$$

In principle it is possible to compensate reduced life times by the reduction of the stored current. The same calculation as above for $I_0 = 200$ mA results in $\tau = 3.3$ h, the injected charge is the same per shot and per year. But the reduction of charge within the bunch will also have effects on the bunch shape and the bunch length.

The life time will be determined by the Touschek rate, which is proportional to the charge density of the bunch. A promising ansatz is to keep the charge density in the long and short bunches on the same level by having more electrons in the long bunches as described in Chapter 2.

9.3 Doses Prediction of Cavity Tests by FLUKA Calculations

The doses and dose rates due to the TopUp operation of BESSY II have been calculated in detail. We used the multi particle transport code FLUKA [1–3] to calculate the doses through the opened beam-shutters and walls for different loss scenarios and discussed the resulting safety measures [4].

In the following we present calculations of dose rates due to cavity tests within the storage ring tunnel. The cavity tests of the super conducting cavities will produce electrons by field emission. Field emission is difficult to predict because it depends on the smooth surface of the individual cavity. To make our calculations conservative we use 20 MeV as energy of the field emission electrons and as maximum dose rate the value of 1 Sv/h, which corresponds to the value of the worst cavity ever investigated at HoBiCaT.

We considered two scenarios depicted in Figure 9.1:

- a) The field emission electrons start as a pencil like beam in the straight section and the 1.3 T dipole field acts as magnetic mirror. The reflected electrons hit the vacuum chamber of the dipole.
- b) The field emission electrons start again as a pencil like beam in the straight section, the dipole has no field, the electrons hit the downstream part of the dipole chamber, downstream the chamber is a local lead shield of 5 cm.

Neutrons are not relevant, because only a very small part of the bremsstrahlung is above the threshold energy of (γ, n) nuclear reaction.

If we compare the two scenarios we see, that the overall dose distribution is more favorable at the second scenario. In that case it is possible to create an effective local shielding. At the first scenario we have a wide spread gamma radiation distribution inside the storage ring tunnel. A local shielding is not possible because the places

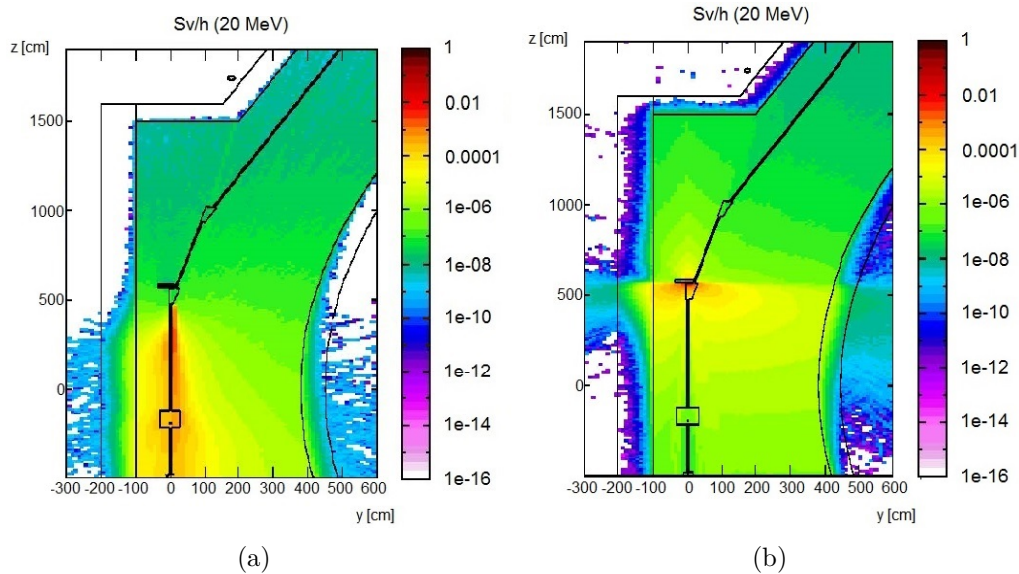


Figure 9.1: The γ dose rate is shown in Sv/h for a magnetic field of (a) $B = 1.3$ T and (b) $B = 0$ T.

where the electrons hit the dipole chamber are not predictable. It is even possible that the reflected electrons do not hit the dipole chamber because their energy is lower and the trajectory has a smaller radius, so that they flow back upstream and hit the vacuum system or the cavity elsewhere. Especially if there are more than one sources of field emission electrons the energy distribution could be broad and therefore always a part of the electrons will be reflected by the dipole field and hit the vacuum system upstream.

The test of the cavities requires the status of the storage ring tunnel as interlock saved exclusion area.

9.4 Dose Measurements

At synchrotron light sources we have two main sources of systematic measurement errors:

1. the high energy parts of both, γ and neutron spectra and
2. the dead time effects due to the pulsed radiation.

We developed methods to compensate errors due to high energy (> 10 MeV) neutrons and photons by calculation of the respective spectra with high accuracy [5,

6]. For high energy neutrons we developed a moderator which expands the measurement range of standard neutron monitors from 10 MeV to several GeV. The upgrade of our neutron monitors with these moderators is in progress.

We developed correction formulas for the dead time effects of neutron monitors and we reduced the measurement errors by exchanging the preamplifiers by faster ones [7].

9.5 Conclusion

The interlock conditions and safety measures for the TopUp operation are also sufficient to provide the radiation safety for BESSY VSR. The reduction of the Touschek rate is the most important method to decrease the annual dose. One of the possibilities is the electron distribution among the short and long bunches. Others are the vertical excitation of the beam (or a part of the bunches) up to a maximum emittance limit that has to be defined or the reduction of the stored current.

Additional doses by the possible increased numbers of stochastic beam dumps can be compensated by a supplement to the interlock system: Beam dumps due to machine protection circuits should be done with a delay of 5 s, within this time all beam-shutters are closed. Beam dumps due to the personal safety interlock must be always conducted without delay.

Test operation of the superconducting cavities is possible, if the dipole field is interlock controlled switched off and a local lead shielding of 5 cm is placed downstream the dipole chamber. This test operation is only possible, if the storage ring tunnel is interlock monitored exclusion area (same prerequisite as for storage ring operation). In this cavity section no 0° beamline exist, so field emission electrons cannot reach the experimental hall even if the dipole field is switched off. Field emission is inverse proportional to the cavity quality. A good cavity quality is the prerequisite for the every day's operation, so the test operation must reach a low field emission or the cavity has to be replaced. The usage of the cavity with the dipole field is acceptable if the dose rate due to field emission is below 10 % of the values shown in Figure 9.1.

The accurate measurement of doses is possible also for BESSY VSR by our improved ambient dose measurement system combined with our effective methods to compensate systematic measurement errors.

References

- [1] G. Battiston et al. “The FLUKA code: Description and benchmarking”. In: *Proceedings of the Hadronic Shower Simulation Workshop 2006* Fermilab 6-8 (2006) (cit. on p. 191).
- [2] M. Albrow and R. Raja. In: *AIP Conference Proceeding* 896 (2007), pp. 31–49 (cit. on p. 191).
- [3] A. Fassio and A. Ferrari. “FLUKA: a multi-particle transport code”. In: *CERN-2005-10 (2005), INFN/TC_05/11, SLAC-R-773* (2005) (cit. on p. 191).
- [4] K. Ott. “Radiation Protection Issues of the TopUp Operation of BESSY”. In: *Proc. 7th Intern. Workshop on Radiation Safety at Synchrotron Radiation Facilities* (2013) (cit. on p. 191).
- [5] P. Kuske et al. “Preparations of BESSY for TopUp Operation”. In: *Proceedings of EPAC08* WEPC037 (2008), pp. 2067–2069. URL: <http://accelconf.web.cern.ch/AccelConf/e08/papers/wepc037.pdf> (cit. on p. 192).
- [6] K. Ott and Y. Bergmann. “FLUKA calculations of gamma spectra at BESSY”. In: *Proceedings of IPAC2014* MOPRO059 (2014), pp. 219–221. URL: <http://accelconf.web.cern.ch/AccelConf/IPAC2014/papers/mopro059.pdf> (cit. on p. 192).
- [7] K. Ott et al. “Dead-time effects of neutron detectors due to pulsed radiation”. In: *Rad. Prot. Dosi.* 155.2 (2013), pp. 125–140 (cit. on p. 193).

10 Testing Equipment

In order to assembly and verify the new SRF components, new testing equipment is required. The infrastructure development currently underway expanding the SRF testing equipment at HZB will benefit the BESSY VSR project. There are presently capabilities to test SRF cavities which are integrated into a helium vessel in the horizontal test cryostat, HoBiCaT [1], shown in Figure 10.1. Furthermore a vertical test stand for 2-cell cavities has just been commissioned.

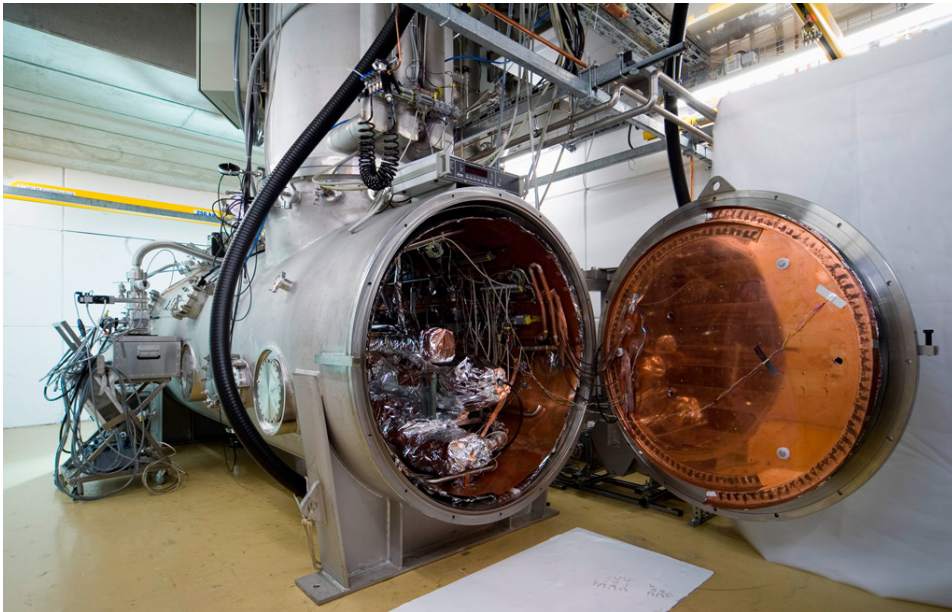


Figure 10.1: The horizontal test cryostat HoBiCaT at HZB.

There is a need for the ability to chemically etch and test cavities prior to helium vessel welding. Infrastructure upgrades are currently underway at HZB for both of these needs to be met. A chemical processing facility as well as a new large vertical testing Dewar, capable of handling a 9-cell TESLA cavity, are currently part of the expansion of the SRF cavity processing and testing facilities at HZB and should become available for use in the fall of 2016. A list of the necessary cavity processing and testing infrastructure is shown in Table 10.1 and an indication of the current status of the equipment is shown by the color coding listed in the table title.

Table 10.1: SRF cavity and cryomodule processing and testing infrastructure status at HZB (items in gray are under construction, items in red are planned).

Cryomodule & Cavity status	Process required	Infrastructure needed	Delivery date
Bare cavity from vendor	Cavity tuning	Beadpull and tuning bench	12/2015
Bare cavity requires chemical etching	Chemical processing of SRF cavities	Chemical processing facility	8/2016
Bare cavity	SRF cavity HPR and assembly	HPR and cleanroom	Operational
Bare cavity (9-cell TESLA cavity)	Vertical 1.8 K RF test	Vertical testing Dewar in Testing Hall 1 and LLRF for 1.5 GHz and 1.75 GHz	7/2016
Coupler processing	RF conditioning of power couplers	RF processing system	11/2016
Cavity in HV with high power coupler	Horizontal test with high power coupler	Cleanroom	Operational
Cavity in HV with high power coupler	Horizontal test with high power coupler	HoBiCaT	Operational
Assembly of CM beamline parts	Cold mass assembly	Cleanroom and HPR	Operational
Assembly of cryomodule	Cryomodule Assembly		Q3/2017
Cryomodule commissioning	Cryomodule RF test	LLRF and HPRF 1.5 GHz and 1.75 GHz	Q4/2017

The two, previously mentioned, key items that are currently being constructed at HZB which directly benefit the BESSY VSR project are the chemical processing facility at the HZB Wannsee site as well as the Testing Hall 1 being built at the HZB Adlershof site adjacent to the Schwerlasthalle where HoBiCaT testing facility, the cleanroom, and the high-pressure rinsing facility (HPR) are located. The chemical processing facility in Wannsee will have a buffered chemical processing (BCP)

cabinet for chemical etching of SRF cavities. For the performance which we require for the BESSY VSR project the BCP process should be adequate, although there are collaborative options available where the electropolishing of the cavity may be possible. The layout of the chemical processing laboratory is shown in Figure 10.2.

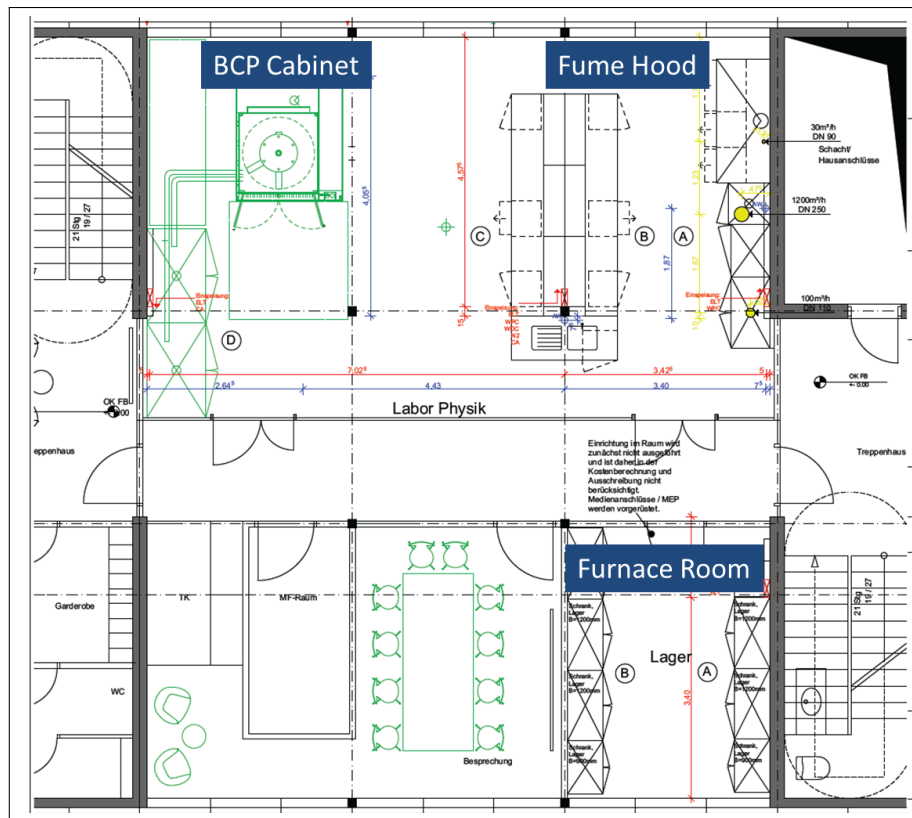


Figure 10.2: The layout of the chemical processing facility at Wannsee.

Perhaps the more important piece of testing infrastructure is the new vertical testing Dewar in the Testing Hall 1. This large testing Dewar will accommodate the SRF cavities required for the BESSY VSR project and will allow us to measure the cavity performance in a facility with a quick turn-around time for cavity measurements. The Dewar is designed to operate down to 1.5 K, allowing us to fully explore the cavity performance as a function of temperature.

Following the successful vertical cavity tests the cavities will be fitted with high power couplers and mounted inside HoBiCaT for further evaluation. These tests are significantly different from the vertical tests due to the change in the cooling scheme to only cooling the cavity inside the HV, not a full submersion of the cavity

and endgroups, as well as the addition of the high power coupler and the previously mentioned heat load from the exterior of the cryostat that must be managed.

After these horizontal tests have been carried out the cold mass must be assembled in the cleanroom and be prepared for cryomodule assembly. Finally the module needs to pass the crucial RF test in the module test facility. As a back-up plan the BESSY VSR module may be able to be tested in the bERLinPro bunker.

References

- [1] J. Knobloch et al. “HoBiCaT - A Test Facility for Superconducting RF Systems”. In: *Proceedings of the 11th Workshop on RF Superconductivity* MOP48 (2003), p. 173 (cit. on p. 195).

11 Cost and Schedule

This chapter summarizes the investment costs and schedule for the BESSY VSR upgrade project. The costs have been broke down by the project phases.

11.1 Costs

The major components and hardware upgrades for the BESSY VSR project can be broken down into five main categories and spread across the preparatory and the final BESSY VSR phase as listed in Table 11.1.

The cost breakdown derived from Table 11.1 is shown in Table 11.2. The total for the different categories has been separated by phase. Critical spares for the SRF cavities as well as the RF components must be maintained as described earlier. For the cavities this results in a complete spare cryomodule, while for the RF systems the spare transmitters will be used in the Cryomodule Test Facility (CTF) ready for use in BESSY VSR.

In addition to the cavities which make up the spare cryomodule at least one spare cavity of each frequency will also be ordered. This will be done in order to ensure that there is at least one spare cavity during each phase of the project as the cavity procurement will be at least 18 months in duration. This means that for the preparatory phase with both frequencies, a total of 4 cavities must be ordered, three 1.5 GHz cavities and one 1.75 GHz cavity. In addition copper prototypes must first be built in order to measure the field pattern of the higher order modes and compare them to the simulations to ensure no dangerous HOMs are trapped in the cavity. The number of copper cavities with ancillary components are listed in brackets in the preparatory phase in the table below.

11.2 Schedule

The abbreviated BESSY VSR schedule is shown in Table 11.3. The schedule provides a view of the many activities that must take place in parallel in order for the

Table 11.1: The breakdown of the major components and spares required for different BESSY VSR phases. The "X" indicates the phase in which different parts will be required when a quantity is not specified. The number of prototype cavities made of copper and its ancillary components for final design testing are listed in brackets.

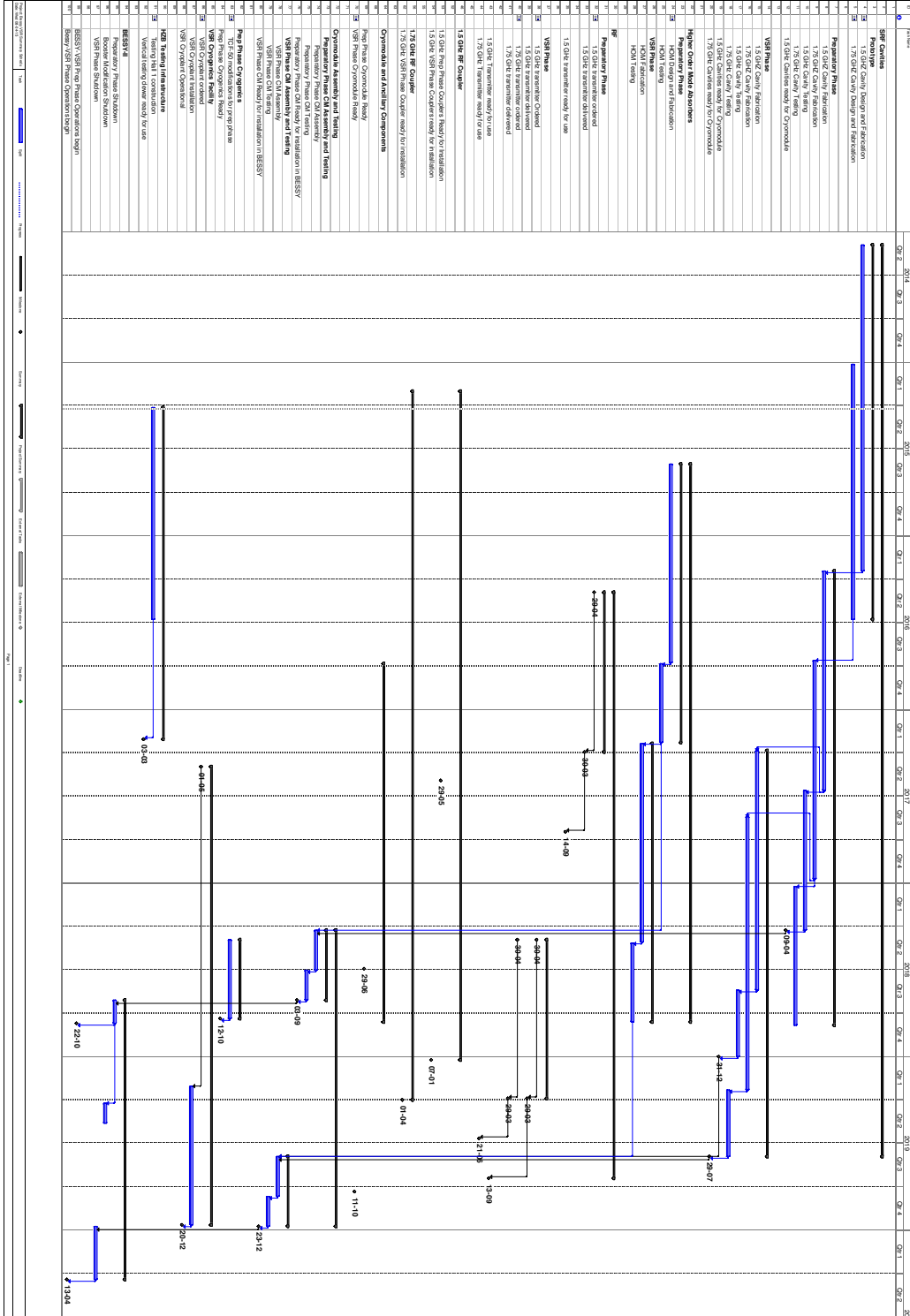
Item	Preparatory phase	Final project phase
SRF components		
1.5 GHz cavity	(1) 3	2
1.75 GHz cavity	(1) 1	4
RF power couplers	4	8
HOM absorbers	(1) 20	30
Cryomodule and ancillary components	1 X	1 X
Cryogenics		
TCF-50 upgrade	X	
New 1.8 K Cryogenic facility		X
Cryogenic connection to CTF	(X)	
RF Components		
1.5 GHz RF transmitters	2	1
1.75 GHz RF transmitters	0	3
Low Level RF	(2) 2	4
RF distribution	X	X
BESSY II Modifications		
Booster synchrotron upgrade	X	X
BESSY II storage ring	X	X
MHz Chopper	X	X
Diagnostics	X	X

project to be successful. The schedule also shows how the work for the preparatory and BESSY VSR phase must proceed and when the key procurements need to be made.

Table 11.2: The cost breakdown for the two BESSY VSR phases.

Item	Preparatory phase Cost/k€	Final project phase Cost/k€
SRF components		
1.5 GHz cavity	665 k€	398 k€
1.75 GHz cavity	335 k€	707 k€
RF power couplers	350 k€	350 k€
HOM absorbers	315 k€	375 k€
Cryomodule and ancillary components	799 k€	898 k€
Cryogenics		
TCF-50 upgrade	125 k€	400 k€
New 1.8 K Cryogenic facility		7870 k€
Cryogenic connection to CTF	1335 k€	
RF Components		
1.5 GHz RF transmitters	1068 k€	534 k€
1.75 GHz RF transmitters		1601 k€
Low Level RF	135 k€	67 k€
1.5 GHz RF distribution	175 k€	87 k€
1.75 GHz RF distribution	90 k€	179 k€
BESSY II Modifications		
Booster synchrotron upgrade	685 k€	2816 k€
BESSY II storage ring (vacuum)	530 k€	330 k€
Digital feedback system upgrade	248 k€	372 k€
Digital BPM system		1700 k€
Pseudo single bunch kicker	300 k€	200 k€
MHz Chopper	380 k€	405 k€
Diagnostics		
Diagnostic beamline equipment	930 k€	
X-ray diagnostics		1175 k€
Subtotals	8465 k€	20 464 k€
Project total	28 929 k€	

Table 11.3: The schedule for the BESSY VSR project.



12 Future Upgrade Options

When the basic scheme of BESSY VSR is operating well further upgrades might be of interest. There are four topics presented here, which still require more detailed work. The first one concerns the optimization of the Touschek life time. This can be achieved by populating four further longitudinal fixed points to relax the peak current. This implies a more complicated cavity operation, to control the energy exchange between the cavities. Another approach would be to moderately modify the transverse beam optics to relax the transverse charge density. A third topic are the NC cavities, which partly become redundant if BESSY VSR is operating well. The 4th topic is the low α optics, which could be optimized with reduced natural emittance and in this way enhance the brilliance of the photon beam.

Population of Further Fixed Points

For the proposed BESSY VSR scheme only fixed points are populated, where all individual harmonic cavity voltages vanish, which produces the long and short bucket types. There are more stable fixed points for short bunches, where only the sum of the voltage vanishes, not their individual contributions, see Figure 2.3. Per period of 250 MHz there is one long bucket and five short buckets, and only the long and one of the short buckets is considered up to now. A population of the additional fixed points could lead to an energy exchange between the cavities. However, if the currents in these bunches are exactly equal, there will be no energy exchange, averaged over 4 ns. If each of these questionable fixed points is populated with, for example, 30 mA than the current in the five short bunches becomes 150 mA and in the long bunches 150 mA. The five short buckets have three slightly different synchrotron frequencies and zero current bunch lengths. The growth rate of the CBI depends on the synchrotron frequency, and the long bunches with the smaller synchrotron frequency are more affected by the CBI than the short bunches. If these additional fixed points are populated, their synchrotron frequencies are all different and the multi bunch motion is decoupled which reduces the risk of CBIs. The reduced long bunch current relaxes the longitudinal CBI for BESSY VSR and has to be balanced against an increased impedance heating by the short bunches.

This redistribution of the charges lowers the peak current and reduces the Touschek loss rate.

Optimization of the BESSY II Optics

If not in conflict with user demands, the Touschek lifetime could be optimized by the following two modifications of the present beam optics:

- Dispersion in the straight sections is presently zero to achieve an emittance damping effect by the SC 7 T multipole wiggler. For BESSY VSR, the wiggler will be removed and relaxes this constrain. A final dispersion in the straights of about 10 cm could affect the bunch volume and reduce the dispersion also inside the achromatic sections, where Touschek events are limited by the chamber dimension. This could improve the Touschek life time but still keeps the beam size in the straights at the present value.
- The Touschek loss rate is above average in the low beta straights. There is a chance to enhance the vertical beta function in the straights from 1.2 m to 4 m and reduce this specific loss rate.

NC Cavities

The present NC, 0.5 GHz cavities are mostly used for longitudinal beam focusing. Only a small fraction of the RF voltage amplitude replaces the beam energy lost by synchrotron radiation, indicated by the small phase angle of few degrees. At BESSY VSR, the task of the beam focusing will be performed by the SC cavities, and, if the operation of the scheme is well settled, one could reduce the number of NC cavities to one unit only or apply even an explicitly designed RF cavity for on crest operation. Even a complete removal of the NC cavities seems possible, if the SC cavities could additionally feed the required power to the beam.

Optimization of Low α Operation

The emittance of the present low α optics is 7 times larger compared to the user optics. With the installed hardware of BESSY II, a different quadrupole tuning of the optics is possible, to reduce the emittance to a value of 5 nm rad, comparable to the emittance of the BESSY II user optics. The horizontal beta function in the straights will be reduced to 1 m, which makes the beam injection difficult. To

overcome this injection problem, one could try to have one local beta function injection bump of about 20 m amplitude. In case of symmetry breaking problems of the optics, a second bump opposite to the injection straight could be helpful. A careful beam optics design is required to find a solution, especially for the sextupole tuning to achieve a good dynamic aperture.

HZB Helmholtz
Zentrum Berlin
 **BESSY VSR**

Helmholtz-Zentrum Berlin für
Materialien und Energie GmbH
Hahn-Meitner-Platz 1
14109 Berlin

und

Albert-Einstein-Strasse 15
12489 Berlin

www.helmholtz-berlin.de